MEASUREMENT OF THE DIFFUSION OF GROUP III ELEMENTS INTO CADMIUM SULPHIDE

by

E. D. JONES

Thesis submitted for the degree of Doctor of Philosophy
at the University of Warwick

Department of Applied Sciences,
Lanchester Polytechnic,
Rugby.

1977

The contents of this thesis have been written solely for submission to the University of Warwick for the Degree of Doctor of Philosophy and have not been submitted for similar purposes to any other University. In addition, the work described is original, has been carried out by the author and in the cases, where the work of other scientists has been included, references are given.

Measurement of the diffusion of group III elements into CdS

by E. D. Jones

ABSTRACT

This thesis is concerned with the measurement of the rate of diffusion of the group III elements In, Ga and Al into CdS using a radiotracer sectioning technique, an optical method and an electron microprobe analyser. The diffusion anneals were carried out over the temperature range 920 K to 1550 K in silica ampoules in the presence of excess group III metal. The diffusion coefficient was linearly proportional to the concentration of the group III metal and the interface between the doped and the undoped part of the CdS was sharply defined. The surface concentration of the dopant in the CdS was dependent on the ratio of the number of Cd to trivalent metal atoms in the metal globule. When Cd metal was added to the ampoule the diffusion changed to being concentration independent.

In the case of the concentration dependent diffusions the optical method was sufficiently sensitive to measure the diffusion anisotropy of the hexagonal CdS. Diffusion was fastest in directions perpendicular to the c-axis and the ratio of the diffusion coefficients varied from unity at the highest temperatures up to five at the lowest temperatures. The results were consistent with the diffusion taking place via the compound defect $(M^{\bullet}_{Cd}\ V''_{Cd})'$ where M is the trivalent metal ion. As the results were normalised to a trivalent ion concentration of 1% of the cation sites, the temperature variation of the normalised diffusion coefficient gave the activation energy of motion of the mobile defect, which were (1.82 ± 0.12) eV and (1.55 ± 0.12) eV for $(In^{\bullet}_{Cd}\ V''_{Cd})'$ in the two principal directions. In the normalisation for the concentration, the surface concentration of the In and Ga were determined as a function of the annealing temperature. This enabled the activation energy of solution for dissolving the group III metal in CdS to be determined, giving (0.48 ± 0.09) eV for In and (0.75 ± 0.06) eV for Ga.

Measurement of the diffusion of group III elements into CdS

by E. D. Jones

ABSTRACT

This thesis is concerned with the measurement of the rate of diffusion of the group III elements In, Ga and Al into CdS using a radiotracer sectioning technique, an optical method and an electron microprobe analyser. The diffusion anneals were carried out over the temperature range 920 K to 1550 K in silica ampoules in the presence of excess group III metal. The diffusion coefficient was linearly proportional to the concentration of the group III metal and the interface between the doped and the undoped part of the CdS was sharply defined. The surface concentration of the dopant in the CdS was dependent on the ratio of the number of Cd to trivalent metal atoms in the metal globule. When Cd metal was added to the ampoule the diffusion changed to being concentration independent.

In the case of the concentration dependent diffusions the optical method was sufficiently sensitive to measure the diffusion anisotropy of the hexagonal CdS. Diffusion was fastest in directions perpendicular to the c-axis and the ratio of the diffusion coefficients varied from unity at the highest temperatures up to five at the lowest temperatures. The results were consistent with the diffusion taking place via the compound defect $(M^{\bullet}_{Cd}\ V''_{Cd})'$ where M is the trivalent metal ion. As the results were normalised to a trivalent ion concentration of 1% of the cation sites, the temperature variation of the normalised diffusion coefficient gave the activation energy of motion of the mobile defect, which were (1.82 ± 0.12) eV and (1.55 ± 0.12) eV for $(In^{\bullet}_{Cd}\ V''_{Cd})'$ in the two principal directions. In the normalisation for the concentration, the surface concentration of the In and Ga were determined as a function of the annealing temperature. This enabled the activation energy of solution for dissolving the group III metal in CdS to be determined, giving (0.48 ± 0.09) eV for In and (0.75 ± 0.06) eV for Ga.

DIFFUSION FRONT FOR THE DIFFUSION OF In INTO CdS

approximate magnification x 400

CONTENTS

List of Illustrations

List of Tables

Acknowledgements

The author wishes to thank the following people for their assistance and guidance which has been received during the project.

Dr. H. Mykura, Reader in the School of Physics, The University of Warwick, Coventry, who acted as the supervisor for the project. He has given invaluable guidance throughout the experimental programme, in the interpretation of the results and in the writing of this thesis. In addition, he carried out the X-ray investigations on the doped CdS specimens using the X-ray set at the University.

Dr. R. F. Y. Randall, Head of the Department of Applied Sciences, Lanchester Polytechnic, Rugby, who made it possible for the author to do this project by providing the necessary equipment, materials and laboratory space. In addition he read through the final draft checking for errors.

Dr. P. D. Fochs, The General Electric Company Limited, The Hirst Research Centre, Wembley, who suggested the initial part of the project which was on the diffusion of In into CdS.

Mr. C. Gilson, laboratory technician, Department of Applied Sciences, Lanchester Polytechnic, Rugby, who assisted with the experimental work. He prepared the ampoules for the diffusion anneals and helped with the measurement of the diffusion profiles using the radiotracer sectioning technique.

Mrs. P. Gillison, laboratory technician, Department of Applied Sciences, Lanchester Polytechnic, Rugby, who assisted with the project for the eighteen months prior to its completion, in tasks such as computer programming, in preparing the CdS slices

for the electron microprobe analyser and in reading through a draft of the thesis checking for errors.

Dr. M. Hall, Centre for Materials Science, University of Birmingham, for carrying out the measurement of the diffusion profiles using an electron microprobe analyser.

Mr. D. R. Clarke, Principal lecturer, Department of Computer Science, Lanchester Polytechnic, Rugby, who wrote the computer program which was used on the University of Warwick ICL 4100 computer.

Mr. K. Waller, Draughtsman, Department of Combined Engineering Sciences, Lanchester Polytechnic, Rugby, who traced all the diagrams which are included in this thesis.

Miss. S. Callanan, Departmental typist, School of Physics, University of Warwick, Coventry, who typed the thesis.

List of important abbreviations and symbols

A	Pre-exponential entropy term used in the relationship for C_o/C_f	dimensionless
Cd/In ratio	Atomic ratio of Cd to In atoms produced in the metal globule in the ampoule during a diffusion	dimensionless
CSE	Computed stoichiometric exchange	
C	Concentration of group III metal atoms in CdS	atoms m^{-3}
C_f	Concentration of cation sites in CdS	atoms m^{-3}
C_x	Concentration of group III metal atoms at a depth x inside the CdS crystal	atoms m^{-3}
C_o	Near-surface concentration of group III metal atoms in the CdS crystal (that is at x = 0)	atoms m^{-3}
Ci	Radiation source strength	Curies
D	Diffusion coefficient for tracer atoms in a chemical gradient	$m^2\ s^{-1}$
D^*	Isoconcentration diffusion coefficient	$m^2\ s^{-1}$
D^C	Diffusion coefficient at concentration C for the concentration dependent diffusion	$m^2\ s^{-1}$
D_M	Experimentally measured diffusion coefficient	$m^2\ s^{-1}$
D_o	Diffusion coefficient of the trivalent metal atoms at the crystal surface, at x = 0, for the concentration dependent diffusion	$m^2\ s^{-1}$
$D_{o\parallel}, D_{o\perp}$	Values of D_o for diffusions in directions parallel and perpendicular to the c-axis in a hexagonal crystal	$m^2\ s^{-1}$
D_o'	Diffusion coefficient at a concentration due to the trivalent metal atoms of 1% for the concentration dependent diffusion	$m^2 s^{-1}$ at $\%^{-1}$
$D_{o\parallel}', D_{o\perp}'$	Values of D_o' for diffusions in directions parallel and perpendicular to the c-axis in a hexagonal crystal	$m^2 s^{-1}$ at $\%^{-1}$
$D_{o\parallel max}$, $D_{o\parallel min}$	Values of $D_{o\parallel}$ for the diffusion of Al atoms in from opposite flat surfaces of the CdS slice at x = 0	$m^2 s^{-1}$
D_f	Pre-exponential factor in the general Arrhenius equation	$m^2 s^{-1}$
D_f'	Pre-exponential factor in the Arrhenius equation for the diffusion coefficient D_o'	$m^2\ s^{-1}$ at $\%^{-1}$
E	Activation energy	eV
E_F	Activation energy for the heat of solution for dissolving the trivalent metal atoms in CdS	eV

E_M	Activation energy for the migration of the mobile defect through the crystal lattice	eV
$E_{M_{\parallel}}, E_{M_{\perp}}$	Values of E_M for diffusions in directions parallel and perpendicular to the c-axis in a hexagonal crystal	eV
E_t	Experimentally determined activation energy which gives the combined value for the heat of solution for dissolving the trivalent metal atoms and for the migration of the mobile defect through the crystal lattice	eV
$E_{t_{\parallel}}, E_{t_{\perp}}$	Values of E_t for diffusions in directions parallel and perpendicular to the c-axis in a hexagonal crystal	eV
e, p	Electrons and holes	
'erfc'	Complementary error function	
enc	Electro-neutrality condition	
F	Helmholtz free energy	eV $(atom)^{-1}$
H	Internal energy	eV $(atom)^{-1}$
J	Diffusion current	atoms $m^{-2}s^{-1}$
K	Equilibrium constant	
K_{CdS}	Equilibrium constant which relates the partial vapour pressure of Cd and S in the vapour with the solid	$(atm)^{3/2}$
k	Boltzmann's constant	eV T^{-1}
n	A power constant usually an integer that relates the diffusion coefficient with the concentration of the trivalent metal atoms ($D \alpha C^n$)	dimensionless
N	Mole fraction of atoms in solution	$(mole)^{-1}$
OM	Optical/microprobe	
P	Partial vapour pressure	atm
P'	Compound defect which is formed due to the pairing of V''_{Cd} and a trivalent metal atom $M^{\bullet}_{Cd}$ in the Cd sub-lattice to form $(M^{\bullet}_{Cd}\ V''_{Cd})'$	
$P^{\bullet}$	Compound defect which is formed due to the pairing of V^{*}_{Cd} and a trivalent metal atom $M^{\bullet}_{Cd}$ in the Cd sub-lattice to form $(M^{\bullet}_{Cd}\ V^{*}_{Cd})^{\bullet}$	
R_x	Normalised count rate of a section removed in a diffusion profile measurement using the radiotracer sectioning technique	kg^{-1}
RTS	Radiotracer sectioning	
S	Entropy of mixing	eV T^{-1} $(atom)^{-1}$
T	Absolute temperature	K
$T_{\frac{1}{2}}$	Half-life	s
t	Duration of the diffusion anneal	s

X	Depth of the diffusion front for the concentration dependent diffusion	m
$X_{\parallel}$, $X_{\perp}$	Values of X for diffusions in directions parallel and perpendicular to the c-axis in a hexagonal crystal	m
$X_{\parallel max}$, $X_{\parallel min}$	Values of X for the diffusion of Al atoms diffusing in from opposite flat surfaces of a CdS slice in a direction parallel to the c-axis	m
x, y, z	Cartesian coordinate axes	m
x, y, z	Atomic proportions of elements in a binary or ternary compound	
x	General variable used for representing the depth in a partially doped CdS slice in a direction perpendicular to the flat surface of the slice	m
δ	Power constant that relates electrical carrier concentration with partial vapour pressure (that is $[e'] \alpha P^{\delta}$)	dimensionless
γ	Activity coefficient	dimensionless
$[\ ]$	Concentration of species enclosed with brackets	species m^{-3}

The convention used in this thesis for expressing stoichiometric deviations is the same as the one used by Van Gool in his book on 'Principles of Defect Chemistry of Crystalline Solids', on page 75.

1. Introduction

The growth of semiconductor technology in the early 1950s highlighted the limitations of Ge and Si of which perhaps the character and magnitude of the forbidden energy gap were the most disadvantageous. The extension in the range of energy gaps was sought in the III-V and II-VI compounds and the latter possessed certain limited advantages over the other type of compounds in that CdS and CdSe are highly photoconducting and ZnS is strongly luminescent. The properties of the II-VI compounds have been reviewed by Aven and Prener (1), Ray (2), Thomas (3), Stevenson (4) and Moss et al (5).

In the broadest sense, II-VI compounds comprise compounds formed from the elements of group II and group VI of the periodic table, but in the semiconductor industry they include the chalcogenides of Cd, Hg and Zn. The majority of these semiconducting compounds take on one of two crystalline structures which are zinc blende and wurtzite, both of which are characterised by tetrahedral lattice sites. The most commonly used of these compounds have band gaps in the range 1.5 to 3.7 eV.

Some other important generalisations can be made on II-VI compounds. The larger band gap materials are expected to exhibit atomic disorder and there is a tendency for one carrier type to predominate. All of the II-VI compounds, except CdTe, are one carrier type in their pure state irrespective of stoichiometry and this carrier type is not readily changed by diffusion doping; only high resistivity crystals of the opposite carrier may be obtained. This behaviour has been explained by the tendency of crystals with larger band gaps to self-compensate electrically active impurities (6) and has limited the use of such materials for many device applications.

The application of II-VI compounds to photoconductivity, luminescence and acoustoelectric devices is reviewed extensively in the literature (2, 1). The manufacture of such devices from II-VI compounds usually involves the doping of these compounds with impurities which are diffused into the pure semiconductor material at high temperatures using precisely controlled conditions. The general pattern of impurity behaviour is that elements from groups III and VII and anion vacancies act as donors whereas elements of groups I and V and cation vacancies act as acceptors. The majority of diffusion coefficients for the diffusion of impurities in II-VI compounds have been calculated approximately from impurity doping experiments rather than from carrying out the diffusion experiments under controlled conditions.

The interpretation of diffusion studies for the diffusion of impurities in the II-VI compounds is somewhat limited because there is not sufficient information on the thermodynamics in the relevant ternary systems. One such example, which has been studied extensively, is the GaAs - Zn system (7); it shows how much work is necessary to interpret fully diffusion studies in the ternary compounds. In fact, there is very little published information on the diffusion of group III elements in II-VI compounds and this thesis will make a significant addition to the measurement of diffusion rates in these compounds. The basic theory on the stoichiometry, phase equilibria and the defect chemistry of semiconductor binary compounds is adequately described in the literature (8-11) and will not be reproduced in this thesis.

The project described in this thesis is a continuation of the measurement of the self-diffusion of Cd into CdS which commenced in 1968 and was carried out in collaboration with the former

Associated Electrical Industries Research Laboratories, Rugby. This collaboration was later continued in conjunction with The General Electric Company Limited, The Hirst Research Centre, Wembley, when the development work on CdS was transferred from Rugby to Wembley. The collaboration was later extended to include the study of the diffusion of In into CdS. These metals were used to make electrical contacts to CdS devices.

Unfortunately, development work on CdS was terminated in 1972 but as sufficiently interesting results were obtained it was felt worthwhile continuing with the project and in fact the project was extended to include the study of the diffusion of other group III elements in CdS. This thesis reports on the measurements of the diffusion of Al, Ga and In into CdS using a radiotracer sectioning (abbreviated to RTS in this thesis) technique and an optical/microprobe (abbreviated to OM) technique which is a combination of the uses of an optical microscope and an electron microprobe analyser.

In fact, the experimental conditions described in this thesis for the diffusion of In into CdS were requested by the Industrial collaborator as these conditions were similar to the ones that were being used in the fabrication of the semiconductor devices. These conditions may not have necessarily been the ones that one would have chosen if the project was devoted solely to determining the defect structure involved in the diffusion of In into CdS. The diffusion of In was the major part of the project and for the purposes of consistency it was decided to use similar conditions with the Ga and Al diffusions which were studied to a lesser extent.

The results obtained for the self-diffusion of Cd in CdS are described in the author's M.Sc. thesis (12) and for completeness the results are reviewed briefly in appendix A1. Further work has been carried out on the properties of the radioactive Cd metal

since the author's M.Sc. thesis was published. This later work is also given in detail in appendix A1.

A review of the literature on diffusion studies into II-VI compounds and in particular into CdS is given in chapter 2. The concentration profiles of certain diffusion processes do not obey the mathematical solutions to Fick's second law where the diffusion coefficient D is assumed to be constant. In these cases more complex solutions, which are reviewed by such authors as Crank (13) and Carslaw and Jaeger (14), have to be used. One such set of solutions described by Crank and by Weisberg and Blanc (15), where the diffusion coefficient is proportional to the spatial concentration of the diffusing impurity (that is $D \alpha C^n$ where n = 1, 2 or 3), is discussed in chapter 2.

A review of all the available methods, which can be used for measuring diffusion rates, is given by Boltaks (16) and Yeh (17). The experimental procedures used by the author in this project are described in chapter 3. The experimental results obtained in the diffusion of In into CdS, which was studied in great detail, are presented in chapters 4 to 8 inclusive. The results obtained using the RTS technique and the CM technique are described in chapters 5 and 6 respectively and the changes that took place in the physical properties of the CdS during the diffusion anneals are discussed in chapter 4. The diffusion mechanism and a tentative identification of the mobile defect are considered in chapter 7.

In the diffusion anneals described in this thesis the CdS and the In metal were sealed in evacuated silica ampoules. The relative amounts of In and CdS placed in the ampoules remained reasonably constant (±30%) for the diffusion measurements, which were obtained using

the RTS technique and the OM technique, but the proportions were different for the two techniques. As each diffusion proceeded the metal globule, which started off as pure In, soon became a dilute Cd/In alloy due to the loss of Cd from the surface of the CdS slice. The different proportions of materials placed in the ampoules in the two sets of measurements, were expressed in terms of the ratio of the concentration of Cd and In atoms in the metal globule at the end of the diffusion anneal and was designated the final Cd/In ratio. Different near-surface In concentrations were obtained in the CdS slices in the two sets of measurements. A third set of measurements was also carried out in which Cd metal was sealed in the ampoule along with the In metal and the RTS technique was used to measure the diffusions. The effect of the variation in the final Cd/In ratio on the diffusion coefficient in the three sets of measurements is discussed in chapter 8.

The results on the diffusion of Ga and Al into CdS are presented and discussed in chapters 9 and 10 respectively. The results are presented in this order because the work on In has been investigated fully and conclusive results have been obtained. The Ga diffusions were complicated by the formation of an outer chemical reaction layer and also by a departure from the $D \propto C$ relationship at high Ga concentrations in the diffusions which were carried out at low temperatures; consequently the Ga diffusions were not studied as comprehensively as the In diffusions. The Al proved to be so chemically reactive that only a limited amount of information was obtained. The results obtained on the diffusion of the three elements are compared and discussed in the conclusions in chapter 11.

In the tabulations presented in this thesis a procedure, which is in common practice in computer usage, has been adopted for

presenting the large and small numbers that are obtained in diffusion studies. That is, when a power of ten is used (for example 3.70×10^{-16}), the ten has been omitted and all the figures have been presented at the same level (for example 3.70, -16). This makes typing of the tables much easier. This practice has not been adopted in the main text of the thesis.

1.1 References

1. Physics and Chemistry of II-VI Compounds (Edited by M. Aven and J. S. Prener), North Holland Publishing Company, Amsterdam (1967).
2. B. RAY, II-VI Compounds, Pergamon Press Limited, Oxford (1969).
3. II-VI Semiconducting Compounds (International conference held at Brown University, Providence, Rhode Island, U.S.A., held on September 6, 7, 8, 1967, edited by D. G. Thomas), W. A. Benjamin Inc., New York (1967).
4. D. A. STEVENSON, Atomic Diffusion in Semiconductors (Edited by D. Shaw), P432, Plenum Press, London (1973).
5. T. S. MOSS, G. J. BURRELL and B. ELLIS, Semiconductor Opto-electronics, Butterworth and Company Limited, London (1973).
6. G. MANDEL, Phys. Rev., 134, A1073 (1963).
7. H. C. CASEY Jr., Atomic Diffusion in Semiconductors (Edited by D. Shaw), P351, Plenum Press, London (1973).
8. R. A. SWALIN, Thermodynamics of Solids, John Wiley and Sons Inc., New York (1972).
9. W. VAN GOOL, Principles of Defect Chemistry of Crystalline Solids, Academic Press (1966).
10. Solid State Chemistry and Physics (Edited by P. F. Weller), Marcel Dekker Inc., New York (1974).
11. F. A. KRÖGER, The Chemistry of Imperfect Crystals, North Holland Publishing Company, Amsterdam (1964).

12. E. D. JONES, Measurement of the Self-Diffusion of Cd into CdS using Radiotracer Sectioning Techniques, M.Sc. Thesis, University of Warwick (1971).

13. J. CRANK, The Mathematics of Diffusion Oxford University Press, London (1970).

14. H. S. CARSLAW and J. C. JAEGER, Conduction of Heat in Solids, Oxford University Press (1959).

15. L.R. WEISBERG and J. BLANC, Phys. Rev., 131, 4, P1548 (1963).

16. B. C. BOLTAKS, Diffusion in Semiconductors (Translated by J. I. Carasso, edited by H. J. Goldsmid), Infosearch Limited, London (1963).

17. T. H.YEH, Atomic Diffusion in Semiconductors (Edited by D. Shaw), P155, Plenum Press, London (1973).

2. Diffusion in II-VI compounds

Diffusion in II-VI compounds is often anomalous, that is concentration dependent and native defect dependent, and interactions between impurity atoms and the native defects take place readily in these compounds. As the elements of II-VI compounds often have high vapour pressures, the majority of diffusion anneals are carried out in a closed system. As a result, the concentration of defects is strongly dependent on the partial vapour pressure of the component elements and this in turn is dependent on the temperature of the diffusion and on the physical conditions used. This is because the partial vapour pressure of the major constituents will determine the concentration of native defects at that temperature. In addition, the presence of several per cent of dissolved impurities of a different valency in the diffusion crystal can also affect the defect concentration. The diffusion rates in these compounds are consequently not only governed by the temperature of the diffusion but also by the partial vapour pressure of the components and the foreign atom concentration.

The dependence of the diffusion coefficient on various interdependent parameters is responsible for the poor reproducability of the data and, giving significance to the systematic classification, involves not only careful control of experimental conditions but also a scrupulous characterisation of the sample material. Ascoli (1) reports that comparing previous data on II-VI compounds with his, which refers to the three years prior to the publication of his paper, an intensification of research had become evident probably because improved techniques for the precise characterisation of materials have begun to reduce the scatter of results. Sets of independent results are piling up on the self-diffusion and

diffusion of noble metals in II-VI compounds and more complex defects are being used to explain the diffusion process in these materials.

Diffusion in II-VI compounds has been reviewed by Ascoli (1), Stevenson (2) and Sharma (3). This thesis is concerned with the diffusion of group III elements into CdS and the review of diffusion measurements given in this chapter will be confined mainly to the self-diffusion in high purity and In-doped CdS and to the diffusion of group III elements into CdS. In addition, the results of similar measurements, which have been carried out in other II-VI compounds, are included if the results obtained are relevant to this thesis. For the self-diffusion measurements a systematic pattern of diffusion has been established but this is certainly not the case for impurity diffusion.

The majority of the II-VI compounds crystallize either with the cubic zinc blende structure (sphalerite) or with the hexagonal wurtzite structure. It is possible for CdS to exist in both forms but crystals possessing the hexagonal structure were used in this investigation. Cubic CdS samples heated above 673 K change from the cubic form to the hexagonal form (4) so that the hexagonal type is the only form that is stable above this temperature. The diffusion coefficient can be regarded as a second rank tensor (5,6) and for a hexagonal lattice two independent diagonal elements are required: one for diffusion perpendicular to the basal plane and one for diffusion (isotropic) in the basal plane.

2.1 Phase diagrams and stoichiometry of II-VI compounds

In contrast to their constituent elements the II-VI compounds have high melting points and relatively low vapour pressures.

Shiozawa and Jost (7) have compiled phase diagrams of the Zn and Cd chalcogenides from data that was already available in the literature. For some of the systems only the congruent melting points of the compounds have been reported and estimates of the complete diagrams have been made based on relationships with the known diagrams of the other II-VI systems. The phase diagram for the Cd - S system is shown in figure 2.1a.

Shiozawa and Jost have also compiled relationships expressing the temperature dependence of the equilibrium constant K_{MX}, which relates the partial pressures of the metal and the diatomic species of the nonmental in the gas in equilibrium with the solid. The equilbrium constant for CdS is given by

$$\log K_{CdS} = \frac{-17.029}{T} + 10.302 \qquad 2.1$$

where:

K_{CdS} is expressed in $(atm)^{3/2}$;

T is the absolute temperature.

At each temperature II-VI crystals have a definite maximum range of deviation from the stoichiometric composition. This composition range, the solid stability field, arises from the presence of native defects which are electrically active. Therefore, in order to explain and control the electronic properties of these crystals adequately, an understanding of the relationships that control these deviations is required. For a two component system the temperature and the equilibrium pressure of one of the elemental components is sufficient to define the equilibrium state of the system and, therefore, the composition of the crystal. Precipitation techniques (8) have proved to be the most reliable and direct method of investigating

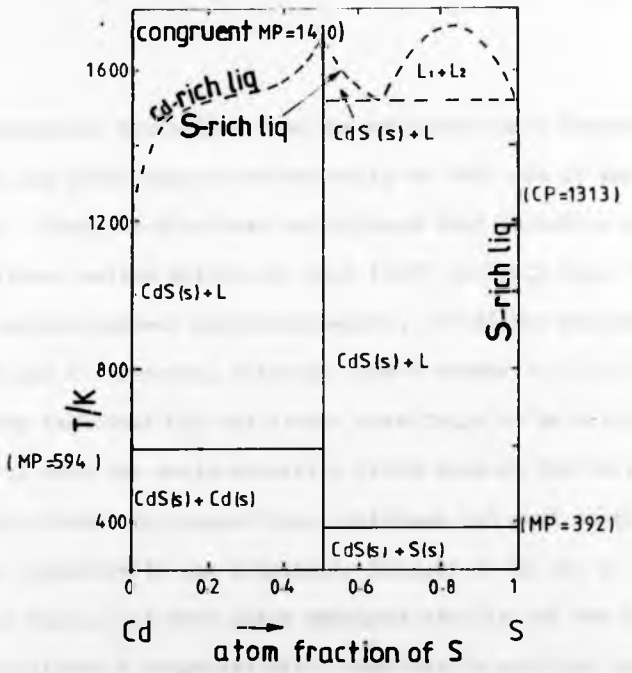

Fig 2·1a PHASE DIAGRAM OF THE Cd–S SYSTEM (FROM SHIOZAWA AND JOST (7))

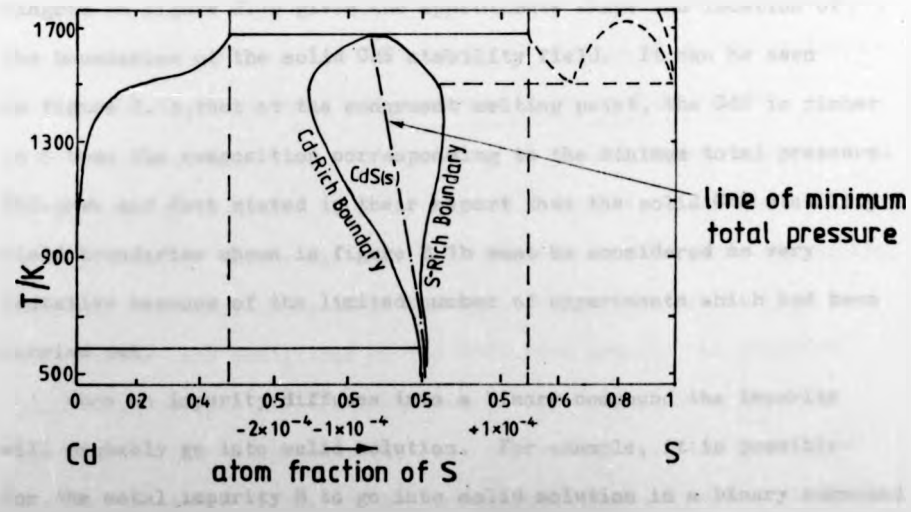

Fig2·1b PHASE DIAGRAM OF THE Cd-S SYSTEM SHOWING THE TENTATIVE SOLID CdS STABILITY FIELD ON AN EXPANDED SCALE
(FROM SHIOZAWA AND JOST (7))

Figs 2·1a,2·1b

the problem of deviations from the stoichiometric compositions. This method was first applied successfully to ZnTe and it was then extended to CdS. These studies have established that vacancies are the only significant native defects in pure II-VI crystals under the conditions used in their growth and consequently, in CdS, the dominant defects are the Cd and S vacancies, although the S vacancies usually predominate.

The fact that CdS has always been found to be n-type or insulating suggests that the solid stability field lies on the Cd-rich side of the stoichiometric composition. Shiozawa and Jost stated that the n-type conductivity was originally thought to be due to a shallow foreign donor, but they later proposed that it was due to the residual unprecipitated S vacancies which remained in solution during the controlled cooling of the CdS crystals. They also observed that precipitation occurs in crystals which were treated under high S pressures. This indicated that the solid stability field also extends into the S-rich side of the stoichiometric composition. The phase diagram in figure 2.1b gives the approximate shape and location of the boundaries of the solid CdS stability field. It can be seen in figure 2.1b, that at the congruent melting point, the CdS is richer in S than the composition corresponding to the minimum total pressure. Shiozawa and Jost stated in their report that the solid CdS stability field boundaries shown in figure 2.1b must be considered as very tentative because of the limited number of experiments which had been carried out.

When an impurity diffuses into a binary compound the impurity will probably go into solid solution. For example, it is possible for the metal impurity B to go into solid solution in a binary compound AC to form $A_x B_y C$ where the elements A and B are completely soluble

on the cation lattice for all values of x and y. It is also possible that intermediate compounds will form at fixed values of x and y. Compounds $Cd_{1-x}Zn_xSe$ (9) and $GaAs_{1-x}P_x$ (10) are examples of the former type and $CdGa_2S_4$ which was formed in the Ga diffusions described in chapter 9, and $CdIn_2S_4$ are examples of the latter (11-13). $CdIn_2S_4$ possesses a spinel structure. A typical example of a spinel is $MgAl_2O_4$ which is an intermediate compound on the MgO - Al_2O_3 phase diagram (14), and it has marked non-stoichiometric deviations on the trivalent metal side of the true stoichiometric composition.

It is only possible to construct hypothetical ternary phase diagrams from the known binary phase diagrams and known thermodynamic data. An attempt has been made at constructing an isothermal section of the CdS-In ternary system at a temperature of approximately 1200 K and the solid single phase regions only are shown in figure 2.2a. The binary compounds CdS and In_2S_3 and the ternary compound $CdIn_2S_4$ are shown on the diagram. The pseudo-binary diagram of the CdS-In_2S_3 system shown in figure 2.2b is a vertical section along the stoichiometric plane through the Cd-In-S system shown in figure 2.2a.

The deviation from stoichiometry of pure CdS, due to changes in Cd or S_2 partial pressures, is less than 10^{-3} but it is important to point out at this stage that the corresponding In or Ga solubility can take any value up to 10%. The exact value depends on the temperature and conditions of the diffusion anneal. An expanded isothermal section through the solid CdS stability field is shown in figure 2.2c. This means that the deviation from the S to metal one to one atomic ratio, in the experimental conditions described in this thesis, is completely dominated by the trivalent atom concentrations. As this thesis is concerned only with diffusions into

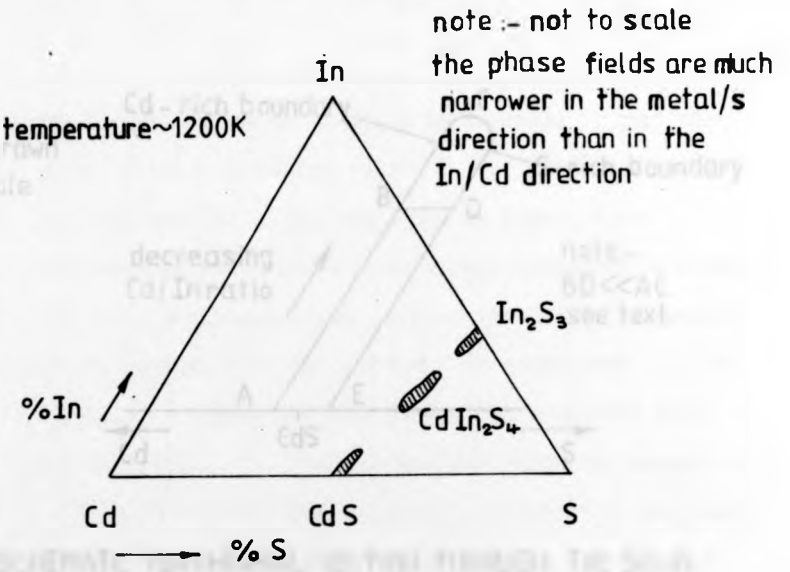

FIG 2.2a AN ISOTHERMAL SECTION THROUGH THE Cd-In-S PHASE DIAGRAM SHOWING SOLID SINGLE PHASE FIELDS ONLY

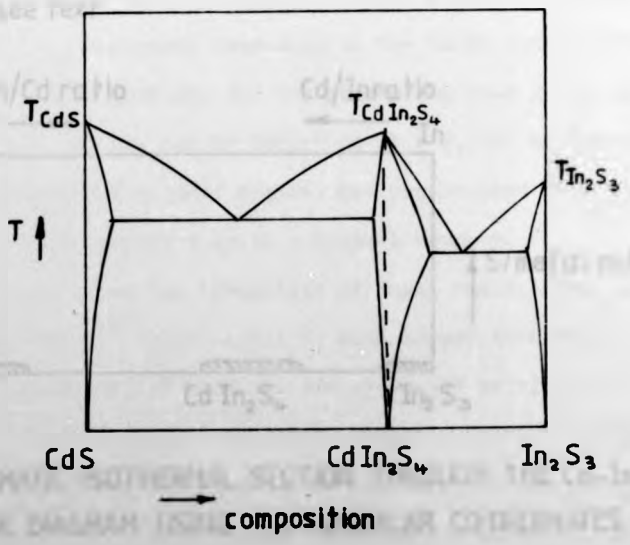

FIG 2.2b A SIMPLE PHASE DIAGRAM FOR THE CdS- In_2S_3 SYSTEM

FIGS 2.2a, 2.2b

CdS in vapours containing excess metal, it is feasible to omit that part of the phase diagram involving excess S and to draw rectangular isothermal sections similar to the one shown in figure 2.2d.

It is customary in the literature of binary compounds to represent departures from true stoichiometry by quoting the partial pressures of the vapours in contact with the crystal. If comparisons are to be made with previously published work then it is essential that these pressures are known. In this project the diffusion anneals were carried out in closed ampoules and it proved convenient to use atomic ratios as shown in figure 2.2d (see chapter 8).

It will be seen later in sections 2.4 and 2.5 that extensive Cd and S self-diffusion studies have been carried out into pure and In-doped CdS under varying Cd and S pressure conditions. Such conditions are represented respectively by line AE and a line parallel to AE, of which BD is one example, as is shown in figure 2.2c. The diffusions described in this thesis are under excess metal vapours and the composition of the CdS crystal surface will be along the side ABC in figure 2.2c, the point depending on the Cd/In ratio in the metal globule. It is possible for the conditions used in the self diffusion studies carried out by Kröger et al (15, 16) to coincide with the work described in this thesis when represented on a phase diagram. Point B in figure 2.2c is a typical example.

It can be seen from the tabulation of ionic radii, given in table 2.1, that the S^{2-} ionic radius is much larger than the corresponding values of Cd^{2+} and all the group III metal ions. Consequently the S^{2-} ions will be fairly immobile relative to the ions on the cation sub-lattice, but this does not rule out the possibility of S^{2-} ions switching to a more mobile charge state for diffusion. In fact S diffusion in CdS can occur by a neutral interstitial (table 2.2).

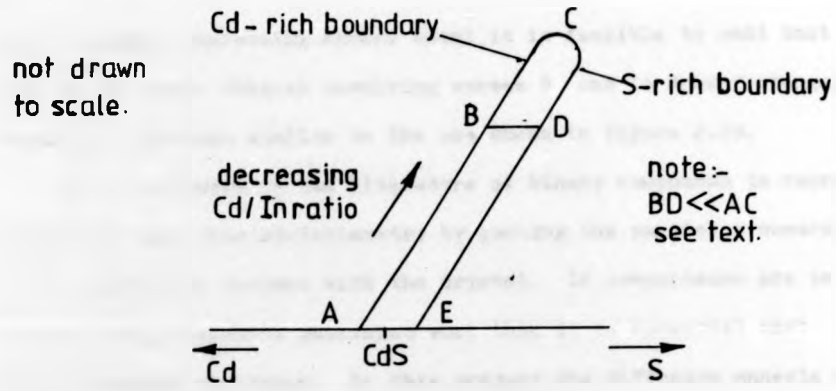

FIG 2.2c SCHEMATIC ISOTHERMAL SECTION THROUGH THE SOLID CdS STABILITY FIELD ON AN EXPANDED SCALE.

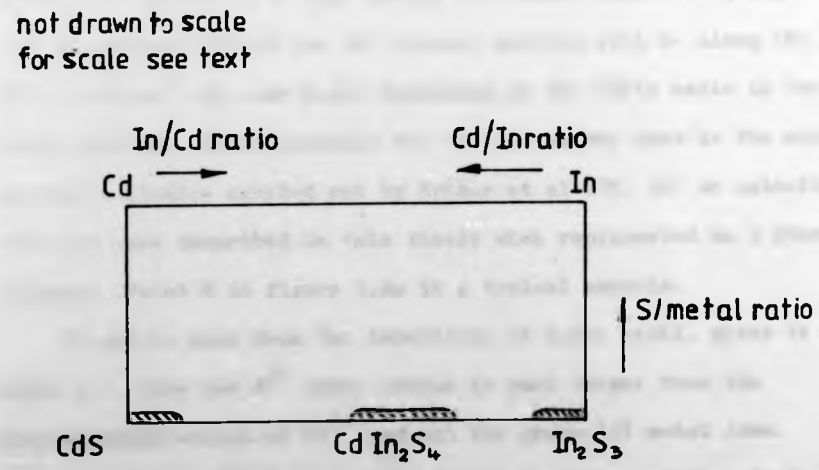

FIG 2.2d SCHEMATIC ISOTHERMAL SECTION THROUGH THE Cd-In-In_2S_3-CdS PHASE DIAGRAM USING RECTANGULAR CO-ORDINATES.

FIGS 2.2c 2.2d

CdS in vapours containing excess metal, it is feasible to omit that part of the phase diagram involving excess S and to draw rectangular isothermal sections similar to the one shown in figure 2.2d.

It is customary in the literature of binary compounds to represent departures from true stoichiometry by quoting the partial pressures of the vapours in contact with the crystal. If comparisons are to be made with previously published work then it is essential that these pressures are known. In this project the diffusion anneals were carried out in closed ampoules and it proved convenient to use atomic ratios as shown in figure 2.2d (see chapter 8).

It will be seen later in sections 2.4 and 2.5 that extensive Cd and S self-diffusion studies have been carried out into pure and In-doped CdS under varying Cd and S pressure conditions. Such conditions are represented respectively by line AE and a line parallel to AE, of which BD is one example, as is shown in figure 2.2c. The diffusions described in this thesis are under excess metal vapours and the composition of the CdS crystal surface will be along the side ABC in figure 2.2c, the point depending on the Cd/In ratio in the metal globule. It is possible for the conditions used in the self diffusion studies carried out by Kröger et al (15, 16) to coincide with the work described in this thesis when represented on a phase diagram. Point B in figure 2.2c is a typical example.

It can be seen from the tabulation of ionic radii, given in table 2.1, that the S^{2-} ionic radius is much larger than the corresponding values of Cd^{2+} and all the group III metal ions. Consequently the S^{2-} ions will be fairly immobile relative to the ions on the cation sub-lattice, but this does not rule out the possibility of S^{2-} ions switching to a more mobile charge state for diffusion. In fact S diffusion in CdS can occur by a neutral interstitial (table 2.2).

TABLE 2.1: TABULATION OF IONIC RADII

Ion	Atomic number	Radius nm
Al^{3+}	13	0.051
S^{2-}	16	0.184
Ga^{3+}	31	0.062
Cd^{2+}	48	0.097
In^{3+}	49	0.081
Tl^{3+}	81	0.095

2.2 Defects in crystals

In a crystalline solid diffusion takes place with the aid of defects which are inherent in the thermodynamics of the crystal (17-19) and also with the aid of non-equilibrium defects. In addition, charge neutrality must be maintained at all times. In an elemental crystal such defects are interstitials and vacancies whereas in an ionic crystal the defects, which aid diffusion on either sub-lattice, are Schottky and Frenkel pairs. A semiconductor crystal will also contain electrons and holes.

In reality, a perfect crystal does not exist as it will contain additional defects such as crystal surfaces, isotopes of various masses, impurities, dislocations and stacking faults.

When an impurity diffuses into a crystal the impurity atoms are incorporated in the host crystal either interstitially or substitutionally. The impurity atoms can also be incorporated in a neutral state or they can become charged, either by donating or acquiring one or more electrons. In an ionic compound charge neutrality can be maintained by an exchange of the impurity atoms with the host atoms in the appropriate ratio - for example two Na^+ ions leaving the NaCl crystal for every Cd^{2+} ion which is incorporated onto the cation lattice. In a semiconductor the impurity atoms can be incorporated onto the crystal lattice and charge neutrality is maintained by the production of atomic defects of opposite polarity or possibly by the production of electrons or holes.

There is an analogy between the solution of a defect in a crystal and a conventional dilute solution of one material in another. When the defect in question is a foreign atom, the distinction disappears altogether; the combination of defect and crystal is a

solid solution in the conventional sense. The formation of any defect in a crystal must involve a change in enthalpy and entropy of the crystal and a free energy of formation can therefore be assigned to the defect. The defects are then subject to the laws of chemical thermodynamics. A chemical potential function can be assigned, for example, to vacancies and, within certain limits, the law of mass action can be used when quasichemical reactions take place between defects. This provides a useful technique for analysing defect interactions in solids.

Because of the presence of electrons and holes and the fact that many atomic defects carry a charge, interactions between charged defects are especially important. They can be divided into two main types. In the first, complexing takes place between defects of opposite sign by the simple mechanism of coulombic attraction. The second type, which is more important in semiconductors, is the way in which the density of electrons and holes is influenced by the concentration of donors and acceptors.

In the diffusion of divalent impurites in alkali halides, Cd^{2+} in NaCl for example, Lidiard (20) assumed that the Cd diffused as a neutral complex $(Cd^{\bullet}_{Na}\ V'_{Na})^{*}$ on the cation sub-lattice. This type of diffusion has also been described in detail for an ionic crystal by several other workers including Wagner (21), who found that the diffusion coefficient was linearly proportional to the concentration of the diffusing impurity, and also by Beniere et al (22). Lidiard's theory had not been applied or tested for compounds with more covalent bonding and predominant electronic conduction until Perkins and Rapp (23) investigated the diffusion Cr in NiO. They obtained a reasonable fit of Lidiard's theory to the experimental concentration dependent Cr diffusion which indicated that, at 1273 K and above, Cr diffuses

in NiO by a mechanism involving Cr-cation vacancy two member complexes of the form $(Cr_{Ni}^{\cdot} V_{Ni}^{''})^{'}$. Charge neutrality was maintained on the cation lattice by three Ni^{2+} ions leaving the crystal for every two Cr^{3+} ions that entered the crystal. This resulted in the formation of the cation vacancy $V_{Ni}^{''}$ for every two Cr^{2+} ions that entered the crystal.

Sharma (3) reports that rapid changes have been observed in the electrical and optical properties in II-VI compounds with alternate firings in chalcogen and metal vapours. It is evident that crystalline point defects both intrinsic and extrinsic, play a dominant role and attempts have been made by several people to establish what defects are involved. Stevenson (2) has reviewed the defect structure involved in the self-diffusion studies in these compounds generally and additional contributions have been made to the self-diffusion studies in CdS by Sysoev et al (24), Hershman and Kröger (25), Hershman, Zlomanov and Kröger (16) but the most detailed contribution is by Kumar and Kröger (15). These will be reviewed in later sections. There is little information available on the diffusion of impurities, particularly those from group III, in these compounds.

2.3 Diffusion

Diffusion into crystalline materials can be studied from two separate aspects. The first is to treat the solid as a continuous medium and then the diffusion equations due to Fick can be set up. If the boundary conditions of the problem are known then the diffusion equation can be solved. The second is based on the atomic structure of a solid and diffusion occurs by atoms jumping from one site to another.

The basic diffusion equation which is given by Fick's second

law is

$$\frac{\partial C}{\partial t} = - \nabla J = + \nabla (D \nabla C) \qquad 2.2$$

where:

J is the diffusion current which has dimensions (atoms) $(\text{area})^{-1}\ (\text{time})^{-1}$;

D is the diffusion coefficient which has dimensions $(\text{area})\ (\text{time})^{-1}$;

C is the concentration of the diffusion species which has dimensions $(\text{atoms})\ (\text{volume})^{-1}$.

For diffusion in one dimension this becomes

$$\frac{\partial C}{\partial t} = \frac{\partial}{\partial x} \left(D \frac{\partial C}{\partial x} \right) \qquad 2.3$$

The majority of the mathematical solutions of the equation assume that D is constant at any given temperature. Solutions to the above equation both for a constant D and a variable D are given by Crank (26) and by Carslaw and Jaeger (27). Two of the most common solutions with a constant D are reviewed in the author's M.Sc. thesis (28); these are the thin film solution (limited source) and the semi-infinite source solution.

If D is not constant then the type of dependency that the coefficient does possess must be established, but solutions of the diffusion equation with a variable D are usually complex. One such example is where D varies as the first, second or third power of the concentration of a diffusing impurity (that is $D \propto C^n$ where n = 1, 2 or 3). Weisberg and Blanc (29) have published results for these three cases for a constant surface impurity concentration and a semi-infinite medium. The solutions are plotted in figure 2.3 along with

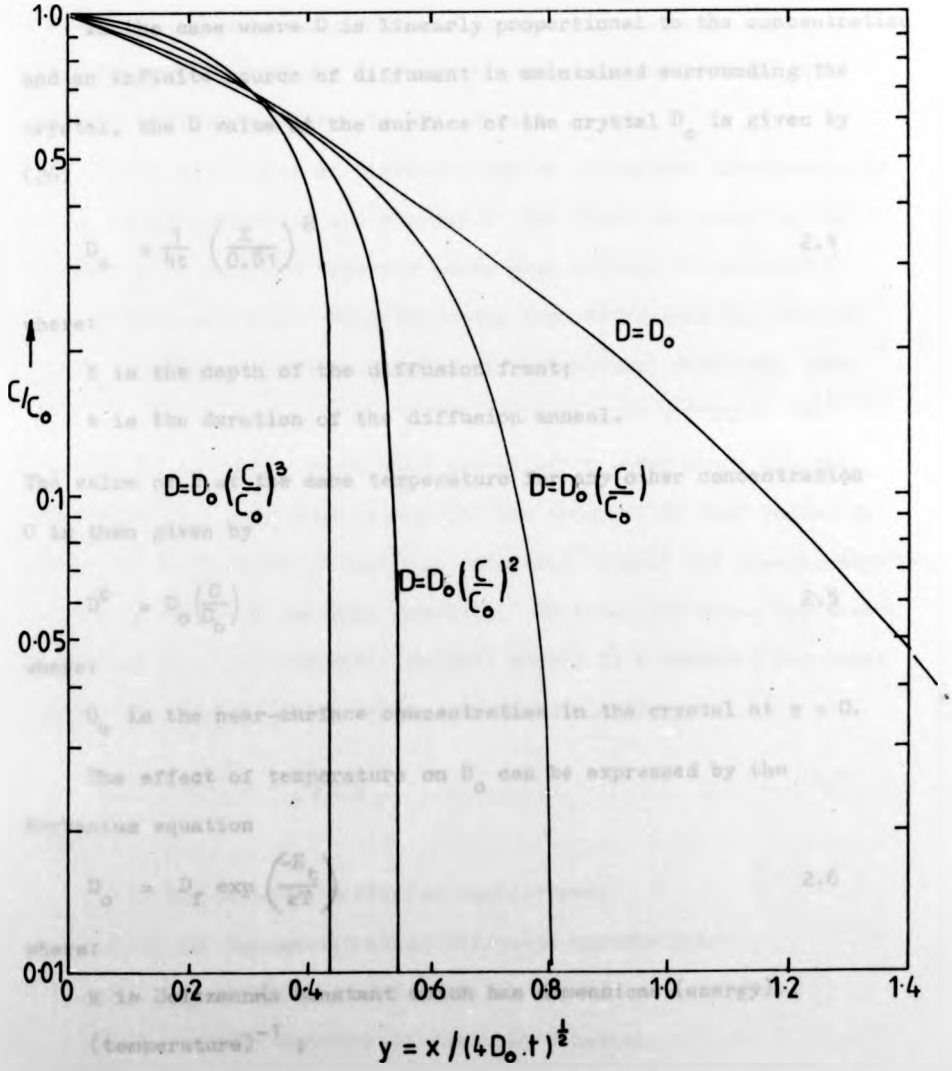

SOLUTIONS TO THE DIFFUSION EQUATION FOR A CONCENTRATION DEPENDENT DIFFUSION OF THE FORM $D \propto C^n$ (29)

FIG 2·3

the solution for an invariant D. Such solutions have been used by Cunnell and Gooch (30) and by Tuck and Kadhim (31) in their analysis of the diffusion of Zn into GaAs where diffusion is assumed to take place by a substitutional - interstitial mechanism.

In the case where D is linearly proportional to the concentration and an infinite source of diffusant is maintained surrounding the crystal, the D value at the surface of the crystal D_o is given by (26)

$$D_o = \frac{1}{4t}\left(\frac{X}{0.81}\right)^2 \qquad 2.4$$

where:

X is the depth of the diffusion front;

t is the duration of the diffusion anneal.

The value of D at the same temperature for any other concentration C is then given by

$$D^C = D_o\left(\frac{C}{C_o}\right) \qquad 2.5$$

where:

C_o is the near-surface concentration in the crystal at x = 0.

The effect of temperature on D_o can be expressed by the Arrhenius equation

$$D_o = D_f \exp\left(\frac{-E_t}{kT}\right) \qquad 2.6$$

where:

k is Boltzmann's constant which has dimensions (energy) (temperature)$^{-1}$;

E_t is the activation energy for the diffusion mechanism which will be expressed in electron volts in this thesis;

T is the absolute temperature;

D_f is the pre-exponential diffusion factor which has

dimensions $(\text{length})^2\ (\text{time})^{-1}$.

As the diffusion anneals described in this thesis were carried out at a constant temperature and with a virtually constant vapour pressure in the ampoule, it would be more appropriate to use the term activation enthalpy in preference to activation energy. As it is more conventional in the literature to use the latter term this procedure will be adopted in this thesis.

Three main types of diffusion can be recognised experimentally: self, isoconcentration and chemical. The first two refer to the diffusion of host and impurity atoms respectively in chemically homogeneous crystals. Experimentally such diffusions can only be followed using an isotope, stable or radioactive, differing from that in the crystal matrix. In isoconcentration diffusion the crystal is uniformly doped with the impurity under study and the diffusion of a different isotope of the impurity is then followed. There is no gradient of chemical potential in self and isoconcentration diffusion, only an isotopic gradient. Chemical diffusion (or inter-diffusion as it is sometimes called) occurs in a chemical potential gradient and it is given by the relationship (5)

$$D = D^* \left(1 + \frac{d \ell n\ \gamma}{d \ell n\ N}\right) \qquad 2.7$$

where:

D is the chemical diffusion coefficient;

D^* is the isoconcentration diffusion coefficient;

γ is the activity coefficient of the diffusing impurity;

N is the mole fraction of atoms in solution.

For the experiments described in this thesis the quantity $\frac{d \ell n\ \gamma}{d \ell n\ N}$ is significant but its magnitude is not known.

2.4 Self-diffusion into high purity CdS

The self-diffusion of Cd into CdS was first investigated extensively by Woodbury (32) where the diffusion profiles were obtained using a RTS technique. The work carried out by the author of this thesis on the self-diffusion of Cd into CdS, which was submitted to the University of Warwick for an M.Sc. degree, is reviewed in appendix A1.

Shaw and Whelan (33) studied both the dependence of D^{*}_{Cd} in CdS on component partial pressure at 1123 K and the electrical conductivity as a function of Cd-partial pressure P_{Cd}, in the temperature range 933 - 1223 K, using the same samples. Diffusion was studied parallel to the c-axis and the diffusion profiles invariably indicated two distinct regions corresponding to a fast and slow diffusion process which the authors interpreted as dislocation and bulk diffusions respectively. Only the slow component was considered by Shaw and Whelan in the treatment of their data and a significant increase in the D^{*}_{Cd} with P_{Cd} was observed - roughly a factor of 250 over the entire phase field. Three distinct regions were apparent: S-saturation and Cd-saturation with $D^{*}_{Cd} \propto P_{Cd}$ and an intermediate region with D^{*}_{Cd} independent of P_{Cd} (table 2.2).

The measurement of the electrical conductivity as a function of P_{Cd} gave a series of carrier density isotherms in which the pressure dependence of $[e']$ could be expressed as $[e'] \propto P_{Cd}^{\delta}$. The parameter δ took on values ranging from 0.38 at the highest temperature to 0.05 at the lowest temperature. The data at the highest temperature are consistent with a $Cd_i^{\bullet\bullet}$ or $V_S^{\bullet\bullet}$ defect but the decrease in δ with falling temperature indicated the influence of an impurity defect. At a diffusion temperature of 1123 K, Shaw and Whelan assumed a model involving singly and doubly ionised Cd interstitials and vacancies

2.4 Self-diffusion into high purity CdS

The self-diffusion of Cd into CdS was first investigated extensively by Woodbury (32) where the diffusion profiles were obtained using a RTS technique. The work carried out by the author of this thesis on the self-diffusion of Cd into CdS, which was submitted to the University of Warwick for an M.Sc. degree, is reviewed in appendix A1.

Shaw and Whelan (33) studied both the dependence of D^*_{Cd} in CdS on component partial pressure at 1123 K and the electrical conductivity as a function of Cd-partial pressure P_{Cd}, in the temperature range 933 - 1223 K, using the same samples. Diffusion was studied parallel to the c-axis and the diffusion profiles invariably indicated two distinct regions corresponding to a fast and slow diffusion process which the authors interpreted as dislocation and bulk diffusions respectively. Only the slow component was considered by Shaw and Whelan in the treatment of their data and a significant increase in the D^*_{Cd} with P_{Cd} was observed - roughly a factor of 250 over the entire phase field. Three distinct regions were apparent: S-saturation and Cd-saturation with $D^*_{Cd} \propto P_{Cd}$ and an intermediate region with D^*_{Cd} independent of P_{Cd} (table 2.2).

The measurement of the electrical conductivity as a function of P_{Cd} gave a series of carrier density isotherms in which the pressure dependence of $[e']$ could be expressed as $[e'] \propto P_{Cd}^{\delta}$. The parameter δ took on values ranging from 0.38 at the highest temperature to 0.05 at the lowest temperature. The data at the highest temperature are consistent with a $Cd_i^{\bullet\bullet}$ or $V_S^{\bullet\bullet}$ defect but the decrease in δ with falling temperature indicated the influence of an impurity defect. At a diffusion temperature of 1123 K, Shaw and Whelan assumed a model involving singly and doubly ionised Cd interstitials and vacancies

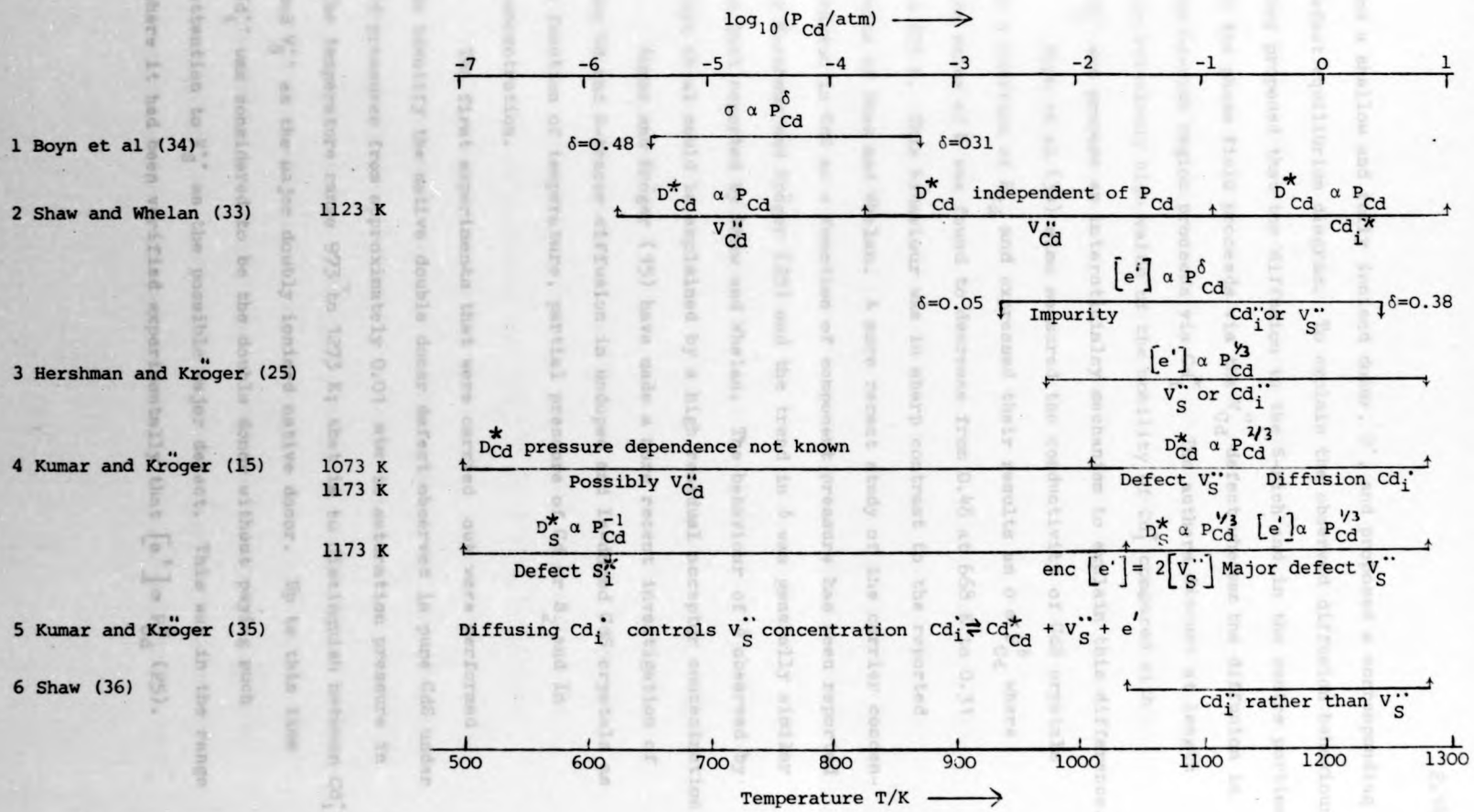

Table 2.2 Summary of the proposed defect structure models for self-diffusion measurements into high purity CdS

and a shallow and fully ionised donor, $D^{\cdot}$, and proposed a corresponding defect equilibrium diagram. To explain the observed diffusion behaviour they proposed that the diffusion in the S-rich and in the centre portion of the phase field proceeds via the V''_{Cd} defect whereas the diffusion in the Cd-rich region proceeds via Cd_i^{*}. The authors discuss at length the relatively high value of the mobility of Cd_i^{*} compared with $Cd_i^{\cdot\cdot}$ and propose an intersticialcy mechanism to explain this difference.

Boyn et al (34) also measured the conductivity of CdS crystals as a function of P_{Cd} and expressed their results as $\sigma \propto P_{Cd}^{\delta}$ where the value of δ was found to decrease from 0.48 at 668 K to 0.31 at 873 K. This behaviour was in sharp contrast to the reported value of Shaw and Whelan. A more recent study of the carrier concentration in CdS as a function of component pressure has been reported by Hershman and Kröger (25) and the trend in δ was generally similar to that reported by Shaw and Whelan. The behaviour of δ observed by Boyn et al could be explained by a high residual acceptor concentration.

Kumar and Kröger (15) have made a more recent investigation of the Cd and S-tracer diffusion in undoped and In-doped CdS crystals as a function of temperature, partial pressure of Cd or S_2 and In concentration.

The first experiments that were carried out were performed to identify the native double donor defect observed in pure CdS under Cd pressures from approximately 0.01 atm to saturation pressure in the temperature range 973 to 1273 K; that is to distinguish between $Cd_i^{\cdot\cdot}$ and $V_S^{\cdot\cdot}$ as the major doubly ionised native donor. Up to this time $Cd_i^{\cdot\cdot}$ was considered to be the double donor without paying much attention to $V_S^{\cdot\cdot}$ as the possible major defect. This was in the range where it had been verified experimentally that $[e'] \propto P_{Cd}^{\frac{1}{3}}$ (25).

Results of the Cd-tracer diffusion in pure crystals for the 1073 K and 1173 K isotherms showed that $D^*_{Cd} \propto P^{\frac{2}{3}}_{Cd}$. The absolute values of D^*_{Cd} reported by Shaw and Whelan, which show that $D^*_{Cd} \propto P_{Cd}$, are in agreement with the results of Kumar and Kröger. Kumar and Kröger state that over the range of pressures for which their measurements extended the results of Shaw and Whelan will in fact fit a line with a slope 2/3 almost as well as the one with a slope of unity which they prefer.

With $D^*_{Cd} \propto P^{\frac{2}{3}}_{Cd}$, the defect responsible for Cd-tracer diffusion cannot be the majority defect controlling charge neutrality since $[e'] \propto P^{\frac{1}{3}}_{Cd}$. It must be $V^{\cdot\cdot}_S$ which is the doubly ionised donor species. S-tracer diffusion was studied and the 1173 K isotherms of D^*_S and $[e']$ as a function of P_{Cd} possessed slopes of 1/3. This is consistent with the neutrality condition $[e'] = 2[V^{\cdot\cdot}_S]$, $V^{\cdot\cdot}_S$ being the major doubly ionised native donor. The dependence $D^*_{Cd} \propto P^{\frac{2}{3}}_{Cd}$ automatically follows from this if Cd-tracer diffusion takes place by singly ionised Cd interstitials $Cd^{\cdot}_i$.

By comparing the magnitudes of D^*_{Cd} and D^*_S , which differ by a factor of 10^4, and realising that $[Cd^{\cdot}_i] < [V^{\cdot\cdot}_S]$ it is clear that $Cd^{\cdot}_i$ is by far the fastest moving point defect under these conditions and should be the one involved in bringing about changes in stoichiometry in response to a change in pressure or temperature.

When passing from high P_{Cd} to low P_{Cd} it was found that a change in the diffusion mechanism in pure CdS occurs for both Cd- and S-tracer diffusion. Results taken at 1173 K show that $D^*_S \propto P^{-1}_{Cd}$ and strongly suggest the neutral S interstitial S^*_i as the dominant defect responsible for the S-exchange. There was no observable change in D^*_S

when the CdS crystals were doped with 10^{25} In m^{-3} and thus $S_i^{\cdot}$ must be the species with the largest concentration - mobility product responsible for S-tracer exchange. Observed values of D^*_{Cd} showed considerable scatter obviating a determination of the exact pressure dependence. The observed values were significantly higher than the values extrapolated from the corresponding values obtained at high values of P_{Cd} indicating a different mechanism or a different electrical neutrality condition. The influence of In-doping on D^*_{Cd} isotherms was independent of P_{Cd} and Kumar and Kröger proposed V''_{Cd} as the dominant mobile defect.

Kumar and Kröger (35) also measured the coefficient of chemical diffusion in CdS at high Cd activities as a function of temperature. Their results showed a good agreement with the single result obtained by Shaw and Whelan but not with the results of Boyn et al. The results were analysed assuming that the defect $V_S^{\cdot\cdot}$ is the dominant defect for controlling non-stoichiometry in CdS under these conditions of temperature and P_{Cd}. As $Cd_i^{\cdot}$ is the most rapidly diffusing species the assumption was made that the diffusing $Cd_i^{\cdot}$ adjusted the $V_S^{\cdot\cdot}$ concentration by the reaction $Cd_i^{\cdot} \rightleftharpoons Cd^*_{Cd} + V_S^{\cdot\cdot} + e'$.

Shaw (36) showed that the conclusion reached by Kumar and Kröger, where they proposed that the dominant native donor in CdS at high Cd-pressures was $V_S^{\cdot\cdot}$, contains an assumption which is inconsistent with this conclusion. The results of their experiments do not rule out the possibility that $Cd_i^{\cdot\cdot}$ rather than $V_S^{\cdot\cdot}$ is the major native donor.

2.5 Self-diffusion studies in In-doped CdS

Kumar and Kröger (15) carried out Cd-tracer diffusion experiments on In-doped crystals. Figure 2.4 shows isotherms for D^*_{Cd} as a

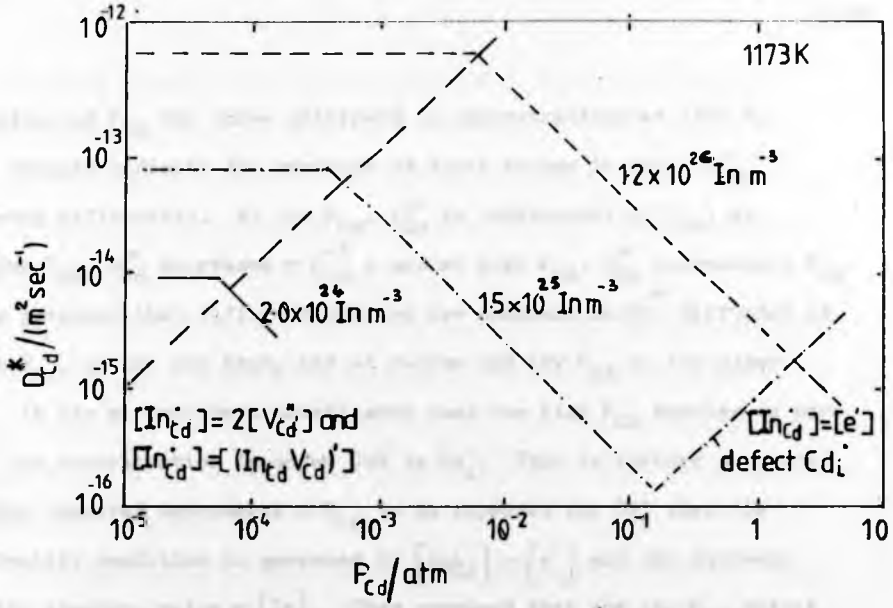

FIG 2·4 ISOTHERMS SHOWING THE VARIATION OF D^*_{Cd} WITH P_{Cd} FOR In-DOPED CdS CRYSTALS. (FROM KUMAR AND KRÖGER (15).)

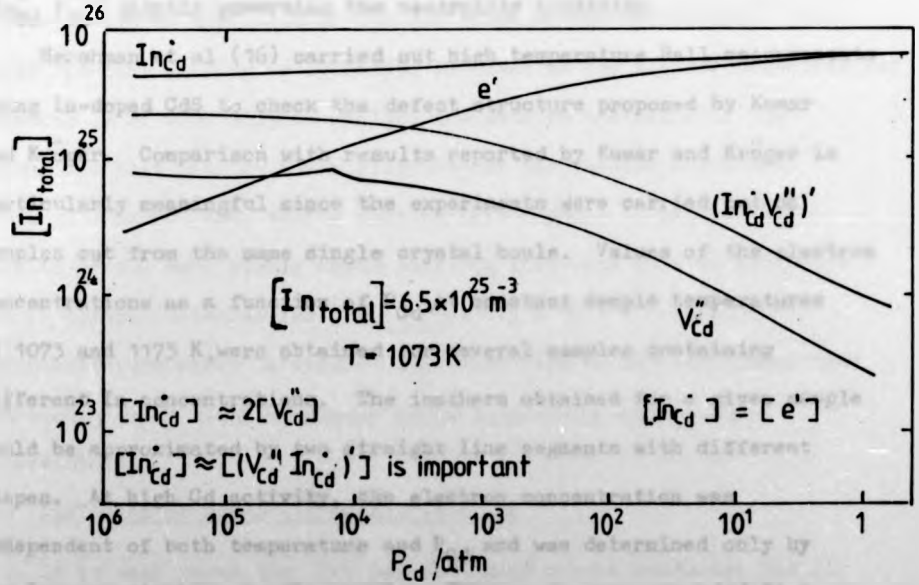

FIG 2·5 DEFECT ISOTHERMS FOR In-DOPED CdS (FROM HERSHMAN et al (16))

FIGS 2·4, 2·5.

function of P_{Cd} for three different In concentrations at 1173 K. The results indicate the presence of three ranges in which D^*_{Cd} behaves differently. At low P_{Cd}, D^*_{Cd} is independent of P_{Cd}; at medium P_{Cd}, D^*_{Cd} decreases α P_{Cd}^{-1} ; and at high P_{Cd}, D^*_{Cd} increases α P_{Cd}. They proposed that different species are dominant in Cd^* diffusion at high P_{Cd}, on the one hand, and at medium and low P_{Cd} on the other.

It has already been established that the high P_{Cd} species in pure and low concentration In-doped CdS is $Cd_i^{\cdot}$. This is further supported by the observed dependence α P_{Cd} to be expected for $Cd_i^{\cdot}$ when the neutrality condition is governed by $\left[In_{Cd}^{\cdot}\right] = \left[e'\right]$ and the decrease in the absolute value α $\left[In\right]$. They proposed that the low P_{Cd} defect must be a charged species V_{Cd}', V_{Cd}'' or $(In_{Cd}^{\cdot}\ V_{Cd}'')'$. By considering the variation with $\left[In_{\ total}\right]$ of transition pressure from P_{Cd} - independent D^*_{Cd} to where D^*_{Cd} α P_{Cd}^{-1} , they were able to rule out V_{Cd}' as the major species and this left a mixed regime with V_{Cd}'' and $(In_{Cd}^{\cdot}\ V_{Cd}'')'$ jointly governing the neutrality condition.

Hershman et al (16) carried out high temperature Hall measurements using In-doped CdS to check the defect structure proposed by Kumar and Kröger. Comparison with results reported by Kumar and Kröger is particularly meaningful since the experiments were carried out on samples cut from the same single crystal boule. Values of the electron concentrations as a function of P_{Cd}, at constant sample temperatures of 1073 and 1173 K, were obtained for several samples containing different In concentrations. The isotherm obtained for a given sample could be approximated by two straight line segments with different slopes. At high Cd activity, the electron concentration was independent of both temperature and P_{Cd} and was determined only by the In concentration in the sample. This region corresponded to a

condition of impurity controlled conductivity with $[e'] = [In^{\cdot}_{Cd}]$. Under sulfurizing conditions it was found that $[e'] \propto P_{Cd}^{\delta}$ where δ varied from approximately 0.5 for the heaviest doped samples of 6.5×10^{25} In m^{-3} to approximately 0.2 for a dopant concentration of 1.55×10^{23} m^{-3}.

It was possible to explain the value of $\delta = 0.5$ for the strongly doped samples by a compensation mechanism of the form of either $[In^{\cdot}_{Cd}] = 2[V''_{Cd}]$ or $[In^{\cdot}_{Cd}] = [(V''_{Cd}\ In^{\cdot}_{Cd})]$. The reason for the smaller slopes found in the weakly doped samples is to be found in the closeness of the range boundary.

Differentiation between the possible compensation models at high P_{S_2} was made by studying the variation between the In concentration and the Cd pressure $(P_{Cd})_{tr}$ marking the intersection of the two asymptotic solutions for $[e']$ for low and high Cd activity. It was discovered that the 1173 K data was in reasonable agreement with $[In^{\cdot}_{Cd}] = 2[V''_{Cd}]$, but the 1073 K data showed a concentration dependence somewhat between that expected on the basis of the two compensation mechanisms. This indicated that pairing is important at least at the higher concentrations. Hershman et al were able to analyse the data on the basis of the assumption that pairing was negligible for the samples doped with 1.6×10^{24} In m^{-3} and, taking pairing into account to explain the results of the more highly doped samples, they were able to produce a set of defect isotherms for $[In_{total}] = 6.5 \times 10^{25}$ m^{-3} at 1073 K. The results are shown in figure 2.5. They came to the conclusion that the theory which they developed agreed with their experimental observations.

2.6 Diffusion of group III metals into CdS

It is well known that CdS can be a good n-type conductor but it cannot be made p-type. The doping of CdS by trivalent elements (37, 38)

and by the halogens (39, 40) has been reported in the literature. In fact the amount of published information on the diffusion of group III elements in II-VI compounds is sparse compared with the diffusion of elements from groups II, VI and I and, in the main, diffusion coefficients have been estimated from doping experiments. As this thesis is concerned mainly with the diffusion of group III elements in CdS, the published information that does exist on this topic will be reviewed extensively.

The earliest reports of quantitative diffusion measurements being carried out in the preparation of In-doped CdS were made by Woodbury. The first (40) is where CdS crystals were fired for three to seven days at 1173 K in liquid S with a small amount of added In. This gave a diffusion coefficient of about 5×10^{-13} $m^2 s^{-1}$. The second (41) is where very degenerate In-doped CdS specimens have been prepared by firing in excess In and S for several days at 1073 K. The samples were very dark red but did not show any precipitates. Spectroscopic analysis on one of the samples indicated an In content of 1×10^{26} m^{-3} ($\pm$ 30%) which is believed to represent the In solubility in CdS under the conditions noted. Hall measurements indicated a carrier concentration of 6×10^{23} m^{-3}. One of the samples was then fired in saturated Cd vapour at 1073 K for a few hours and a carrier concentration of 6×10^{25} m^{-3} was then measured which is in excellent agreement with the In content. However, the Cd-fired sample showed black precipitates indicating that the In concentration now exceeded the solubility limit and was precipitated during the Cd vapour anneal. By introducing a smaller amount of In in the first firing the In content can be controlled to any desired level. For lower In concentrations there appears to be no problem of In precipitation under the uncompensating Cd firing and a 1:1 correspondence can be

obtained between the In content, as determined spectroscopically, and the room temperature carrier concentration down to the residual donor impurity level of about 10^{23} m^{-3}. The In content, in crystals prepared as described above, can be simply estimated since essentially all the In added to the firing tube goes into the CdS crystals up to the solubility limit. There is no segregation due to the excess S.

O'Tuama and Richter (42) used an electron microprobe analyser to measure the In concentration profile of CdS platelets which had been obtained from various sources and had been exposed to a diffusion anneal in In vapour. One typical result, which was obtained using CdS obtained from Clevite Corporation, Cleveland, Ohio, was that after a diffusion time of 60 min at 793 K the surface concentrations, by mass per cent, were 66.1% Cd, 22.8% S and 11.9% In and the In concentration profile close to the surface was equivalent to a diffusion coefficient of 1.8×10^{-18} $m^2 s^{-1}$. This value of the In surface concentration does, in view of the measurements reported in this thesis, appear to be exceptionally high. O'Tuama and Richter came to the conclusion in their studies that the displacement of Cd by In was the dominant diffusion mechanism.

Chern and Kröger (43) showed that the diffusion coefficient D_P of In-Cd vacancy pairs in CdS and CdTe, is smaller than that of free vacancies. In addition, their analysis showed that the chemical diffusion coefficient D_{In} initially increases with increasing In concentration; it then passes through a maximum before starting to decrease at high In concentrations where almost half the In is present as $(In_{Cd}^{\bullet} V_{Cd}^{''})'$ pairs.

Chern and Kröger carried out measurements on the diffusion of In into CdS at 1083 K and 1173 K in an atmosphere of saturated S_2 vapour. The profiles obtained are shown in figure 2.6a. It was not

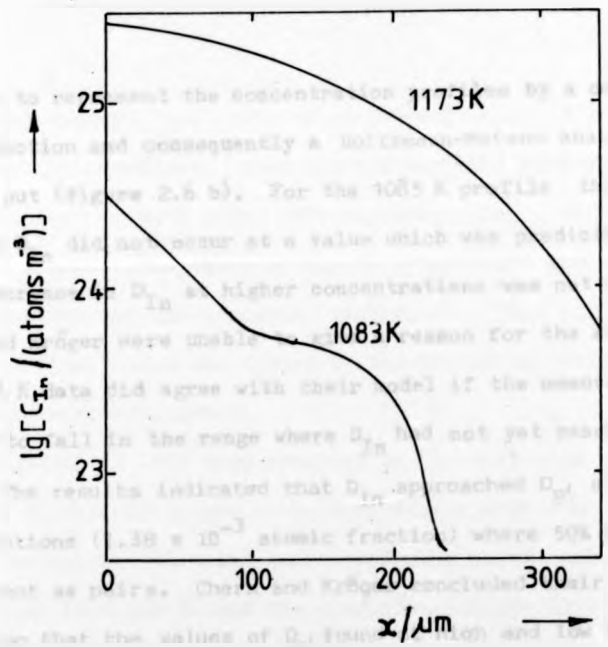

FIG 2·6a PENETRATION PROFILES OF In DIFFUSING INTO CdS (FROM CHERN AND KROGER(43))

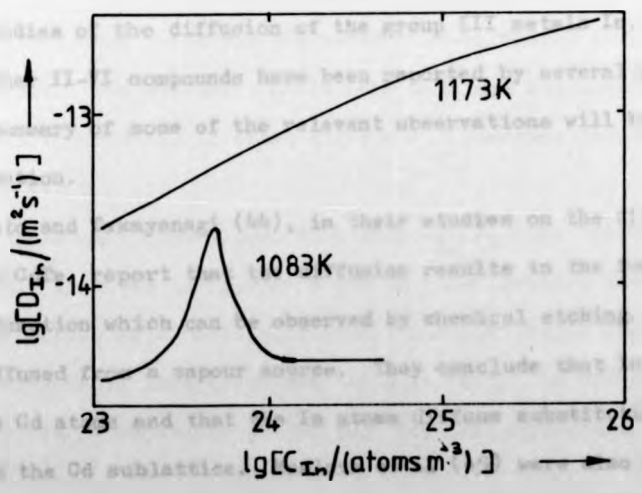

FIG 2·6b VARIATION OF D_{In} WITH C_{In} IN CdS
(FROM CHERN AND KROGER(43))

FIGS 2·6a,2·6b.

possible to represent the concentration profiles by a complementary error function and consequently a Boltzmann-Matano analysis was carried out (figure 2.6 b). For the 1083 K profile the maximum value of D_{In} did not occur at a value which was predicted from theory and a decrease in D_{In} at higher concentrations was not observed. Chern and Kröger were unable to give a reason for the abnormal profile. The 1173 K data did agree with their model if the measurements were assumed to fall in the range where D_{In} had not yet reached a maximum value. The results indicated that D_{In} approached $D_{p'}$ at medium In concentrations (1.38×10^{-3} atomic fraction) where 50% of the In was present as pairs. Chern and Kröger concluded their investigations by stating that the values of $D_{p'}$ found at high and low In concentrations offered support for the model used and the value of $K_{p'}$, the equilibrium constant for the pairing of V''_{Cd} and $In^{\bullet}_{Cd}$ to form $(V''_{Cd}\ In^{\bullet}_{Cd})'$, calculated by Hershman et al (16).

2.7 Diffusion of group III metals into other II-VI compounds

Studies of the diffusion of the group III metals In, Al and Ga into other II-VI compounds have been reported by several people. A brief summary of some of the relevant observations will be given in this section.

Kato and Takayanagi (44), in their studies on the diffusion of In into CdTe, report that the diffusion results in the formation of a p-n junction which can be observed by chemical etching. The In was diffused from a vapour source. They conclude that In atoms replace Cd atoms and that the In atoms diffuse substitutionally through the Cd sublattice. Maslova et al (45) were also able to observe the p-n junction, which formed in their experiments on the diffusion of In into CdTe, using an optical microscope.

Several workers have reported on the diffusion of group III elements into the Zn chalcogenides. Aven and Kreiger (46) have investigated the diffusion of Al into ZnSe, ZnTe and $ZnSe_{0.5}Te_{0.5}$ using a Zn-Al alloy as a source. The depth of the Al penetration was measured using electrical and luminescence techniques. They concluded that the p-n junction, which was formed in the diffusion, coincided with the Al luminescence boundary.

Yokozawa et al (47) have reported on the diffusion and the solid solubility of In into p-type cubic ZnTe single crystals. The diffusions were carried out in evacuated quartz ampoules which contained radioactive In and inactive Zn and the concentration profiles due to the volume diffusion gave standard 'erfc' distributions. An Arrhenius plot of D_{In} is shown in figure 2.7a. The constant surface concentration was considered to be the solid solubility of In in ZnTe and it is shown as a function of temperature in figure 2.7b. The corresponding results on the diffusion of In into CdTe (48) are included along with those for the metal self-diffusion into ZnTe (49) and CdTe (50). The diffusion of In into ZnTe was considered to be substitutional in which In atoms diffuse by a vacancy mechanism on the Zn sublattice.

It can be seen from figure 2.7a that D_{In} for the diffusion of In into CdTe and ZnTe is between 5 and 50 times greater than D^* for the corresponding metal self-diffusion. The activation energy for the In diffusion in ZnTe is greater than it is in the CdTe and this difference can be explained by the fact that ZnTe possesses a smaller lattice constant.

The vapour pressure of Zn during the diffusion was changed to examine the effect of the vacancy concentration on the Zn sublattice

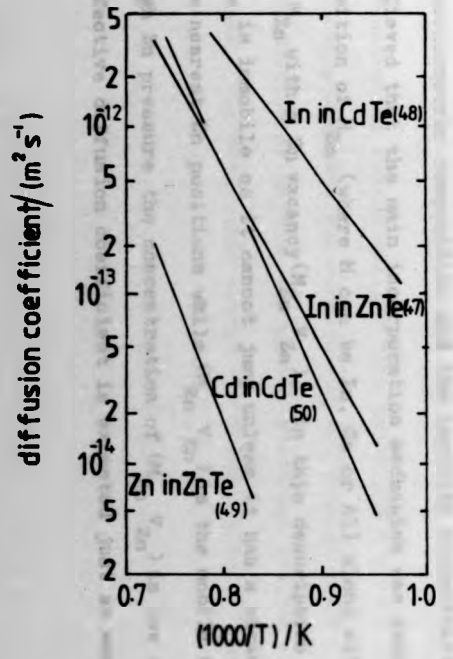

FIG 2·7a AN ARRHENIUS PLOT FOR THE DIFFUSION OF In INTO Zn Te AND Cd Te
(FROM YOKAZAWA et al (47))

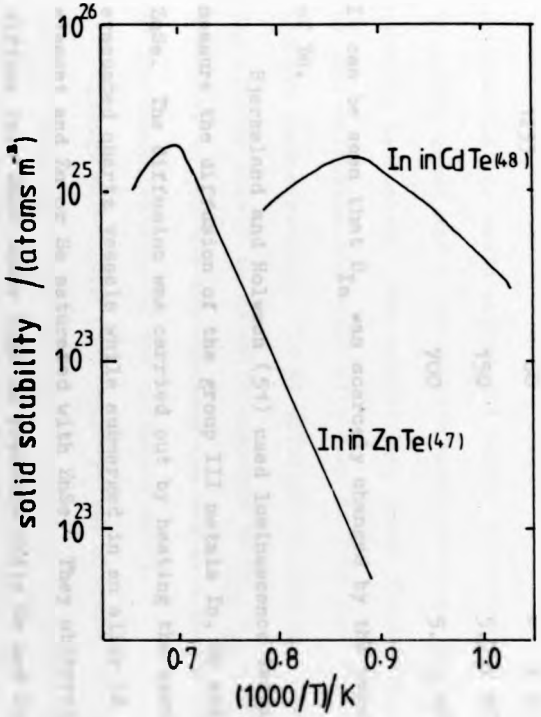

FIG 2·7b SOLID SOLUBILITY OF In IN Zn Te AND Cd Te
(FROM YOKAZAWA et al (47))

FIGS 2·7a 2·7b.

on D_{In}. The following results were obtained:

Temperature K	Zn vapour pressure Torr	Diffusion coefficient D_{In}/m^2s^{-1}
1233	60	6×10^{-13}
	150	5.7×10^{-13}
	700	5.3×10^{-13}

It can be seen that D_{In} was scarcely changed by the vapour pressure of Zn.

Bjerkeland and Holwech (51) used luminescence techniques to measure the diffusion of the group III metals In, Ga and Al into ZnSe. The diffusion was carried out by heating the specimens in evacuated quartz vessels while submerged in an alloy of the doping element and Zn or Se saturated with ZnSe. They observed that Al can diffuse into ZnSe under high Zn pressure while Ga and In will only diffuse under high Se pressure. The impurity profiles were concentration dependent but they did not follow a relationship of the form $D \propto C^n$, where n is an integer.

The authors stated that the rate of diffusion is a function of stoichiometric composition and the impurity concentration. They believed that the main incorporation mechanism was substitution on a position of M_{Zn} (where M can be In, Ga or Al) along with an association of M_{Zn} with a Zn vacancy($M_{Zn}\ V_{Zn}$). In this description the defect M_{Zn} is immobile as it cannot jump unless it has a vacancy on one of the nearest Zn positions while ($M_{Zn}\ V_{Zn}$) is the mobile form. Under high Zn pressure the concentration of ($M_{Zn}\ V_{Zn}$) is low and a low effective diffusion coefficient is expected just as was observed for

Ga and In. The comparatively large diffusion coefficient which was observed for Al must then be due to either a very large binding energy for the complex (Al_{Zn} V_{Zn}), even under high Zn pressure, or to the presence of a small number of highly mobile defects such as interstitials. For high doping levels similar to the ones covered in these experiments one would expect the number of acceptors and donors to be nearly equal and clusters with basic structure (M_{Zn} V_{Zn} M_{Zn}) will probably be formed. They stated that these clusters would be paths of easy diffusion and could give rise to very fast diffusion at the highest concentrations. It is difficult to see how this happens as the cluster itself is immobile compared to (M_{Zn} V_{Zn}). It is also difficult to see how the clusters can act as a short circuit path at low concentrations of the trivalent metal.

Koshiga and Sugano (52) measured the diffusion of Al into ZnS by measuring the Al concentration profile using a Schottky barrier capacitance method. Zn and Al were vacuum sealed in a silica ampoule along with the ZnS. Zn was added to suppress the formation of acceptor Zn vacancies and to prevent the direct reaction of ZnS with Al to form a ternary alloy. The authors indicated that the Al and the ZnS did form a ternary alloy during some of the diffusions. The standard 'erfc' relationship was fitted to the concentration profiles. Concentration values smaller than those given by the 'erfc' relationship were obtained near the surface and the reasons given for this were the introduction of defects during the diffusion and the formation of new phases. The activation energy for the diffusion is 3.6 eV.

2.8 Anisotropy in II-VI compounds

It is possible that diffusion anisotropy can be observed in II-VI compounds that possess the hexagonal structure, where diffusion coefficients are measured both parallel and perpendicular to the c-axis. It is also possible that the anisotropy will be greater for impurities that diffuse via an associated secondary defect than if the individual primary defects acted independently. The magnitude of the anisotropy will depend on such factors as the c/a ratio of the crystal, the diameter of the individual ions of the crystal and of the impurity, on the type of defect formed and on the physical conditions of the diffusion. If diffusion does take place via the $(In^{\bullet}_{Cd}\ V^{''}_{Cd})'$ defect it can depend greatly on the orientation of the defect in the lattice particularly if it has preferred orientation.

There is no published information available on the anisotropy for self-diffusion studies in the II-VI compounds. Sullivan (53), who studied the diffusion of Cu in CdS, noticed a marked anisotropy was found which favoured diffusion in a direction perpendicular to the c-axis by one or two orders of magnitude. Sullivan (54) also measured the diffusion of Cu, Ag and Au in CdS and found that there was no significant anisotropy for the diffusion of Ag.

2.9 References

1. A. ASCOLI, Energia Nucleare, 20, 8-9, P467(1973).
2. D. A. STEVENSON, Atomic Diffusion in Semiconductors (Edited by D. Shaw), P431, Plenum Press, London and New York (1973).
3. B. L. SHARMA, Diffusion in Semiconductors, Trans. Tech. Publications, Germany (1970).
4. National Bureau of Standards Circular No. 539, 4, 15-16 (1955).

5. B. TUCK, Introduction to Diffusion in Semiconductors, Peter Peregrinus Limited, Stevenage (1974).

6. A. KELLY and G. W. GROVES, Crystallography and Crystal Defects, Longman Group Limited, London (1970).

7. L. R. SHIOZAWA and J. M. JOST, Research on Improved II-VI Crystals, Aerospace Research Laboratories Report 69-0107, Office of Aerospace Research, United states Air Force, Wright-Patterson Air Force Base, Ohio (1969).

8. L. R. SHIOZAWA, J. M. JOST and G. A. SULLIVAN, Research on Improved II-VI crystals, Aerospace Research Laboratories Report 68-0153, Office of Aerospace Research, United States Air Force, Wright-Patterson Air Force Base, Ohio (1968).

9. M. R. LORENZ, Physics and Chemistry of II-VI Compounds (Edited by M. Aven and J. S. Prener), P73, North-Holland Publishing Company, Amsterdam (1967).

10. N. A. GORYUNOVA, F. P. KESAMANLY and D. N. NASLEDOV, Semiconductors and Semimetals (Edited by K. R. Willardson and A. C. Beer), P413, Physics of III-V Compounds, Volume 4, Academic Press, New York (1968).

11. H. HAHN and W. KLINGER, Z. Anorg. Allg. Chem., 263, P178 (1950).

12. H. HAHN, G. FRANK, W. KLINGER, A.D. STORGER and G. STORGER, Z. Anorg. Allg. Chem., 279, P241 (1955).

13. H. KOELMANS and H. G. GRIMMEIS, Physica, 25, P1287 (1959).

14. L. H. VAN VLACK, Materials Science for Engineers, Addison - Wesley Publishing Company (1970).

15. V. KUMAR and F. A. KRÖGER, J. Sol. State Chem., 3, P387 (1971).

16. G. H. HERSHMAN, V. P. ZLOMANOV and F. A. KRÖGER, J. Sol. State Chem., 3 , P401 (1971).

17. R. A. SWALIN, Thermodynamics of Solids, John Wiley and Sons Inc., New York (1972).

18. W. VAN GOOL, Principles of Defect Chemistry of Crystalline Solids, Academic Press (1966).

19. Solid State Chemistry and Physics (Edited by P. F. Weller), Marcel Dekker Inc., New York (1974).

20. A. B. LIDIARD, Handbuch der Physik (Edited by S. Flugge), 20, P298, Springer-Verlag OHG, Berlin (1957).

21. C. WAGNER, J. Chem. Phys., 18, P1227 (1950).

22. F. BENIERE, M. BENIERE and M. CHEMLA, J. Chem. Phys., 56, P549 (1972).

23. R. A. PERKINS and R. A. RAPP, Metal. Trans., 4, P193 (1973).

24. L. A. SYSOEV, A. Ya. GILFMAN, A. D. KOVALEVA and W. G. KRAVCHENKO, Izv. Akad. Nauk. S.S.S.R., Neorgan. Mater. (In Russian), 5, 12, P2208 (1969).

25. G. H. HERSHMAN and F. A. KRÖGER, J. Sol. State Chem., 2, P483 (1970).

26. J. CRANK, The Mathematics of Diffusion,Oxford University Press, London (1970).

27. H. S. CARSLAW and J. C. JAEGER, Conduction of Heat in Solids, Oxford University Press (1959).

28. E. D. JONES, Measurement of the Self-Diffusion of Cd into CdS using Radiotracer Sectioning Techniques, M.Sc. Thesis, University of Warwick (1971).

29. L. R. WEISBERG and J. BLANC, Phys. Rev., 131, P1548 (1963).

30. F. A. CUNNELL and C. H. GOOCH, J. Phys. Chem. Solids, 15, P127 (1960).

31. B. TUCK and M. A. H. KADHIM, J. Mat. Sci., 7, P585 (1972).

32. H. H. WOODBURY, Phys. Rev., 134, PA492 (1964).

33. D. SHAW and R. C. WHELAN, Phys. Stat. Sol., 36, P705 (1969).

34. R. BOYN, O. GOEDE and S. KUSCHNERUS, Phys. Stat. Sol., 12, P57 (1965).

35. V. KUMAR and F. A. KRÖGER, J. Sol. State. Chem., 3, P406 (1971).

36. D. SHAW, Phys. Stat. Sol. (b), 60, K45 (1973).

37. F. A. KRÖGER, H. J. VINK and J. VAN DEN BOOMGARD, Z. Physik Chem., 203, P1 (1954).

38. W. W. ANDERSON and H. J. CHANG, J. Electrochem.Soc., Solid State Science, 118, 9, P1451 (1971).

39. H. R. VYDYANETH, S. S. CHERN and F. A. KRÖGER, J. Phys. Chem. Solids, 34, 8, P1317 (1973).

40. H. H. WOODBURY, Physics and Chemistry of II-VI Compounds (Edited by M. Aven and J. S. Prener), P223, North Holland Publishing Company, Amsterdam (1967).

41. H. H. WOODBURY, II-VI Semiconducting Compounds (Edited by D. G. Thomas), P244, W. A. Benjamin Inc., New York (1967).

42. S. S. O'TUAMA and J. RICHTER, J. Appl. Phys., 41, 4, P1861 (1970).

43. S. S. CHERN and F. A. KRÖGER, Phys. Stat. Sol. A, 25, 1, P215 (1974).

44. H. KATO and S. TAKAYANAGI, Japan.J. Appl. Phys., 2, P250 (1963).

45. L. V. MASLOVA, O. A. MATSEEV, Yu. V. RAD and A. K. V. SANIN, Physics of p-n junctions and semiconductor devices (Edited by S. M. Ryvkin and Yu. K. Shmartsev, translated from Russian), P234, Consultants bureau, New York (1971).

46. M. AVEN and E. L. KREIGER, J. Appl. Phys., 41, 5, P1935 (1970).

47. M. YOKOZAWA, H. KATO and S. TAKAYANAGI, Denki. Kagaku., 36, 4, P282, (1968).

48. H. KATO and S. TAKAYANAGI, Japan. J. Appl. Phys., 2, P250 (1963).

49. R. A. REYNOLDS and D. A. STEVENSON, J. Phys. Chem. Solids, 30, P139 (1969).

50. P. M. BORSENBERGER and D. A. STEVENSON, J. Phys. Chem. Solids, 29, P1277 (1968).

51. H. BJERKELAND and I. HOLWECH, Phys. Norv., 6, 3-4, P139 (1972).

52. F. KOSHIGA and T. SUGANO, Shinku., 16, 5, P174 (1973).

53. G. A. SULLIVAN, Phys. Rev., 184, 3, P796 (1969).

54. J. L. SULLIVAN, J. Phys. D, 6, P552 (1973).

3. Experimental techniques

There are very many methods available for measuring diffusion rates into solids. It is possible to measure diffusion profiles directly using chemical, spectrographic, optical, X-ray and radiochemical methods, or it is possible to use an indirect method such as microhardness or electrical conductivity. Available methods have been reviewed by several people (1-4).

It is possible that a particular method for measuring diffusion profiles may have one or more advantages over all other possible ones in a particular application. For example: electrical conductivity measurements can be used for measuring the diffusion of electrically active impurities in a semiconductor and luminescence methods can be used for measuring the diffusion of the optically active impurities. It is possible that not all the impurity atoms are electrically or optically active in such a semiconductor and so if the total impurity concentration is required, other suitable methods will have to be used. If the impurity exists in a convenient radioactive form, then it is possible to use a RTS method to measure the concentration profile of the total number of impurity diffusing atoms. If no convenient radioisotope exists, then it may be possible to use an electron microprobe analyser.

Optical techniques can be used to measure diffusion profiles and the actual technique used will depend on the optical properties of the material under investigation. For example: with transparent materials, it is possible to obtain the concentration profiles in an interdiffusion problem using quantitative measurements of refractive index or of absorption coefficients. For opaque materials, variations in the reflective properties can be used.

In the investigations described in this thesis, three experimental techniques were used for the measurements. They were a RTS technique, an

optical method and an electron microprobe analyser and all three methods are described briefly in this chapter. The actual uses to which the techniques were put are given and compared in section 3.5.

The diffusion profiles that were obtained for some of the In diffusions (those described in section 5.1 for example) indicated the presence of slow and fast diffusion processes similar to the ones observed by Shaw and Whelan (5, section 2.4). The former was the bulk diffusion and was the one on which all the measurements were made. The latter, which contributed less than 10^{-3} of the total impurity concentration at the surface of the slice at $x = 0$, was probably due to diffusion along dislocations. A convention is adopted in this thesis, although not strictly correct, in which the part of the CdS crystal that contains the bulk diffusion is referred to as the doped part, and the remainder as the pure or undoped part.

3.1 The diffusion anneal

The method used in preparing the samples for the diffusion anneal and the diffusion anneal procedure are described in detail in the author's M.Sc. thesis (6), and only a brief outline of the procedures will be given in this section. These procedures were similar, irrespective of which technique was used for measuring the diffusion rates, and they will be described in the three following subsections.

3.1.1 Ampoule preparation

For the RTS technique, slices of CdS were cut from a boule of single crystal material of known orientation (figure 3.1) which had been checked using both polarised light and a Laue back reflection X-ray technique. The slices, which were approximately 1 mm thick and 8 mm diameter, were cut in such a way that the surface of the slice

EXPERIMENTAL TECHNIQUES USED FOR MEASURING DIFFUSION COEFFICIENTS.

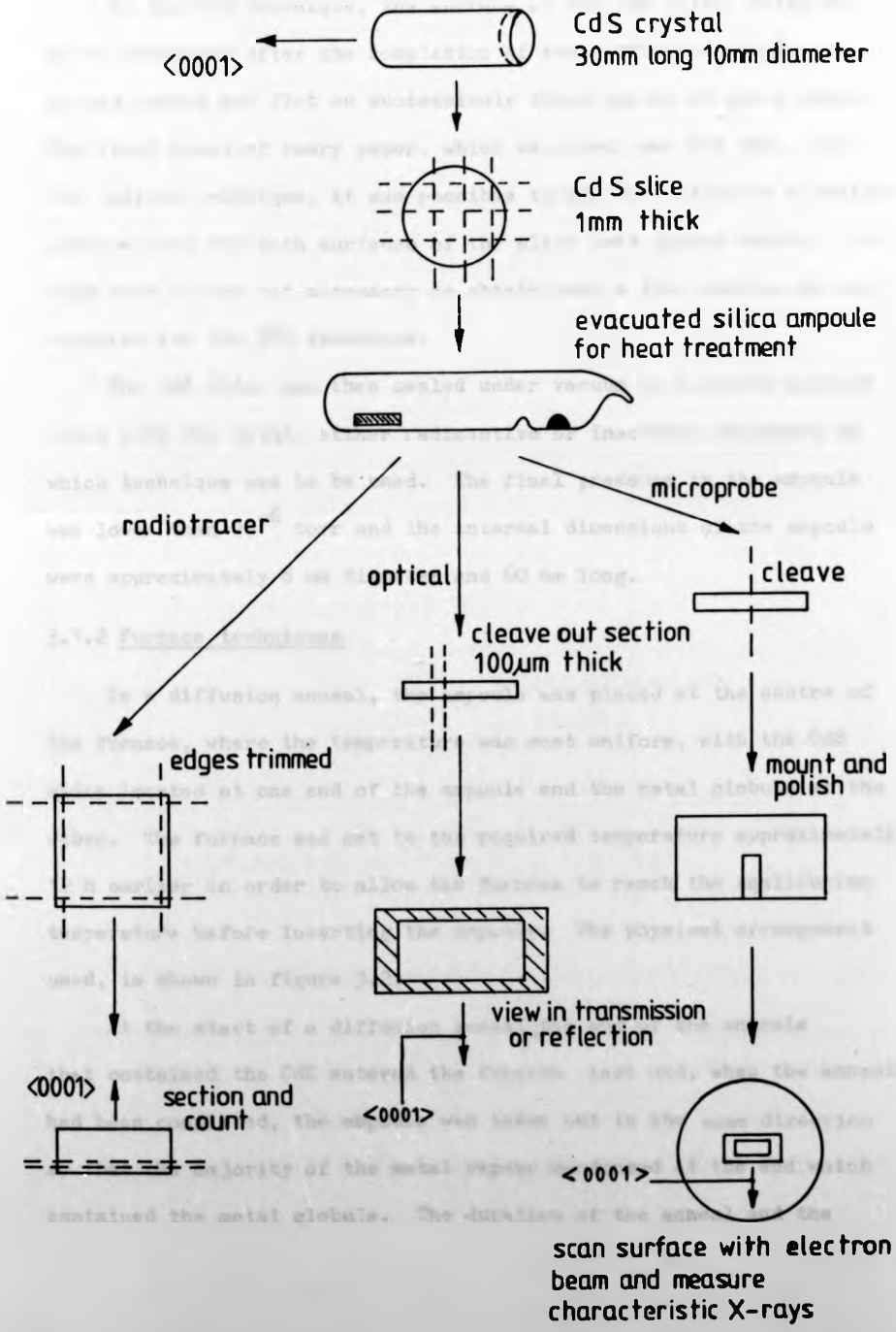

Fig 3.1

was perpendicular to the [0001] direction.

In the RTS technique, the surface of the CdS slice, which was to be sectioned after the completion of the diffusion anneal, was ground smooth and flat on successively finer grades of emery paper. The final grade of emery paper, which was used, was SIA 7XO. For the optical technique, it was possible to use CdS slices of a smaller surface area and both surfaces of the slice were ground smooth. In this case it was not necessary to obtain such a flat surface as was required for the RTS technique.

The CdS slice was then sealed under vacuum in a silica ampoule along with the metal, either radioactive or inactive, depending on which technique was to be used. The final pressure in the ampoule was lower than 10^{-6} torr and the internal dimensions of the ampoule were approximately 8 mm diameter and 60 mm long.

3.1.2 Furnace techniques

In a diffusion anneal, the ampoule was placed at the centre of the furnace, where the temperature was most uniform, with the CdS slice located at one end of the ampoule and the metal globule at the other. The furnace was set to the required temperature approximately 12 h earlier in order to allow the furnace to reach the equilibrium temperature before inserting the ampoule. The physical arrangement used, is shown in figure 3.2.

At the start of a diffusion anneal, the end of the ampoule that contained the CdS entered the furnace last and, when the anneal had been completed, the ampoule was taken out in the same direction so that the majority of the metal vapour condensed at the end which contained the metal globule. The duration of the anneal and the

DETAILS OF THE ANNEAL FURNACE.

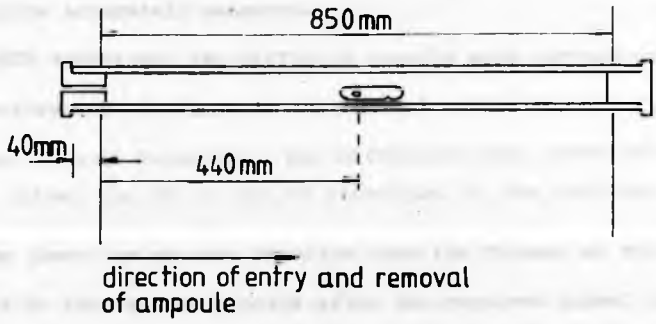

(a) LOCATION OF AMPOULE IN THE FURNACE

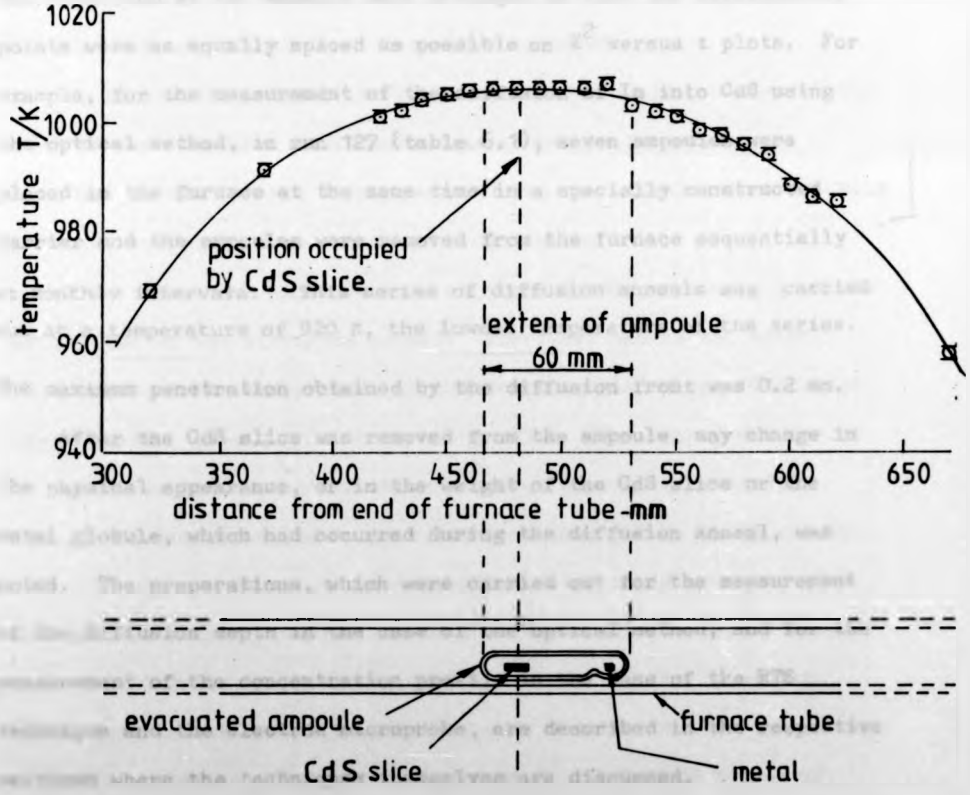

(b) TEMPERATURE DISTRIBUTION ALONG THE AXIS OF THE FURNACE

Fig 3.2

temperature were accurately measured.

In the RTS technique, the diffusion anneals were carried out singly and this practice was also used in the optical method for anneals that were less than 24 h in duration. For diffusions that lasted for more than 24 h in either the RTS or the OM technique, it was sometimes more convenient to place two or more ampoules into the furnace at the same time and to remove each ampoule after the required anneal time. This procedure proved successful for the optical technique, where between six and eight anneals were carried out at each temperature. The durations of the anneals were arranged so that the experimental points were as equally spaced as possible on x^2 versus t plots. For example, for the measurement of the diffusion of In into CdS using the optical method, in run 127 (table 6.1), seven ampoules were placed in the furnace at the same time in a specially constructed carrier and the ampoules were removed from the furnace sequentially at monthly intervals. This series of diffusion anneals was carried out at a temperature of 920 K, the lowest temperature of the series. The maximum penetration obtained by the diffusion front was 0.2 mm.

After the CdS slice was removed from the ampoule, any change in the physical appearance, or in the weight of the CdS slice or the metal globule, which had occurred during the diffusion anneal, was noted. The preparations, which were carried out for the measurement of the diffusion depth in the case of the optical method, and for the measurement of the concentration profile in the case of the RTS technique and the electron microprobe, are described in the respective sections where the techniques themselves are discussed.

3.1.3 Measurement of the temperature of the anneal

The temperature of each anneal was measured, using a Pt - 87% Pt 13% Rh thermocouple, by placing it in the hot zone of the furnace

before the start of the diffusion anneal and again after the ampoule had been removed from the furnace. In a run where two or more ampoules were placed in the furnace simultaneously in a special holder and the ampoules were removed sequentially after the required diffusion time had elapsed, the temperature was measured before the carrier was placed in the furnace and again when it was removed from the furnace. The mean of the starting and finishing temperatures was taken to be the temperature of the anneal. As the thermocouple did not possess a cold junction, which would have been made up of an ice and water mixture, the ambient temperature of the laboratory was noted each time the temperature of the furnace was measured.

As it was not possible to place the thermocouple junction at the required position when a diffusion anneal was in progress, any variation in the furnace temperature during the anneal was noted using the scale on the furnace temperature controller.

There were four major sources of error in the measurement of the temperature of the diffusion anneal. The first was in the actual measurement of the temperature of the thermocouple using a Cambridge potentiometer, type 44228, which was $\pm$ 0.5 K. The second was due to the variation in temperature which occurred during the diffusion anneal, and the error due to this was less than $\pm$ 2 K, which was the limit of accuracy to which the controller meter could be read. The manufacturer's specification quoted that the controller would keep the temperature of the furnace to within closer limits than this and no such variations in temperature were detected on the temperature controller meter in a long diffusion anneal. The third source of error was due to the variation in the position to which the CdS slice was placed in the furnace, and this contributed an uncertainty in the

temperature of ± 1 K. The fourth was the variation in the ambient temperature of the laboratory, which was ± 2 K.

The overall error in the temperature of the anneal was approximately ± 3 K.

3.2 The RTS technique

After the completion of the diffusion anneal, the CdS slice was mounted in a lapping jig by attaching the slice to a removable stainless steel platelet using Araldite, as shown in figure 3.3. The edges of the slice were then removed using a diamond saw, leaving the centre portion of the slice, which had been doped only by the diffusion of atoms in from the flat surfaces of the slice.

Parallel sections were removed from the exposed surface of the slice by lapping the surface on discs of SIA 7x0 emery paper using the lapping jig. A dry lapping method was used and during the lapping all the material that was removed from the slice got embedded in the emery paper. The thickness of each section removed was obtained by weighing the slice and plate assembly before, and again after each lapping process using an Oertling microbalance, type 147. The area of the surface of the slice was measured by photographing the surface of the slice using a known magnification and measuring the area of the image by placing a grid, which was calibrated in millimetres, over the photographic plate and counting squares.

The activity of the CdS section, which was embedded in the emery disc, was measured either on a gamma scintillation counter or on an anticoincidence low background Geiger counter, depending on the count rate. When the count rate on the scintillation counter, which was used at the start of a profile measurement, dropped below 100 counts per second, counting was transferred to the low background Geiger counter. The relative properties of these counters are discussed extensively

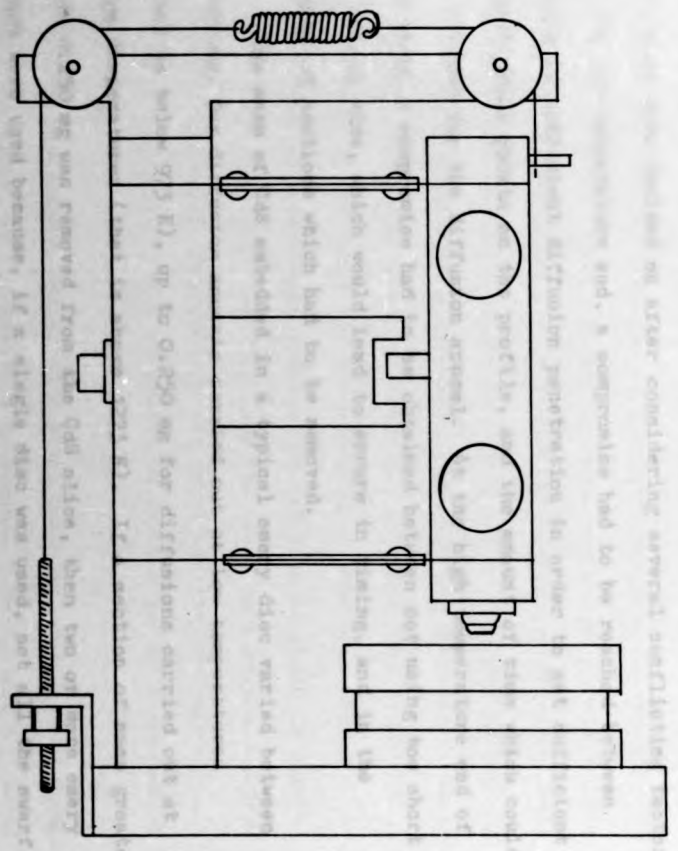

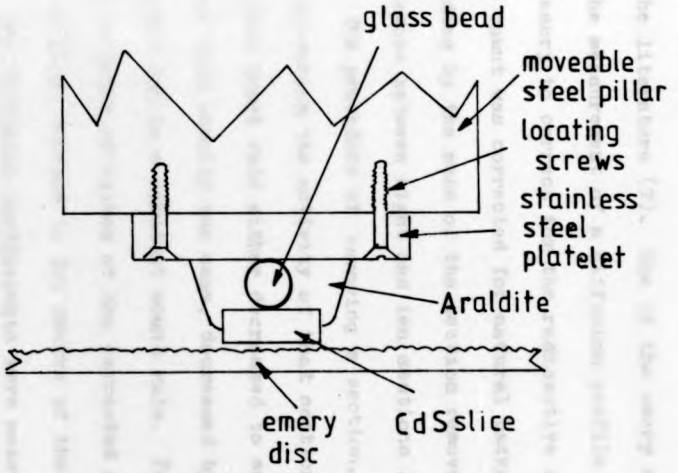

enlarged view showing CdS assembly in position

THE LAPPING JIG

Fig 3·3

in the literature (7). One of the emery discs was used as a standard in the measurement of a diffusion profile and consequently it was not necessary to correct for the radioactive decay of the Cd or the In. Each count was corrected for natural background and was normalised by dividing by the mass of the section removed. It was possible to remove between eight and ten sections in a normal working day.

The procedure of removing a section, weighing the slice assembly and measuring the activity of that section was continued until the specific count rate either decreased to an undetectable level or, as was more usually the case, decreased by two or three decades and levelled out to a constant count rate. For each diffusion profile, sets of pairs of values of the corrected count rate and the depth from the original surface to the centre of the section were obtained.

The diffusion coefficients were measured over as great a range of temperatures as possible and the limiting temperatures at both ends of the range were decided on after considering several conflicting factors. At the low temperature end, a compromise had to be reached between obtaining sufficient diffusion penetration in order to get sufficient experimental points on the profile, and the amount of time which could be allowed for the diffusion anneal. At the high temperature end of the range a compromise had to be obtained between not using too short an anneal time, which would lead to errors in timing, and in the number of sections which had to be removed.

The mass of CdS embedded in a typical emery disc varied between 0.080 mg, for diffusion anneals carried out at low temperatures (that is below 973 K), up to 0.250 mg for diffusions carried out at high temperatures (that is above 1273 K). If a section of mass greater than 0.250 mg was removed from the CdS slice, then two or more emery discs were used because, if a single disc was used, not all the swarf would be firmly embedded in the emery disc.

Several tests were developed to measure the depth of the scratches in the surface of the CdS slice, which were caused by the lapping process, and also to check how parallel the lapped surface remained to the original surface of the slice throughout the profile measurement. The scratch depths were measured mechanically using a Taylor Hobson Talysurf (8) and optically using an interference microscope. These tests showed that the depth of the scratches produced an error of less than $\pm$ 3% in the specific activity of a typical section. The parallelism of the sections removed was checked by taking radiographs of the surface of the slice at various stages during the measurement of the diffusion profile. The results obtained gave a maximum scatter in the angle between the normal to the lapped surface of the slice and the axis of the lapping jig of $\pm$ 0.02 degrees.

3.3 The optical technique

This method, which involved the use of non-radioactive materials, was used for measuring the rate of diffusion of group III metals into CdS in anneals where excess group III metal was placed in the ampoule. Such diffusions possessed a sharply defined observable diffusion front, as shown in figure 3.4 , whose depth X could be measured by looking at a cleaved section with a microscope. It was not possible to obtain any information on the impurity concentration using this technique. The sharpness of the front was demonstrated by passing a narrow parallel beam of white light through the front as is shown in figure 3.5. At a critical angle of incidence the green part of the spectrum is totally internally reflected by the front and the red part of the spectrum is refracted. This is discussed further in the introduction to chapter 6.

As CdS possesses a hexagonal crystal structure and $D_{||}$ and $D_{\perp}$ are probably different, it was possible to measure both $X_{||}$ and $X_{\perp}$ using

THE DIFFUSION FRONT FOR THE DIFFUSION OF In INTO CdS

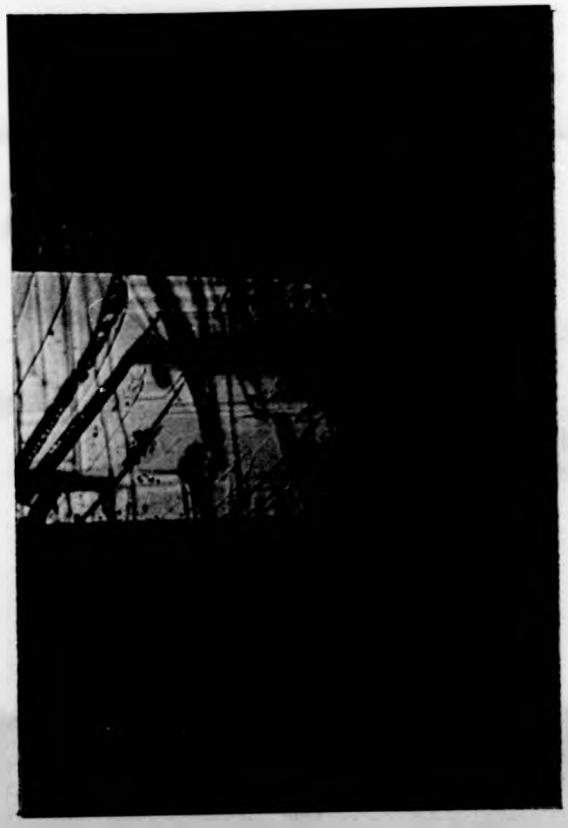

magnification x 150

Fig 3.4

DEMONSTRATION OF THE DISPERSION OF A NARROW BEAM OF WHITE LIGHT AT THE DIFFUSION INTERFACE.

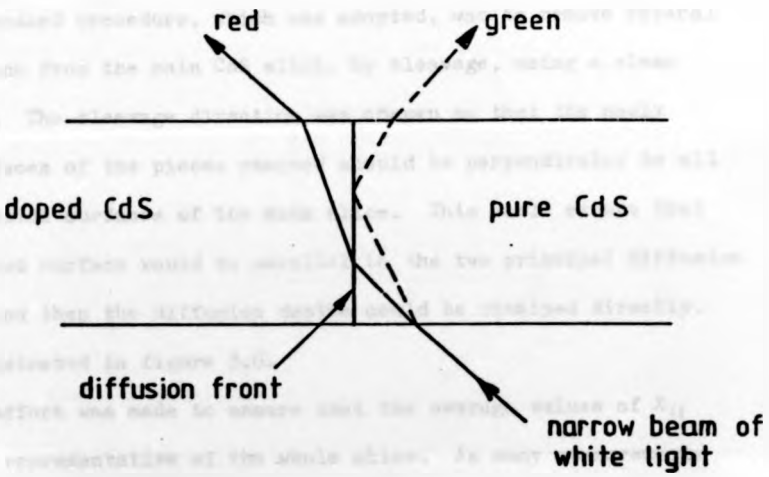

approximate magnification x 400

Fig 3.5

DEMONSTRATION OF THE DISPERSION OF A NARROW BEAM OF WHITE LIGHT AT THE DIFFUSION INTERFACE.

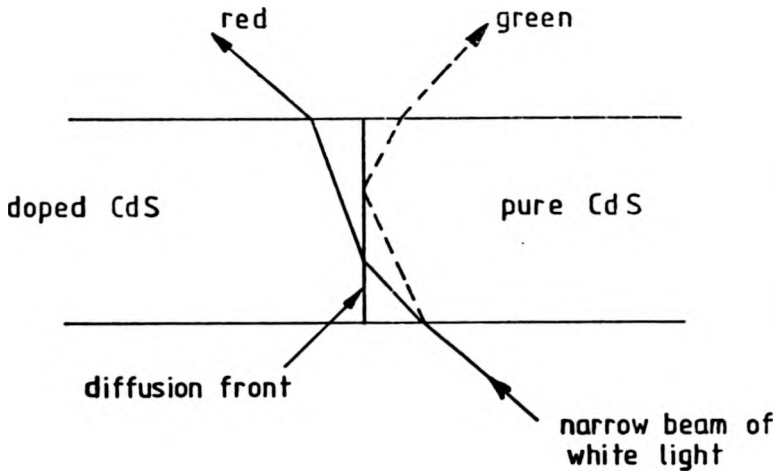

approximate magnification x 400

Fig 3.5

this method. If a CdS slice is cleaved in the correct manner, it is possible to expose a corner of a cleaved surface of the slice where both $X_{\parallel}$ and $X_{\perp}$ could be measured.

The standard procedure, which was adopted, was to remove several small sections from the main CdS slice, by cleavage, using a clean sharp knife. The cleavage direction was chosen so that the newly exposed surfaces of the pieces removed should be perpendicular to all adjacent outside surfaces of the main slice. This would ensure that such a cleaved surface would be parallel to the two principal diffusion directions and then the diffusion depths could be obtained directly. This is illustrated in figure 3.6.

Every effort was made to ensure that the average values of $X_{\parallel}$ and $X_{\perp}$ were representative of the whole slice. As many measurements as possible were obtained up to a maximum of fifteen in each of the two directions. Not more than four measurements, for diffusions in each direction, were taken from any single cleaved surface. In addition, the pieces of crystal, which were used for the measurement, were taken from as widely differing parts of the slice as possible and up to a maximum of six such pieces were used.

In practice these aims were not always achieved because, in certain instances, the slice would not cleave in the required orientation. CdS possesses three natural cleavage planes, which are parallel to the c-axis and are mutually inclined at 60° to each other, and a natural cleavage plane in a direction perpendicular to the c-axis. If the orientation of the CdS slice was such that one of the natural cleavage planes coincided with the direction in which the slice itself was to be cleaved, then the operation worked out as required. In other cases the natural cleavage planes were not always orientated

GENERAL ARRANGEMENT USED FOR MEASURING DIFFUSION DEPTHS USING THE OPTICAL METHOD

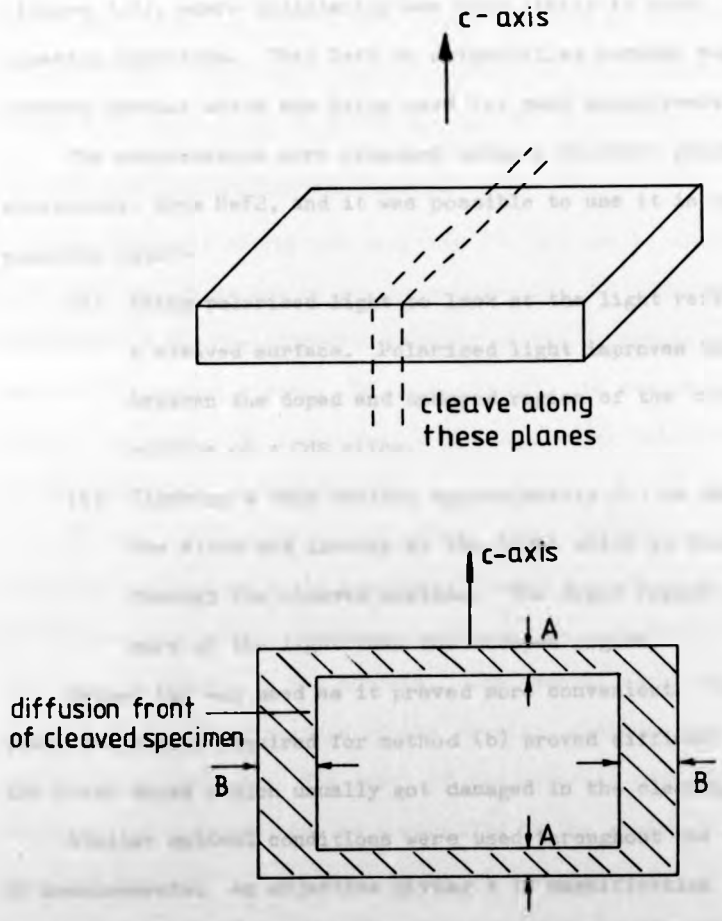

Fig 3·6

in the required direction and under these conditions the cleaving operation became more of a 'hit or miss' type of operation.

In general, it proved more difficult to obtain the desired fifteen measurements of $X_{\perp}$ than it did of $X_{\parallel}$. This is because taking measurements of $X_{\perp}$ involved taking measurements at the edge of the CdS slice (figure 3.6), where splintering was more likely to occur in the cleaving operation. This left an unidentified outside edge to the cleaved surface which was being used for such measurements.

The measurements were obtained using a Reichart projection microscope, type MeF2, and it was possible to use it in one of two possible ways:-

(a) Using polarised light to look at the light reflected from a cleaved surface. Polarised light improves the contrast between the doped and undoped region of the cleaved surface of a CdS slice.

(b) Cleaving a thin section approximately 0.1 mm thick from the slice and looking at the light which is transmitted through the cleaved section. The doped region absorbs more of the light than the undoped region.

Method (a) was used as it proved more convenient. The thin cleaved sections required for method (b) proved difficult to obtain as the outer doped region usually got damaged in the cleaving operation.

Similar optical conditions were used throughout the whole series of measurements. An objective giving x 16 magnification and an eyepiece giving x 8 magnification were used. The diffusion depths were measured using a graduated scale in the eyepiece, which had 100 divisions, where 1 division was equivalent to a distance of 0.917×10^{-2} mm. The depth of the doped region could be measured to an accuracy of $\pm$ 0.2 divisions.

Greater accuracy could have been obtained by using a higher magnification for the smaller depths, but it was decided to sacrifice the greater accuracy and use the same combination of eye-piece and objective throughout. It reduced the possibility of errors occurring due to any uncertainty which would have arisen in the magnification if several combinations had been used. The range of depths measured extended from a minimum of five divisions for the measurement of $X_{\parallel}$ and up to a maximum of 40 divisions for the measurement of $X_{\perp}$.

3.4 The electron microprobe analyser

The electron microprobe analyser (9, 10) can be used to obtain the same information as can be obtained using the RTS technique, which is the shape of the concentration profile of the diffusing atoms and the depth of the doped region. In this project, the measurements were carried out using the apparatus at the Centre for Materials Science at the University of Birmingham.

In this instrument the CdS slice, whose cleaved surface is to be analysed, is mounted in an evacuated chamber and the electron beam from an electron microscope is focussed onto a small circular area, smaller than 1 μm diameter, on the surface. The beam of electrons generates characteristic X-ray spectra of the chemical elements contained in the volume being analysed. The depth of the material under the surface, which can be analysed, can be controlled by the energy of the electron beam and the depth of penetration is of the order of 1 to 2 μm for an electron beam of 50 kV. The characteristic X-rays, which are generated, can be analysed using either a crystal diffractometer or a semi-conductor spectrometer. In this case a crystal diffractometer was used.

This type of analysis can be carried out with the electron beam

stationary or with the electron beam scanning over a small area. In this application one slow scan was made across the width of the cleaved surface of the CdS, as shown in figure 3.1, in order to measure the concentration profile of the impurity atoms diffusing into the slice from both flat surfaces.

A CdS slice, which had undergone diffusion, was cut in two by cleaving in a direction perpendicular to the flat surfaces. One part of the slice was mounted in cold setting metallurgical mounting plastic with the cleaved surface of the CdS slice exposed. As it was necessary for the plastic mount to be conducting when it was used on the electron microprobe, Zn dust was mixed in with the plastic before the liquid hardener was added. An equal volume of Zn dust and powder was used. After the plastic mounting material had set, the CdS specimen was then polished using successively finer grades of emery paper and diamond paste. The final polish used was 6 micron diamond paste.

A small piece of the dopant metal was embedded in the polished surface of the plastic mount and this was used as a reference standard. It was used to take a standard count before the start of a profile measurement and again after the completion of the profile. Appropriate correction factors (11) had to be applied to the measured signal from both the doped CdS slice and the metal standard to correct for variations in the penetration of the electron beam, the scattering coefficient of the targets and the self-absorption of the characteristic X-rays.

In this particular application the crystal diffractometer possessed a sufficiently high resolution to measure the intensity of the characteristic X-rays of the three metals which were used as dopants in the CdS.

3.5 Comparison of the experimental techniques used for measuring diffusion coefficients

The three experimental techniques, which are described in this chapter for measuring diffusion coefficients, are compared in this section and the uses, to which each of the techniques was put in this project, are also described.

The RTS technique can be used to study the self-diffusion and the inter-diffusion of any element as long as a convenient radioisotope of that element is available. The radioisotope must possess a long half-life and it must be possible to isolate, detect and measure the radiation that it emits. The technique can be used to measure the shape of the concentration profile of the total number of diffusing species, from which it is possible to obtain a mathematical model for the diffusion. This will also give information on the type of mechanism by which diffusion is taking place. It is possible to determine if diffusion is taking place by more than one mechanism and in fact such an observation has been made by several workers. For example: Zmija and Demianiuk (12) in their studies on the diffusion of noble metals into CdS and Shaw and Whelan (5) in their studies on the self-diffusion of Cd into CdS observed that there were two diffusing components. For the concentration dependent diffusion it is possible to determine both C_o and X using this technique.

The electron microprobe, like the RTS technique, can also be used to measure the total number of diffusing impurity atoms, but it does not possess such a range of sensitivities as the RTS technique. At low concentrations the signal obtained using the electron microprobe is swamped by the general background that is obtained from the

host material. For the diffusion measurements described in this thesis impurity concentrations as low as approximately 0.1% can be measured using the microprobe , whereas concentrations which are a factor of 100 lower than this can be measured using the RTS technique.

The optical method used in this project was very limited in its application. It can be used for measuring the depth of the doped region provided the diffusion front is sharp and can be viewed optically using a microscope. In fact such a situation is produced for the diffusion of a group III metal, such as In, into CdS where the diffusion anneal takes place in an ampoule containing excess group III metal and $D \propto C$. It was not possible to measure C_o or the shape of the concentration profile of the diffusing atoms using the optical method described in section 3.3.

Another comparison which is worthwhile making between the three experimental methods is the time it takes to carry out the measurements after the diffusion anneal has been completed. In the RTS technique, it takes between three and five days to prepare the CdS slice and to measure the diffusion profile. In the case of the electron microprobe the whole operation can be carried out in one day, whereas in the optical method the whole operation is very quick, it can be carried out in approximately one hour.

In general the three techniques described in this chapter can be used independently to measure the diffusion coefficient for the concentration dependent diffusion. It is seen in the introduction to chapter 5 of this thesis that,in order to evaluate the results fully, it was necessary to measure C_o and, as it is not possible to do this with each of the techniques described earlier in this chapter, combinations of techniques were used to get a full analysis.

For the diffusion of In into CdS in an excess In metal, where the diffusion is concentration dependent, two methods were used and one method acted as a check on the other. In the first method, the RTS technique was used for measuring both the diffusion profile and C_o in the CdS slices. In the second (OM technique) X and hence D_0 were obtained using the optical technique and the electron microprobe was used to measure C_o. In addition different proportions of CdS and In were sealed in the ampoules in the two techniques and the actual masses used are given in table 3.1.

For the measurements on the diffusion of In into CdS where excess In and Cd metals were placed in the ampoule, the RTS technique was used to measure the diffusion rate. Only one or two spot measurements were taken of C_o and these were obtained using the electron microprobe.

In the case of the Ga diffusions a full analysis was obtained using the OM technique as there was no convenient radioisotope of Ga. In the case of the Al diffusions there was only sufficient time to measure the diffusion rate using the optical method.

3.6. Sources of the material

In this section a brief description of the consumable materials (table 3.2) used in the project is given. In any project similar to the one described in this thesis, it is essential that high purity materials are used and that clean working conditions are used for preparing the ampoules for the diffusion anneal. The silica tubing was washed in dilute HNO_3 and ethyl methyl ketone and then it was baked out under vacuum to expel O_2 and H_2O from the inside walls of the tube. The metal and the CdS slice were washed in dilute HNO_3, ethyl methyl ketone and distilled water and were dried in a stream

TABLE 3.1: NOMINAL MASSES OF THE COMPONENTS PLACED IN EACH AMPOULE FOR THE DIFFUSION ANNEAL

Material diffusing into CdS	Technique used	Mass of components placed in the ampoule mg	Mass of metal* required to give a saturated vapour pressure in the ampoule at the highest temperature at which anneals were carried out.
Cd self-diffusion	RTS	CdS 150 Cd 20	60 mg at 1528 K
In	RTS	CdS 150 In 15	12×10^{-6} mg at 1275 K
In in the presence of inactive Cd	RTS	CdS 150 In 15 Cd 50	12×10^{-6} mg at 1275 K 19 mg at 1275 K
In	OM	CdS 60 In 50	55×10^{-6} mg at 1411 K
Ga	OM	CdS 60 Ga 30	120×10^{-6} mg at 1558 K
Al	OM	CdS 50 Al 30	500×10^{-9} mg at 1336 K

* due to pure metal, assuming no interaction

TABLE 3.2: DETAILS OF INACTIVE MATERIALS USED IN THE DIFFUSION ANNEALS

MATERIAL	MANUFACTURER	DETAILS
CdS	(a) The General Electric Co. Ltd., The Hirst Research Centre, Wembley, Middlesex.	Single crystal and polycrystalline material of unknown orientation. No impurities of concentration greater than 1 ppm.
	(b) Eagle-Picher Industries Incorporated, Miami Research Laboratories, Oklahoma, U.S.A.	Ultra high purity single crystal material. Resistivity 0.01 to 0.1 Ω m. Mobility greater than $0.0250\ m^2\ v^{-1}\ s^{-1}$.
	United Kingdom Distributors: New Metals & Chemicals Ltd., Chancery House, Chancery Lane, London WC 2.	Major impurity was Si, concentration < 5 ppm.
	(c) The Post Office Research Laboratories Dollis Hill, London.	Polycrystalline material, unknown orientation.
In	Johnson Matthey Chemicals Ltd., 74, Hatton Garden, London EC 1.	Grade 1. Maximum impurity 5 parts per million.
Ga	Koch-Light Laboratories Ltd., Colnbrook, Buckinghamshire.	Purity 99.999%
Al	Koch-Light Laboratories Ltd., Colnbrook, Buckinghamshire.	Purity 99.999%
Silica	Thermal Syndicate Ltd., P.O. Box 6, Wallsend, Tyne and Wear.	Transparent vitreous silica (Vitreosil). Contained over 99.9% SiO_2. Major impurities:- Al 30 parts per million; Ca 4 " " "; Li, Na 4 " " "

of warm air.

RTS techniques involve the handling of unsealed radioactive sources of relatively high specific activity and consequently the Code of Practice, set out by the International Commission for Radiological Protection (13), was followed. All the necessary precautions, that were used in the handling of the radioactive Cd for the measurement of the self-diffusion of Cd into CdS, are described in the author's M.Sc. thesis (6). As the specific activity of the radioactive In was similar to that of the Cd, similar precautions were taken for the handling of the radioactive In.

3.6.1. Cadmium Sulphide

In the investigations on the self-diffusion of Cd into CdS, CdS from three different sources was used. These are given in table 3.2. The material from The General Electric Company Limited was used for determining the activation energy and only spot measurements at a single temperature were carried out using CdS from the other two sources. For the measurements on the diffusion of group III metals into CdS, CdS from Eagle-Picher Industries Incorporated only was used. For this latter project cylindrical boules, approximately 10 mm in diameter and 10 g in weight, of ultra high purity single crystal material were purchased from the United Kingdom distributor. The boules were supplied with the c-crystallographic axis parallel to the axis of the cylinder. The orientation of the boules was checked using X-rays and polarised light (section 4.3). The CdS was produced by the vapour phase technique and a typical spectrographic analysis showed that the major impurity in the material was Si whose concentration was less than 5 parts per million. CdS slices, whose flat surfaces were perpendicular to the c-axis, were cut from the cylindrical boules with

a circular diamond saw for use in the majority of the diffusion measurements, but CdS slices of other standard orientations were used occasionally.

3.6.2 Radioactive Cd and In metal

The radioactive Cd and In metals were purchased in foil form from the Isotope Production Unit at the Atomic Energy Research Establishment, Harwell. High purity metal foil was sealed in a silica ampoule, then packed in a standard Al isotope can and placed in either the Dido or Pluto reactors. Suitable values of the neutron flux and the exposure times were arranged to give the required specific activity.

Five consignments of radioactive In were purchased at different times, each one containing 0.5 g of high purity In foil, which had been irradiated to give an activity of approximately 3 mCi due to the radioisotope $^{114m}_{49}In$ ($T_{\frac{1}{2}}$ = 50 d). At the end of the neutron exposure, each consignment of In was stored for two to three days at Harwell to allow the short lived activity, due to $^{116m}_{49}In$ ($T_{\frac{1}{2}}$ = 54.0 m), to decay away before it was despatched to Rugby by rail. The half-life of the radioactive In was measured over a long period of time and, in addition, gamma spectra of some of the samples were obtained. The results of these measurements are discussed in appendix A2.

3.6.3. Inactive In, Ga and Al

These metals were used for measuring the diffusion of group III elements into CdS using the OM technique. High purity materials were used and the full details are given in table 3.2.

3.6.4. Silica tubing

The ampoules were made from pure transparent vitreous silica tubing (Vitreosil) which contained over 99.9% SiO_2. Tubing possessing a range of diameters was used, the smallest possessed an internal diameter of 4 mm and the largest an internal diameter of 10 mm. The full details are given in table 3.2. SiO_2 does react with certain materials at high temperatures. Two of these materials are Al and Al_2O_3 where the reactions become significant at temperatures of 1073 K and 1273 K respectively. This point is discussed further in section 3.7.

3.7. Energy of formation of the oxides

When diffusion anneals are carried out in an evacuated silica ampoule, it is necessary that the elemental components used do not react with the CdS, the O_2 gas left in the ampoule or the SiO_2 of the ampoule itself. The energy of formation of the oxides of all the metals of group III have been calculated (14) and are tabulated in table 3.3. Crystalline forms of the oxides at 1000 K have been assumed in the calculations for two reasons: firstly, for ease of calculation and secondly, as this is a typical temperature at which the diffusion anneals were carried out.

The results presented in table 3.3 confirm the statement made in sub-section 3.6.4 about the reactivity between Al and SiO_2 at high temperatures. The oxide of Al is the most stable, which is then followed by SiO_2. The other metals listed, Tl, Cd, In and Ga are less reactive and are not likely to react with the SiO_2 of the ampoule during a diffusion anneal. The reaction, that was involved between the Al and the silica ampoule, is discussed in section 10.3, but there was no evidence at all of any of the other metals reacting with the SiO_2 during a diffusion anneal.

TABLE 3.3: ENERGY OF FORMATION OF THE OXIDES OF THE METALS USED IN THE DIFFUSION STUDIES

Reaction	Physical Form	Free energy F Cal $mole^{-1}$	Free energy F eV (O atom in oxide)$^{-1}$
$2Tl + \frac{3}{2}O_2 \rightarrow Tl_2O_3$	Crystal	-5.58×10^4	- 0.046
$\frac{1}{2}Cd + \frac{1}{2}O_2 \rightarrow CdO$	Crystal	-4.39×10^4	- 0.109
$2In + \frac{3}{2}O_2 \rightarrow In_2O_3$	Crystal	-18.3×10^4	- 0.151
$2Ga + \frac{3}{2}O_2 \rightarrow Ga_2O_3$	Crystal	-23.0×10^4	- 0.191
$Si + O_2 \rightarrow SiO_2$	β Cristobalite	-15.7×10^4	- 0.195
$2Al + \frac{3}{2}O_2 \rightarrow Al_2O_3$	Corundum	-30.6×10^4	- 0.253

Calculations are for 1000 K.

The free energy equation used is the one due to Helmholtz $F = H - TS$.

3.8 References

1. W. SEITH, Diffusion in Metallen (Second edition revised by T. Heuman), Springer - Verlag, Berlin (1955).
2. B. I. BOLTAKS, Diffusion in Semiconductors (Translated by J. I. Carasso, edited by H. J. Goldsmid), Infosearch Limited, London (1963).
3. T. H. YEH, Atomic Diffusion in Semiconductors (Edited by D. Shaw), P155, Plenum Press, London (1973).
4. B. TUCK, Introduction to Diffusion in Semiconductors, Institute of Electrical Engineers Monograph Series, Peter Peregrinus Ltd., Stevenage (1974).
5. D. SHAW and R. C. WHELAN, Phys. Stat. Sol., 36, P705 (1969).
6. E. D. JONES, Measurement of the Self-Diffusion of Cd into CdS using Radiotracer Sectioning Techniques, M.Sc. Thesis, University of Warwick (1971).
7. W. G. PRICE, Nuclear Radiation Detection, McGraw Hill Book Company, New York (1964).
8. L. MILLER, Engineering Dimensional Metrology, Edward Arnold Limited, London (1962).
9. P. J. GOODHEW, Electron Microscopy and Analysis, Wykeham Publications (London) Limited, London (1975).
10. P. R. THORNTON, Scanning Electron Microscopy, Chapman and Hall Limited, London (1968).
11. R. THEISEN, Quantitative Electron Microprobe Analysis, Springer-Verlag, Berlin (1965).
12. J. ZMIJA and M. DEMIANIUK, Acta Phys. Pol., A39, 5, P539 (1971).
13. Department of Employment and Productivity, Code of Practice for the Protection of Persons Exposed to Ionising Radiations in Research and Teaching, Her Majesty's Stationery Office, London (1968).
14. Handbook of Chemistry and Physics (Edited by R. C. Weast), Chemical Rubber Company Press, Cleveland, U.S.A. (1973).

4. Changes in the physical parameters for the diffusion of In into CdS

The changes, which occurred in the physical appearance and in the mass of the components placed in the ampoule for the In diffusion anneals, are described in this chapter. The relatively small number of diffusions described in chapter 8 were not included in this analysis. The majority of the diffusions carried out using In were used in the investigations described in chapters 5 and 6 and all of these have been included in the analysis described in this chapter. In addition, optical and X-ray investigations were carried out on the diffused specimens and the results of these are also described in this chapter.

4.1. Physical appearance

After the completion of the diffusion anneal, the outer surfaces of the CdS slices took on a darker appearance with the slices, which had been annealed with excess In metal in the ampoule, being much darker than the slices which had been annealed with excess In and Cd metals placed in the ampoule. In addition, for diffusion anneals carried out at temperatures above 1273 K, the inner surface of the ampoule possessed a slight yellow colouration. The metal globule itself, which was located at the end of the ampoule, which emerged from the furnace first at the end of a diffusion anneal, possessed a shiny bright surface. This indicated that the metal globule had not oxidised to any noticeable extent.

The doped regions of the CdS slices were much harder and more brittle than the undoped part. In the RTS technique the sectioning became easier as the number of sections that were removed increased. The ease with which sectioning could be carried out improved gradually for the slices, which had been annealed in excess In and Cd metals, whereas for the slices which had been annealed in excess In

metal only, there was little noticeable change for the first few sections and then there was an abrupt change. To avoid any possibility of breaking the CdS slice in the sectioning operation, care had to be taken not to apply too much pressure when grinding the first few sections from the slice. As the number of sections removed from any slice was increased, it was possible to increase the pressure applied to the slice gradually. For the sections, which were removed from the inner part of the slice, it was possible to let the whole mass of the pillar of the grinding jig (figure 3.3) rest on the CdS slice.

For the diffusions which were carried out in excess In metal only, occasionally the doped region broke away from the main part of the slice at the diffusion front during the sectioning. The brittleness problems, that were encountered in the sectioning of the CdS slices in the measurement of the diffusion coefficient using the optical method, are described in section 3.3.

4.2. Change in mass

The individual masses of all the components, that were placed in each ampoule for a diffusion anneal, were measured before they were sealed in the ampoule and again when they were removed from the ampoule after the diffusion anneal had been completed. For the anneals carried out in excess In metal only, the change in mass of the CdS slice, the mass of the In metal globule and the combined mass of the CdS and the In taken together, were obtained. For the anneals carried out in excess Cd and In metals, the change in mass of the CdS slice, the combined mass of the In and Cd taken together and the combined mass of all three components, were obtained.

All the mass changes, which occurred during the diffusion anneals,

are given as percentages of the original values. As the nominal masses of the components, which were placed in the ampoules, are given in table 3.1 the absolute mass changes can be calculated if they are required. This information is sometimes useful, as a total mass balance gives some idea of the weighing errors and of the deposits that remain on the inside of the ampoule.

It was not possible to determine all the mass changes listed above in all the diffusion anneals. In some of the anneals the In metal adhered to the inside surface of the ampoule with the result that it was not possible to remove it, in its entirety, from the ampoule. In other cases the CdS slice got broken as the ampoule was either pushed into the centre of the furnace at the start of a diffusion anneal, or as it was removed from the furnace at the end of the anneal. On other occasions the CdS slice and the molten metal globule ended up attached to each other after they had been removed from the furnace. In the early days of the project, when diffusion anneals involving the RTS technique were carried out, only the change in mass of the CdS slice was measured.

It was possible to measure the complete set of mass changes listed above in 75% of all the diffusion anneals carried out. In the remaining 25% a complete set of weighings was not obtained because of the reasons listed above. It was possible to calculate the change in mass of the CdS slice in 95% of all the diffusion anneals carried out.

The CdS slices were not treated in any way at the end of the diffusion anneal to remove any metallic vapour which may have condensed on to the surface of the slice when it was taken out of the diffusion furnace. As the metal globule and the CdS slice were located at opposite ends of the ampoule during the diffusion anneal,

it was assumed that the major portion of the metal vapour condensed onto the metal globule, as it was located at the end of the ampoule that emerged first from the hot zone of the furnace.

The results obtained will be discussed under three separate sub-headings. The most comprehensive set of results was obtained for the diffusion anneals carried out in excess inactive In metal only and these results, which are discussed first, will be discussed in detail. The results obtained for the diffusions carried out in excess radioactive In metal only will be discussed second and the diffusions carried out in excess inactive Cd and radioactive In metals will be discussed third.

4.2.1. Diffusions carried out in excess inactive In metal

In this series of measurements 76 diffusion anneals were carried out and a complete set of all the mass changes, listed at the beginning of this section, was obtained in 59 of the diffusions. The details of the diffusion runs are given in table 6.1.

The mass changes, obtained in each of the runs listed in table 6.1, were averaged and it is these average values that are plotted in figure 4.1 as a function of the anneal temperature. The CdS showed a steady decrease in mass with increase in temperature, whereas the In metal showed a steady increase. The results for run 122b did not fall into this general pattern and the reason will be given later. The change in the combined mass of both components remained constant with temperature.

It was not possible to detect any other correlation between the change in the mass of the components of the ampoule and any other diffusion parameter. The overall average decrease in the mass of the CdS slice was 4.2% whereas the In showed an increase of 4.3%.

THE CHANGE IN MASS OF THE CONTENTS OF THE AMPOULES FOR THE DIFFUSION OF In INTO CdS

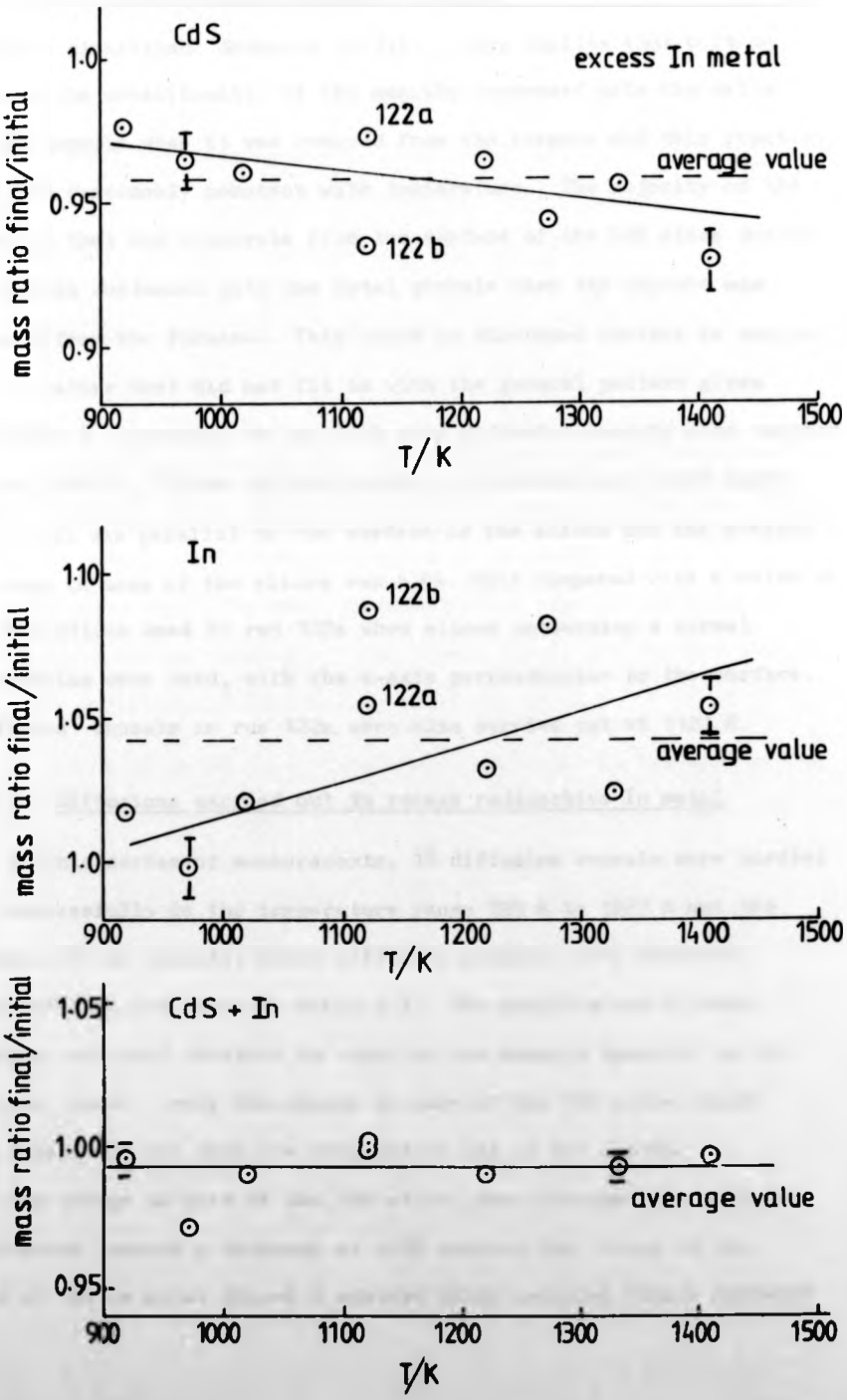

Fig 4-1

The change in the combined masses of the constituents of the ampoule showed a significant decrease (0.7%). This implies that 0.7% by mass of the constituents of the ampoule condensed onto the walls of the ampoule when it was removed from the furnace and this fraction remained reasonably constant with temperature. The majority of the material that did evaporate from the surface of the CdS slice during the anneal condensed onto the metal globule when the ampoule was removed from the furnace. This point is discussed further in chapter 8.

A feature that did not fit in with the general pattern given in figure 4.1 occurred in run 122b when diffusion anneals were carried out at 1120 K. Slices of non-standard orientation were used where the c-axis was parallel to the surface of the slices and the average decrease in mass of the slices was 6.6%. This compared with a value of 2.8% for the slices used in run 122a when slices possessing a normal orientation were used, with the c-axis perpendicular to the surface. Diffusion anneals in run 122a were also carried out at 1120 K.

4.2.2. Diffusions carried out in excess radioactive In metal

In this series of measurements, 18 diffusion anneals were carried out successfully in the temperature range 729 K to 1287 K and the details of the anneals, where diffusion profiles were measured successfully, are given in table 5.1. The complete set of mass changes was only obtained in eight of the anneals because, in the earlier ones, only the change in mass of the CdS slice itself was determined and this was obtained in all of the anneals.

The change in mass of the CdS slice, when averaged over all the diffusions, showed a decrease of 1.8% whereas the change in the mass of the In metal showed a scatter which extended from a decrease

of 1.5% to an increase of 10.7%. The average value was an increase of 3.7%. A possible reason for this variation was due to the fact that the mass of In placed in the ampoule was much lower than for the optical measurements which are described in sub-section 4.2.1. The overall change in the combined mass of the constituents of the ampoule showed a decrease of 1.1%.

4.2.3. Diffusions carried out in excess radioactive In and inactive Cd metals.

In this series of measurements, 14 diffusion anneals were carried out in the temperature range 727 K to 1286 K and the details of the diffusion anneals, in which profiles were successfully measured, are given in table 5.4. The complete set of mass changes was measured in only five of the anneals and the change in the mass of the CdS slice was successfully measured in 12 of the anneals.

In this case there was a much smaller decrease in the mass of the CdS slice; an average value of 0.3% was obtained. This relatively small decrease in mass was probably due to the presence of excess Cd metal in the ampoule, during the diffusion anneal, suppressing any evaporation of Cd and S atoms from the surface of the CdS slice.

The average change in the combined mass of the In and Cd metal showed a decrease of 2.9% and the change in the combined mass of all the constituents in the ampoule was a decrease of 1.1%.

4.3. X-ray measurements

The CdS used in this project was purchased in single crystal 10 g boules, which were cylindrical in shape, with the axis of the cylinder in the [0001] direction. The details are given in sub-section 3.6.1. The orientation of the cylindrical boules was checked

using Laue back reflection techniques. A total of five such boules were purchased at periodic intervals and the orientation of all of the boules was found to be correct to within $\pm$ 3 degrees except for the second one. In this case the cylindrical axis of the boule was found to be perpendicular to the $[0001]$ direction.

X-ray Laue photographs were obtained from several different parts of each boule in order to ensure that it was a single crystal throughout its entire volume. In addition, this was also checked using polarised light. In fact all the boules were found to be single crystal material.

Unfortunately, the orientation of the first two boules of CdS used in this project was not checked until the majority of the diffusion profiles had been measured using the RTS technique. When it was discovered that the second boule did not possess the expected orientation, the orientation of all the CdS slices, which had previously been used in this part of the project, were checked individually using Laue back reflection techniques. This point affected the measurements described in chapter 5.

A rotating crystal technique using Cu K_α X-rays was used to test if there was any difference between the lattice parameters of the In-doped part of the crystal and the pure undoped part for the slices which were diffused in an ampoule containing excess In metal. The experimental details on this investigation are discussed further in appendix A3. The conclusions reached were that the doped part of the crystal possessed the same crystal structure as the undoped part and it was not possible, to within an accuracy of 500 parts in 10^6, which can be obtained at high Bragg angles, to detect

any change in the lattice spacing.

In the diffusions that were carried out in excess In metal, it has been established (section 7.2) that the In is incorporated into the Cd sub-lattice with three Cd atoms diffusing out of the crystal for every two In atoms that diffuse into the crystal. This results in an increase in the vacancy concentration in the doped part of the crystal which is much greater than the thermal equilibrium concentration of the undoped material. It was suspected that this would result in the In-doped part of the crystal possessing a slightly smaller lattice spacing than the undoped part. The X-ray result indicated that if there was any such change produced in the lattice spacing it must have been very small (less than 0.1%, see sub-section 1 of appendix A3).

In spite of the fact that it was not possible to detect any change in the lattice parameters of the doped part of the CdS slice using X-ray techniques, a small relaxation did occur in the crystal structure at the interface which did produce a strain in the lattice. This has been confirmed optically and is described in section 4.4. An additional point which confirms this is discussed in section 4.1 where, in certain instances, the doped region did break away from the main part of the slice at the interface between the two regions.

4.4. Microscopic investigations

After the completion of the diffusion anneals, the surfaces of the CdS slices were examined using an optical microscope to see if there had been a deterioration in the quality of the surfaces. In fact no such deterioration was observed.

Microscopic methods were also used to examine the cleaved surfaces of sections approximately 0.5 mm thick, which were removed from the

CdS slices that had undergone a diffusion with excess In metal in the ampoule. The pattern of the cleavage steps that were present in the cleaved surfaces often changed at or near the diffusion boundary indicating that there was a strain in the lattice at this interface. In fact the use of reflected illumination in this instance was very restricted because it was only possible to observe defects on the surface. It was advantageous to examine cleaved sections using transmitted illumination because it was then possible to focus on defects that were present in the volume of the slice.

5. Diffusion of In into CdS using the RTS technique.

In this chapter the results of the measurements of the diffusion of In into CdS, which have been obtained using the RTS technique, are discussed. In fact, two different sets of conditions were used in the diffusion anneals. In the first set, the CdS slices were annealed with excess radioactive In metal only in the ampoule - where the calculated final value of the atomic ratio of Cd to In atoms in the metal globule was 2×10^{-3}. This ratio was calculated from the stoichiometric exchange between the In atoms from the metal globule with Cd atoms of the CdS slice on a two to three basis when In diffuses into CdS as is explained in the next paragraph. The significance of the Cd/In ratio on the diffusion anneals will be discussed in chapter 8. In the second set, excess inactive Cd and radioactive In metals were placed in the ampoule. The calculated final Cd/In ratio in this case was 3.4 and in addition to being much higher than the value obtained in the first set of measurements, it remained reasonably constant throughout the anneal. The radioactive In used in these experiments was naturally occurring neutron irradiated metal.

The diffusion profiles in the former set of measurements were found to be concentration dependent with $D \propto C$. It will be shown in chapter 7, using the In concentration measurements presented in this chapter, that diffusion probably took place via the mobile defect $(In_{Cd}^{\bullet} V_{Cd}^{''})'$ and that the In was incorporated onto the Cd sub-lattice with three Cd^{2+} ions leaving the lattice for every two In^{3+} ions that enter.

The measured diffusion coefficient D_o varied with temperature according to the equation

$$D_o = D_f \exp\left[\frac{-E_T}{kT}\right] \qquad 5.1$$

where:

D_f is a pre-exponential frequency factor which has dimensions $(\text{length})^2\ (\text{time})^{-1}$;

E_T is the total activation energy and is expressed in eV per atom in this thesis.

The measurement of the near-surface In concentration C_o, described in section 5.2, showed that C_o increased exponentially with temperature (1) as given by the following equation

$$\frac{C_o}{C_f} = A \exp\left[\frac{-E_F}{kT}\right] \qquad 5.2$$

where:

C_f is the concentration of cation sites in the crystal and has dimensions atoms $(\text{volume})^{-1}$;

A is a pre-exponential entropy term which is dimensionless;

E_F is the activation energy for dissolving In in CdS under these conditions and is expressed in eV per atom in this thesis.

In the case of the concentration dependent diffusions it was possible to normalise the experimental values of the diffusion coefficients D_o, which is the diffusion coefficient corresponding to an In concentration C_o. An In concentration of 1% was chosen and the variation of the normalised diffusion coefficient D'_o with temperature is given by the following equation

$$D'_o = D'_f \exp\left[\frac{-E_M}{kT}\right] \qquad 5.3$$

where:

D_f' is a pre-exponential factor which has dimensions $(\text{length})^2 (\text{time})^{-1}$ $(\text{at \%})^{-1}$;

E_M is, as can be seen from equation 2.5, the activation energy of motion of the mobile defect in CdS and is equal to $(E_t - E_F)$.

It has been assumed in the above equations that the nature and the proportion of the defects causing the diffusion remains constant over the range of temperatures covered.

As is mentioned in section 2.6, Chern and Kröger (2) obtained concentration dependent profiles for the diffusion of In into CdS but they were unable to explain the curves fully. An analysis similar to the one described above was used by Perkins and Rapp (3) in the measurement of the diffusion of Cr in single crystals of NiO. Trivalent Cr ions occupy Ni sites when dissolved in NiO and charge neutrality is maintained by the formation of V''_{Ni} (4). $NiCr_2O_4$, which has a spinel structure, is known to exist with NiO and when equilibrium between the two is obtained defect equilibrium is described by

$$NiCr_2O_4 \rightleftharpoons 4O_o + Ni_{Ni} + 2Cr^{\bullet}_{Ni} + V''_{Ni} . \qquad 5.4$$

NiO is a metal deficient semiconductor with vacancies in the Ni sub-lattice. If the concentration of native vacancies is greatly exceeded by the Cr ion concentration the electro-neutrality condition becomes

$$\left[Cr^{\bullet}_{Ni}\right] = 2\left[V''_{Ni}\right] . \qquad 5.5$$

An electro-neutrality condition of a similar form was used by Kumar and Kröger (5) for their Cd self-diffusion measurements in In-doped CdS and in the present work for diffusions which were carried out with

excess In metal in the ampoule. For the diffusion of Cr into NiO, Perkins and Rapp stated that because of their electrostatic attraction, the defects exist in two forms $(Cr^{\bullet}_{Ni}\ V''_{Ni})^{i}$ and $(Cr^{\bullet}_{Ni}\ V''_{Ni}\ Cr^{\bullet}_{Ni})^{*}$ and diffusion will occur by a vacancy mechanism. At low temperatures the triple defect will predominate but as the temperature increases $\left[Cr^{\bullet}_{Ni}\ V''_{Ni}\ Cr^{\bullet}_{Ni}\right]$ will decrease and $\left[Cr^{\bullet}_{Ni}\ V''_{Ni}\right]$ will increase. Perkins and Rapp predicted that at low temperatures diffusion is concentration independent becoming concentration dependent at high temperatures where the two member complexes predominate. At temperatures of 1273 K and above, their diffusion profiles showed a reasonable fit to the theoretical model developed where Cr diffuses by a two member complex.

The diffusion of Cr into NiO has also been studied by Greskovich (6) where again he obtained concentration dependent profiles and the graphs he obtained showing the $D \propto C$ relationship are reproduced in figure 5.4a.

The diffusion of Cr into NiO and MgO has also been studied respectively by Chen et al (7) who used a tracer sectioning technique, and by Weber et al (8), who used a surface activity loss method, but in these cases concentration independent profiles were obtained. This can probably be ascribed to the use of much smaller quantities of radioactive tracer in the diffusion anneal. Solaga and Mortlock (9) studied the diffusion of Sc^{3+} into MgO using a surface activity loss method and noticed that at concentrations above 50 parts per million the concentration profiles were indicative of a concentration dependent diffusion, but below this concentration the profiles were concentration independent.

The diffusion profiles in the second set of In diffusion measurements, described in section 5.4, were found to be consistent with what was

observed by Chen et al, Weber et al and by Solaga and Mortlock for low dopant levels. The diffusion profiles were concentration independent, the diffusion coefficients and the In concentrations in the CdS were lower than for the concentration dependent case described in section 5.1. This is because the addition of inactive Cd metal to the ampoule possibly decreased the In vapour pressure in the ampoule during the anneal. The diffusion mechanism in this case was probably a simple vacancy one.

An attempt has been made to propose a defect model for the diffusion mechanism in each set of experiments. In order to do this it has been necessary to calculate the Cd partial pressure in the ampoule and to evaluate the defect structure proposed by Kröger et al (5) from their self-diffusion studies using pure CdS and In-doped CdS. It has also been necessary to consider the results obtained by the workers mentioned above on the diffusion of group III metals into NiO and MgO. This will be discussed in chapter 7.

The half-lives of the consignments of radioactive In, which were purchased from the Isotope Production Unit at Harwell, were checked throughout the duration of the project. In addition, gamma-ray spectra of some of the consignments and of some of the In-doped CdS slices were measured. All the consignments, except for the second one, decayed with the expected half-life of 40.0 d due to the isotope $^{114m}_{49}In$. The second consignment of In did contain a radioactive impurity whose half-life was slightly shorter than that due to $^{114m}_{49}In$ and the consignment did contain minute traces of long lived radioactive impurities. The presence of these impurities did not affect the accuracy of the results of the diffusion measurements in any way. These measurements are discussed in detail in appendix A2.

5.1. The diffusion of In into CdS in the presence of low Cd/In metal ratios.

The diffusions described in this section were carried out with excess In metal only in the ampoule and the profiles were found to fit very closely to a one dimensional spatial solution to the diffusion equation given by Wagner (section 2.3), where it was assumed that $D \propto C$ and the surface concentration C_o was constant. The diffusion coefficient D_o can be determined from the depth of the doped region X which is sharply defined for this type of diffusion.

5.1.1. General considerations

After the completion of the diffusion anneal, the concentration profile of the In, which had diffused into the CdS from the flat surfaces, was measured using the procedure described in section 3.2. Eighteen diffusion runs were carried out successfully in the temperature range 729 K to 1287 K and the full diffusion details are given in table 5.1. A typical concentration profile is plotted on semi-logarithmic paper in figure 5.1 and the analysis of the diffusion profiles will be discussed in more detail in sub-section 5.1.2.

All the discs of emery paper used in the sectioning of the CdS slices were counted on the low background counter, where the maximum count rate obtained was 25 counts per second. The majority of the counts were of 1000 s duration, except for the sections which were removed from the slice near the end of a diffusion profile, where the count rates from the removed section alone were comparable with natural background. In these cases count periods of up to 10^5 s were used. Background counts were either measured overnight or over a weekend and such counts were usually obtained before the measurement

TABLE 5.1. EXPERIMENTAL DATA FOR THE DIFFUSION OF In INTO CdS IN THE PRESENCE OF EXCESS In METAL USING THE RTS TECHNIQUE

Run number	Temperature T K	1000/T K^{-1}	Duration s	Orientation	Area $10^{-6} m^2$	Diffusion depth X $10^{-6} m$	$D_o = 0.3811 \left(\frac{\chi^2}{t}\right)$ $m^2 s^{-1}$	$D'_o = D_o \left(\frac{C_f}{C_o}\right)$ $m^2 s^{-1}$ ☆$^{-1}$	Number of slices removed	Number of points used in curve fitting	Average amount removed per section	
											thickness $10^{-6} m$	mass $10^{-3} kg$
102b	829	1.206	2.259,6	Parallel	14.18	27.0	1.230,-16	1.268,-15	14	8	3.150	3.011
103	1078	0.928	1.494,5	Parallel	13.68	155	6.128,-14	1.075,-13	17	14	10.54	11.81
105	983	1.017	2.641,5	Parallel	8.43	85.0	1.043,-14	3.161,-14	18	13	6.155	4.501
105a	1193	0.838	1.440,5	Parallel	8.03	147	5.719,-13	5.552,-13	27	21	6.770	7.073
106b	1193	0.838	1.440,5	Parallel	5.60	210	1.167,-12	1.133,-12	16	11	16.67	7.201
107	778	1.285	2.065,5	Parallel	19.18	8.00	1.181,-17	2.010,-16	12	7	1.912	2.120
108a	1282	0.777	3.600,3	Parallel	8.39	175	3.242,-12	2.161,-12	13	11	14.91	7.791
109f	1143	0.875	8.670,4	Parallel	13.22	240	2.506,-13	3.094,-13	47	40	5.176	15.51
109g	1126	0.888	2.625,5	Parallel	13.91	285	1.180,-13	1.580,-13	36	25	8.830	21.31
109j	1126	0.888	1.800,4	Parallel	11.21	104	2.268,-13	3.036,-13	26	20	4.961	6.972
109m	1129	0.886	5.670,4	Perpendicular	11.79	270	4.900,-13	6.447,-13	52	48	5.459	16.13
109w	1137	0.880	1.730,5	Perpendicular	3.15	433	4.130,-13	5.238,-13	46	34	12.53	8.755
114	729	1.372	8.454,6	Perpendicular	11.92	5.03	1.127,-18	3.364,-17	11	4	3.237	2.046
115a	981	1.019	1.296,6	Perpendicular	3.83	340	3.394,-14	1.054,-13	40	33	10.99	8.105
116a	1027	0.974	7.738,5	Perpendicular	15.52	270	3.590,-14	8.407,-14	43	37	7.553	24.30
118a	772	1.295	1.313,7	Perpendicular	20.96	16.0	7.430,-18	1.356,-16	14	8	2.250	3.152
119a	880	1.136	2.089,6	Perpendicular	12.89	63.0	7.241,-16	4.733,-15	19	16	4.674	5.520
120a	1275	0.784	1.080,4	Perpendicular	7.49	330	3.843,-12	2.669,-12	34	32	11.08	13.60

CONCENTRATION PROFILE FOR THE DIFFUSION OF In INTO Cd S.

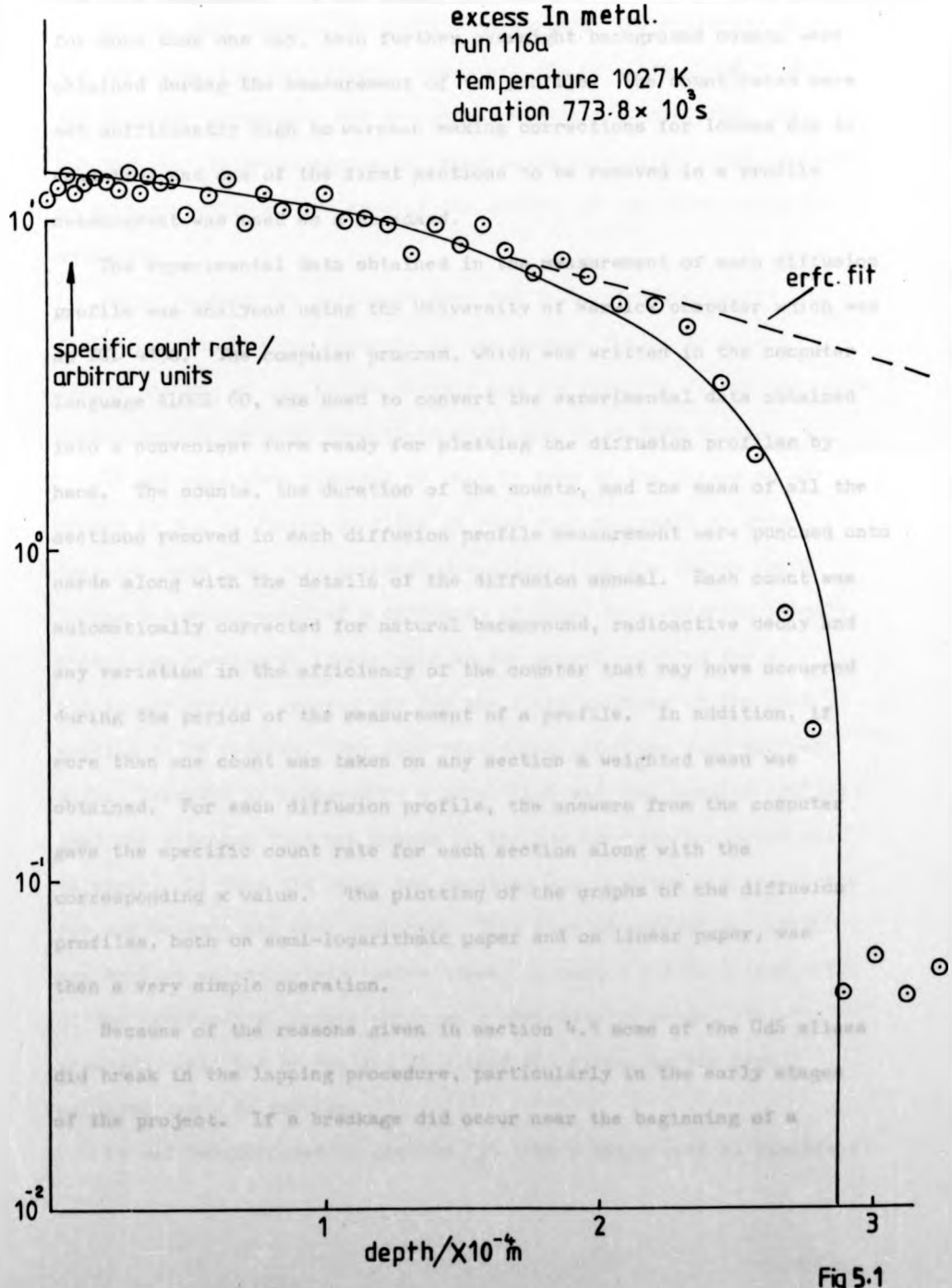

Fig 5.1

of the profile commenced and again when the measurement of the profile had been completed. If the measurement of a diffusion profile continued for more than one day, then further overnight background counts were obtained during the measurement of the profile. The count rates were not sufficiently high to warrant making corrections for losses due to dead time and one of the first sections to be removed in a profile measurement was used as a standard.

The experimental data obtained in the measurement of each diffusion profile was analysed using the University of Warwick computer which was an ICL 4130. The computer program, which was written in the computer language ALGOL 60, was used to convert the experimental data obtained into a convenient form ready for plotting the diffusion profiles by hand. The counts, the duration of the counts, and the mass of all the sections removed in each diffusion profile measurement were punched onto cards along with the details of the diffusion anneal. Each count was automatically corrected for natural background, radioactive decay and any variation in the efficiency of the counter that may have occurred during the period of the measurement of a profile. In addition, if more than one count was taken on any section a weighted mean was obtained. For each diffusion profile, the answers from the computer gave the specific count rate for each section along with the corresponding x value. The plotting of the graphs of the diffusion profiles, both on semi-logarithmic paper and on linear paper, was then a very simple operation.

Because of the reasons given in section 4.1 some of the CdS slices did break in the lapping procedure, particularly in the early stages of the project. If a breakage did occur near the beginning of a

profile measurement then the run was usually abandoned. In certain cases the slice broke cleanly into two pieces and, if it was possible to measure their areas, the profile measurement was continued with the larger of the two pieces. Sometimes the breakage occurred after the specific count rate had decayed by a factor of more than 100, but the profile measurements in these cases were still valid provided an accurate value of the area of the surface of the slice could be obtained.

Other reasons why diffusion runs had to be abandoned were: failure of the heating elements in the furnace during an anneal, faulty sealing of the silica ampoule and the breakage of the CdS slice during one of the many operations which had to be undertaken.

It was sometimes possible to rectify some of the points on the graphs of the diffusion profiles if they were obviously in error, that is, more than five standard deviations from the fitted curve. During the measurement of a diffusion profile, each weighing usually served two functions; it was used as the second weighing for a particular section removed and for the first weighing of the next section to be removed. Any incorrect point,which was high and was either preceded or followed by a point that was low, usually implied that the weighing that was common to the two sections concerned was in error. If this did occur the weighing was rejected and the counts for the two sections were combined. This type of correction, which was applied approximately twelve times, accounted for more than half of the experimental points which were obviously in error. This practice could not be applied to either the first, or the last weighing taken in any day.

It was demonstrated in section 3.3 that a sharp optical interface

existed between the doped and the undoped parts of the crystal. The RTS technique showed that the concentration of the diffusing In atoms dropped rapidly at the interface but the method did not possess a sufficiently good resolution to show that the interface was sharply defined.

5.1.2. Verification of the concentration dependent diffusion

The main aim of this section is to establish what type of concentration dependency the In concentration profiles possessed.

From an inspection of the shape of the In concentration profiles it was suspected that the curves possessed a similar shape to the concentration dependent profiles computed by Weisberg and Blanc (10) where $D \propto C^n$ with n = 1, 2 or 3. The most convenient way of showing this was to calculate the diffusion coefficient as a function of concentration using the Boltzmann-Matano formula (11) for each profile. The formula is

$$D(C_1) = -\frac{1}{2t}\left(\frac{dx}{dC}\right)_{C_1}\int_0^{C_1} x\,dC \,. \qquad 5.6$$

The diffusion coefficient in each profile was determined as a function of the normalised In concentration C/C_o. A typical plot is shown in figure 5.2 and the values of n which were obtained are tabulated in table 5.2.

Very little weighting was given to the experimental points which were more than three standard deviations from the best hand fitted curve drawn through the set of points. The first two points on each diffusion profile were ignored in the hand fit as these points were liable to be in error. The possible reasons for this were the condensation of radioactive In on to the surface of the CdS slice as

A TYPICAL PLOT OF THE DIFFUSION COEFFICIENT AS A FUNCTION OF In CONCENTRATION.

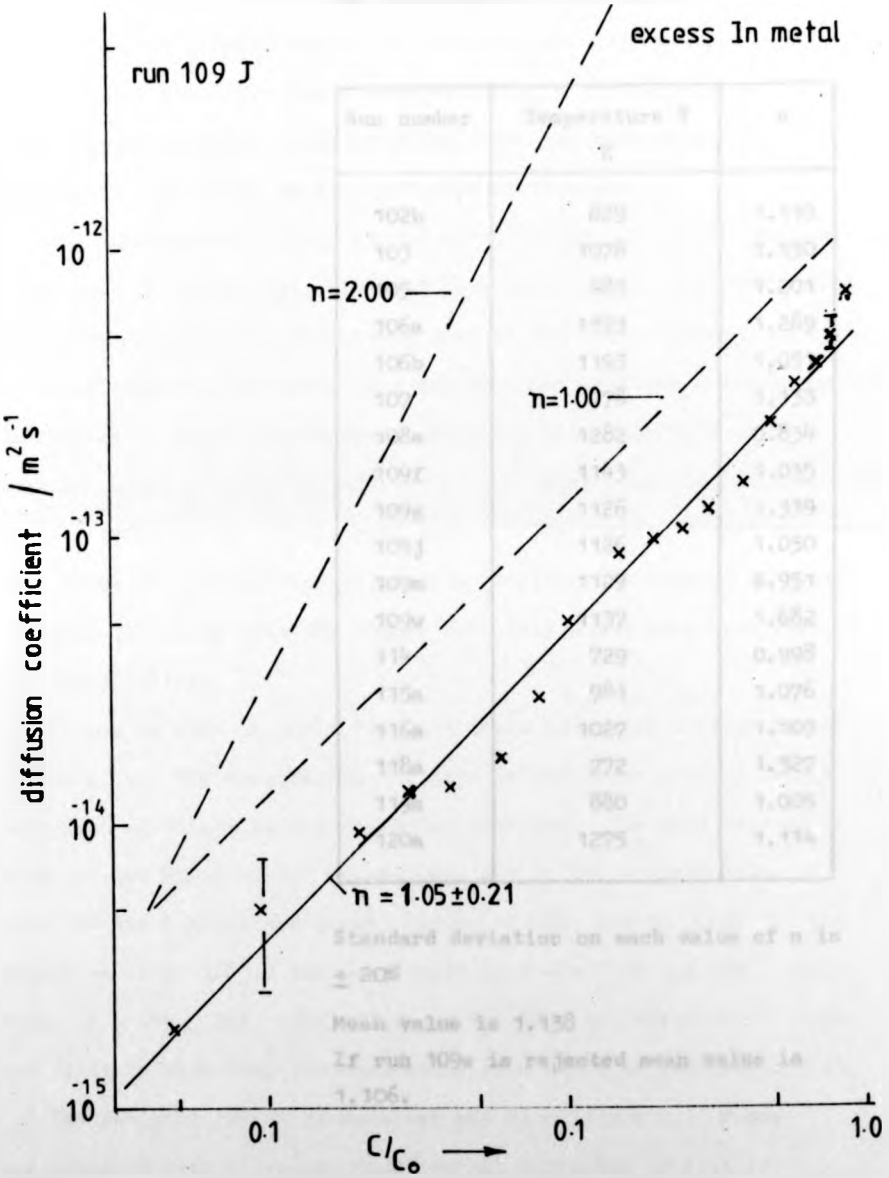

Fig 5.2

TABLE 5.2. TABULATION OF VALUES OF n OBTAINED IN THE BOLTZMANN-MATANOANALYSIS.

Run number	Temperature T K	n
102b	829	1.110
103	1078	1.150
105	983	1.201
106a	1193	1.289
106b	1193	1.051
107	778	1.133
108a	1282	0.834
109f	1143	1.035
109g	1126	1.339
109j	1126	1.050
109m	1129	0.951
109w	1137	1.682
114	729	0.998
115a	981	1.076
116a	1027	1.109
118a	772	1.327
119a	880	1.005
120a	1275	1.114

Standard deviation on each value of n is ± 20%

Mean value is 1.138

If run 109w is rejected mean value is 1.106.

the ampoule was removed from the furnace at the end of the diffusion anneal. In addition it is possible that the deviation at high values of C/C_o may be genuine due to the drop in the surface concentration with time as the Cd/In ratio changes during a diffusion anneal. This would result in a low value of dC/dx near the surface and a spuriously high value of the diffusion coefficient.

The experimental points at the end of a profile, where the specific count rate flattened out, have not been used in the Boltzmann-Matano analysis. The points, which were used in the curve fitting, contained a contribution to the count rate due to a fast diffusion mechanism that was present. This contribution, which was less than 0.1% of the specific count rate at the surface of the slice, did not influence the curve fitting to any significant extent. The number of sections, which were removed from each CdS slice in a profile measurement, is given in table 5.1 along with the number of points which have been used in the curve fitting.

It can be seen in table 5.2 that there is a wide scatter in the values of n. The main reason for this is the large scatter in the experimental points in the diffusion profiles. The main sources of error in the Boltzmann-Matano analysis are in the determination of dx/dC at the highest and lowest values of C/C_o and in $\int xdC$ at the lowest value of C/C_o. The mean value of n was 1.14 and the overall error in n was $\pm$ 20%. The value for run 109w is exceptionally high and if it is rejected, the mean value of n would be reduced to 1.11.

The computed curves of Weisberg and Blanc for n = 1, 2 and 3 are compared with a typical experimental diffusion profile in figure 5.3. The experimental curve is the best hand fit through the experimental points in concentration profile run 116a shown in figure 5.1 and the computed curves were normalised to the experimental

A TYPICAL DIFFUSION PROFILE SHOWING THE COMPUTED CONCENTRATION DEPENDENT CURVES.

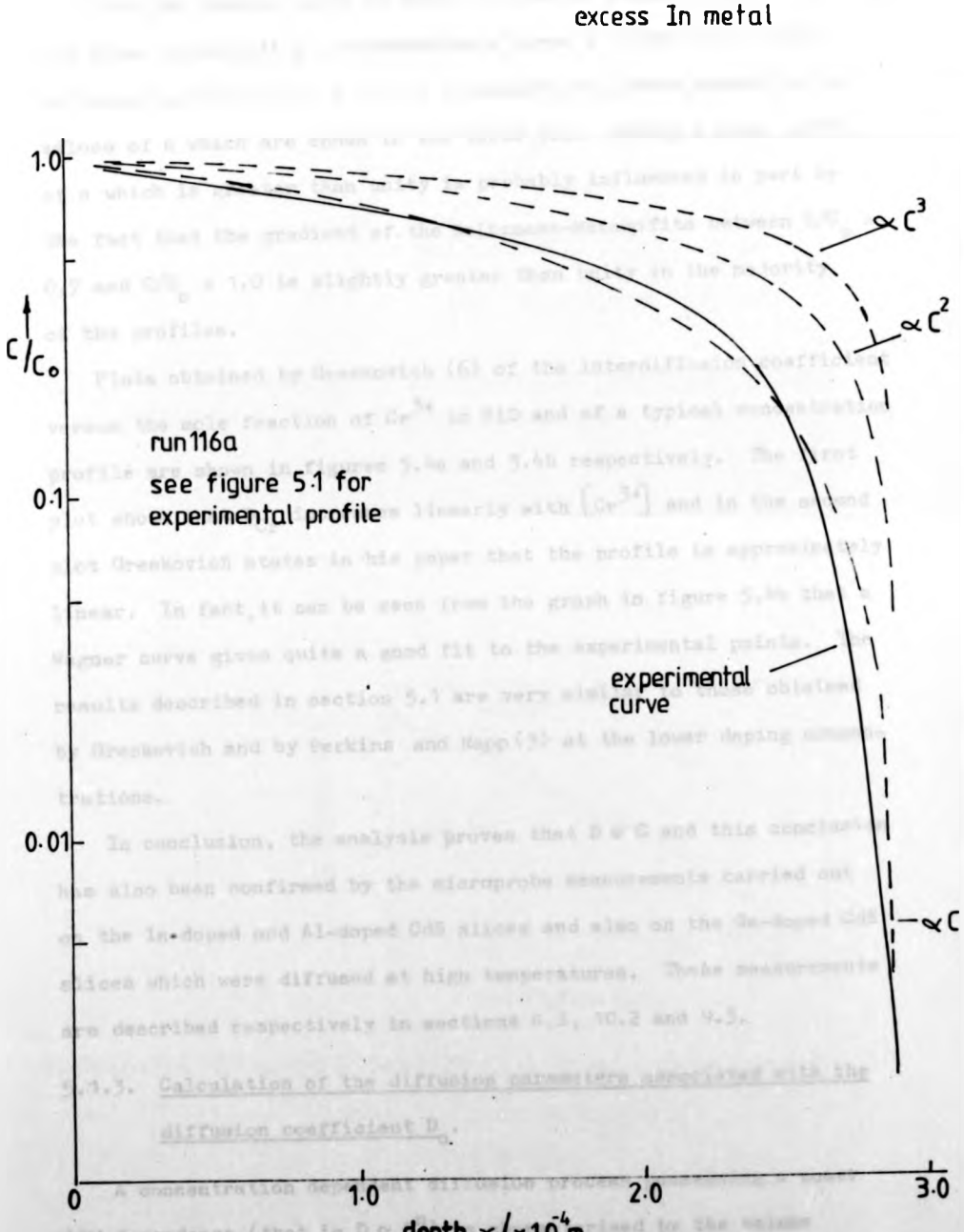

Fig 5.3

curve at x = 0 and at x = 2.9 x 10^{-4} m.

From the results given in table 5.2 and in figure 5.3 the Weisberg and Blanc curve with n = 1 undoubtedly gives a better fit to the diffusion profiles than n = 2 or 3, despite the large spread in the values of n which are shown in the table 5.2. Having a mean value of n which is greater than unity is probably influenced in part by the fact that the gradient of the Boltzmann-Matano fits between C/C_o = 0.7 and C/C_o = 1.0 is slightly greater than unity in the majority of the profiles.

Plots obtained by Greskovich (6) of the interdiffusion coefficient versus the mole fraction of Cr^{3+} in NiO and of a typical concentration profile are shown in figures 5.4a and 5.4b respectively. The first plot shows that D_{Cr} increases linearly with $[Cr^{3+}]$ and in the second plot Greskovich states in his paper that the profile is approximately linear. In fact, it can be seen from the graph in figure 5.4b that a Wagner curve gives quite a good fit to the experimental points. The results described in section 5.1 are very similar to those obtained by Greskovich and by Perkins and Rapp (3) at the lower doping concentrations.

In conclusion, the analysis proves that $D \propto C$ and this conclusion has also been confirmed by the microprobe measurements carried out on the In-doped and Al-doped CdS slices and also on the Ga-doped CdS slices which were diffused at high temperatures. These measurements are described respectively in sections 6.3, 10.2 and 9.3.

5.1.3. Calculation of the diffusion parameters associated with the diffusion coefficient D_o.

A concentration dependent diffusion process possessing a power law dependence (that is $D \propto C^n$) is characterised by the volume

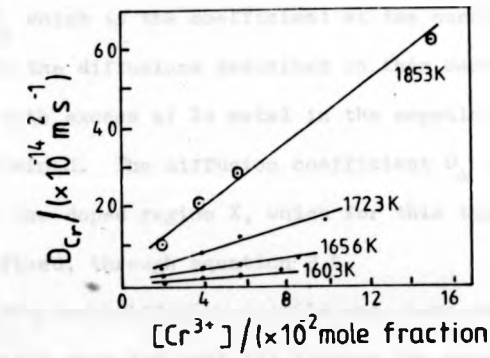

Fig 5.4a LINEAR DEPENDENCE OF INTERDIFFUSION COEFFICIENT ON MOLE FRACTION Cr^{3+} IN NiO (FROM GRESKOVICH (6))

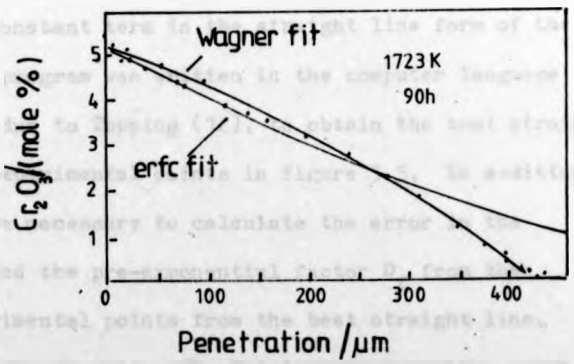

Fig 5.4b CONCENTRATION PROFILES OF Cr_2O_3 IN NiO (FROM GRESKOVICH (6))

Fig 5.4a,5.4b

diffusion coefficient D_o which is the coefficient at the surface of the slice at x = 0. For the diffusions described in this section, which were carried out with excess of In metal in the ampoule, a $D \propto C$ dependence was obtained. The diffusion coefficient D_o is related to the depth of the doped region X, which for this type of diffusion is sharply defined, through equation 2.4.

The magnitude of X for each diffusion profile was where the Weisberg-Blanc curve, which gave the best fit through the experimental points, intercepted the horizontal axis. These values are given in table 5.1 along with the corresponding value of the diffusion coefficient D_o and an Arrhenius plot of the diffusion coefficients is given in figure 5.5.

The parameters that define the rate of diffusion of In in CdS, which are given in the Arrhenius equation, are the activation energy E_t and the pre-exponential factor D_f. They can be determined from the gradient and the constant term in the straight line form of the equation. A computer program was written in the computer language BASIC, using formulae due to Topping (12), to obtain the best straight line fit through the experimental points in figure 5.5. In addition the formulae, which are necessary to calculate the error in the activation energy E_t and the pre-exponential factor D_f from the deviation of the experimental points from the best straight line, were also included in the program. The Polytechnic computer, which is an ICL 1900, was used to do this.

The diffusion coefficient is given by the following Arrhenius expression:

$$D_o = \left(6^{+3}_{-2}\right) \times 10^{-4} \left(m^2 s^{-1}\right) \exp\left[\frac{-(2.09 \pm 0.08)\ eV}{kT}\right] \qquad 5.7$$

AN ARRHENIUS PLOT OF THE DIFFUSION COEFFICIENT D_o
FOR THE DIFFUSION OF In INTO CdS IN EXCESS In METAL

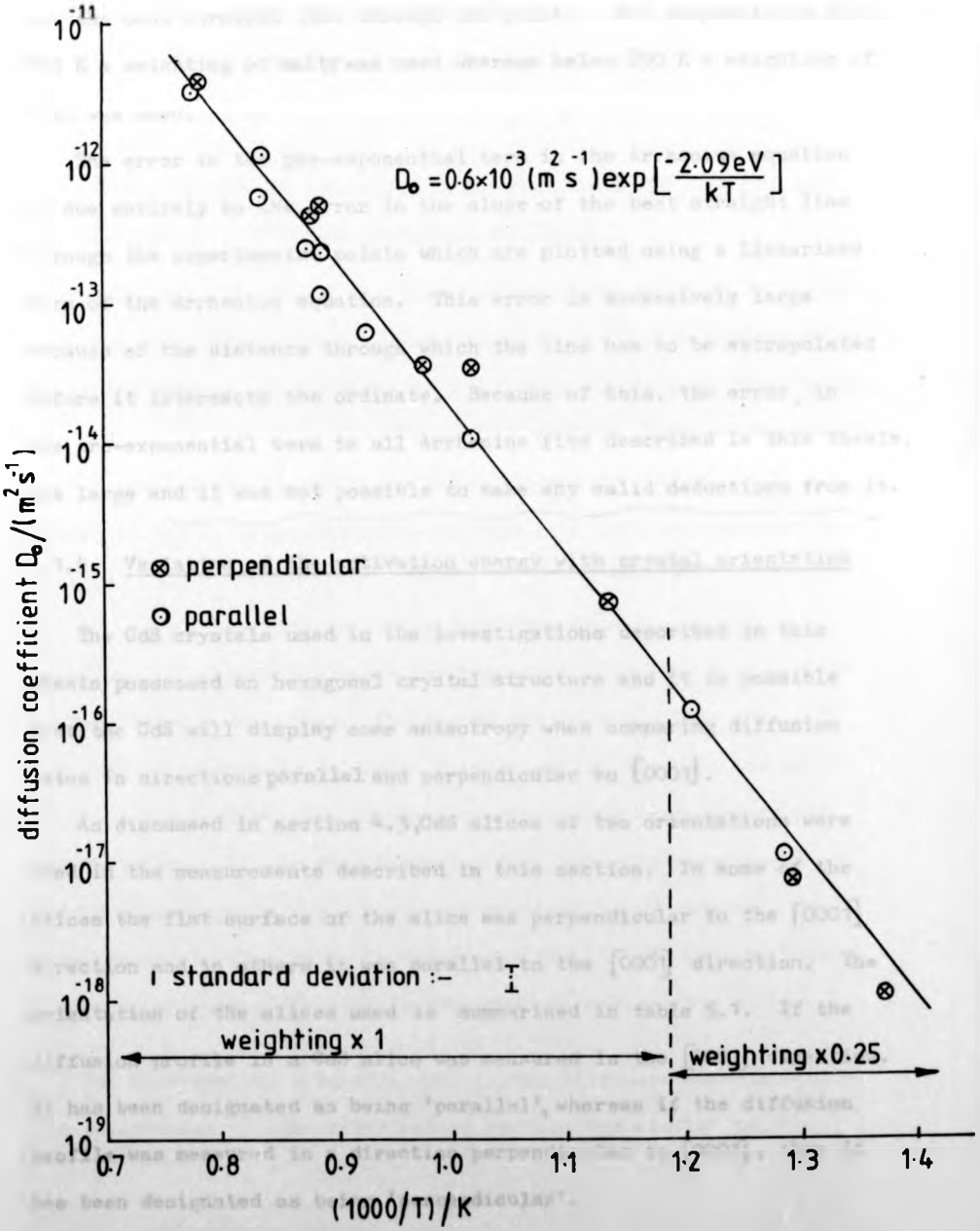

Fig 5.5

As the diffusion coefficients for anneals carried out at temperatures below 850 K possessed an error which was approximately twice the average value, the experimental values were weighted in the fit to get the best straight line through the points. For temperatures above 850 K a weighting of unity was used whereas below 850 K a weighting of 0.25 was used.

The error in the pre-exponential term in the Arrhenius equation is due entirely to the error in the slope of the best straight line through the experimental points which are plotted using a linearised form of the Arrhenius equation. This error is excessively large because of the distance through which the line has to be extrapolated before it intersects the ordinate. Because of this, the error in the pre-exponential term in all Arrhenius fits described in this thesis, was large and it was not possible to make any valid deductions from it.

5.1.4. Variation of the activation energy with crystal orientation

The CdS crystals used in the investigations described in this thesis possessed an hexagonal crystal structure and it is possible that the CdS will display some anisotropy when comparing diffusion rates in directions parallel and perpendicular to [0001].

As discussed in section 4.3, CdS slices of two orientations were used in the measurements described in this section. In some of the slices the flat surface of the slice was perpendicular to the [0001] direction and in others it was parallel to the [000$\bar{1}$] direction. The orientation of the slices used is summarised in table 5.1. If the diffusion profile in a CdS slice was measured in the [0001] direction, it has been designated as being 'parallel', whereas if the diffusion profile was measured in a direction perpendicular to [000$\bar{1}$], then it has been designated as being 'perpendicular'.

It can be seen from the results which are plotted in figure 5.5 that $D_{o_\perp}$ is, on average, twice as great as $D_{o_\parallel}$. As the optical measurements, which are described in chapter 6, gave a more accurate measurement of the diffusion anisotropy than could be obtained with the RTS technique, the subject of diffusion anisotropy is discussed in detail in chapter 6.

5.2 Determination of the near-surface concentration of In in CdS for the concentration dependent diffusion

In order to determine the possible mechanism by which In diffuses into the CdS it is helpful to know what the maximum In concentration is at the surface of the slice at x = 0 as a function of temperature. The results of the experiments described in this section were also used to deduce the shape of the phase diagram of the CdS/In_2S_3 system at low In concentrations and this item will be discussed in section 8.2.

It was not possible to derive this data from the experiments described in section 5.1 where the measurements of the diffusion of In into CdS are described. The reason for this was that four different consignments of radioactive In metal were used and no accurate intercalibration of the activity of the consignments had been obtained. It was thought that a more accurate measurement of the In concentration could have been obtained by purchasing a new consignment of radioactive In metal specifically for this purpose. This was consignment 5 which is described in sub-section 3.6.2.

The experimental procedure used in the diffusion anneals and in the measurement of the concentration profile was similar to that

described in sub-section 5.1.1, except for two points.

The first was that the anneal time was longer than the time that was necessary for the diffusion fronts, diffusing into the slice from both surfaces, to meet at the centre of the CdS slice. In fact, as long a time as was convenient was allowed for the anneal so that the doping level throughout the volume of the slice was as near uniform as possible. The second difference was that only sufficient sections were removed from the slice and measured to give an accurate value of C_o. This value was obtained from a graphical plot of the specific count rate versus x by extrapolating the profile back to x = 0. Again the first two experimental points in each profile were not included in the fit. Usually between 10 and 15 sections were removed from each CdS slice. A typical profile is shown in figure 5.6.

Seven diffusion anneals were carried out in the temperature range 1020 K to 1476 K and the full details of the anneals and of the experimental results are given in table 5.3.

The count rates of all the sections removed from the CdS slices were normalised using a standard source, which was made up from the same consignment of radioactive In metal (number 5). A small piece of the metal, 3.90 mg in weight, was dissolved in dilute HCl in a graduated flask and the solution was made up to 50 ml by adding distilled water. A micro-pipette was used to measure out 0.05 ml onto a planchet and the solution was then evaporated slowly to dryness. The radioactive salt was then covered with a thin layer of Al foil. The source gave approximately 170 counts per second when counted on the low background Geiger counter and the mass of In metal in the source was 3.90×10^{-9} kg. All the sections, which were removed from

Fig5.6 A TYPICAL PROFILE OF THE NEAR-SURFACE In CONCENTRATION IN A CdS SLICE

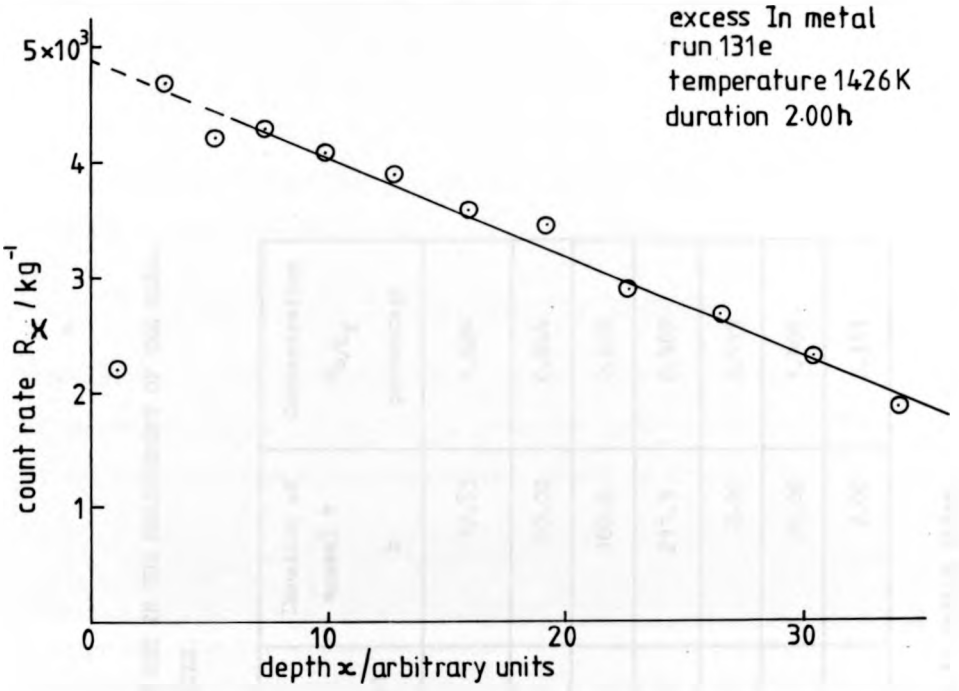

Fig5.7 AN ARRHENIUS PLOT OF THE NEAR-SURFACE In CONCENTRATION IN THE CdS SLICES

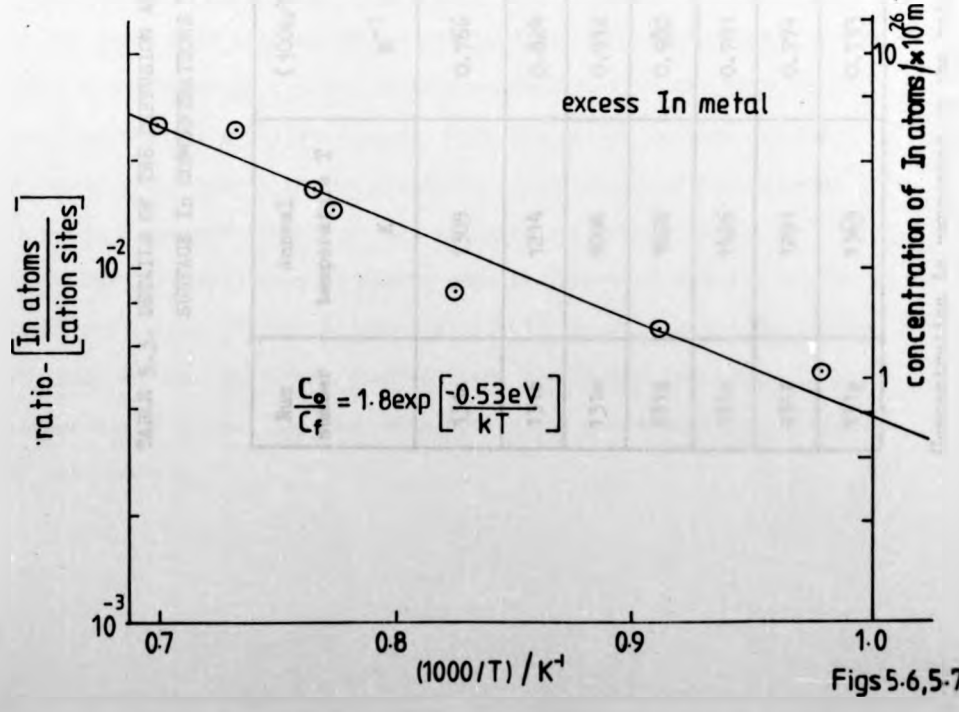

Figs 5.6, 5.7

TABLE 5.3. DETAILS OF THE DIFFUSION ANNEALS CARRIED OUT IN THE MEASUREMENT OF THE NEAR-SURFACE In CONCENTRATIONS IN THE CdS SLICES.

Run number	Anneal temperature T K	(1000/T) K^{-1}	R_o $x10^3/kg^{-1}$	Duration of anneal t h	Concentration C_o/C_f percentage
131a	1305	0.766	3.31	17.83	1.624
131b	1214	0.824	1.72	57.00	0.844
131c	1096	0.912	1.36	160.0	0.668
131d	1020	0.980	0.951	211.3	0.467
131e	1426	0.701	4.92	2.00	2.415
131f	1291	0.774	2.87	24.00	1.409
131g	1365	0.733	4.75	2.00	2.331

Concentration is expressed as the ratio of In atoms to cation sites

the CdS slices, were counted on the low background counter in the normal manner.

The normalised count rate R_x, for each section, was calculated using the following relationship

$$R_x(kg^{-1}) = \frac{\text{count rate of section}}{(\text{count rate of standard})\ (\text{mass of section})} \qquad 5.8$$

Graphs of the normalised count rate R_x versus x were plotted. It can be seen in figure 5.7 that C_o/C_f increases exponentially with T and the best fit through the experimental points is given by

$$\frac{C_o}{C_f} = \left(1.8^{+1.2}_{-0.7}\right) \exp\left[\frac{-(0.53 \pm 0.06)\ eV}{kT}\right] \qquad 5.9$$

This implies that the activation energy for the heat of solution for dissolving In in CdS in the presence of excess In metal is (0.53 ± 0.06) eV.

Both Greskovich (6) and Perkins and Rapp (3) obtained maximum doping levels for the diffusion of Cr^{3+} in NiO which were comparable to the maximum In concentrations obtained for the concentration diffusion. These concentrations are the maximum solubilities in the crystal for the experimental conditions used. Only the latter workers actually obtained measurements on the temperature dependence of the maximum impurity concentration and it did not increase exponentially as T increased. In addition, as can be seen in figures 2.4 and 2.5 both Kumar and Kröger (5) and Hershman et al (13) used In-doped CdS slices in their Cd self-diffusion studies where the doping level was comparable with what has been obtained in the measurements described in this section.

5.3. Determination of the diffusion parameters at a constant In concentration.

The experimentally determined values of C_o were used to normalise the diffusion coefficients D_o presented in section 5.1 to a uniform In concentration, and a value of C_o/C_f of 1% was chosen.. The results are summarised in table 5.1 and are plotted in figure 5.8. The best exponential fit through the experimental points is given by

$$D_o' = \left(3^{+1}_{-1}\right) \times 10^{-6} \left(m^2\ s^{-1}\ \text{at}\ \%^{-1}\right) \exp\left[\frac{-(1.54 \pm 0.08)\ eV}{kT}\right] \qquad 5.8$$

For the definition of the activation energy used in equation 5.8, refer to page 5.3 and to equation 7.17.

5.4. The diffusion of radioactive In into CdS in the presence of high Cd/In ratios.

In this section the results of diffusions, which were carried out with excess radioactive In and inactive Cd metals in the ampoule, are described. The Cd and In atoms will interact with each other and the partial pressure due to both metals will probably be reduced below the saturation vapour pressure value of the individual metals. In fact, it has been verified that the solubility of the In in the CdS is substantially reduced when Cd metal is added to the ampoule (section 8.1).

The diffusion mechanism is of a type in which the diffusion coefficient is concentration independent and its magnitude is much lower than for the concentration dependent case. It is very probable that the defect chemistry for the diffusions described in this section

AN ARRHENIUS PLOT OF THE DIFFUSION COEFFICIENT D_o'
FOR THE DIFFUSION OF In INTO CdS

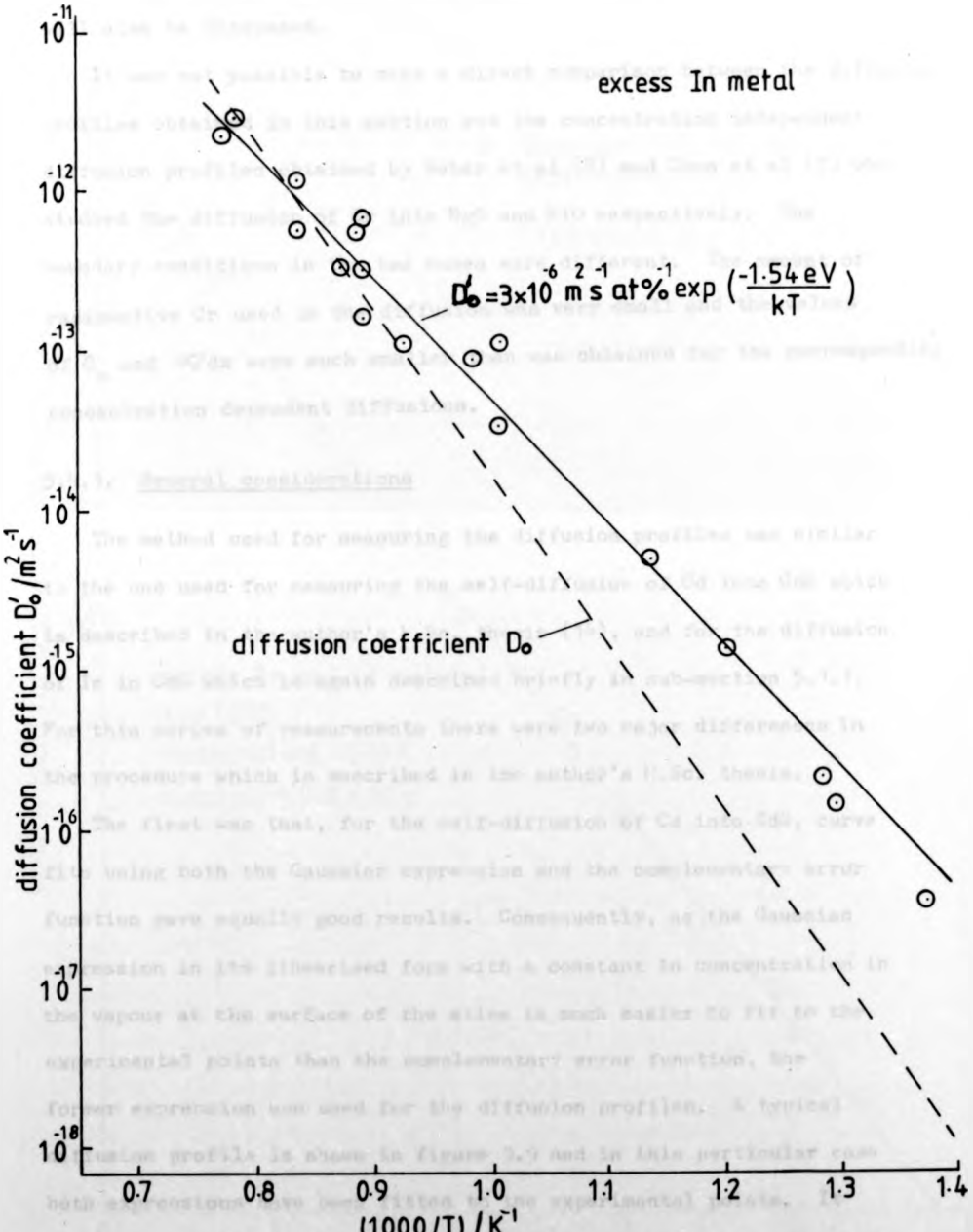

Fig 5·8

will also be different. The partial pressure conditions will be evaluated in chapter 7 and its likely influence on the defect chemistry will also be discussed.

It was not possible to make a direct comparison between the diffusion profiles obtained in this section and the concentration independent diffusion profiles obtained by Weber et al (8) and Chen et al (7) who studied the diffusion of Cr into MgO and NiO respectively. The boundary conditions in the two cases were different. The amount of radioactive Cr used in the diffusion was very small and the values of C_o and dC/dx were much smaller than was obtained for the corresponding concentration dependent diffusions.

5.4.1. General considerations

The method used for measuring the diffusion profiles was similar to the one used for measuring the self-diffusion of Cd into CdS which is described in the author's M.Sc. thesis (14), and for the diffusion of In in CdS which is again described briefly in sub-section 5.1.1. For this series of measurements there were two major differences in the procedure which is described in the author's M.Sc. thesis.

The first was that, for the self-diffusion of Cd into CdS, curve fits using both the Gaussian expression and the complementary error function gave equally good results. Consequently, as the Gaussian expression in its linearised form with a constant In concentration in the vapour at the surface of the slice is much easier to fit to the experimental points than the complementary error function, the former expression was used for the diffusion profiles. A typical diffusion profile is shown in figure 5.9 and in this particular case both expressions have been fitted to the experimental points. It can be seen that away from the origin both functions give equally good fits except that the diffusion coefficient calculated from the

A GAUSSIAN PLOT FOR THE DIFFUSION OF RADIOACTIVE In INTO CdS

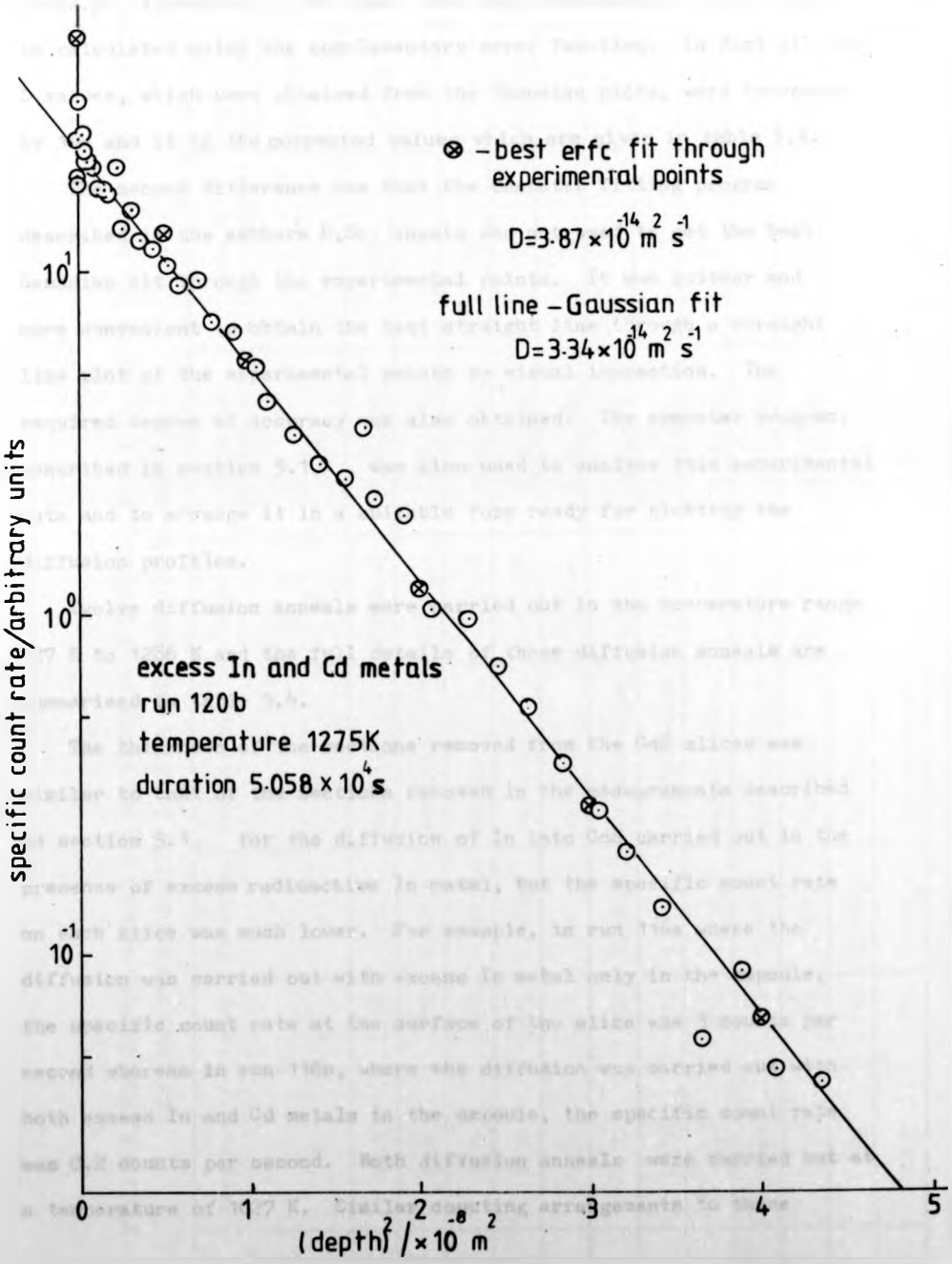

Fig 5·9

Gaussian expression is 16% lower than the corresponding value which is calculated using the complementary error function. In fact all the D values, which were obtained from the Gaussian plots, were increased by 16% and it is the corrected values which are given in table 5.4.

The second difference was that the computer fitting program described in the author's M.Sc. thesis was not used to get the best Gaussian fit through the experimental points. It was quicker and more convenient to obtain the best straight line through a straight line plot of the experimental points by visual inspection. The required degree of accuracy was also obtained. The computer program, described in section 5.1 , was also used to analyse this experimental data and to arrange it in a suitable form ready for plotting the diffusion profiles.

Twelve diffusion anneals were carried out in the temperature range 727 K to 1286 K and the full details of these diffusion anneals are summarised in table 5.4.

The thickness of the sections removed from the CdS slices was similar to that of the sections removed in the measurements described in section 5.1 for the diffusion of In into CdS carried out in the presence of excess radioactive In metal, but the specific count rate on each slice was much lower. For example, in run 116a where the diffusion was carried out with excess In metal only in the ampoule, the specific count rate at the surface of the slice was 3 counts per second whereas in run 116b, where the diffusion was carried out with both excess In and Cd metals in the ampoule, the specific count rate was 0.2 counts per second. Both diffusion anneals were carried out at a temperature of 1027 K. Similar counting arrangements to those

TABLE 5.4. EXPERIMENTAL DETAILS FOR THE DIFFUSION OF RADIOACTIVE In INTO CdS IN THE PRESENCE OF EXCESS INACTIVE Cd METAL AND RADIOACTIVE In METAL USING THE RTS TECHNIQUE

Run number	Temperature K	1000/T K^{-1}	Duration s	Orientation	Area m^2	Diffusion coefficient D $m^2 s^{-1}$	Number of slices removed	Average amount removed per section	
								Thickness m	Mass kg
101	1079	.927	1.636,5	Parallel	2.646,-5	7.38,-16	17	2.263,-6	0.2886,-6
108b	1286	.778	2.520,4	Parallel	1.871,-5	3.57,-15	12	3.026,-6	0.2728,-6
109h	1129	.886	1.494,5	Parallel	6.267,-6	1.45,-15	13	5.424,-6	0.1638,-6
1091	1124	.890	6.102,5	Parallel	1.721,-5	9.36,-16	35	2.697.-6	0.2237,-6
110	1229	.814	1.422,5	Parallel	1.535,-5	1.05,-14	39	4.526,-6	0.3349,-6
112	729	1.372	9.398,6	Perpendicular	1.751,-5	7.53,-19	7	1.358,-6	0.1146,-6
113	727	1.376	9.398,6	Perpendicular	1.340,-5	4.24,-19	9	1.962,-6	0.1267,-6
115b	982	1.018	1.298,6	Perpendicular	7.772,-6	6.94,-17	11	2.952,-6	0.1106,-6
116b	1027	.974	7.738,5	Perpendicular	1.403,-5	3.59,-16	20	2.073,-6	0.1402,-6
118b	772	1.295	1.313,7	Parallel	1.115,-5	8.53,-19	8	1.749,-6	0.0940,-6
119b	880	1.136	2.089,6	Parallel	1.713,-5	2.04,-17	14	2.336,-6	0.1928,-6
120b	1275	.784	5.058,4	Perpendicular	1.871,-1	3.87,-14	42	4.964,-6	0.4328,-6

described in section 5.1 were used, except that because of the lower activity of the sections removed, longer count periods were used.

In the diffusion profiles the logarithm of the count rate decayed linearly with x^2 right down to zero activity. There was little evidence of the activity levelling off to give a constant background due to a faster diffusing mechanism of any kind, similar to the one obtained in the diffusion profiles given in section 5.1.

As with the other sets of diffusion measurements, the first two points in each diffusion profile were not considered when the best straight line through the points was drawn. In addition, as the activity of the sections decreased right to zero, there was no reason for rejecting any of the experimental points at the lower activity end of the profile. The count rates of the last sections to be removed were comparable with the count rate due to natural background and so the statistical accuracy of these points is very low. In certain cases the errors on these innermost points were as large as $\pm$ 300%.

5.4.2. Determination of the diffusion parameters

All the diffusion profiles gave reasonable straight line fits when the logarithm of the specific count rate was plotted against x^2. The diffusion coefficients are given in an Arrhenius plot in figure 5.10 and the best exponential fit through the experimental points is given by:-

$$D = \left(2^{+6}_{-1}\right) \times 10^{-5} \ m^2 s^{-1} \ \exp\left[\frac{-(2.27 \pm 0.12)\ eV}{kT}\right] \qquad 5.10$$

This implies that the activation energy for the diffusion of In into CdS is (2.27 $\pm$ 0.12) eV.

From the results plotted in figure 5.10 it can be seen that the three diffusion anneals carried out at temperatures below 835 K show

AN ARRHENIUS PLOT FOR THE DIFFUSION OF RADIOACTIVE In INTO CdS IN THE PRESENCE OF INACTIVE Cd METAL

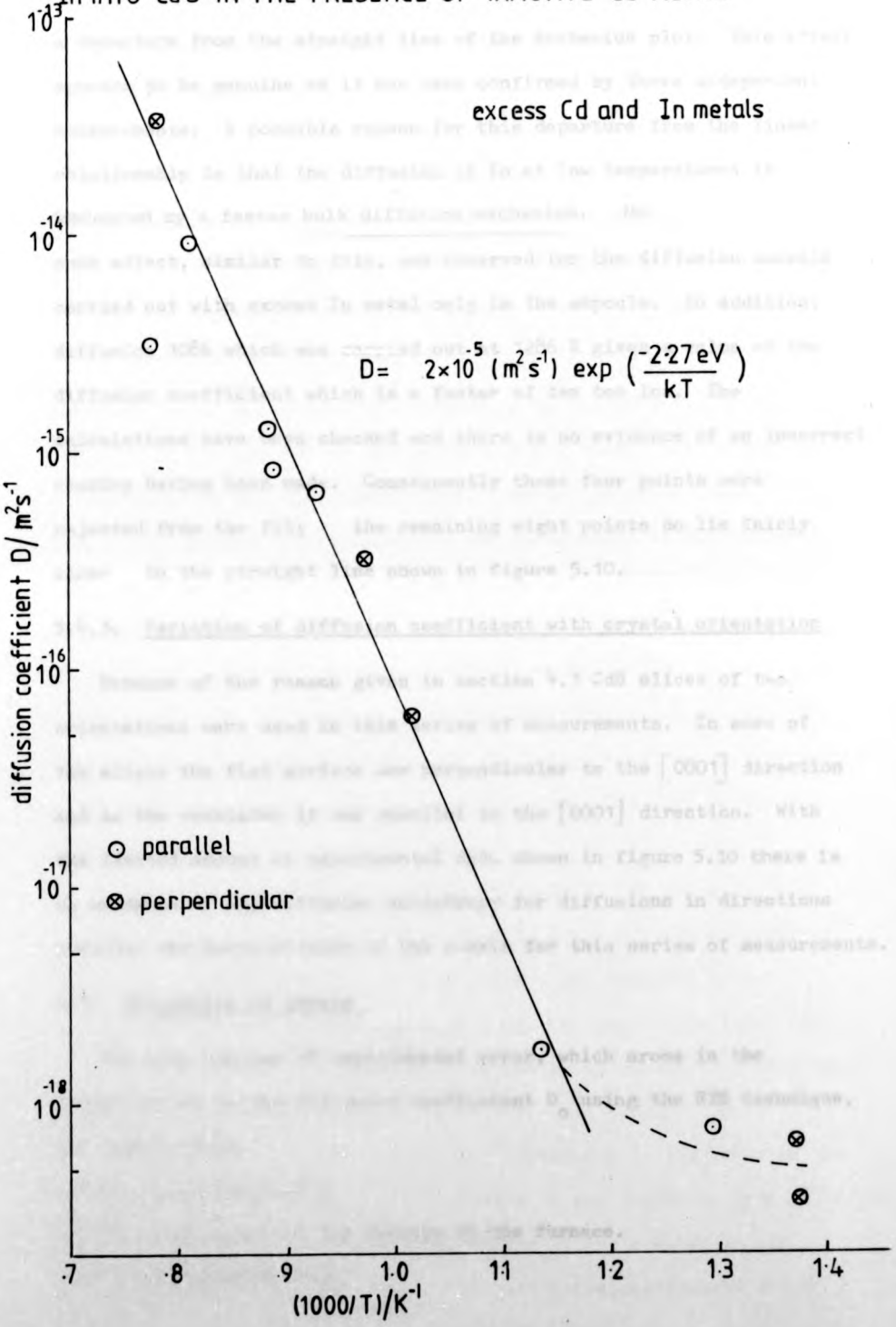

Fig 5.10

a departure from the straight line of the Arrhenius plot. This effect appears to be genuine as it has been confirmed by three independent measurements. A possible reason for this departure from the linear relationship is that the diffusion of In at low temperatures is dominated by a faster bulk diffusion mechanism. No such effect, similar to this, was observed for the diffusion anneals carried out with excess In metal only in the ampoule. In addition, diffusion 108b which was carried out at 1286 K gives a value of the diffusion coefficient which is a factor of ten too low. The calculations have been checked and there is no evidence of an incorrect reading having been made. Consequently these four points were rejected from the fit; the remaining eight points do lie fairly close to the straight line shown in figure 5.10.

5.4.3. Variation of diffusion coefficient with crystal orientation

Because of the reason given in section 4.3 CdS slices of two orientations were used in this series of measurements. In some of the slices the flat surface was perpendicular to the [0001] direction and in the remainder it was parallel to the [0001] direction. With the limited amount of experimental data shown in figure 5.10 there is no evidence of any diffusion anisotropy for diffusions in directions parallel and perpendicular to the c-axis for this series of measurements.

5.5. Discussion of errors

The main sources of experimental error, which arose in the determination of the diffusion coefficient D_o using the RTS technique, are listed below:-

(a) The measurement of T.

(b) The positioning of the ampoule in the furnace.

(c) The measurement of t.

(d) In counting both the sections removed from the CdS slice and the natural background.

(e) The weighing of the sections removed.

(f) The parallelism of the sections removed.

(g) The measurement of the area of the surface of the slice.

(h) The depth of the scratches in the lapped surface of the slice.

(j) Possible systematic errors due to mass loss in the CdS slice during the diffusion anneal.

These sources of error have been discussed in connection with the self-diffusion of Cd into CdS in the author's M.Sc. thesis (14) and will not be discussed to the same extent here. The way in which these experimental errors are reflected in the measurement of the diffusion coefficient is different for the diffusion of In in CdS, where the diffusion is concentration dependent, compared with the self-diffusion of Cd in CdS, where the diffusion coefficient is assumed to be constant. In the former case the errors are reflected in the measurement of the depth of the doped region, whereas in the latter case they are reflected in the measurement of the gradient of the linearised form of the Gaussian equation.

The errors (that is 67% confidence limits) due to items (a) and (b), which have been discussed in sub-section 3.1.3., can be combined to give an overall error of $\pm$ 3 K in T and t was measured to an accuracy of $\pm$ 15 s. In fact the errors in the first three items are so small compared with the remainder of the items listed that they can by neglected in this assessment.

The items (d) to (h) inclusive all contribute to the error in the specific count rate, which is the ordinate in the diffusion profile plots, and the magnitude of the error is reflected in the scatter in the points on the graphs. The error in the diffusion coefficient due to

items (f) and (h) were dealt with extensively in the author's M.Sc. thesis. The error in the diffusion coefficient due to lack of parallelism in the sections removed from the slice was ± 3% and the error in the count rate due to the scratches formed in the surface of the slice was less than ± 3%. The error in the count rate of a section removed from the CdS slice at the beginning of a diffusion profile was ± 3% and the error increased to as high as ± 300% for sections, which were removed from the slice, at the end of a profile measurement.

The largest experimental error was in the mass of each section removed from the CdS slice which was ± 10 μg. In addition, for reasons given in section 5.1 , a section whose mass was low was invariably preceded or followed by a section whose mass was high and fortunately when the masses of two or more consecutive sections were added together, the error on the combined mass was probably very much less than the combined errors of each individual section.

The depth, from the original surface of a slice to the midpoint of a section, is obtained by adding the weights of all the preceding sections, which have been removed, and one half the weight of the section under consideration. Then if the area of the surface of the slice is known the corresponding depth can be calculated. The main source of error in the abscissa of the diffusion profiles, which is the depth, is in the measurement of the area of the surface of the slice which is ± 4%.

For the diffusion of In into CdS, with excess In metal in the ampoule, the scatter in the experimental points in the diffusion profiles will lead to a possible error of ± 10% in X and this will lead to an error of ± 20% in D_o. An investigation of the scatter in the

experimental points from the best straight line in the Arrhenius plot in figure 5.4 indicates that this value is reasonably accurate.

For the diffusion of In into CdS, which was carried out with excess radioactive In metal and inactive Cd metal in the ampoule so that the diffusion proved to be concentration independent, the possible sources of error should be the same as those which were obtained for the self-diffusion of Cd into CdS. In fact the main source of experimental error in the diffusion profiles will be in the abscissae. The error in the diffusion coefficient in this type of diffusion is reflected in the slope of the linearised form of the Gaussian expression which, as is described in section 5.4 , was used in preference to the error function for computing convenience. The errors for the diffusion coefficient were estimated to be $\pm$ 40% at 910 K and $\pm$ 20% at 1540 K. It can be seen from the scatter of the experimental points, from the best straight line in the Arrhenius plot in figure 5.10., that the errors quoted in the author's M.Sc. thesis appear to be too great in this instance. Values equal to approximately one half of the quoted ones would appear to be more reasonable. A possible explanation for this increased accuracy is that there has been an improvement in the experimental technique used since the author's M.Sc. thesis was written.

The mass loss, which occurred in the CdS slices during a diffusion anneal, was due mainly to the evaporation of Cd and S atoms from the surface of the slice. The most likely occasions when this evaporation takes place is either at the beginning or at the end of the diffusion anneal. For the concentration dependent diffusions there is a certain mass loss occurring at the beginning of the anneal due to Cd and S atoms leaving the CdS to provide the Cd and S partial pressures during the anneal. When the ampoule is removed from the furnace at the end

of the anneal, the walls of the ampoule will cool considerably more quickly than the CdS slice itself and it is possible that this will cause some evaporation to occur. From the discussion of the errors which arose in the OM technique described in section 6.5, it was concluded that the majority of the mass loss occurred at the beginning of the anneal and did not affect the measurement of the diffusion coefficient D_o.

In the determination of the near-surface In concentration in the CdS errors arose, due to counting and weighing, similar to those which were obtained in the measurement of the diffusion profiles. An additional source of error occurred in the mass of the standard source which was made up for the concentration determinations decribed in section 5.2. The error in the ratio C_o/C_f was $\pm$ 10% and the final error in the diffusion coefficient D_o' was $\pm$ 15% .

5.6. References

1. R. A. SWALIN, Thermodynamics of Solids, John Wiley and Sons Inc., New York (1972).
2. S. S. CHERN and F. A. KRÖGER, Phys. Stat. Sol. (a), 25, 1, P215 (1974).
3. R. A. PERKINS and R. A. RAPP, Metal. Trans., 4, P193 (1973).
4. G. H. MEIER and R. A. RAPP, Z. Physik. Chem., 74, P168 (1971).
5. V. KUMAR and F. A. KRÖGER, J. Sol. State Chem., 3, P387 (1971).
6. C. GRESKOVICH, J. Amer. Cer. Soc., 53, 9, P498 (1970).
7. W. K. CHEN, N. L. PETERSON and L. C. ROBINSON, J. Phys. Chem. Solids, 34, P705 (1973).
8. G. W. WEBER, W. R. BITLER and V. S. STUBICAN, J. Amer. Cer. Soc., 60, P61 (1977).
9. T. SOLAGA and A. J. NORTLOCK, Phys. Stat. Sol. (a), 3, K247 (1970).

10. L. R. WEISBERG and J. BLANC, Phys. Rev., 131, 4, P1548 (1963).

11. B. TUCK, Introduction to Diffusion in Semiconductors, Institute of Electrical Engineers Monographs Series 16, Peter Peregrinus Ltd., Stevenage, Herts (1974).

12. J. TOPPING, Errors of Observation and their treatment, The Institute of Physics, London (1957).

13. G. H. HERSHMAN, V. P. ZLOMANOV and F. A. KRÖGER, J. Sol. State Chem., 3, P401 (1971).

14. E. D. JONES, Measurement of the Self-Diffusion of Cd into CdS using Radiotracer Techniques, M.Sc. Thesis, University of Warwick, (1971).

6. Diffusion of In into CdS using the optical/microprobe technique

When In is diffused into CdS with excess In metal in the ampoule, the diffusion is concentration dependent and the diffusion front is sharply defined as can be seen in figure 3.4. In this chapter the determination of the diffusion parameters using the OM technique is described and in addition, as the optical method proved extremely sensitive for measuring the diffusion anisotropy, these measurements are also described in this chapter.

The optical boundary is rather similar in appearance to a p - n junction which defines the boundary between two regions with different electroneutrality conditions. Nykura (1) has used a scanning electron microscope to investigate the cathodoluminescence on the diffusion front of CdS samples which have been doped with trivalent metals. He found that the cathodoluminescence is very localised at and near the diffusion front and, that the intensity profile across the diffusion front varies with the concentration gradient of the diffusing species and the crystal orientation of the CdS slice. Comparison of the optical and cathodoluminescence images showed that the inner sharp edge of the cathodoluminescence band coincided with the optical position of the diffusion front to better than 1 μm. The reason suggested by Nykura, for the much higher radiative efficiency at the diffusion front, is an increase in the oscillator strength of the transition which is probably due to the perturbation of the CdS lattice by a very low concentration of the fastest moving defect. A possible electric field at the diffusion front is called in to explain an observed anisotropy effect in the cathodoluminescence.

A sharp diffusion front has also been observed in GaP (2) and $GaAs_{1-x}P_x$ (3) when Zn has been diffused into these materials. In

addition it is stated in section 2.7 that both Kato and Takayanagi (4) and Maslova et al (5), in their studies on the diffusion of In into CdTe, both report that the diffusion results in the formation of a p - n junction which is observable. No such observation has been reported by Perkins and Rapp (6) or by Greskovich (7) in their studies on the concentration dependent diffusion of Cr into NiO. It has been verified in a comparison experiment described in section 8.1 that the diffusion front which is measured using the RTS technique coincides, to within the limits of experimental error, with the optical measurement of the interface.

The masses of In and CdS, which were placed in each ampoule for the diffusion anneals described in this chapter, were different from those used in section 5.1, where the concentration dependent measurements were obtained using the RTS technique. The amount of In used in each ampoule in the RTS technique was cut to a minimum because of the high cost of the radioactive In and also to keep radiation levels to a minimum. The amount used in both methods was more than sufficient to maintain a saturated vapour pressure in the ampoule throughout the diffusion anneal provided the In did not interact with any other element in the ampoule. The calculated final Cd/In ratio in the metal globule, due to the stoichiometric exchange between the In atoms of the vapour and the Cd atoms in the CdS slice, for the measurements described here was approximately equal to 2×10^{-4}; the comparable value using the RTS technique was 2×10^{-3}.

6.1. Optical measurements

In this series of measurements, 71 diffusion anneals were successfully carried out at eight different temperatures in the range 920 K to 1411 K and a summary of the results obtained is given in table 6.1. From the typical set of results for a single temperature,

TABLE 6.1: EXPERIMENTAL DATA FOR THE DIFFUSION OF In INTO CdS IN THE PRESENCE OF EXCESS In METAL USING THE OPTICAL METHOD.

Run number	Temperature T K	1000/T K^{-1}	Number of experimental points	Maximum duration of the diffusion anneal h	$D_{o_{\parallel}} = 0.3811\left(\frac{X_{\parallel}^2}{t}\right)$ $m^2 s^{-1}$	$D_{o_{\perp}} = 0.3811\left(\frac{X_{\perp}^2}{t}\right)$ $m^2 s^{-1}$	$D'_{o_{\parallel}} = \frac{0.3811}{c}\left(\frac{X_{\parallel}^2}{t}\right)$ $m^2 s^{-1}$	$D'_{o_{\perp}} = \frac{0.3811}{c}\left(\frac{X_{\perp}^2}{t}\right)$ $m^2 s^{-1}$	Ratio $X_{\perp}/X_{\parallel}$
127	920	1.087	7	3426	1.482, -15	6.909, -15	2,117, -15	9.870, -14	2.175
126	972	1.029	6	1506	5.578, -15	2.386, -14	5.751, -15	2.460, -14	2.037
125	1020	0.980	10	125.1	3.382, -14	1.200, -13	2.642, -14	9.375, -14	1.885
122a	1120	0.893	12	26.50	2.968, -13	7.565, -13	1.427, -13	3.637, -13	1.598
122b	1120	0.893	4	18.95	2.968, -13	8.213, -13	1.427, -13	3.949, -13	1.671
123	1220	0.820	7	5.22	1.546, -12	3.289, -12	4.939, -13	1.051, -12	1.457
124, 128	1273	0.786	10	5.00	2.551, -12	5.377, -12	6.784, -13	1.430, -12	1.423
129	1333	0.750	9	1.68	6.421, -12	1.131, -11	1.396, -12	2.459, -12	1.340
130	1411	0.707	6	0.583	1.125, -11	1.787, -11	1.923, -12	3.055, -12	1.275

which is plotted in figure 6.1, it can be concluded that $x^2 \propto t$.

In run 122, in addition to using CdS slices which possessed the normal orientation with the surface of slice perpendicular to the [0001] direction, slices with the surface parallel to the [0001] direction were also used. The two runs were designated 122a and 122b respectively and there was no measurable difference in the slopes of the corresponding graphs in the two runs. As the straight line graphs passed very close to the origin, it was included as an experimental point when the best straight line was drawn through the points. Eight such lines were drawn representing eight different temperatures with the ninth being a repeat of run 122 using the slices with the non-standard orientation.

The values of the diffusion coefficients D_o are shown as Arrhenius plots in figure 6.2 and, for temperatures below 1220 K, the best exponential fits through the experimental points are given by:

PARALLEL $$D_{o_{\parallel}} = \left(6^{+9}_{-4}\right) \times 10^{-3} \ (m^2 s^{-1}) \exp\left[\frac{-(2.30 \pm 0.08)\ eV}{kT}\right] \quad 6.1$$

PERPENDICULAR $$D_{o_{\perp}} = \left(1^{+2}_{-1}\right) \times 10^{-3} \ (m^2 s^{-1}) \exp\left[\frac{-(2.03 \pm 0.08)\ eV}{kT}\right] \quad 6.2$$

This implies that the activation energies E_t for diffusions in directions parallel and perpendicular to the c-axis are (2.30 ± 0.08) eV and (2.03 ± 0.08) eV respectively and the difference, which is a measure of the diffusion anisotropy, is given by

$$E_{t_{\parallel}} - E_{t_{\perp}} = (0.27 \pm 0.11)\ eV \quad 6.3$$

This topic will be discussed further in section 6.2.

For the diffusions carried out at 1220 K and at temperatures below this value the experimental points all lie, to within the limits of experimental error, along a straight line. For diffusions carried out

A PLOT OF THE SQUARE OF DIFFUSION DEPTH X VERSUS THE DURATION OF THE ANNEAL FOR THE DIFFUSION OF In INTO CdS

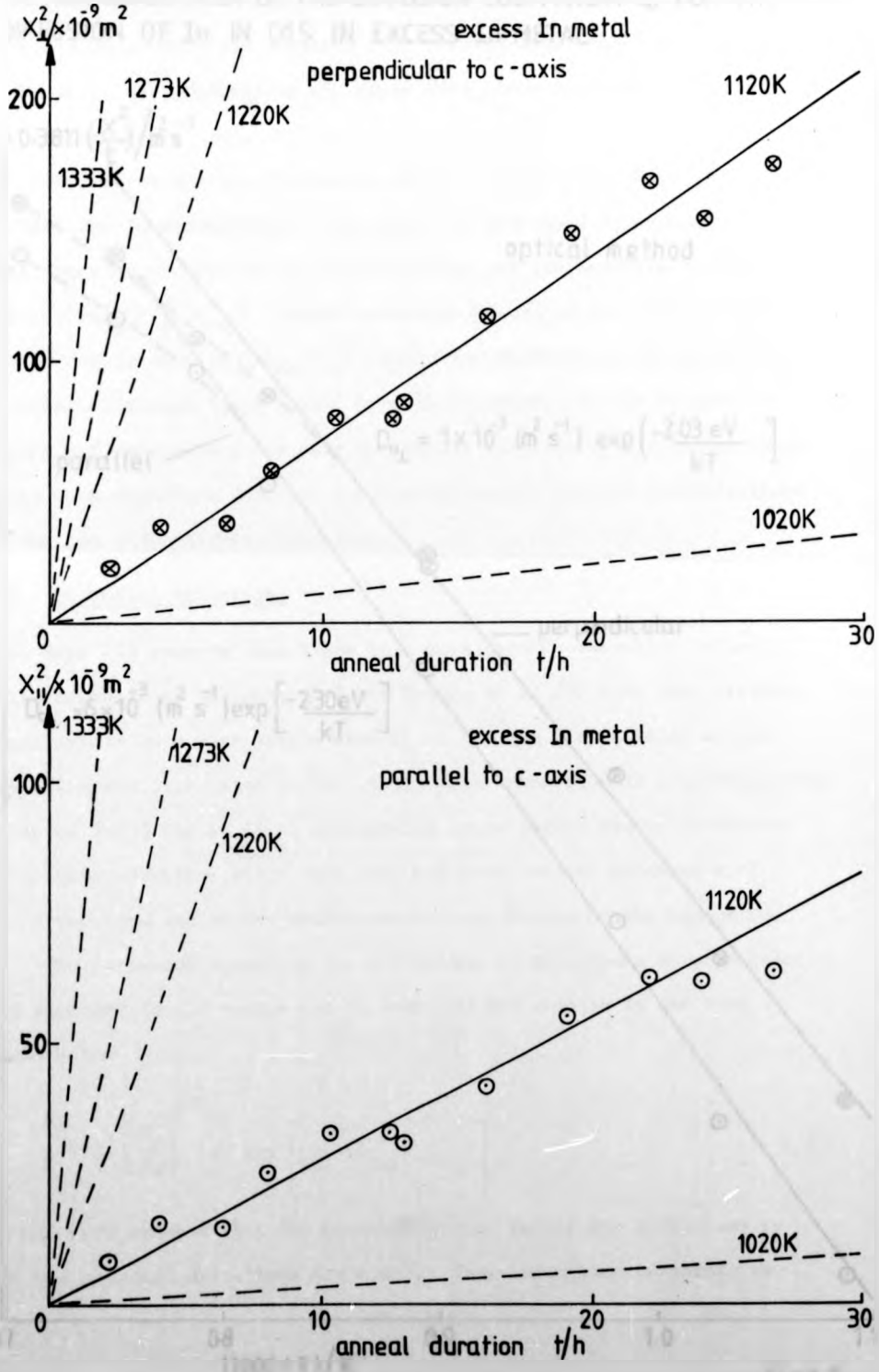

Fig 6.1

AN ARRHENIUS PLOT OF THE DIFFUSION COEFFICIENT D_o FOR THE DIFFUSION OF In IN CdS IN EXCESS In METAL

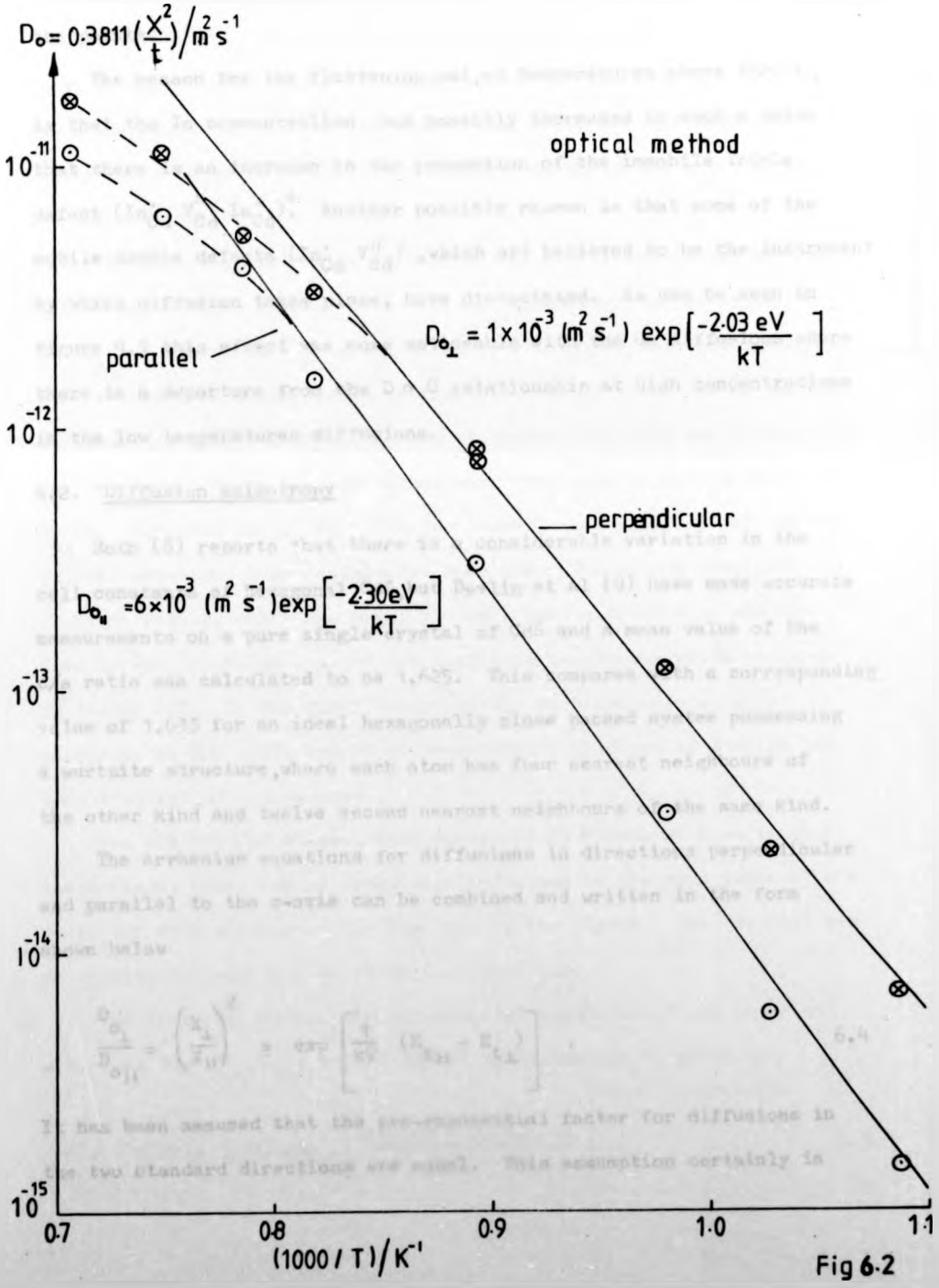

Fig 6.2

at temperatures above 1220 K the experimental points indicate that there is a departure from the straight line relationship, where there is a decrease in the gradient of the curve that gives the best fit through the points.

The reason for the flattening out, at temperatures above 1220 K, is that the In concentration has possibly increased to such a value that there is an increase in the proportion of the immobile triple defect $(In^{\bullet}_{Cd}\ V''_{Cd}\ In^{\bullet}_{Cd})^{*}$. Another possible reason is that some of the mobile double defects $(In^{\bullet}_{Cd}\ V''_{Cd})'$, which are believed to be the instrument by which diffusion takes place, have dissociated. As can be seen in figure 9.1 this effect was more noticeable with the Ga diffusions where there is a departure from the $D \propto C$ relationship at high concentrations in the low temperatures diffusions.

6.2. Diffusion anisotropy

Roth (8) reports that there is a considerable variation in the cell constants of hexagonal CdS, but Devlin et al (9) have made accurate measurements on a pure single crystal of CdS and a mean value of the c/a ratio was calculated to be 1.625. This compares with a corresponding value of 1.633 for an ideal hexagonally close packed system possessing a wurtzite structure, where each atom has four nearest neighbours of the other kind and twelve second nearest neighbours of the same kind.

The Arrhenius equations for diffusions in directions perpendicular and parallel to the c-axis can be combined and written in the form shown below

$$\frac{D_{o_\perp}}{D_{o_{||}}} = \left(\frac{X_\perp}{X_{||}}\right)^2 = \exp\left[\frac{1}{kT}\ (E_{t_{||}} - E_{t_\perp})\right] . \qquad 6.4$$

It has been assumed that the pre-exponential factor for diffusions in the two standard directions are equal. This assumption certainly is

true for an ideally close packed system, where the factors such as the jump distances and the probability of jumping will be equal for the two directions. For CdS, where the departure from the close packed geometry is small, the activation energy difference can still be measured even if the pre-exponential frequency terms are not equal, but provided they are constant. If the pre-exponential terms are not constant, the error involved in assuming that they will cancel in the above equation is probably small.

The following averaging procedure was used to obtain the diffusion anisotropy at each temperature; it is represented by the ratio $D_{o_\perp}/D_{o_{||}}$. Values of $X_{||}$ and $X_\perp$, which were obtained for each CdS slice, were averaged as described in section 3.3. Any reading, which was obviously outside the normal spread of results for that particular slice, was rejected. These average values were then used to give a value of $D_{o_\perp}/D_{o_{||}}$ for each CdS slice. Then the overall mean ratio of all the CdS slices, which had been annealed at each temperature, was obtained. It is these values, which are shown for each run in table 6.1, and are used in the Arrhenius plot of the diffusion anisotropy which is shown in figure 6.3. In the final averaging the readings were weighted according to the total number of experimental readings of X which had been measured on each slice.

For all the CdS slices, that underwent an anneal at a particular temperature, there was no detectable variation in the mean value of the ratio for each slice with the duration of the anneal. One typical set of results for run 122a is shown in figure 6.4.

The best fit through the experimental points, which are shown on a plot of $\log (D_{o_\perp}/D_{o_{||}})$ versus 1000/T in figure 6.3, is given by

$$\frac{D_{o_\perp}}{D_{o_{||}}} = (0.20 \pm 0.02) \exp\left[\frac{-(0.250 \pm 0.008)\ eV}{kT}\right] . \qquad 6.5$$

Fig 6 3 AN ARRHENIUS PLOT OF THE DIFFUSION ANISOTROPY FOR THE DIFFUSION OF In INTO CdS.

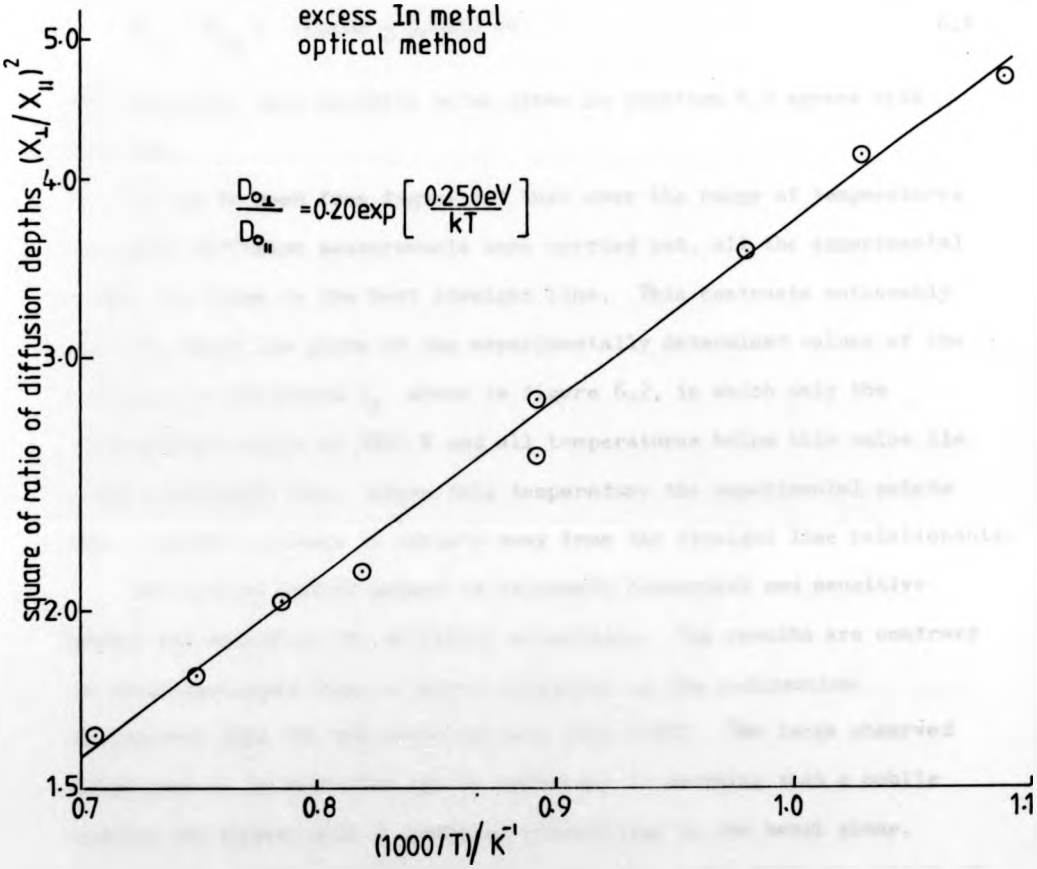

Fig6.4 PLOT OF THE MEAN RATIO $(X_\perp / X_\parallel)$ FOR EACH CdS SLICE AGAINST THE DURATION OF THE ANNEAL

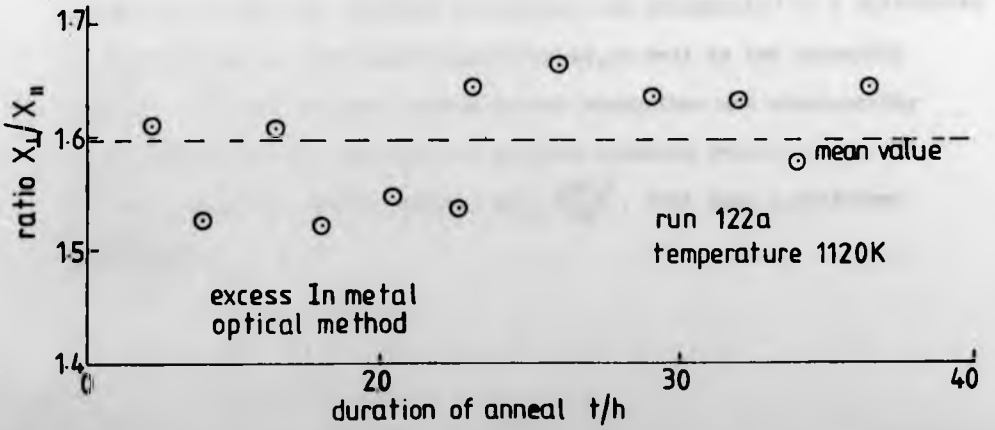

Figs6.3,6.4

This implies that the difference in the activation energies is given by

$$E_{t_{\parallel}} - E_{t_{\perp}} = (0.250 \pm 0.008)\ \text{eV} \quad . \qquad 6.6$$

The relatively less accurate value given in equation 6.3 agrees with this one.

It can be seen from figure 6.3 that over the range of temperatures for which diffusion measurements were carried out, all the experimental points lie close to the best straight line. This contrasts noticeably with the Arrhenius plots of the experimentally determined values of the diffusion coefficients D_o shown in figure 6.2, in which only the experimental points at 1220 K and all temperatures below this value lie along a straight line. Above this temperature the experimental points show a marked tendency to deviate away from the straight line relationship.

The optical method proved an extremely convenient and sensitive method for measuring the diffusion anisotropy. The results are contrary to those envisaged where a faster diffusion in the c-direction is expected when the c/a ratio is less than 1.633. The large observed anisotropy of In diffusion can be explained by assuming that a mobile complex has formed with a preferred orientation in the basal plane. In his measurements on the cathodoluminescence on the diffusion front of CdS doped with trivalent metals, Nykura (1) observed that the diffusion anisotropy in the two standard directions was accompanied by a difference in the spectrum of the cathodoluminescence, as well as the intensity profile. CdS does possess piezoelectric properties and consequently it is likely that an electrically charged extended defect, which is believed to be the mobile defect $(In_{Cd}^{\bullet}\ V_{Cd}^{''})^{'}$, will have a preferred orientation.

6.3. Determination of the In concentration using the electron microprobe

The main use of the electron microprobe was to measure the temperature dependence of C_o in the CdS slices in which the diffusion depths had been determined optically. Five partly doped CdS slices were chosen for the measurements from among the ones which had been used in the optical measurements described in section 6.1. A description of the experimental procedure used for measuring the In concentration profiles using the microprobe is described in section 3.4 and a summary of the diffusion details and the results obtained is given in table 6.2. A typical recorder chart scan of the In concentration in a partially doped CdS slice is shown in figure 6.5. The flat part of the profile is the background signal that was obtained from the inner undoped part of the CdS slice.

In the analysis of the recorder chart profiles, the scatter in the signal was reduced by drawing a smooth line through the traces. The outside edge of each slice was taken as the point half way between where the trace reached its maximum signal, due to the In, and the point where the background from the plastic mounting started. The smoothed curve for each profile was corrected for the background signal due to the pure CdS, the variation in the reference standard counts and the microprobe correction factors which are listed in section 3.4. Plots of the In atomic concentration, expressed as C/C_f, were obtained. The two plots of the concentration for each CdS slice were superposed on one another and the best Wagner fit through the two sets of experimental points was obtained.

Taking the origin of the distance scale as the interface between the diffusion layer and the pure part of the slice produced a closer

TABLE 6.2: DETAILS OF THE DIFFUSION ANNEALS CARRIED OUT IN THE MEASUREMENT OF C_o USING THE ELECTRON MICROPROBE.

Specimen number	Anneal temperature T K	1000/T K^{-1}	Duration of anneal s	X (optical) μm	X (microprobe) μm	Ratio of X values microprobe/optical	C_o/C_f
125j	1020	0.980	4.201,5	200.8	219	1.09	0.0146
122s	1120	0.893	9.540,4	252.8	268	1.06	0.0160
123e	1220	0.820	1.440,4	240.2	304	1.27	0.0370
128c	1273	0.786	1.800,4	327.8	348	1.06	0.0380
129f	1333	0.750	5.904,3	254.8	251	.99	0.0460

A TYPICAL MICROPROBE PROFILE OF THE In CONCENTRATION IN A CdS SLICE.

(a) RECORDER TRACE

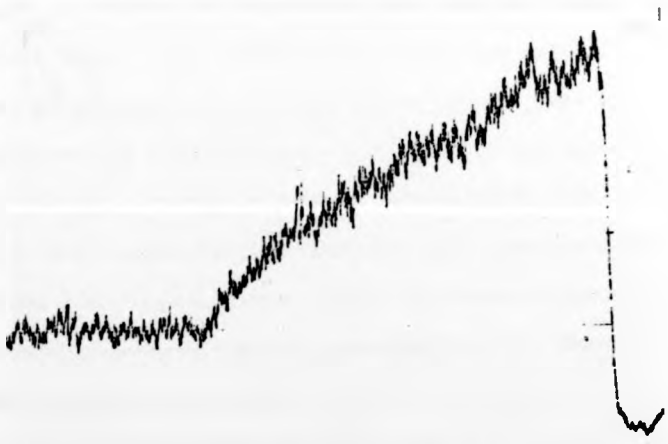

horizontal magnification x 195

(b) WAGNER FIT TO EXPERIMENTAL POINTS

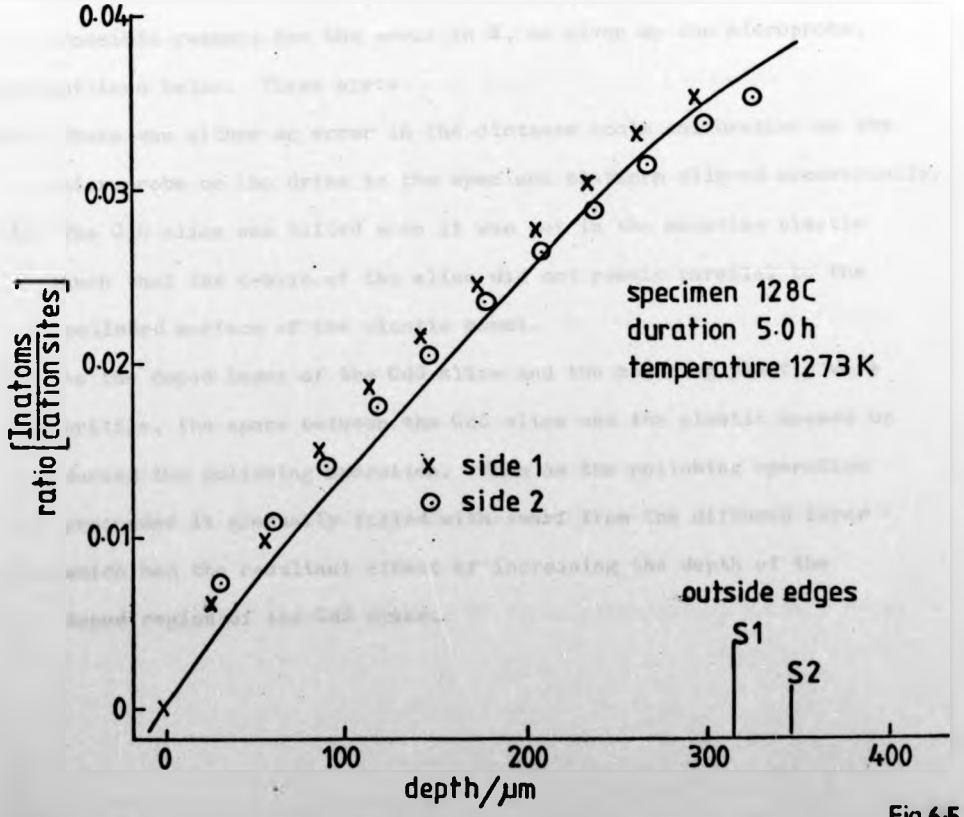

Fig 6·5

agreement in the experimental results than taking the origin at the outside edge of the slice. The agreement between the two profiles for each slice, which were superposed on one another and with the Wagner curve that gave the best fit through the experimental points, was better. The resultant inaccuracy in locating the position of the outside edge of the slice did not produce too large an error in C_o because the Wagner curve is reasonably flat in this region. It was estimated to be $\pm$ 10%.

The values of X, which were obtained from the microprobe profiles, did not agree with the corresponding values that were measured optically. The ratio of the X values, as measured with the microprobe to those which were obtained optically, varied from a minimum value of 0.99 up to a maximum value of 1.27. The ratios are shown in table 6.2. The calibration of the microscope was rechecked and was found to be correct. The optical measurements were taken to be the more reliable set of results.

Possible reasons for the error in X, as given by the microprobe, are outlined below. These are:-

(a) There was either an error in the distance scale calibration on the microprobe or the drive to the specimen platform slipped occasionally.

(b) The CdS slice was tilted when it was set in the mounting plastic such that the c-axis of the slice did not remain parallel to the polished surface of the plastic mount.

(c) As the doped layer of the CdS slice and the mounting plastic were brittle, the space between the CdS slice and the plastic opened up during the polishing operation. Then as the polishing operation proceeded it gradually filled with swarf from the diffused layer which had the resultant effect of increasing the depth of the doped region of the CdS slice.

(d) The traverse across the polished microprobe specimen was not perpendicular to the outside surface of the CdS slice and to the diffusion front.

(e) The optical measurements were low due to the edges of the specimen cracking off.

The errors due to all the items listed above, except item (c) and possibly (a), were small and could not account for the discrepancy between the optical and the microprobe measurements. In the optical method for measuring the diffusion depth, which is described in section 3.3, a sufficiently large representative number of measurements were obtained for each CdS slice so that any readings that were low due to the edges of the specimen cracking off would have been immediately obvious. The microprobe traverse across the polished surface of the CdS was within 5 degrees of the normal to the outside surface of the CdS slice (10).

After the measurements were completed the CdS slice, which gave the largest discrepancy, was taken and the tilt of the slice in the mounting plastic was checked. This was done by sawing across a diameter of the plastic mount and through the CdS slice in a direction perpendicular to the sides of the polished surface of the slice. In fact the tilt was less than 5 degrees.

As it was unlikely that there was any error due to item (a) the most feasible cause of the discrepancy was item (c). This is confirmed by the fact that the majority of the depths, which were measured using the microprobe, were greater than the corresponding measurements which were obtained optically. In view of this discrepancy, the readings that were obtained optically were used in the determination of the diffusion parameters.

Corrections for such factors as electron penetration, primary X-ray

emission efficiency, X-ray mass absorption and electron backscatter obtained using the electron microprobe were applied to both the counts from the specimen, which was being analysed, and the reference standard. The calculations were carried out using a computer program which was written and run by the staff at the Centre for Materials Science at the University of Birmingham. The numerical data used in the program was taken from a report to the Science Research Council on microprobe correction procedures (11). The calculations were checked using a procedure due to Theisin (12), where it was assumed that 2 per cent of the cation sites in the CdS crystal were occupied by In atoms. When the data due to Theisin was used, a correction factor of 0.97 was obtained whereas the corresponding value obtained from the computer program was 0.89.

The agreement between these two values was poor, but as the information given in the Science Research Council report was more recent, it was used to calculate the correction factors for the microprobe.

6.4. Determination of the diffusion parameters at a fixed In concentration

The experimentally determined values of C_o, which were determined using the microprobe and are presented in this section, were used to normalise the diffusion coefficents D_o to a value of C_o/C_f of 0.01. The Arrhenius plot of the experimentally determined values of C_o, which is shown in figure 6.6, can be represented by the following relationship

$$\frac{C_o}{C_f} = \left(3.0^{+4.4}_{-1.8}\right) \exp\left[\frac{-(0.478 \pm 0.091)\ eV}{kT}\right] \qquad 6.7$$

This expression gives the activation energy for the heat of solution for dissolving In in CdS. The Arrhenius relationships derived in this thesis rely on C_o remaining constant throughout each diffusion anneal. In fact C_o increases rapidly from zero in some manner at the start of each anneal

Fig 6·6 AN ARRHENIUS PLOT OF THE NEAR -SURFACE In CONCENTRATION IN CdS OBTAINED USING THE ELECTRON MICROPROBE

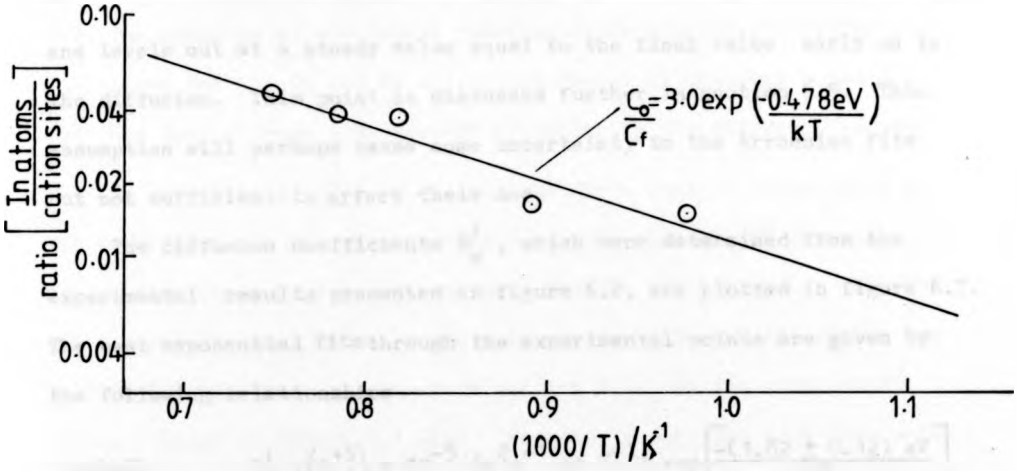

Fig 6·7 AN ARRHENIUS PLOT OF THE DIFFUSION COEFFICIENT D_o' FOR THE DIFFUSION OF In INTO CdS

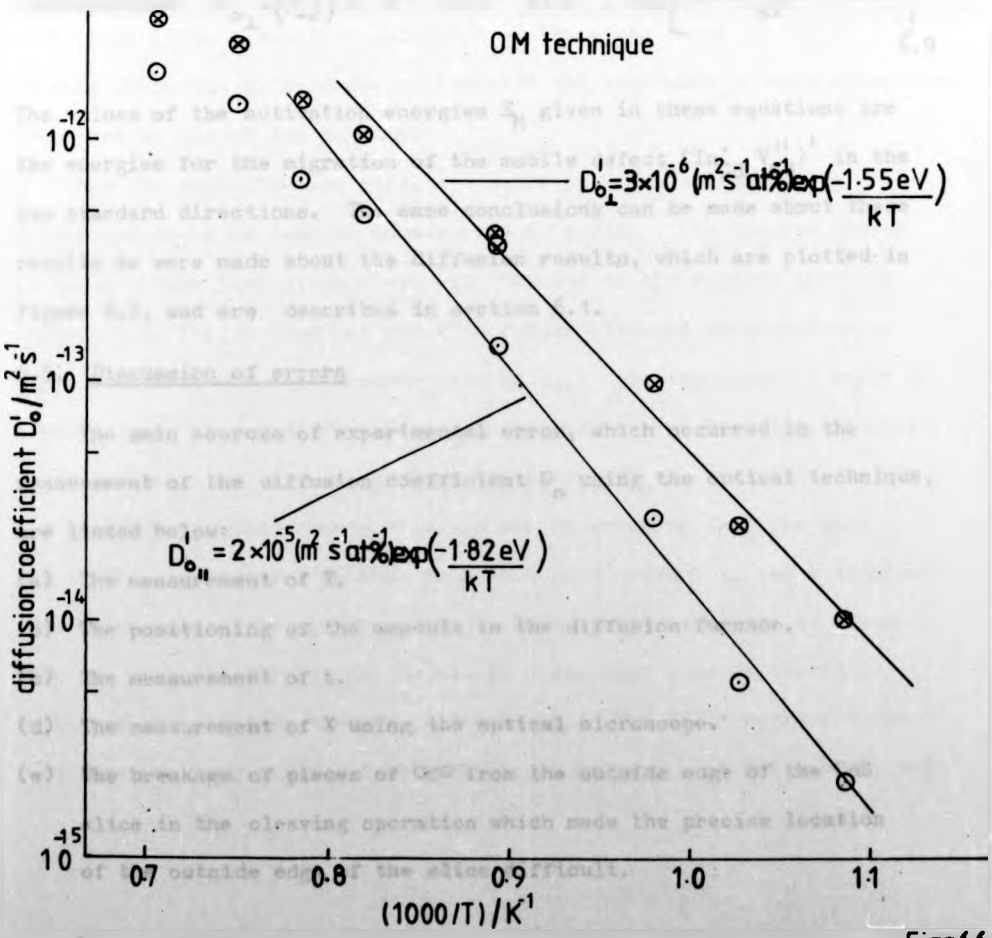

Figs 6·6, 6·7

and levels out at a steady value equal to the final value early on in the diffusion. This point is discussed further in section 6.5. This assumption will perhaps cause some uncertainty in the Arrhenius fits but not sufficient to affect their use.

The diffusion coefficients D_o', which were determined from the experimental results presented in figure 6.2, are plotted in figure 6.7. The best exponential fits through the experimental points are given by the following relationships

PARALLEL $$D_{o_{\parallel}}' = \left(2^{+3}_{-1}\right) \times 10^{-5} \ (m^2 s^{-1} \text{ at } \%^{-1}) \exp\left[\frac{-(1.82 \pm 0.12) \text{ eV}}{kT}\right] \quad 6.8$$

PERPENDICULAR $$D_{o_{\perp}}' = \left(3^{+5}_{-2}\right) \times 10^{-6} \ (m^2 s^{-1} \text{ at } \%^{-1}) \exp\left[\frac{-(1.55 \pm 0.12) \text{ eV}}{kT}\right] \quad 6.9$$

The values of the activation energies E_M given in these equations are the energies for the migration of the mobile defect $(In_{Cd}^{\bullet} \ V_{Cd}^{''})^{'}$ in the two standard directions. The same conclusions can be made about these results as were made about the diffusion results, which are plotted in figure 6.2, and are described in section 6.1.

6.5. Discussion of errors

The main sources of experimental error, which occurred in the measurement of the diffusion coefficient D_o using the optical technique, are listed below:

(a) The measurement of T.

(b) The positioning of the ampoule in the diffusion furnace.

(c) The measurement of t.

(d) The measurement of X using the optical microscope.

(e) The breakage of pieces of CdS from the outside edge of the CdS slice in the cleaving operation which made the precise location of the outside edge of the slice difficult.

(f) The presence of a chemical reaction layer outside the diffusion layer for the Ga and Al diffusions (refer to chapters 9 and 10).

(g) The loss of mass from the CdS slice during the diffusion anneal.

In the plots of X^2 versus t all the above factors contributed to the error in X and the error in the dependent variable X^2 is much larger than it is in the independent variable. The errors in (a), (b) and (c) are the same as those given in section 5.5 and the errors due to item (g) have been discussed in section 5.5. As the plots of X^2 versus t shown in figure 6.1 give reasonable straight line fits which pass through the origin, the majority of the mass loss in the CdS slice must have occurred when the ampoule was placed in the furnace. If the mass loss had occurred at the end of the anneal then the results would have given a negative intercept on the plots shown in figure 6.1. In fact there was no evidence to indicate the existence of such a negative intercept on any of the results.

For the magnification used, the scale in the eyepiece of the microscope could be read to an accuracy of $\pm$ 2μm. The largest source of error in the list given above was, because of the reasons given in section 3.3, due to item (e) and this factor affected measurements of $X_\perp$ more than it affected measurements of $X_{||}$. The experimental error in X was $\pm$ 7 μm but for diffusion anneals carried out at high temperatures it was probably as large as $\pm$ 10 μm (that is $\pm$ 3%).

Another possible source of error was in assuming that the best fit to the experimental points, on a plot of X^2 versus t, was a straight line which passed through the origin. It is only reasonable to assume that the best fit through the points is a straight line if the Cd/In ratio remains constant throughout the anneal. The Cd/In ratio will in fact increase very rapidly from zero at the beginning of the anneal, and

as the anneal proceeds the rate of increase will slow down until the final value is obtained at the end of the anneal. As the X^2 versus t plots described in section 6.1 are all linear and pass through the origin, it indicates that the Cd/In ratio must have remained reasonably constant at a value near the final value throughout the major portion of the anneal. In fact, there was not sufficient evidence in the experimental data obtained to indicate that a straight line passing through the origin was not the best fit to each set of experimental data.

The error in the diffusion coefficient D_o was estimated to be $\pm$ 10%. The scatter in the experimental points in the Arrhenius plots in figure 6.2 indicated that this was a reasonable estimate. The measurement of the diffusion anisotropy involved the determination of $D_{o_\perp}/D_{o_{||}}$ on each CdS slice, and errors due to several factors such as (a), (b),(c), tended to cancel each other out either wholly or partially. The final error in each ratio was estimated to be $\pm$ 3%.

Some of the uncertainties in the measurement of C_o using the electron microprobe have been discussed in section 6.3. One large source of error occurred in estimating the background due to the CdS. This contributed as much as 30% to the total maximum signal which was obtained at the outside edges of the CdS slices at x = 0. The other major source of error was due to uncertainties in the correction factors listed in section 3.4. Greater accuracy could possibly have been obtained if a series of reference standards of low In concentration had been specially manufactured from known masses of In_2S_3 and CdS rather than using pure In metal (13). The uncertainty in the values of C_o increased the error of $\pm$ 10% in D_o to $\pm$ 15% for D'_o.

6.6. References

1. H. MYKURA, J. Phys. D: Appl. Phys., 10, P779 (1977).
2. S. F. NYGREN and G. L. PEARSON, J. Electrochem. Soc., 116, P648 (1969).
3. N. BINDLEY, Diffusion of Zinc into Gallium Arsenide Phosphide, M.Sc. project report, Lanchester Polytechnic (1976).
4. H. KATO and S. TAKAYANAGI, Japan. J. Appl. Phys., 2, P250 (1963).
5. L. V. NASLOVA, O. A. NATSEEV, Ya. V. RAD and A. K. V. SANIN, Physics of p - n junctions and semiconductor devices (Edited by S. F. RYVKIN and Ya. K. SHWARTSEV, translated from Russian), P234, Consultants Bureau, New York (1971).
6. R. A. PERKINS and R. A. RAPP, Metal. Trans., 196, 4, P193 (1973).
7. C. GRESKOVICH, J. Amer. Cer. Soc., 53, P498 (1970).
8. W. L. ROTH, Physics and Chemistry of II-VI Compounds (Edited by M. AVEN and J. S. PRENER), P119, North Holland Publishing Company, Amsterdam (1967).
9. S. S. DEVLIN, J. N. JOST, and L. R. SHIOZAWA, U.S. Dept. Comm. Office Tech. Serv., P.B. Reproductions (1960).
10. M. HALL. Private Communication, University of Birmingham (1976).
11. Report to the Science Research Council on microprobe correction procedures from the University of Sheffield (1973), private communication.
12. R. THEISEN, Quantitative Electron Microprobe Analysis, Springer-Verlag, Berlin (1965).
13. P. J. GOODHEW, Electron Microscopy and Analysis, Wykeham Publications (London) Ltd., (1975).

7. Proposed defect mechanisms for the diffusion of In into CdS

The aim in this chapter is to consider all the experimental data that was obtained in chapters 5 and 6 and to propose defect mechanisms for both the concentration dependent and the concentration independent diffusions. One of the main differences between the two sets of diffusions is that the Cd partial pressures in the ampoules were widely different and the defect mechanism in both cases is probably dependent on this.

The points which are considered in this chapter are: the experimental results which have been obtained, the partial pressure conditions in the ampoule and the experimental work which has been carried out by Kröger and co-workers (1, 2) on the self-diffusion studies into pure and In-doped CdS. As some of the In-doping levels obtained in this thesis were comparable with the In-doping levels used by Kröger et al, some of the experimental conditions used in the two sets of measurements will overlap when they are represented on an isothermal plot of the Cd-In-S ternary phase diagram. In addition, the analysis of the results on the diffusion of group III metals into NiO and MgO (3 - 7), which is described in the introduction to chapter 5, is considered as the diffusion behaviour is similar to what has been obtained in chapters 5 and 6. Perkins and Rapp (3) used a similar method for analysing their results, on the diffusion of Cr into NiO, as is used in this thesis for analysing the concentration dependent In diffusions.

7.1. Pressure conditions in the diffusion ampoule

When a pure CdS crystal is sealed in an evacuated ampoule the Cd and S_2 partial pressures are related by the relationship (8)

$$K_{CdS} = P_{Cd} P_{S_2}^{\frac{1}{2}}. \qquad 7.1$$

When a pure stoichiometric CdS crystal is in equilibrium with its vapour the total pressure is a minimum and the Cd and S_2 partial pressures are

related by

$$P_{Cd} = 2P_{S_2} = 2^{\frac{1}{3}} K_{CdS}^{\frac{2}{3}} \quad 7.2$$

Thermodynamic data for the Cd - S phase system has been compiled by Shiozawa and Jost (9).

When CdS and In were placed in an evacuated ampoule, the partial pressures exerted by the components were estimated by assuming that the In partial pressure was at the metal saturation value and that the Cd and S_2 values were obtained by assuming that the CdS was under conditions of free evaporation. This assumption was valid provided the mass of the In was small compared to the mass of the CdS. In reality this was not so because the effective mass of the CdS, that is, that which was influenced by the diffusion, was much less than the total mass. The errors incurred by this assumption were difficult to estimate, but the calculated metal partial pressures from the In/Cd alloy system were still a useful guide to the In and Cd partial pressures in the ampoule.

When known quantities of In and Cd metals were sealed in the ampoule with the CdS, the metal partial pressures were calculated using the chemical activity data for the In/Cd phase system (10).

The partial pressures in the ampoule for the two sets of In diffusion experiments are plotted as a function of temperature in figure 7.1 and the near-surface In concentration in the CdS slices obtained in the two sets of experimental measurements are replotted in figure 7.2 for convenience.

It is necessary to estimate the partial pressures in the ampoule so that comparisons can be made between this work and the work carried out by Kröger et al where Cd partial pressures have been quoted. For the purpose of the thesis it has been found to be more convenient to

Fig 7.1 A TEMPERATURE PLOT OF THE PARTIAL PRESSURES IN THE DIFFUSION AMPOULE

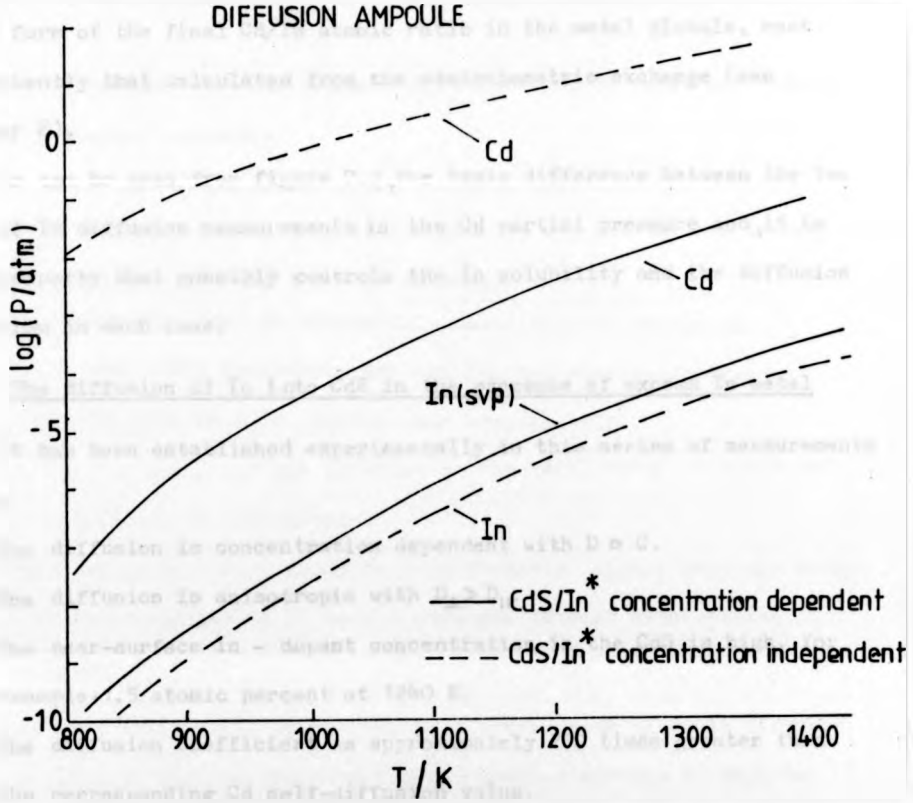

Fig 7.2 A TEMPERATURE PLOT OF THE NEAR-SURFACE In CONCENTRATION IN THE CdS

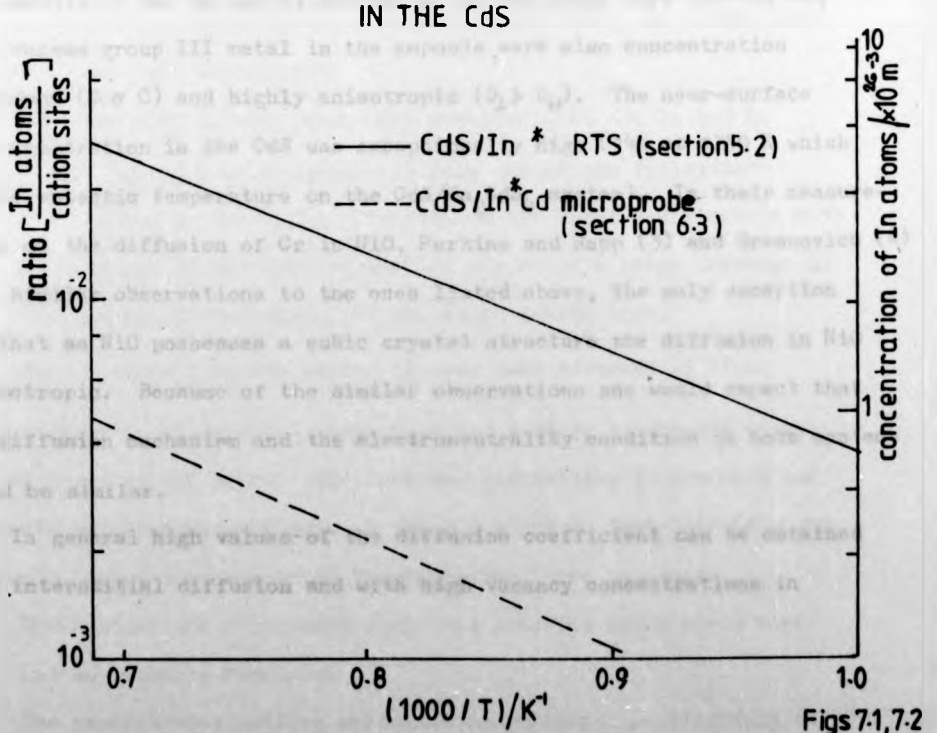

Figs 7.1, 7.2

use a form of the final Cd/In atomic ratio in the metal globule, most conveniently that calculated from the stoichiometric exchange (see chapter 8).

As can be seen from figure 7.1, the basic difference between the two sets of In diffusion measurements is the Cd partial pressure and, it is this property that possibly controls the In solubility and the diffusion mechanism in each case.

7.2. The diffusion of In into CdS in the presence of excess In metal

It has been established experimentally in this series of measurements that:-

(a) The diffusion is concentration dependent with $D \propto C$.

(b) The diffusion is anisotropic with $D_{\perp} > D_{\parallel}$.

(c) The near-surface In - dopant concentration in the CdS is high, for example-1.5 atomic percent at 1240 K.

(d) The diffusion coefficient is approximately 200 times greater than the corresponding Cd self-diffusion value.

The results of the Ga and Al diffusions in CdS, which were carried out with excess group III metal in the ampoule, were also concentration dependent ($D \propto C$) and highly anisotropic ($D_{\perp} > D_{\parallel}$). The near-surface Ga concentration in the CdS was exceptionally high (1% at 1240 K which is the eutectic temperature on the CdS/Ga_2CdS_4 system). In their measurements on the diffusion of Cr in NiO, Perkins and Rapp (3) and Greskovich (4) made similar observations to the ones listed above, the only exception was that as NiO possesses a cubic crystal structure the diffusion in NiO is isotropic. Because of the similar observations one would expect that the diffusion mechanism and the electroneutrality condition in both systems would be similar.

In general high values of the diffusion coefficient can be obtained with interstitial diffusion and with high vacancy concentrations in

vacancy diffusion. In this project the former can be ruled out because of the following reasons:-

(a) It would not be possible to get the high dopant concentrations that were obtained in this experiment, if all the In were interstitial.

(b) It would not give the $D \propto C$ dependency.
It is possible that an interstial-substitutional mechanism could give a $D \propto C$ dependency but not for the electro-neutrality condition used in this section (see equation 7.5).

(c) As the c/a ratio for CdS is close to the ideal value it would not be significantly anisotropic.

(d) The activation energy would be significantly higher than the values that were obtained if it were a straight forward interstitial mechanism.

Van Gool (11) states that, when a group III metal such as Ga is diffused into CdS, interstitial Ga could be the predominant species at high Ga concentrations. In fact, there is an error in Van Gool's book (12) and there is no possibility of interstitial Ga being the predominant species under such conditions.

The high solubilities, that were obtained with the In and Ga diffusions, can only be accommodated with one of the following:-

(a) An increase in the number of cation sites which would result with an increase in the mass of the CdS slice and a large increase in the vacancy concentration on the anion sub-lattice.

(b) When M atoms from the cation lattice have replaced Cd atoms.

The evaporation of Cd and S atoms from the surface of the CdS slice at the start of the anneal ruled out any possibility of carrying out accurate weighing measurements on the CdS slice to test item (a), but it can be ruled out because of the following three reasons:-

(a) The S atoms are relatively large and immobile which would make (a) an unlikely reaction.

(b) The experimental lattice parameter measurements particularly on

Ga-doped CdS indicate that a substantial number of Cd vacancies are formed during the diffusion anneal.

(c) The concentration dependent diffusion gives a substantial vacancy concentration in the Cd sublattice and the corresponding value on the S sublattice would be very small as they are controlled by the Schottky defect equlibrium which is given by

$$\left[V_S^{\cdot\cdot}\right] \left[V_{Cd}^{''}\right] = K_S(T) \qquad 7.3$$

If In is incorporated substitutionally onto the cation lattice as an independent atom or ion it would not be possible to get high values of the diffusion coefficient. If diffusion does take place by a vacancy mechanism, the formation of an associated defect of the form $(In_{Cd}^{\cdot} V_{Cd}^{''})^{'}$ can account for the experimental results which are given at the beginning of this section. In addition, an associated defect of this kind, even if it were uncharged, can have an electric dipole moment and this will have a preferred orientation in the CdS which could automatically account for the high diffusion anisotropy.

If it is accepted that the In atoms enter the Cd sub-lattice substitutionally then the possible ways in which it can be achieved are:-

(a) An exchange of two In^{3+} ions for three Cd^{2+} ions which will result in the formation of Cd vacancies $V_{Cd}^{''}$, which causes no change in stoichiometry.

(b) An exchange of one In^{3+} ion and an electron for one Cd^{2+} ion with the electron entering the conduction band, which changes the metal to chalcogenide stoichiometry.

(c) An excess of In entering the lattice to increase the total metal to S ratio, by adding an In metal atom to the Cd sub-lattice and creating an S vacancy, which will produce a stoichiometry change three times as large as (b) per In atom.

Because of the high band gap energy (approximately 2.5 eV) and the ionicity of CdS, the effect of (b) is likely to be small and the effect of (c) will be small. The effect of (b), while being small will occur to some extent and may be important for low In concentrations. It is possible that (b) controls the electrical properties and (a), as it does not contribute any electrons to the lattice, controls the diffusion in the CdS.

There will be a Coulombic attraction between $In_{Cd}^{\bullet}$ and $V_{Cd}^{''}$ to give $(In_{Cd}^{\bullet}\ V_{Cd}^{''})'$ and $(In_{Cd}^{\bullet}\ V_{Cd}^{''}\ In_{Cd}^{\bullet})^{*}$. The latter defect because of its neutrality will be the stable form of the complex and will exist at low temperatures. At high temperatures it will dissociate to $In_{Cd}^{\bullet}$ and $(In_{Cd}^{\bullet}\ V_{Cd}^{''})'$ and possibly into $2In_{Cd}^{\bullet}$ and $V_{Cd}^{''}$.

It is possible for other less likely defects to form; examples of some of the possibilities are listed below:-

(a) $V_{Cd}^{''}$ could give up one or two electrons to the conduction band;

(b) the associated defect $(In_{Cd}^{\bullet}\ V_{Cd}^{''})'$ could give up one electron;

(c) $In_{Cd}^{\bullet}$ could release a hole or capture an electron from the conduction band to become In_{Cd}^{*};

(d) Interstitial defects could be present.

Defects of types (a) and (b) could lead to n-doping which is discussed in section 7.4. Defects of type (c) would either lead to p-doping, which is unknown in CdS and would not be majority defects, or reduce the existing n-doping. Defects of type (d) could only be present in very small concentrations. Defects of the kind listed above are minority defects and it is not possible to deduce their concentrations as the necessary thermodynamic data are not known accurately.

Diffusion dependent on concentration (but not linearly concentration dependent with $D \propto C$) has been observed by Bjerkeland and Holwech (13)

for the diffusion of the group III metals Al, Ga and In into ZnSe and by Chern and Kröger (14) for the diffusion of In into CdS and CdTe. In the former set of measurements a simple dependency relationship was not obtained whereas in the latter set, which was not very extensive, the authors were unable to explain the results. The results obtained by Bjerkeland and Holwech are discussed further in section 7.3. The results reported in this thesis are far more extensive than the ones reported by these investigators. Both Perkins and Rapp (3) and Greskovich (4) did, as is mentioned earlier, obtain concentration diffusion profiles with $D \propto C$ for the diffusion of Cr into NiO.

There is an overlap in the Cd partial pressure conditions and the In dopant levels for the work on the diffusion of In in CdS described in this thesis and, the work carried out by Kumar and Kröger (2) and by Hershman et al (1) for the self-diffusion of Cd in In-doped CdS. The results of the self-diffusion measurements are shown in figures 2.4 and 2.5. The precise conditions where the overlap occurred for the concentration dependent In diffusion measurements at 1173 K are represented by point A in figure 7.3. The graph also shows isotherms for the dependence of D^{*}_{Cd} upon P_{Cd} for CdS crystals doped with various concentrations of In obtained by Kumar and Kröger (2). It is possible that the CdS will possess similar defects in the two sets of measurements and that a similar electroneutrality condition will apply. The conditions for the concentration independent In diffusion at 1173 K are represented by point B and are discussed in section 7.3.

For the concentration dependent diffusion the full electroneutrality condition will be an expression of the form:-

$$\left[In^{\bullet}_{Cd}\right] = 2\left[V''_{Cd}\right] + \left[\left(In^{\bullet}_{Cd}\ V''_{Cd}\right)'\right] + \left[e'\right] \qquad 7.4$$

A PLOT SHOWING THE OVERLAP BETWEEN THE DIFFUSION CONDITIONS USED BY KRÖGER ET AL AND THE PRESENT WORK.

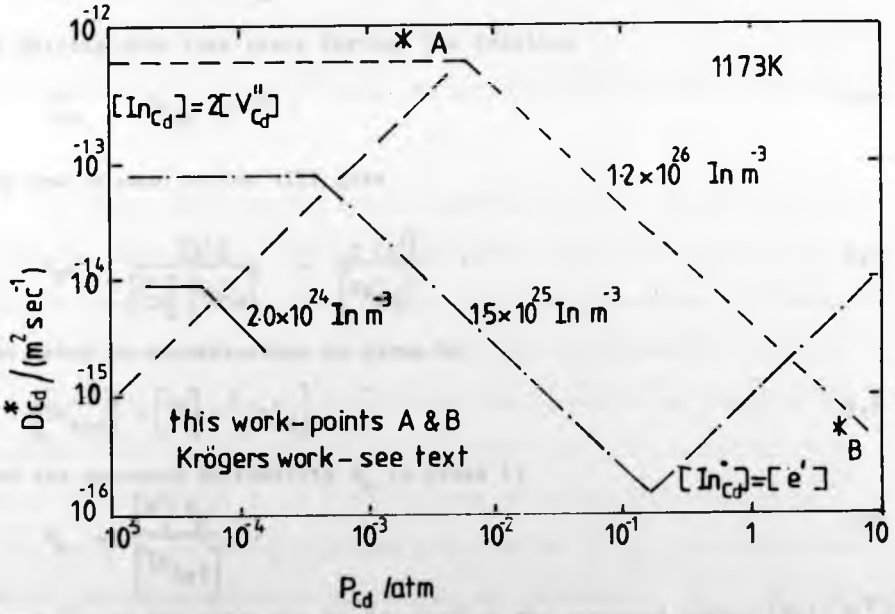

Fig7·3

The third term has been included in the right hand side of the above equation to account for the small proportion of negative carriers which have been measured in section 7.4.

In their experiments on CdS at 1073 K and at low values of Cd partial pressure, Hershman et al calculate $\left[(In_{Cd}^{\bullet}\ V_{Cd}^{''})'\right] / \left[V_{Cd}^{''}\right] \approx 2$ at an In concentration of $6.5 \times 10^{25}\ m^{-3}$ which implies that pairing is important at high In concentrations. At much higher temperatures this ratio will decrease rapidly and the above electroneutrality condition can be approximated to

$$\left[In_{Cd}^{\bullet}\right] \approx 2 \left[V_{Cd}^{''}\right] . \qquad 7.5$$

If pairing does take place through the reaction

$$V_{Cd}^{''} + In_{Cd}^{\bullet} \rightleftharpoons P' , \qquad 7.6$$

the law of mass action will give

$$K_{P'} = \frac{\left[P'\right]}{\left[V_{Cd}^{''}\right]\left[In_{Cd}^{\bullet}\right]} = \frac{2\left[P'\right]}{\left[In_{Cd}^{\bullet}\right]^2} . \qquad 7.7$$

The total In concentration is given by

$$\left[In_{tot}\right] = \left[P'\right] + \left[In_{Cd}^{\bullet}\right] \qquad 7.8$$

and the measured diffusivity D_M is given by

$$D_M = \frac{\left[P'\right] D_{P'}}{\left[In_{tot}\right]} , \qquad 7.9$$

where $D_{P'}$ is the diffusion coefficient of the compound defect $(In_{Cd}^{\bullet}\ V_{Cd}^{''})'$. It is assumed in equation 7.9 that the mobility of $(In_{Cd}^{\bullet}\ V_{Cd}^{''})'$ is much greater than any other defect that may be present. If it is assumed that $\left[P'\right] \ll \left[In_{Cd}^{\bullet}\right]$ then the expression for D_M will reduce to

$$D_M = \tfrac{1}{2} D_{P'} K_{P'} \left[In_{tot}\right] . \qquad 7.10$$

This gives the same dependency between the measured value of the diffusion coefficient D_I, and the total In concentration ($D_I \propto [In_{tot}]$) that was obtained with the concentration dependent measurements described in chapter 5. This assumes that $(In_{Cd}^{\bullet}\ V_{Cd}^{''})'$ is the only mobile form of In and that there is an easy and rapid interchange of In in all its forms in the CdS.

If In is incorporated into the Cd sublattice by the direct exchange of two In^{3+} ions with three Cd^{2+} ions then this can be represented by the following reaction:-

$$In(vap) + 1.5Cd_{Cd}^{*} \rightleftharpoons In_{Cd}^{\bullet} + 1.5Cd(vap) + 0.5V_{Cd}^{''} \quad . \qquad 7.11$$

Application of the law of mass action gives

$$\frac{P_{In}}{P_{Cd}^{1.5}} \propto [In_{tot}]^{1.5} \quad . \qquad 7.12$$

The above defect model looks plausible but to be absolutely certain it is the correct one, further measurements need to be carried out. The partial pressure dependencies of the In and Cd vapours on such parameters as the measured diffusion coefficient D_N and the electrical carrier concentration need to be established. Care needs to be taken in the interpretation, as a different mobile defect and a different electroneutrality condition would normally give different dependencies to those given in equations 7.10 and 7.12; but it is possible occasionally for different conditions to those used in these equations to give similar dependencies to those shown in equation 7.10 and 7.12. For example, if the mobile defect is $(In_{Cd}^{\bullet}\ V_{Cd}^{'})^{*}$ and the electroneutrality condition is

$$[In_{Cd}^{\bullet}] = [V_{Cd}^{'}] \quad , \qquad 7.13$$

then the use of similar assumptions as those that were used for deducing equation 7.8 will also yield a value of $D_N \propto [In_{tot}]$. There was

insufficient time and apparatus available for carrying out additional measurements.

In fact the diffusion mechanism proposed in this section agrees with those put forward by Greskovich (4) and Perkins and Rapp (3) for the diffusion of Cr in NiO. In these diffusions the workers used the solid diffusion sources Cr_2O_3 and $NiCr_2O_4$ respectively which were in contact with the NiO crystal. It is not convenient to discuss this type of Cr diffusion in relation to the Ni/Cr atomic ratio as this is only useful when there is a metal globule in the ampoule. It is also possible to interpret the type of concentration profile obtained for the In and Cr diffusions in terms of the concentration C_o and the concentration gradient dC/dx. Concentration dependent diffusion profiles with $D \propto C$ are produced at high values of C_o and dC/dx (that is a low Cd/In ratio in the diffusions described in this thesis) and concentration independent diffusion profiles are produced at much lower values of C_o and dC/dx (high Cd/In ratios). It is possible that the initial values of C_o and dC/dx in the work reported by Chern and Kröger (14) and Bjerkeland and Holwech (13) were sufficiently high to give concentration dependent profiles, but that insufficient tracer was sealed in the ampoule to maintain high values throughout each diffusion anneal.

This section can be concluded by stating that when In is diffused in CdS in the presence of excess In, diffusion takes place via the mobile defect $(In^{\bullet}_{Cd}\ V''_{Cd})'$ with the In being incorporated onto the Cd sublattice by the stoichiometric exchange where three Cd atoms leave the crystal for every two In atoms that enter from the surrounding vapour.

7.3. The diffusion of In into CdS in the presence of excess In and Cd metals

In this series of measurements the diffusions were carried out with an excess of radioactive In metal and inactive Cd metal in the

ampoule; this gave a Cd/In ratio of approximately 3.4 in the metal globule. The main experimental observations were:-

(a) The diffusion was concentration independent with no visible diffusion front.

(b) The diffusion coefficient was much lower than for the concentration dependent case, the diffusion coefficient and the activation energy values were similar to the values obtained for the self-diffusion of Cd into CdS.

(c) The In concentration values in the CdS were much lower than for the concentration dependent case (for example-0.2 at % at 1240 K as against 1.5 at % at the same temperature for the concentration dependent case).

(d) The Cd partial pressure in the ampoule was much higher than for the corresponding concentration dependent case.

(e) There was no evidence of any diffusion anisotropy for diffusions in the two standard directions.

In the reports in the literature on the diffusion of group III metals into II-VI compounds, some of the workers carried out the diffusion with excess group II metal in the ampoule, whereas others carried out diffusions with no added group II metal present. Some investigators even sealed excess chalcogen into the ampoule along with the II-VI crystal and the group III tracer. There does not appear to be any correlation between the type of diffusion profile obtained and the proportion of materials sealed in the ampoules. For the diffusions which are described in chapters 5 and 6, when Cd is added to the ampoule the diffusions are concentration independent and when no Cd is added the diffusions are concentration dependent. Yokozawa et al (15) and Koshiga and Sugano (16), in their diffusion studies into ZnTe and ZnS

respectively, added excess Zn to the ampoule and obtained concentration independent profiles which are consistent with what is reported in this thesis. Bjerkeland and Holwech (13) in their studies on ZnSe added excess Zn for the Al diffusions and excess Se for the In and Ga diffusions. The profiles they obtained, as was mentioned in section 7.2, were concentration dependent but not of the form $D \propto C$. Chern and Kröger (14), in their investigations on the diffusion of In into CdS and CdTe, added excess chalcogen to the ampoule and as in the case of the former, obtained concentration dependent profiles, but again it was not of the type that has been obtained in this thesis. In the case of the latter concentration independent profiles were obtained.

However, there is a similarity between the results obtained for the concentration independent In diffusions described in this thesis and the results obtained by Chen et al (6) and Weber et al (5) who respectively carried out measurements on the diffusion of Cr into NiO and MgO. The two sets of workers obtained concentration independent profiles which were the result of using extremely small amounts of radioactive tracer. This meant that the Cr concentrations used in these cases was much lower than for the concentration dependent cases of Greskovich (4) and Perkins and Rapp (3) measured at the same temperature. In addition, Chen et al and Weber et al have also observed that the diffusion coefficient in the concentration independent diffusion is much smaller than it was for the corresponding concentration dependent diffusion.

It is rather more difficult to propose a diffusion mechanism for the set of results under discussion in this section than it was for the concentration dependent case. Several investigators have stated that the diffusion of group III metals into II-VI compounds is sub-substitutional (15, 5). As there is no definite evidence of any diffusion anisotropy for diffusions in the two standard directions and as the c/a ratio is close to the ideal value, diffusion is probably by a single

defect which is very likely to be a simple neutral vacancy V^{*}_{Cd}. If associated defects do form in this case they will not possess a preferred orientation in the Cd sublattice, and if there is any interaction between the defects it must be exceedingly weak.

In this case the Cd partial pressure is higher than for the concentration dependent case and hence the vacancy concentration V^{*}_{Cd} will be less (it will be verified later that the vacancy must be neutral). It is also possible that the In atoms in this case enter the Cd sub-lattice by a method that does not cause the vacancy concentration V^{*}_{Cd} to increase as was obtained for the concentration dependent diffusion. The vacancy concentration V^{*}_{Cd} in this case is probably independent of In concentration and is constant at a given temperature.

13 For a pure material it is possible to write $\left[V^{*}_{Cd}\right] \alpha\ P^{-1}_{Cd}$ (11).

In this case the diffusion mechanism can be represented by the following equation

$$In^{\cdot}_{Cd} + V^{*}_{Cd} \rightleftharpoons (In^{\cdot}_{Cd}\ V^{*}_{Cd})^{\cdot} \rightleftharpoons P^{\cdot} \quad , \tag{7.14}$$

and it can be assumed that

$$\left[In^{\cdot}_{Cd}\right] \approx \left[In_{tot}\right] \quad . \tag{7.15}$$

The law of mass action will give

$$K_{P^{\cdot}} = \frac{\left[P^{\cdot}\right]}{\left[In_{tot}\right]\left[V^{*}_{Cd}\right]} \quad , \tag{7.16}$$

and the diffusion coefficient can be written in the form

$$D_{M} = \frac{\left[P^{\cdot}\right] D_{P^{\cdot}}}{\left[In_{tot}\right]} = K_{P^{\cdot}}\left[V^{*}_{Cd}\right] D_{P^{\cdot}} = \frac{const}{P_{Cd}} D_{P^{\cdot}} \quad . \tag{7.17}$$

At a fixed temperature this relationship gives a concentration independent diffusion mechanism.

For Cd self-diffusion measurements into In-doped CdS at high Cd partial pressures the electroneutrality condition which has been proposed is

$$\left[In_{Cd}^{\cdot}\right] = \left[e'\right]. \qquad 7.18$$

The conditions in the ampoule, at the diffusion temperature of 1173 K for the concentration independent In diffusions, are shown in figure 7.3 along with the diffusion isotherms obtained by Kumar and Kröger (2) at the same temperature on the self-diffusion of Cd into In-doped CdS. The conditions obtained here for the In diffusions are represented by point B. As there is an overlap in the Cd partial pressures at high values of the partial pressure it would be reasonable to assume that the electroneutrality condition for the concentration independent diffusion would be similar to that proposed by Kumar and Kröger (2).

It is possible for the neutral Cd vacancies, V_{Cd}^{*}, to interact with the free electrons in the following manner

$$V_{Cd}^{*} + e' \rightleftharpoons V_{Cd}' \qquad 7.19$$

with

$$\left[V_{Cd}'\right] \ll \left[V_{Cd}^{*}\right].$$

The law of mass action will give

$$K_{7.19} = \frac{\left[V_{Cd}'\right]}{\left[V_{Cd}^{*}\right]\left[e'\right]}. \qquad 7.20$$

At a constant temperature

$$\left[e'\right] \propto \left[V_{Cd}'\right] \propto \left[In_{Cd}^{\cdot}\right]. \qquad 7.21$$

By using an analogous equation to 7.17 it is possible to see, that if the defect V_{Cd}' was the dominant mobile defect, that

$$D_M \propto \left[V_{Cd}'\right]. \qquad 7.22$$

The fact that a concentration independent diffusion was found means that the native defect involved must have been neutral.

The In atoms can be incorporated into the Cd sub-lattice through the following reaction

$$In^{*}(vap) + V^{*}_{Cd} \rightleftharpoons In^{\bullet}_{Cd} + e' \quad . \qquad 7.23$$

The law of mass action will give

$$\frac{P_{In}}{P_{Cd}} \propto \left[In_{tot}\right]^2 \quad . \qquad 7.24$$

In addition the diffusion coefficient is given by

$$D_M \propto \frac{1}{P_{Cd}} \quad . \qquad 7.25$$

As with the concentration dependent diffusion the above defect model does satisfy the experimental observations but to be sure that this mechanism is the correct one, further experimental work must be carried out to verify the above pressure dependencies. In fact, it is also possible to obtain concentration independent diffusion by assuming that diffusion takes place via an interstitial-substitutional mechanism.

If in the concentration dependent case the vacancy is charged and in the concentration independent case it is uncharged, then one would expect a much stronger bonding between $In^{\bullet}_{Cd}$ and V''_{Cd} than one would get between $In^{\bullet}_{Cd}$ and V^{*}_{Cd}. This could well be a part of the explanation for the higher diffusivity and greater anisotropy that was obtained in the concentration dependent diffusion.

In conclusion it is possible to state that with the limited amount of experimental information available, the concentration independent diffusion probably takes place substitutionally with the main defects being $In^{\bullet}_{Cd}$ and a neutral vacancy V^{*}_{Cd}.

7.4. Electrical measurements

Resistivity and Hall coefficient room temperature measurements were carried out on a single In-doped CdS slice using the Van der Pauw (17) method. The measurement was carried out by Dr. D. Shaw at the University of Hull. Specimen 150a (table 8.1) was uniformly doped throughout in an atmosphere of excess In at 1241 K to give 2.0 atomic % In. The concentration measurement was obtained using the electron microprobe. The electrical measurement gave a negative carrier concentration of 5.6×10^{25} m^{-3} showing that at room temperature only 14% of the In in the crystal was electrically active. This result does not affect the conclusions which have been drawn for the concentration diffusion where the primary defects are $In_{Cd}^{\bullet}$ and $(In_{Cd}^{\bullet} V_{Cd}^{''})^{'}$.

7.5. References

1. C. H. HERSHMAN, V. P. ZLOMANOV and F. A. KRÖGER, J. Sol. State Chem., 3, P401 (1971).
2. V. KUMAR and F. A. KRÖGER, J. Solid State Chem., 3, P387 (1971).
3. R. A. PERKINS and R. A. RAPP, Metal. Trans., 4, P193 (1973).
4. C. GRESKOVICH, J. Amer. Cer. Soc., 53, 9, P498 (1970).
5. G. W. WEBER, W. R. BITLER and V. S. STUBICAN, J. Amer. Cer. Soc., 60, P61 (1977).
6. W. K. CHEN, N. L. PETERSON and L. C. ROBINSON, J. Phys. Chem. Solids, 34, P705 (1973).
7. T. SOLAGA and A. J. MORTLOCK, Phys. Stat. Sol. (a), 3, K247 (1970).
8. D. A. STEVENSON, Atomic Diffusion in Semiconductors (Edited by D. SHAW) P431, Plenum Press, London (1973).
9. L. R. SHIOZAWA and J. M. JOST, Research on Improved II-VI crystals, Aerospace Research Laboratories Report 69 - 0107, Aerospace Research Laboratories, Office of Aerospace Research, United States Air Force, Wright-Patterson Air Force Base, Ohio, U.S.A. (1969).

10. R. HULTGREN, R. L. ORR, P. D. ANDERSON and K. K. KELLEY, Selected values of Thermodynamic Data of Metals and Alloys, John Wiley, New York (1963).

11. W. VAN GOOL, Principles of Defect Chemistry of Crystalline Solids, Academic Press, New York (1966).

12. W. VAN GOOL. Private Communication, letter to Dr. H. Nykura (1977).

13. H. BJERKELAND and I. HOLMECH, Phys. Norv., 6, P139 (1972).

14. S. S. CHERN and F. A. KRÖGER, Phys. Stat. Sol. (a), 25, P215 (1974).

15. M. YOKOZAWA, H. KATO and S. TAKAYANAGI, Denki. Kagaku., 36, 4, P282 (1968).

16. F. KOSHIGA and T. SUGANO, Shinku., 16, 5, P174 (1973).

17. P. F. KANE and G. B. LARRABEE, Characterisation of Semiconductor Materials, McGraw - Hill Book Company (1970).

8. Diffusion of In into CdS - comparison of experimental techniques

The results obtained for the diffusion of In into CdS using the RTS technique and the OM technique, which are outlined in chapters 5 and 6 respectively, are compared in this chapter. When a CdS slice is diffused in the presence of excess In metal only, the diffusion profiles are concentration dependent with $D \propto C$, whereas when the CdS slice is diffused in the presence of excess In and Cd metals, the diffusion profiles are independent of concentration and the diffusivity is much lower than for the concentration dependent case. The difference between the two experimental conditions can be interpreted in terms of the overall atomic ratio of the number of Cd to In atoms in the metal globule at the end of the diffusion and this quantity is defined as the overall final Cd/In ratio.

The relative amounts of In and CdS placed in the ampoules for the concentration dependent diffusion measurements described in sections 5.1 and 6.1 were different, and so the overall final Cd/In ratio in the metal globule was different for the two sets of measurements. For the concentration independent measurements described in section 5.4, where excess Cd metal is sealed in the ampoule along with the In, the overall final Cd/In ratio is much higher than the overall ratio obtained for the concentration dependent diffusions.

The overall final Cd/In ratio is made up of two components. The first is due to the stoichiometric exchange between the In atoms from the metal globule and the Cd atoms from the CdS slice on a two to three basis, which is required during diffusion to keep charge neutrality in the CdS slice. It is possible to calculate the resulting final Cd/In ratio due to this exchange, and it is referred to as the calculated stoichiometric exchange value; it will be abbreviated to CSE value

in this chapter. The second, which has a much greater value and is more difficult to calculate, is due to the evaporation of Cd and S atoms from the surface of the CdS slice when the ampoule is taken up to temperature in the furnace. It is the CSE final value which has been quoted in earlier chapters and, as this value can be easily calculated, it has been used as a relative scale in place of the overall final ratio.

Corresponding values of C_o for the concentration dependent diffusions determined using the microprobe and the RTS techniques, as can be seen in figure 8.1, give an CN value which is consistently higher than the RTS value at all temperatures by a factor slightly in excess of two. This discrepancy is also reflected in the Arrhenius plots of D_o' which are represented by lines E and B in figure 8.7. The reason for this discrepancy has been investigated by carrying out additional experiments which are outlined in section 8.1 along with the possible reasons for the discrepancy. The shape of the pseudo CdS/In_2S_3 phase diagram at low In concentrations is discussed in section 8.2 and the conclusions drawn from the In diffusion measurements, described in chapters 4 - 7 inclusive, are discussed in section 8.3.

8.1. Comparison of near-surface In concentrations

The near-surface In concentration C_o for the concentration dependent diffusions, which were measured using the RTS technique and the microprobe and are described in sections 5.2 and 6.3 respectively, are shown as Arrhenius plots in figure 8.1. The results are represented by the best straight line fit through each set of experimental points. As is mentioned in the introduction to this chapter, there is a discrepancy slightly in excess of two between the two sets of results with the RTS resul's being smaller than the corresponding microprobe results. In spite of the discrepancy in C_o, the value of the activation energy

SUMMARY OF C_o DETERMINATIONS FOR THE DIFFUSION OF In INTO CdS

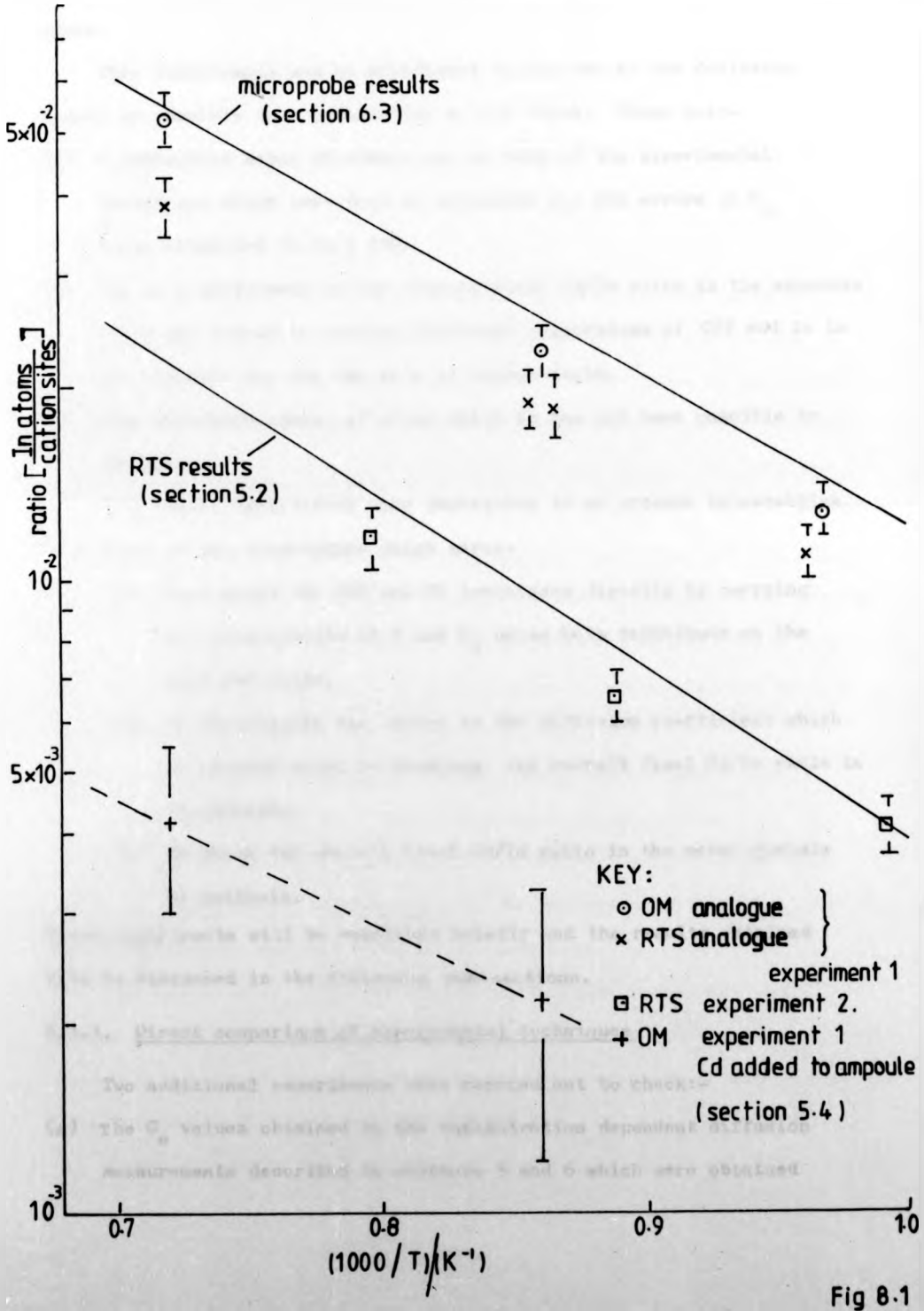

Fig 8.1

for the heat of solution for dissolving In in CdS determined using the two experimental techniques agree to within the limits of experimental error.

This discrepancy can be attributed to any one of the following causes or possibly to a combination of all three. These are:-

(a) A systematic error in either one or both of the experimental techniques which were used to determine C_o; the errors in C_o were estimated to be $\pm$ 10%.

(b) Due to a difference in the overall final Cd/In ratio in the ampoules which was caused by sealing different proportions of CdS and In in the ampoules for the two sets of measurements.

(c) Some undefined source of error which it has not been possible to identify.

Additional experiments were undertaken in an attempt to establish the cause of the discrepancy which were:-

(a) To compare the RTS and OM techniques directly by carrying out measurements of X and C_o using both techniques on the same CdS slice.

(b) To investigate the change in the diffusion coefficient which is brought about by changing the overall final Cd/In ratio in the ampoule.

(c) To check the overall final Cd/In ratio in the metal globule by analysis.

These experiments will be described briefly and the results obtained will be discussed in the following sub-sections.

8.1.1. Direct comparison of experimental techniques

Two additional experiments were carried out to check:-

(a) The C_o values obtained in the concentration dependent diffusion measurements described in chapters 5 and 6 which were obtained

respectively using the RTS and OM techniques. In this case a single measuring technique was used.

(b) To make a direct comparison of the techniques by carrying out measurements of X and C_o using both techniques on the same CdS slice.

Experiment 1

Diffusion anneals were carried out at three different temperatures with the ampoules containing the same masses of CdS, In and Cd (to within ± 10%) as those which were used in the three series of measurements described in chapters 5 and 6. The aim of this experiment was to measure all the values of C_o using one technique, instead of the two, and the microprobe was chosen. This would reduce the errors in C_o as the measurements would not be affected by the systematic errors that the RTS and the OM techniques possess. The full details of the diffusion anneals carried out are given in table 8.1. and the results are plotted in figure 8.1.

In the case of the concentration dependent diffusions, the results obtained using the conditions of the RTS technique are consistently lower than the results obtained using the conditions of the OM technique by 20%. This difference, which is not as great as that between the standard results represented by the full lines in figure 8.1, is attributable to the difference between the overall final Cd/In ratio for the two sets of conditions.

The values of C_o obtained for the diffusions carried out with excess Cd and In metals in the ampoule are, as can be seen in figure 8.1, a factor of ten lower than the corresponding concentration dependent results. This information has been used in chapter 7.

TABLE 8.1: SUMMARY OF THE DIFFUSION DETAILS AND THE RESULTS OBTAINED IN COMPARISON EXPERIMENT 1

Diffusion number	Experiment simulated	Nominal weights of CdS, In, Cd	Temperature of the anneal	1000/T	Estimation of fraction of CdS slice doped	Duration of anneal	Measured surface concentration
		mg	K	K^{-1}		s	C_o/C_f
150a	RTS	150, 15, -	1161	0.861	1.0	1.555, 5	0.0187
150b	RTS	150, 15, -	1161	0.861	1.0	1.555, 5	0.0183
150c	OM	60, 50, -	1161	0.861	1.0	1.555, 5	0.0225
150d	RTS	150, 15, 50	1161	0.861	0.4	1.555, 5	0.00216
151a	RTS	150, 15, -	1036	0.965	0.3	5.103, 5	0.0108
151c	CN	60, 50, -	1036	0.965	0.3	5.103, 5	0.0124
151d	RTS	150, 15, 50	1036	0.965	0.1	5.103, 5	undetectable
152a	RTS	150, 15, -	1388	0.720	1.0	1.272, 4	0.0382
152c	CN	60, 50	1388	0.720	1.0	1.272, 4	0.0525
152d	RTS	150, 15, 50	1388	0.720	0.2	1.272, 4	0.00417

Surface concentration C_o/C_f is expressed as the ratio of In atoms to available cation sites.

Experiment 2

It has not been possible to make a direct comparison in this thesis of X and C_o values that were obtained independently for the concentration dependent diffusion using the RTS and the CM techniques; the different physical conditions used in the ampoule for each set of measurements made this impossible.

In this experiment such a comparison was made by measuring both C_o and X on the same CdS slice, which had been diffused in excess In metal, using both techniques. Sufficient CdS and radioactive In metal were sealed in each ampoule so that all the required measurements could be carried out. Diffusion anneals were carried out at three different temperatures and the full details of the diffusions are given in table 8.2 along with a summary of the results obtained. At the time of writing, the electron microprobe at the University of Birmingham was not operational and it was not possible to include the microprobe determinations of C_o and X.

In this series of measurements a radioactive standard source containing a known mass of In was made up for each of the diffusion anneals and the values of C_o obtained using the RTS technique are, in addition to being presented in table 8.2, plotted in figure 8.1.

Corresponding values of X, obtained at each temperature in experiment 2 using the RTS technique and the optical method, are at the same CSE final Cd/In ratio and so they can be compared directly. It can be seen that the values agree to within the limits of experimental error. Values of X which were obtained using the microprobe proved to be inaccurate; this point has been discussed in section 6.3.

All the results obtained for C_o, which have been obtained using both the RTS technique and the microprobe, are presented in figure 8.1. These

TABLE 8.2: SUMMARY OF THE DIFFUSION DETAILS AND THE EXPERIMENTAL RESULTS OBTAINED IN COMPARISON EXPERIMENT 2

			S1	S2	S4
Diffusion Details	Temperature T	K	1008	1127	1255
	1000/T	K^{-1}	0.992	0.888	0.797
	Duration t	s	7.765,5	6.300,4	3.600,3
	Mass of CdS, In in ampoule	mg	436, 23.9	358, 17.1	440, 16.2
	CSE final Cd/In ratio		1.54, -3	4.16, -3	6.39, -3
Optical results	Depth $X_{\parallel}$	m	1.153, -4	1.479, -4	1.008, -4
	Depth $X_{\perp}$	m	2.338, -4	2.485, -4	1.542, -4
	Anisotropy $D_{\perp}/D_{\parallel}$		4.109	2.823	2.340
RTS	Depth $X_{\parallel}$	m	1.17, -4	1.43, -4	1.10, -4
	Near-surface In concentration C_o/C_f		4.04, -3	6.65, -3	1.17, -2

Near-surface concentration is expressed as the ratio of In atoms/cation sites

include the results that were obtained in:-

(a) the determination of the diffusion parameters using the RTS technique (section 5.2);

(b) the determination of the diffusion parameters using the microprobe (section 6.4);

(c) comparison experiment 1 using the microprobe

(d) comparison experiment 2 using the RTS technique.

The results obtained using the RTS technique (items (a) and (d)) give reasonably consistent results and the same is true of the results obtained using the microprobe (items (b) and (c) microprobe analogue). In spite of this agreement, there is a discrepancy of a factor slightly in excess of two at all temperatures between the results obtained using the two techniques and this can be attributed in part to two causes. The first, which has been dealt with in experiment 1, is due to the variation in the overall final Cd/In ratio between the two sets of conditions used for the concentration dependent diffusion in chapters 5 and 6, and accounts for a discrepancy of approximately 20%. The second one is the possible error of measurement in each of the experimental techniques used which is $\pm$ 10%. In spite of this, these two sources of error cannot possibly account for the discrepancy between the two sets of results which are represented by the full lines in figure 8.1.

8.1.2. Variation of the diffusion coefficient with the overall final Cd/In ratio.

It was mentioned in the introduction to this chapter that the overall final Cd/In ratio is made up of two contributions. The first, which is due to the stoichiometric exchange that takes place between the In and Cd atoms in a diffusion anneal, is easy to calculate and

typical values are given in table 8.3. The second contribution, which is much greater than the first, is due to the evaporation of CdS from the surface of the slice at the beginning of a diffusion anneal. The amount of evaporation will increase with temperature and the contribution to the overall final Cd/In ratio is more difficult to evaluate.

The variation between the diffusion coefficient and the CSE final Cd/In ratio was measured at three different temperatures. Diffusion anneals were carried out in which the relative amounts of CdS, Cd and In placed in each ampoule were varied such that the CSE final Cd/In ratio in the metal globule could be varied over as wide a range of values as possible. The smallest ratio of 10^{-5} was obtained when 2.0 g In and 60 mg CdS were placed in a specially constructed ampoule and the largest ratio was obtained when Cd metal was placed in the ampoule along with the In and CdS; this was when 15 mg Cd, 50 mg In and 150 mg CdS were used and a final ratio of 0.31 was obtained. If larger quantities of Cd than this were used it was not possible to observe the diffusion front. The diffusion coefficients D_o were measured optically and the results obtained for diffusions in a direction parallel to the c-axis are shown in figure 8.2.

It can be seen from the graph in figure 8.2 that for values of the CSE final Cd/In ratio below 0.03 the diffusion is concentration dependent and for values above 0.4, where the diffusion coefficients are approximately two decades smaller, the diffusion is concentration independent. In the range between 0.03 and 0.4 the interface between the doped and undoped parts of the CdS slice became more diffuse as the ratio increased, whereas at values above 0.4 it was not possible to observe the interface optically at all.

The variation of the diffusivity with the CSE final Cd/In ratio

TABLE 8.3: ESTIMATION OF THE OVERALL FINAL Cd/In RATIO IN THE METAL GLOBULE

Run number		150a	122c	122q
Temperature	K	1161	1120	1120
Duration of anneal	s	1.555,5	1.44,4	7.92,4
Fraction of CdS doped with In		1.0	0.35	0.69
Final Cd/In ratio				
Due to stoichiometric exchange		0.03 ± 0.02	0.0005 ± 0.0003	0.0004 ± 0.0002
From analysis of globule		0.32 ± 0.04	0.037 ± 0.010	0.105 ± 0.020
By weighing (chapter 4)		0.36 ± 0.20	0.085 ± 0.040	0.04 ± 0.02

PLOT OF $D_{o_{\perp}}$ AGAINST THE CSE FINAL Cd/In RATIO FOR THE DIFFUSION OF In INTO CdS

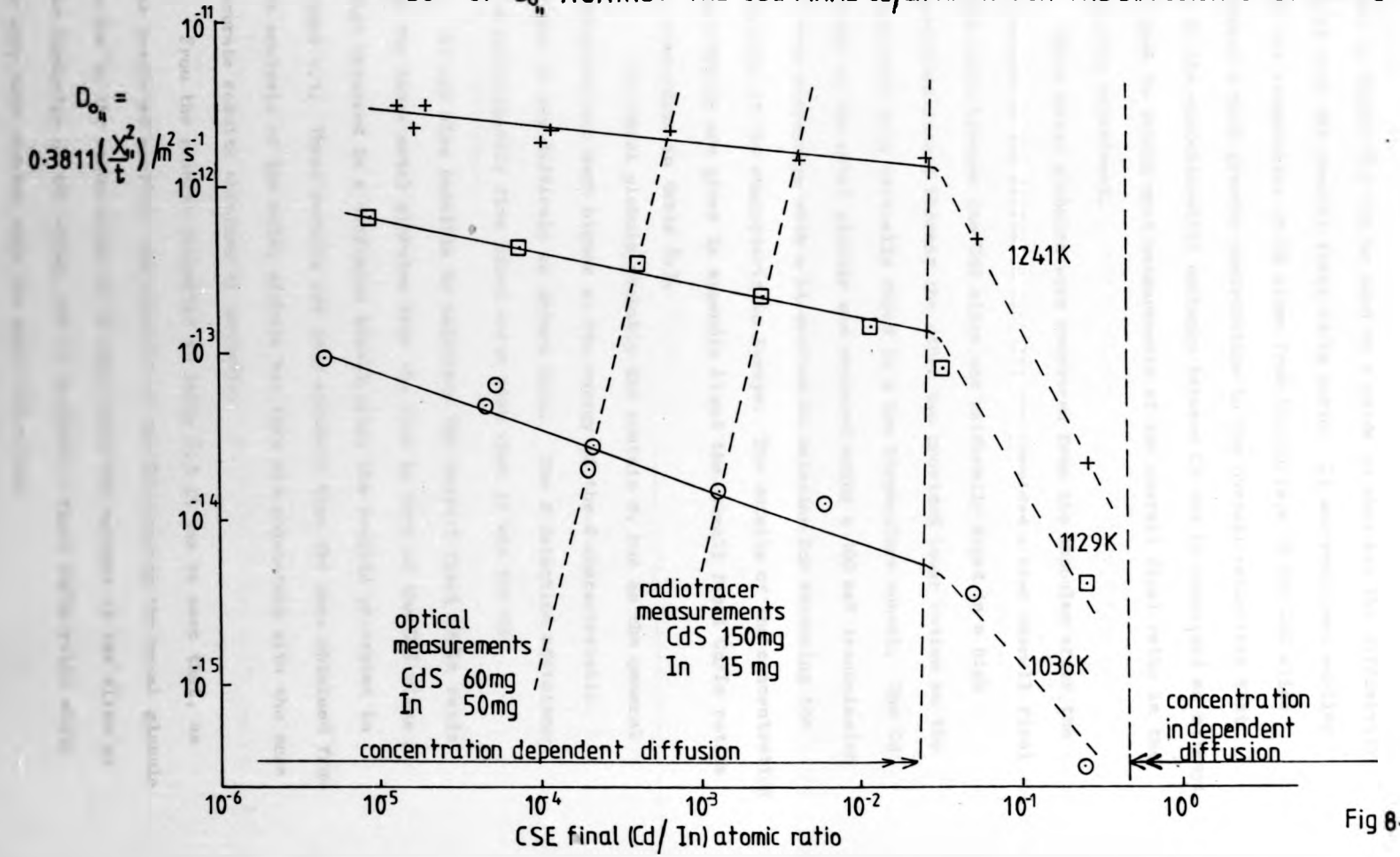

Fig 8.2

shown in figure 8.2 can be used as a guide to show how the diffusivity varies with the overall final Cd/In ratio. It was mentioned earlier that the evaporation of Cd atoms from the surface of the CdS slice produced a much greater contribution to the overall ratio than that due to the stoichiometric exchange between Cd and In atoms;and an attempt was made to obtain spot measurements of the overall final ratio in the following experiment.

Three metal globules were recovered from the ampoules after the completion of the diffusion anneals; one provided a high overall final Cd/In ratio because the CdS slice was uniformily doped in a high temperature anneal whereas the other two provided lower ratios as the slices were only partially doped in a low temperature anneal. The Cd content in the metal globule was measured using a 100 keV transmission electron microscope with a Li-drifted Si detector for measuring the intensity of the characteristic X-rays. The details of the concentration measurements are given in appendix A4 and the overall final Cd/In ratios are summarised in table 8.3.

The metal globule probably did contain S, but as the general background was much higher at the energy of the S characteristic X-rays it was difficult to detect them. The S detection efficiency was approximately five times worse than what it was for Cd.

It was also possible to calculate the overall final Cd/In ratio for the three metal globules from the loss in mass of the CdS slice, which occurred in a diffusion anneal, using the results presented in figure 4.1. These results are less accurate than the ones obtained from the analysis of the metal globule but they are consistent with the more accurate results obtained by analysis.

From the results presented in table 8.3 it can be seen that, as was predicted earlier, the majority of the Cd entering the metal globule is due to the evaporation of Cd atoms from the surface of the slice at the beginning of the anneal and it produces a final Cd/In ratio which is very much greater than the final CSE value.

It was not possible to measure the variation of the diffusion coefficient with the overall final Cd/In ratio, but it is possible with the aid of existing data to draw a schematic variation. As the overall final Cd/In ratio is much greater than the corresponding CSE value, it is reasonable to assume that the resultant effect will be to move the experimental points in figure 8.2, for the concentration dependent diffusion, to the right. The points at the highest temperature and the lowest Cd/In ratio move the greatest amount, and the points at the lowest temperature and the highest Cd/In ratio move least. The resultant effect will be that the three lines will take up approximately the same gradient with the 1241 K line moving furthest to the right and the experimental points closing up together by the greatest amount. The change from the concentration dependent diffusion to the concentration independent diffusion could become more abrupt and occur at numerically higher Cd/In ratios. The corresponding resultant family of curves that would be expected is shown in figure 8.3.

In fact, as can be seen in section 2.7, Yokozawa et al (1) observed a similar behaviour for the diffusion of In in ZnTe with variation in Zn partial pressure, but in this case the diffusion profiles possessed an 'erfc' shape.

The results obtained in this sub-section on the variation of the diffusion coefficient with the overall final Cd/In ratio, despite the fact that they are not very comprehensive, are consistent with the results obtained in sub-section 8.1.1. The variation between the overall final Cd/In ratio for the two sets of measurements causes the C_o values in the RTS standard conditions to be $(20 \pm 5)\%$ lower than the C_o values in the OM standard conditions.

8.1.3. Conclusions and comparison with other published work

The reason for the discrepancy in corresponding values of C_o for the concentration dependent diffusion, which were obtained using the

SCHEMATIC PLOT OF $D_{o_{\parallel}}$ VERSUS OVERALL FINAL Cd/In RATIO FOR THE DIFFUSION OF In INTO CdS

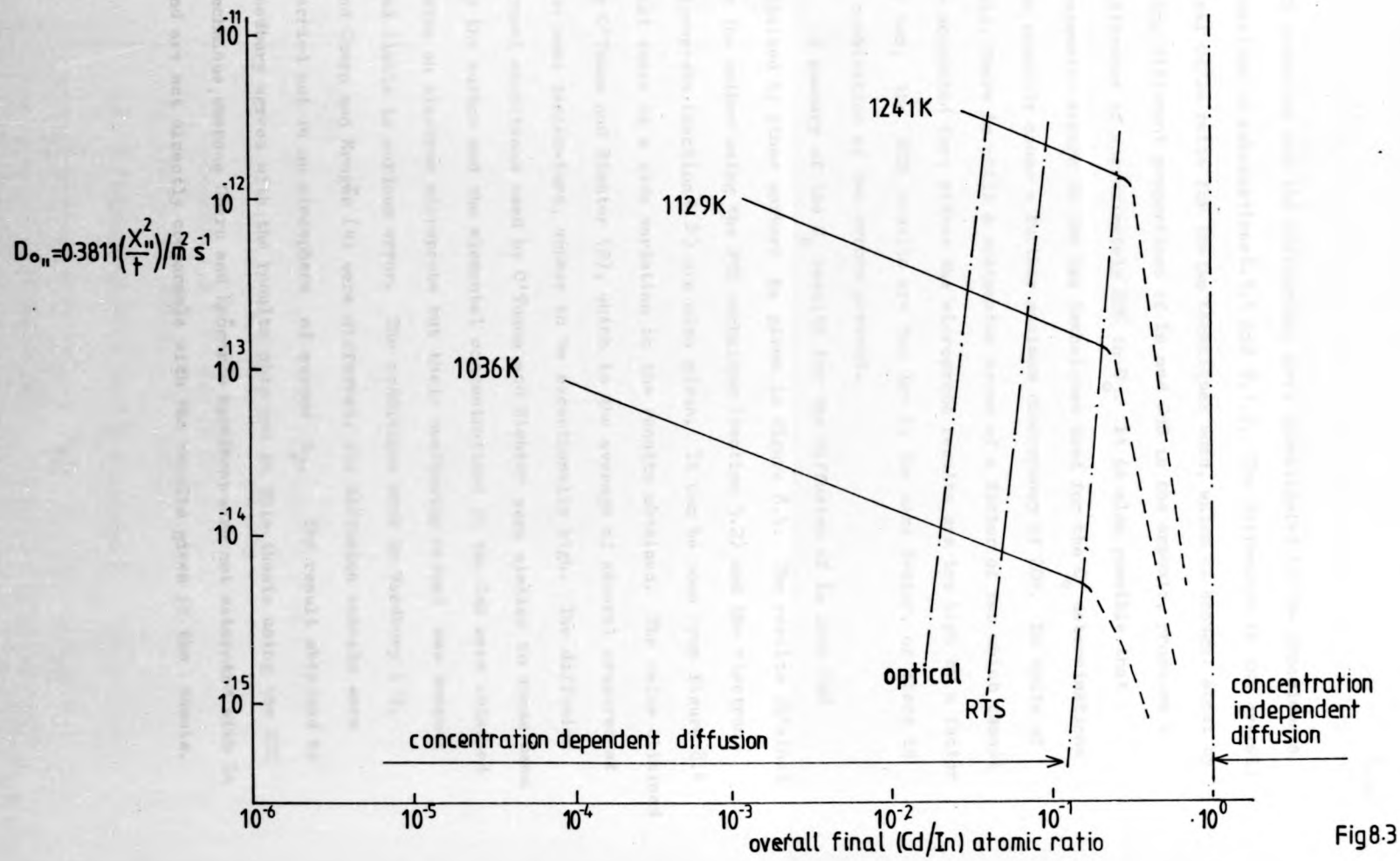

Fig 8.3

RTS technique and the microprobe, were investigated in the experiments described in sub-sections 8.1.1 and 8.1.2. The difference in the overall final Cd/In ratio for the two techniques used, which is brought about by using different proportions of In and CdS in the ampoule, produces a difference of approximately 20% in C_o. It is also possible that systematic errors in the two techniques used for the C_o determinations can possibly cause a further maximum discrepancy of 20%. In spite of this, there is still a systematic error of a factor of two which cannot be accounted for; either the microprobe results are too high by a factor of two, the RTS results are too low by the same factor, or there is a combination of two errors present.

A summary of the C_o results for the diffusion of In into CdS obtained by other workers is given in figure 8.4. The results obtained by the author using the RTS technique (section 5.2) and the electron microprobe (section 6.3) are also given. It can be seen from figure 8.4 that there is a wide variation in the results obtained. The value obtained by O'Tuama and Richter (2), which is the average of several measured at the same temperature, appear to be exceptionally high. The diffusion anneal conditions used by O'Tuama and Richter were similar to those used by the author and the elemental concentrations in the CdS were obtained using an electron microprobe but their sectioning method was suspect and liable to serious error. The conditions used by Woodbury (3), and Chern and Kröger (4) were different, the diffusion anneals were carried out in an atmosphere of excess S_2. The result obtained by Woodbury agrees with the results obtained in this thesis using the RTS technique, whereas Chern and Kröger's specimens were not saturated with In and are not directly comparable with the results given in the thesis.

A COMPILATION OF ALL THE AVAILABLE RESULTS OF THE NEAR-SURFACE In CONCENTRATION IN CdS.

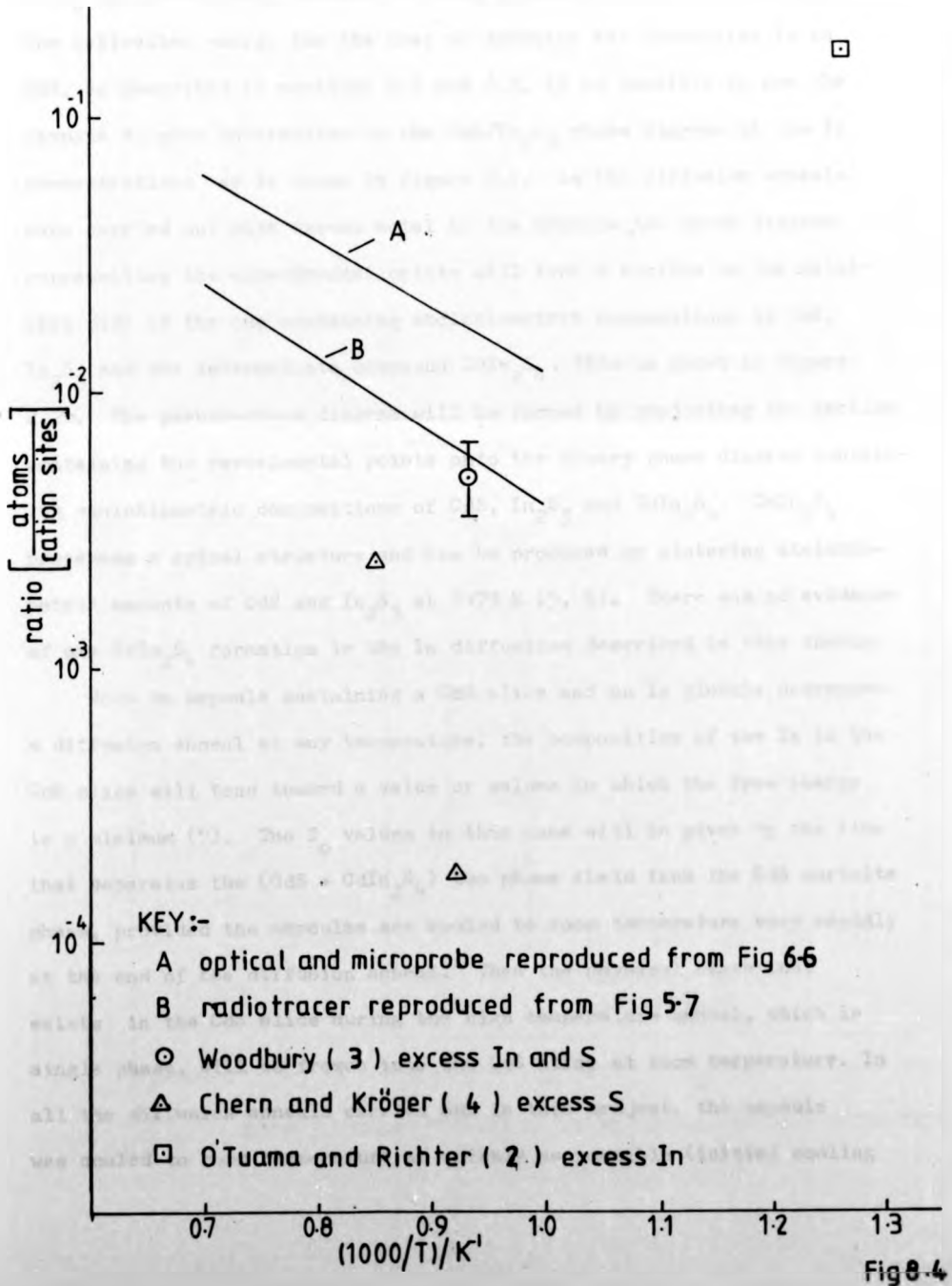

Fig 8·4

8.2. Proposed phase diagram for the CdS/In_2S_3 system .

It is possible to represent the experimentally determined values of C_o in another way; instead of using Arrhenius plots to determine the activation energy for the heat of solution for dissolving In in CdS, as described in sections 5.2 and 6.3, it is possible to use the results to give information on the CdS/In_2S_3 phase diagram at low In concentrations as is shown in figure 8.5. As the diffusion anneals were carried out with excess metal in the ampoule, the phase diagram representing the experimental points will form a section on the metal-rich side of the one containing stoichiometric compositions of CdS, In_2S_3 and the intermediate compound $CdIn_2S_4$. This is shown in figure 2.2b. The pseudo-phase diagram will be formed by projecting the section containing the experimental points onto the binary phase diagram containing stoichiometric compositions of CdS, In_2S_3 and $CdIn_2S_4$. $CdIn_2S_4$ possesses a spinel structure and can be produced by sintering stoichiometric amounts of CdS and In_2S_3 at 1173 K (5, 6). There was no evidence of any $CdIn_2S_4$ formation in the In diffusions described in this thesis.

When an ampoule containing a CdS slice and an In globule undergoes a diffusion anneal at any temperature, the composition of the In in the CdS slice will tend toward a value or values in which the free energy is a minimum (7). The C_o values in this case will be given by the line that separates the (CdS + $CdIn_2S_4$) two phase field from the CdS wurtzite phase, provided the ampoules are cooled to room temperature very rapidly at the end of the diffusion anneal. Then the physical state that exists in the CdS slice during the high temperature anneal, which is single phase, will be frozen into the CdS slice at room temperature. In all the diffusion anneals carried out in this project, the ampoule was cooled to room temperature as quickly as possible (initial cooling

THE PROPOSED PHASE DIAGRAM FOR THE CdS/In_2S_3 SYSTEM

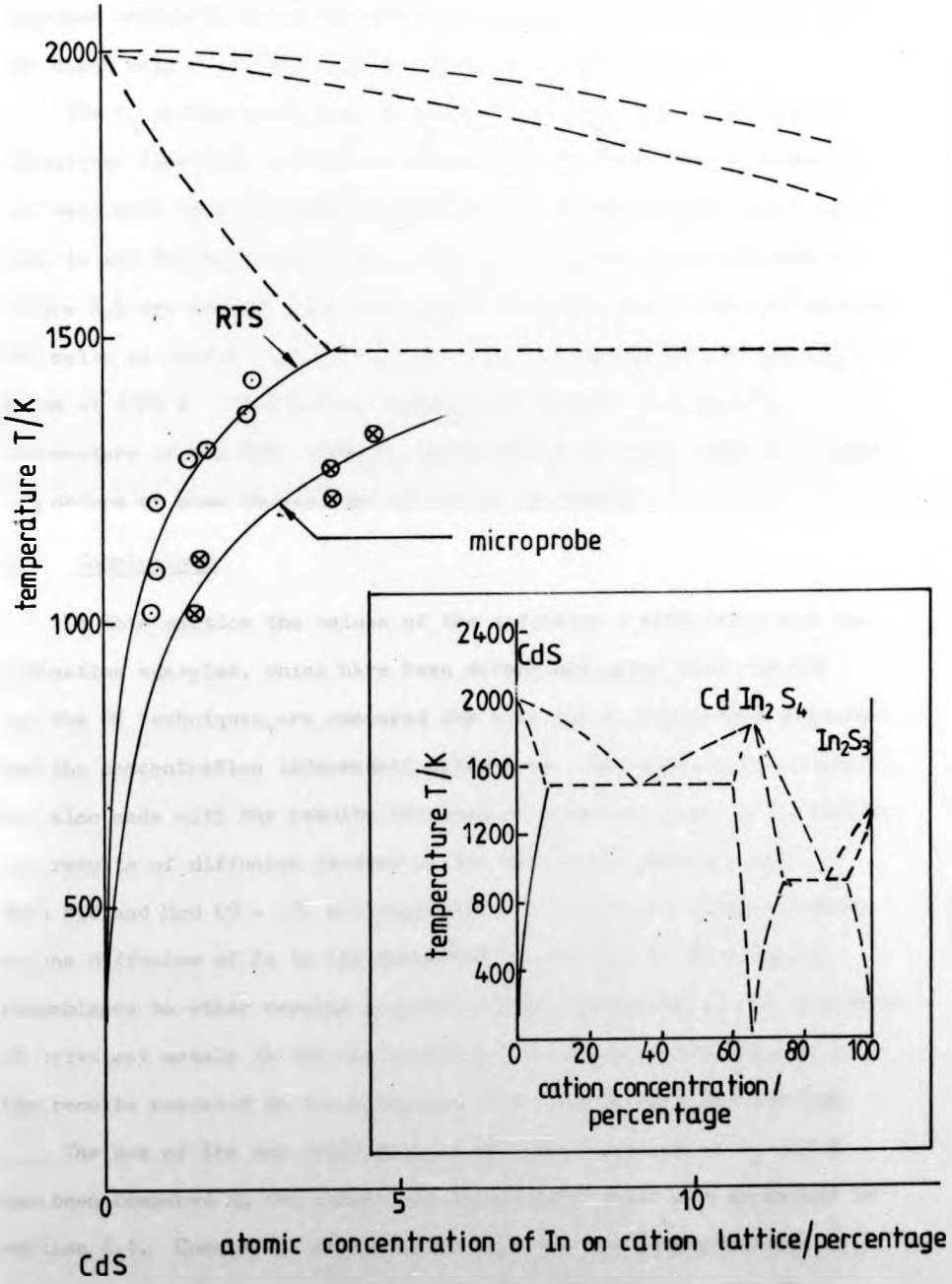

Fig 8.5

THE PROPOSED PHASE DIAGRAM FOR THE CdS/In_2S_3 SYSTEM

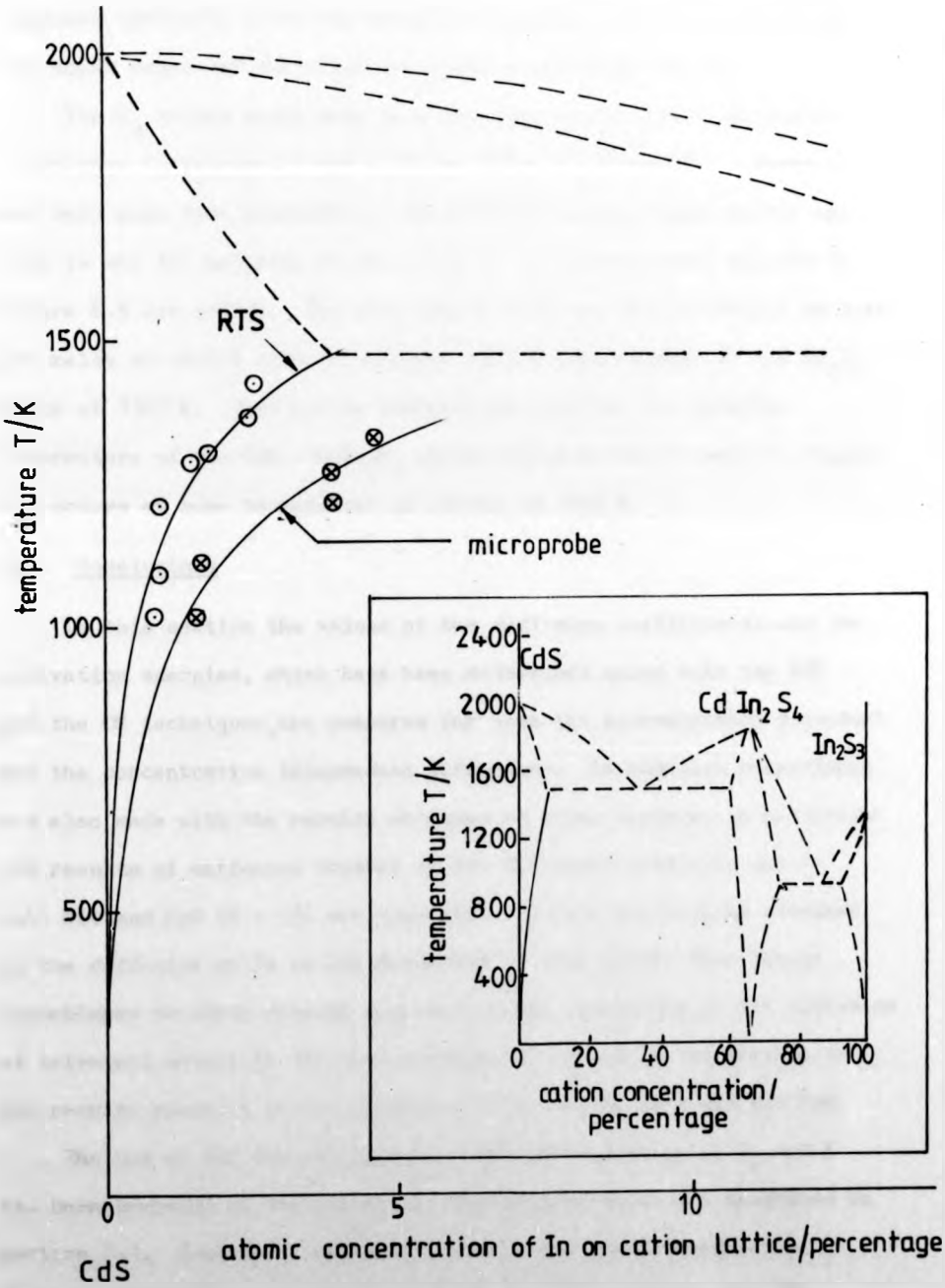

Fig 8.5

rate 20 K s^{-1}) at the end of the anneal. Some of the slices were examined optically after the diffusion anneal had been completed and the doped region of the slice was found to be single phase.

The C_o values which have been obtained using both experimental techniques (sections 5.2 and 6.3) are shown in figure 8.5. There is not very much data available on the Cd/In/S ternary phase system and this is why the majority of the lines in the pseudo-phase diagram in figure 8.5 are dotted. The only other published data available is that CdS melts at 2022 K under a pressure of 100 atmospheres (8) and In_2S_3 melts at 1323 K. This latter temperature is below the eutectic temperature of the CdS - $CdIn_2S_4$ system which, as can be seen in figure 8.5, occurs at some temperature in excess of 1450 K.

8.3. Conclusions

In this section the values of the diffusion coefficients and the activation energies, which have been determined using both the RTS and the OM techniques, are compared for both the concentration dependent and the concentration independent diffusions. In addition comparisons are also made with the results obtained by other workers; in particular the results of diffusion studies of the trivalent metals Cr and Sc into NiO and MgO (9 - 13) are compared. In fact the results obtained on the diffusion of In in CdS described in this thesis bear little resemblance to other results reported in the literature on the diffusion of trivalent metals in the chalcogenides of Cd and Zn but they do to the results reported on the diffusion of Cr and Sc into NiO and MgO.

The use of the two techniques in the determination of C_o and X has been compared in the comparison experiments which are described in section 8.1. Consistent measurements of X for the concentration dependent diffusion were obtained using the RTS technique and the optical method, but the corresponding measurements, which were obtained

with the microprobe, proved to be less reliable. The measurement of C_o was repeated several times using both the RTS technique and the microprobe. The results obtained using each technique were consistent, but when the results obtained using the two techniques were compared with each other there was a discrepancy of a factor slightly in excess of two. A part of this discrepancy can be attributed to the different physical conditions existing in the ampoules for the two sets of measurements and is reflected in the overall final Cd/In ratio. Another part can possibly be attributed to the experimental errors in the techniques used. The major portion of the discrepancy remains unresolved.

All the diffusion results, which have been obtained by the author on the self-diffusion of Cd into CdS and on the diffusion of In into CdS, are summarised in Arrhenius plots in figure 8.6. The key for the graphs is presented separately in table 8.4 and the results are represented by the best straight line through each set of experimental points. In addition, an estimate of the diffusion coefficient in the concentration independent regime was obtained from the microprobe profile for specimen 152d which is one of the diffusions carried out in experiment 1 described in sub-section 8.1.1.

The results obtained by the author and presented in figure 8.6 fall into two general groups. In the first, the In diffusion is concentration dependent with $D \propto C$ and possesses marked diffusion anisotropy with $D_\perp > D_{||}$. In the second, which occurs when the Cd/In ratio is greater than unity, the In diffusion is concentration independent and there is no evidence of any diffusion anisotropy. In this case the diffusion coefficient, which is 0.01 of the corresponding coefficient in the concentration dependent regime, and the activation energy are comparable with the values obtained for the self-diffusion of Cd into CdS in the

A COMPILATION OF THE AVAILABLE DIFFUSION RESULTS FOR THE DIFFUSION OF In INTO CdS

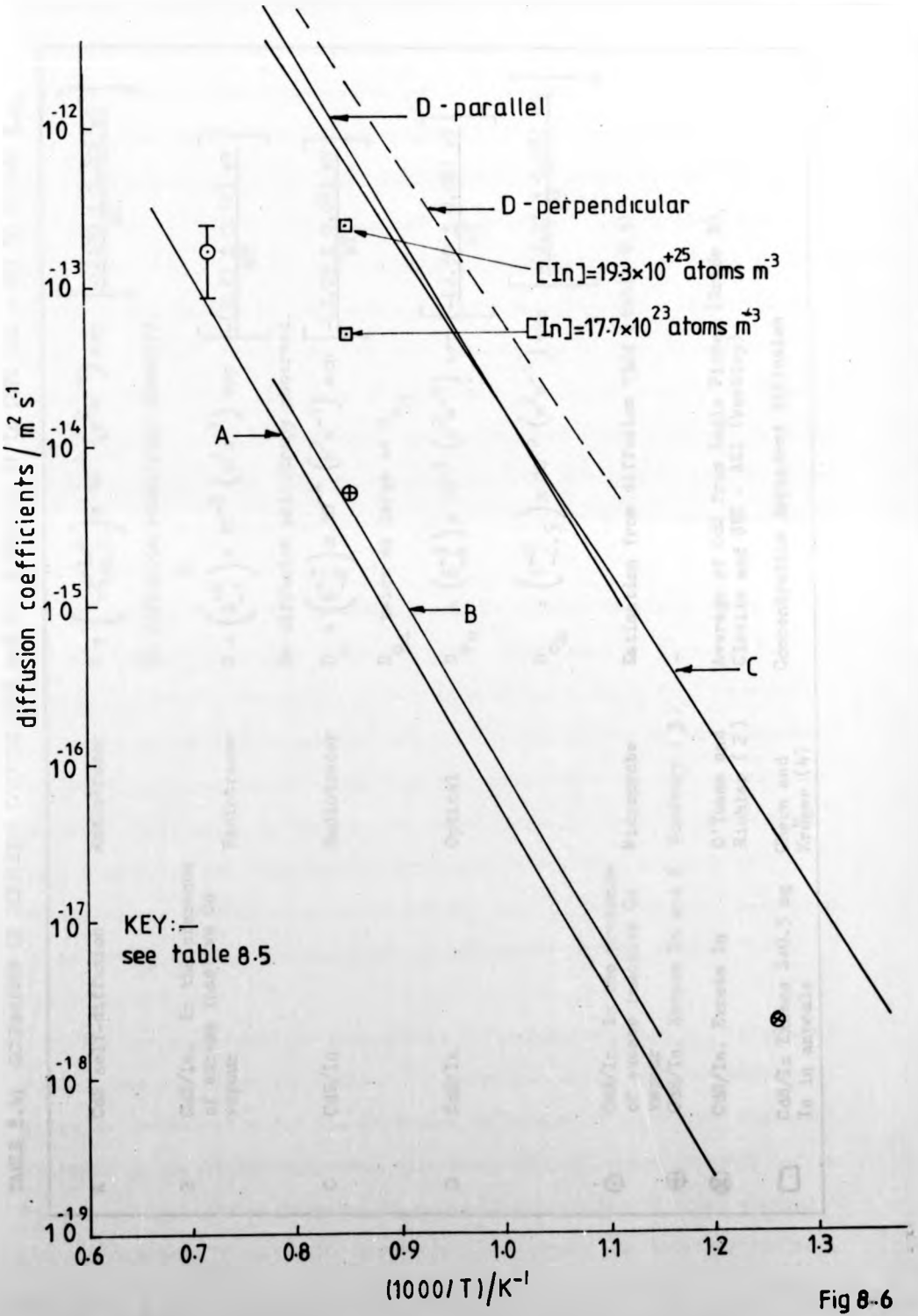

Fig 8·6

TABLE 8.4: COMPARISON OF DIFFUSION COEFFICIENTS FOR THE DIFFUSION OF In INTO CdS - KEY TO FIGURE 8.6.

A	CdS self-diffusion	Radiotracer	$D = \left(1.2^{+3.6}_{-0.4}\right) \times 10^{-4} \left(m^2 s^{-1}\right) \exp\left[\frac{-(2.30 \pm 0.20)\ eV}{kT}\right]$ No diffusion anisotropy observed.
B	CdS/In. In the presence of excess inactive Cd vapour	Radiotracer	$D = \left(2^{+6}_{-1}\right) \times 10^{-5} \left(m^2 s^{-1}\right) \exp\left[\frac{-(2.27 \pm 0.12)\ eV}{kT}\right]$ No diffusion anisotropy observed.
C	CdS/In	Radiotracer	$D_o = \left(6^{+3}_{-2}\right) \times 10^{-4} \left(m^2 s^{-1}\right) \exp\left[\frac{-(2.09 \pm 0.08)\ eV}{kT}\right]$ $D_{o_\perp}$ twice as large as $D_{o_{\parallel}}$
D	CdS/In	Optical	$D_{o_{\parallel}} = \left(6^{+9}_{-4}\right) \times 10^{-3} \left(m^2 s^{-1}\right) \exp\left[\frac{-(2.30 \pm 0.08)\ eV}{kT}\right]$ $D_{o_\perp} = \left(1^{+2}_{-0.5}\right) \times 10^{-3} \left(m^2 s^{-1}\right) \exp\left[\frac{-(2.03 \pm 0.08)\ eV}{kT}\right]$
⊙	CdS/In. In the presence of excess inactive Cd vapour	Microprobe	Estimation from diffusion 152d (table 8.1)
⊕	CdS/In. Excess In and S	Woodbury (3)	-
⊗	CdS/In. Excess In	O'Tuama and Richter (2)	Average of CdS from Eagle Picher (Grade B), Clevite and GEC - AEI (Wembley)
⊡	CdS/In Excess S+0.5 mg In in ampoule	Chern and Kröger (4)	Concentration dependent diffusion

presence of excess Cd metal. In addition it can be seen from figure 8.6 that at a constant temperature the diffusion coefficent increases as the CSE final Cd/In ratio decreases or as C_o increases.

The results obtained by other workers are also shown in figure 8.6. The results obtained by O'Tuama and Richter (2), which are for diffusions carried out in excess In vapour, must be in doubt. The results obtained by Woodbury (3) which are for diffusion anneals carried out in an atmosphere of excess S_2 agree with the second group of measurements. The results obtained by Chern and Kröger (4) fall between the two sets of results shown in figure 8.6. In their diffusions 0.5 mg of In metal was placed in the ampoule with the CdS slice and the diffusion was carried out under saturated S_2 pressure. The penetration profile obtained at 1173 K, which was concentration dependent, but not of a type where $D \propto C$, is shown in figure 2.6.

A summary of all the activation energy values is given in table 8.5. For the concentration dependent diffusion, which occurs at a low P_{Cd} (low Cd/In ratio), the mobile defect is probably a $(In_{Cd}^{\bullet} V_{Cd}^{''})'$ complex. Indium is probably incorporated into the Cd sub-lattice by the stoichiometric exchange of two In atoms from the vapour with three Cd atoms from the CdS. This can also explain the large diffusion anisotropy which has been observed. For this type of diffusion it has been possible to determine the activation energies for the heat of solution for dissolving In in CdS E_F and for the migration of the mobile defect through the Cd sub-lattice E_M.

For the concentration independent diffusion, the high P_{Cd} (high Cd/In ratio) does not allow the vacancy concentration on the cation lattice to increase sufficiently for the diffusion to become concentration dependent. There is no observable diffusion anisotropy and diffusion probably occurs by a simple vacancy mechanism. This has been proposed by other workers (1, 11) who have reported on other similar systems. In this particular

TABLE 8.5: COMPARISON OF ACTIVATION ENERGY VALUES FOR THE DIFFUSION OF In INTO CdS

				PARALLEL	PERPENDICULAR	OVERALL
Self diffusion of Cd into CdS	Radiotracer					2.30 ± 0.20
CdS/In*Cd	Radiotracer					2.27 ± 0.12
CdS/In						
Formation and migration E_t	Radiotracer					2.09 ± 0.08
	Optical			2.30 ± 0.08	2.03 ± 0.08	
Anisotropy ($E_{t_{\parallel}} - E_{t_{\perp}}$)	Optical	Difference	0.27 ± 0.11			
		Ratio	0.250 ± 0.008			
Formation E_F	Radiotracer		0.53 ± 0.06			
	Microprobe		0.48 ± 0.09			
Migration E_M	Radiotracer					1.54 ± 0.08
	Optical/ microprobe			1.82 ± 0.12	1.55 ± 0.12	

All activation energies are expressed in eV

case it was only possible to calculate the total activation energy for the diffusion.

As was mentioned in section 7.3, there is no consistent pattern existing between the type of diffusion profile obtained and the physical conditions existing in the ampoule during the diffusion anneal for the diffusion of In into the chalcogenides of Cd and Zn (1, 4, 14). When a concentration dependent diffusion was observed by other workers it was not of a type with $D \alpha C$. On the other hand, when the diffusion results reported in this thesis were compared with the results obtained by workers on the diffusion of the group III metals Cr and Sc into NiO and MgO (9 - 13), there is a consistent pattern between the two sets of results. Concentration dependent diffusion profiles were obtained by Greskovich (10) and Perkins and Rapp (9) when relatively large amounts of Cr were used; the latter workers also used a method of analysis similar to the one described in this thesis for analysing their results. In addition concentration independent diffusion profiles were obtained by Chen et al (12) and by Weber et al (11), similar to the ones described in section 5.4, when relatively small amounts of tracer were used. In addition Solaga and Nortlock (10) in their measurements of the diffusion of Sc into MgO obtained results which were indicative of a concentration dependent diffusion for surface concentrations in excess of 50 parts per million whereas, below this level, concentration independent diffusion profiles were obtained.

The values of the diffusion anisotropy have been determined directly from the ratio $(X_{\perp}/X_{\parallel})$ and by difference, and as can be seen in table 8.5, give good agreement. The values, which have been calculated by difference, were obtained by taking the difference of the activation energies E_t, for diffusions in the two standard directions. Undoubtedly, the more accurate

method for measuring the diffusion anisotropy is the optical method, where the ratio of $X_{\perp}/X_{||}$ was measured on the same CdS slice, as is described in section 6.2.

Temperature plots of the diffusion coefficients D_o and D_o' for the concentration dependent diffusion are summarised in figure 8.7. The discrepancy of a factor of two existing in the determinations of C_o using the RTS and the OM techniques is reflected in the D_o' values represented by lines B and E in figure 8.7. It is possible to conclude by stating that, for the concentration dependent diffusion, the measurement of D_o using both techniques and the anisotropy are reliable and are not affected by the uncertainties discussed earlier. The discrepancy in the C_o determinations of a factor of two will make the D_o' determinations unreliable by the same factor. However, the results for the concentration independent diffusion are reliable as they are not affected by the discrepancies in C_o.

8.4. References

1. N. YOKOZAWA, H. KATO and S.TAKAYANAGI, Denki. Kagaki., 86, 4, P282 (1968).
2. S. S. O'TUAMA and J. RICHTER, J. Appl. Phys., 41, 4, P1861 (1970).
3. H. H. WOODBURY, Physics and Chemistry of II-VI Compounds (Edited by M. AVEN and J. S. PRENER), P225, North Holland Publishing Company, Amsterdam.
4. S. S. CHERN and F. A. KRÖGER, Phys. Stat. Sol. (a), 25, P215 (1974).
5. H. HAHN and W. KLINGER, Z. Anorg. Allg. Chem., 263, P178 (1950).
6. H. HAHN, G. FRANK, W. KLINGER, A. D. STÖRGER and G. STÖRGER, Z. Anorg. Allg. Chem., 279, P241 (1955).
7. A. REISMAN, Solid State Chemistry and Physics (Edited by P. F. WELLER), P721, Marcel Dekker Inc., New York (1974).

A SUMMARY OF THE DIFFUSION COEFFICIENTS D_o AND D_o'
FOR THE CONCENTRATION DEPENDENT DIFFUSION OF In IN CdS

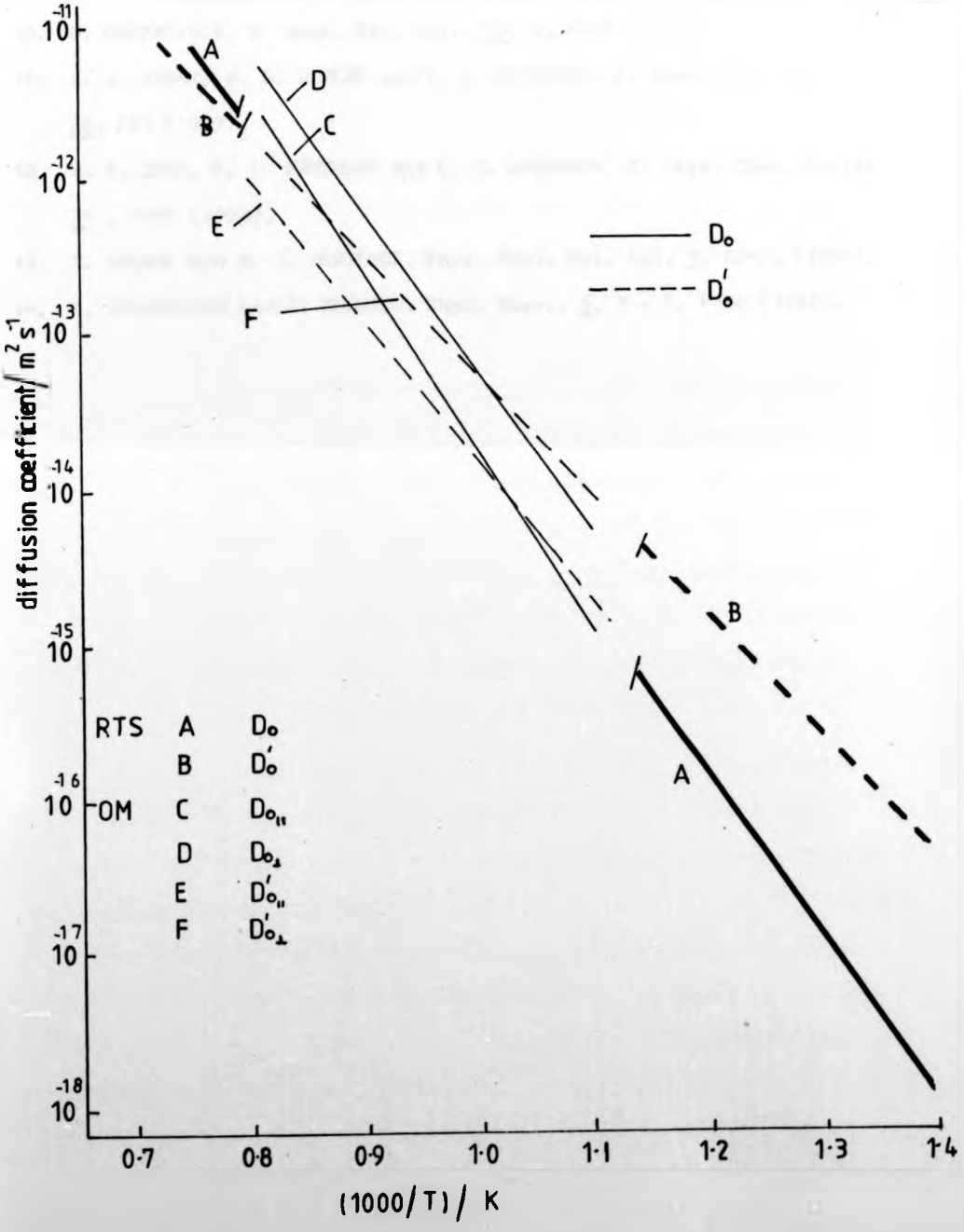

Fig 8·7

8. Handbook of Chemistry and Physics (Edited by R. C. WEAST), Chemical Rubber Company Press, U.S.A. (1973).

9. R. A. PERKINS and R. A. RAPP, Metal. Trans., 4, P193 (1973).

10. C. GRESKOVICH, J. Amer. Cer. Soc., 53, 9, P498 (1970).

11. G. W. WEBER, W. R. BITLER and V. S. STUBICAN, J. Amer. Cer. Soc., 60, P61 (1977).

12. W. K. CHEN, N. L. PETERSON and L. C. ROBINSON, J. Phys. Chem. Solids, 34 , P705 (1973).

13. T. SOLAGA and A. J. MORTLOCK, Phys. Stat. Sol. (a), 3, K247, (1970).

14. H. BJERKELAND and I. HOLWECH, Phys. Norv., 6, 3 - 4, P139 (1972).

9. Diffusions of Ga into CdS

As there is no convenient radioisotope of Ga, it was not possible to measure the rate of diffusion of Ga into CdS using the RTS technique. In this chapter all the CdS slices were annealed with excess Ga metal in the ampoule and, as a sharp optically observable diffusion front was obtained, it was possible to use the OM technique to measure the diffusions. It was also discovered that the doped part of the CdS slice was composed of two regions: an inner diffusion layer and an outer chemical reaction layer which occupied up to one quarter of the doped part of the CdS slice.

The diffusion behaviour of the Ga was in many respects similar to that which was obtained with the In diffusions. Consequently, the method used in the analysis of the Ga diffusions was similar to the one used for the analysis of the In diffusions and the contents of this chapter will be devoted solely to discussing the experimental results obtained. The mobile species by which Ga diffuses in CdS is probably a defect of the form $(Ga_{Cd}^{\bullet}\ V_{Cd}^{''})^{'}$ but there is also evidence which shows the formation of the neutral defect $(Ga_{Cd}^{\bullet}\ V_{Cd}^{''}\ Ga_{Cd}^{\bullet})^{\times}$.

Diffusion anneals were carried out at 10 different temperatures in the range 941 K to 1558 K and typical microprobe concentration profiles are shown in figure 9.1a. Corresponding Boltzmann-Matano fits to the concentration profiles are shown in figure 9.1b. In the diffusion anneals, which were carried out at the lower temperatures, the microprobe profiles showed a departure from the $D \propto C$ behaviour at the high Ga concentrations. As there was not sufficient time available, the analysis of the profiles was carried out assuming a simple $D \propto C$ dependence and a fuller analysis, which is obviously required, has not

TYPICAL Ga CONCENTRATION PROFILES IN DIFFUSED CdS SLICES OBTAINED USING THE MICROPROBE.

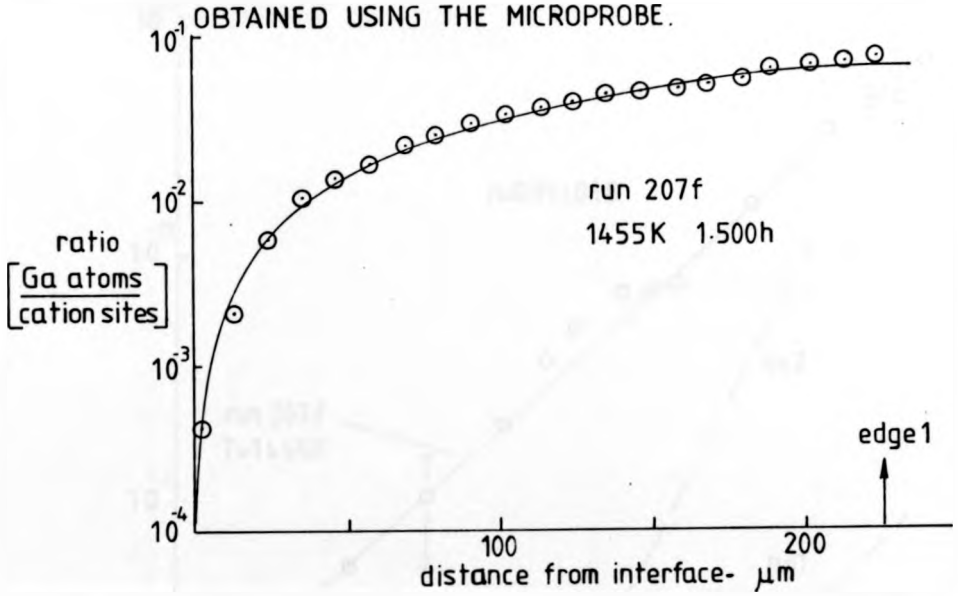

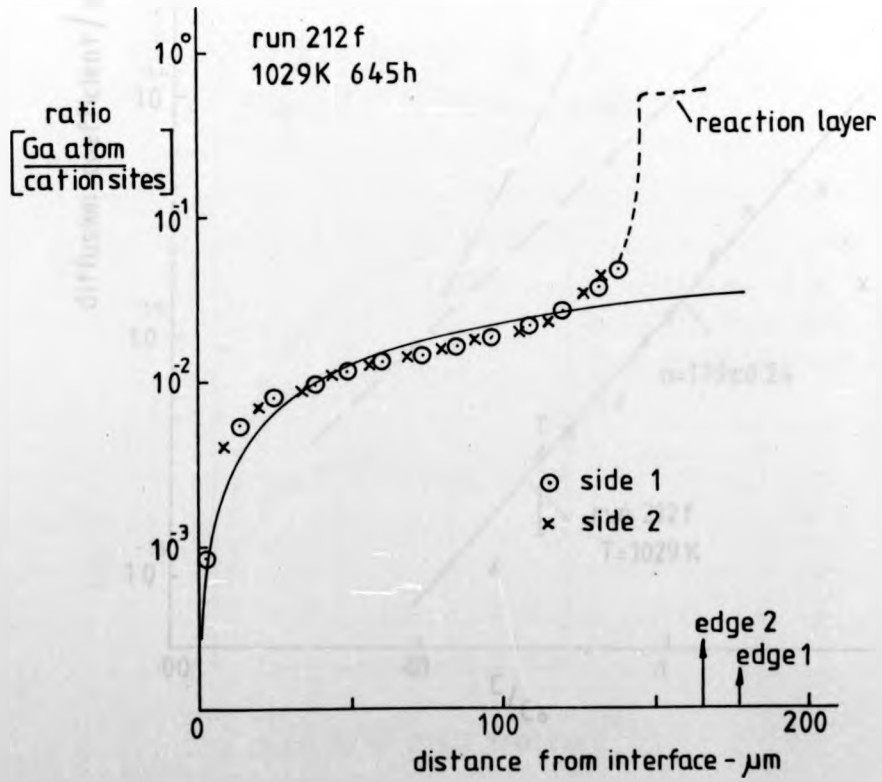

Fig 9·1a

TYPICAL PLOTS OF THE DIFFUSION COEFFICIENT AS A FUNCTION OF Ga CONCENTRATION.

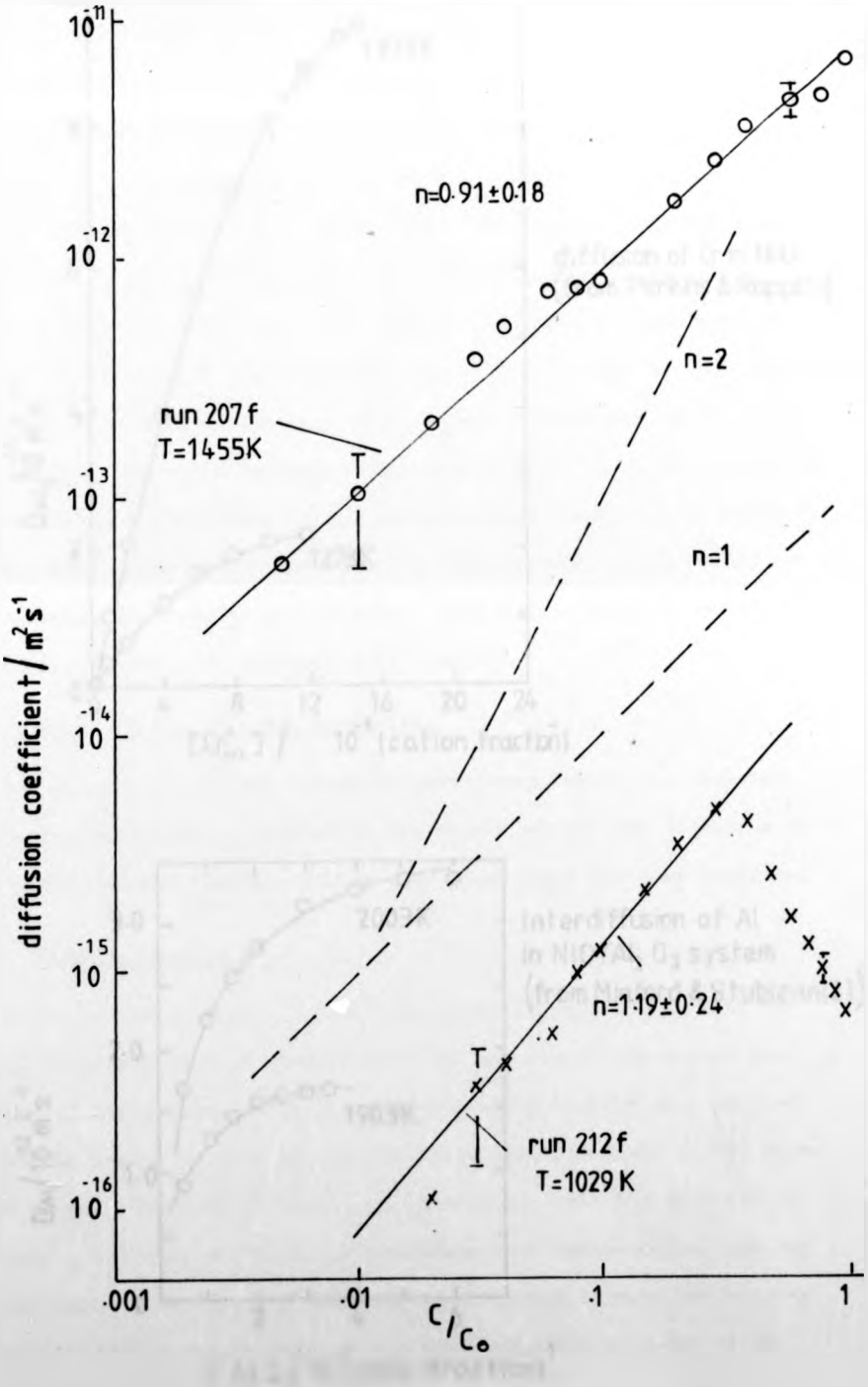

Fig 9.1b

PUBLISHED DIFFUSION DATA SHOWING THE DEPARTURE FROM THE D∝C RELATIONSHIP AT HIGH DOPANT CONCENTRATIONS

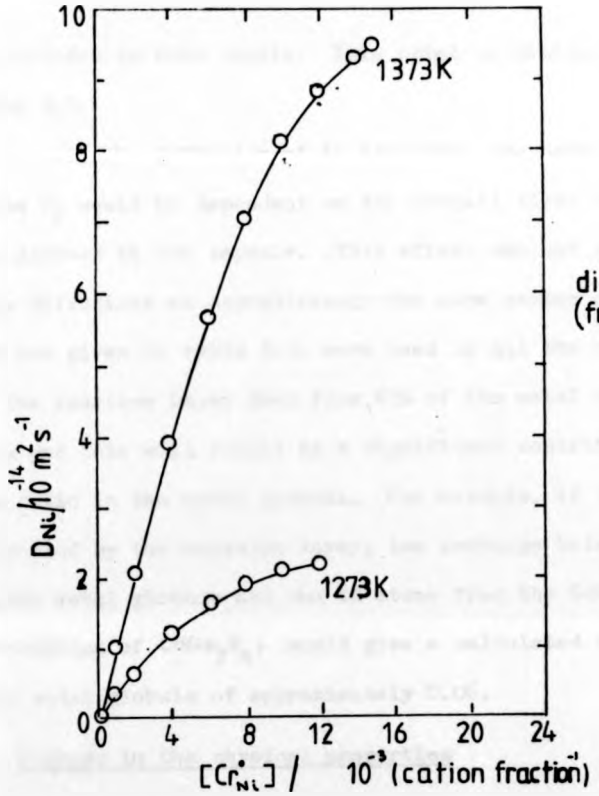

diffusion of Cr in NiO
(from Perkins & Rapp(1))

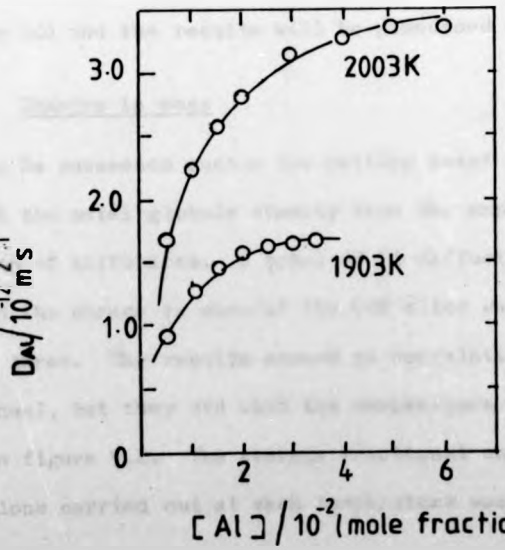

interdiffusion of Al
in NiO/Al_2O_3 system
(from Minford & Stubican(2))

Fig 9.1c

been included in this thesis. This point is discussed further in section 9.3.

As with the diffusion of In into CdS, the near-surface Ga concentration C_o would be dependent on the overall final Cd/Ga ratio in the metal globule in the ampoule. This effect was not investigated with the Ga diffusions as approximately the same masses of Ga and CdS, which are given in table 3.1, were used in all the diffusion anneals. When the reaction layer does form, 67% of the metal atoms in the compound are Ga and this will result in a significant contribution to the final Cd/Ga ratio in the metal globule. For example, if 10% of the CdS slice is occupied by the reaction layer, the exchange between the Ga atoms from the metal globule and the Cd atoms from the CdS, which occurs in the formation of $CdGa_2S_4$, would give a calculated CSE final Cd/Ga ratio in the metal globule of approximately 0.06.

9.1. Changes in the physical properties

The changes in the same physical parameters, which are reported for the In diffusions in chapter 4, are discussed for the diffusion of Ga into CdS and the results will be discussed under the same headings.

9.1.1. Changes in mass

As Ga possesses such a low melting point it proved difficult to extract the metal globule cleanly from the ampoule at the end of the majority of diffusions. A total of 63 diffusion anneals were carried out and the change in mass of the CdS slice was determined in all cases except three. The results showed no correlation with the duration of the anneal, but they did with the temperature of the anneal as can be seen in figure 9.2. The average fractional change in mass for all the diffusions carried out at each temperature was calculated and it is

CHANGE IN MASS OF THE CdS SLICES FOR THE DIFFUSION OF Ga INTO CdS

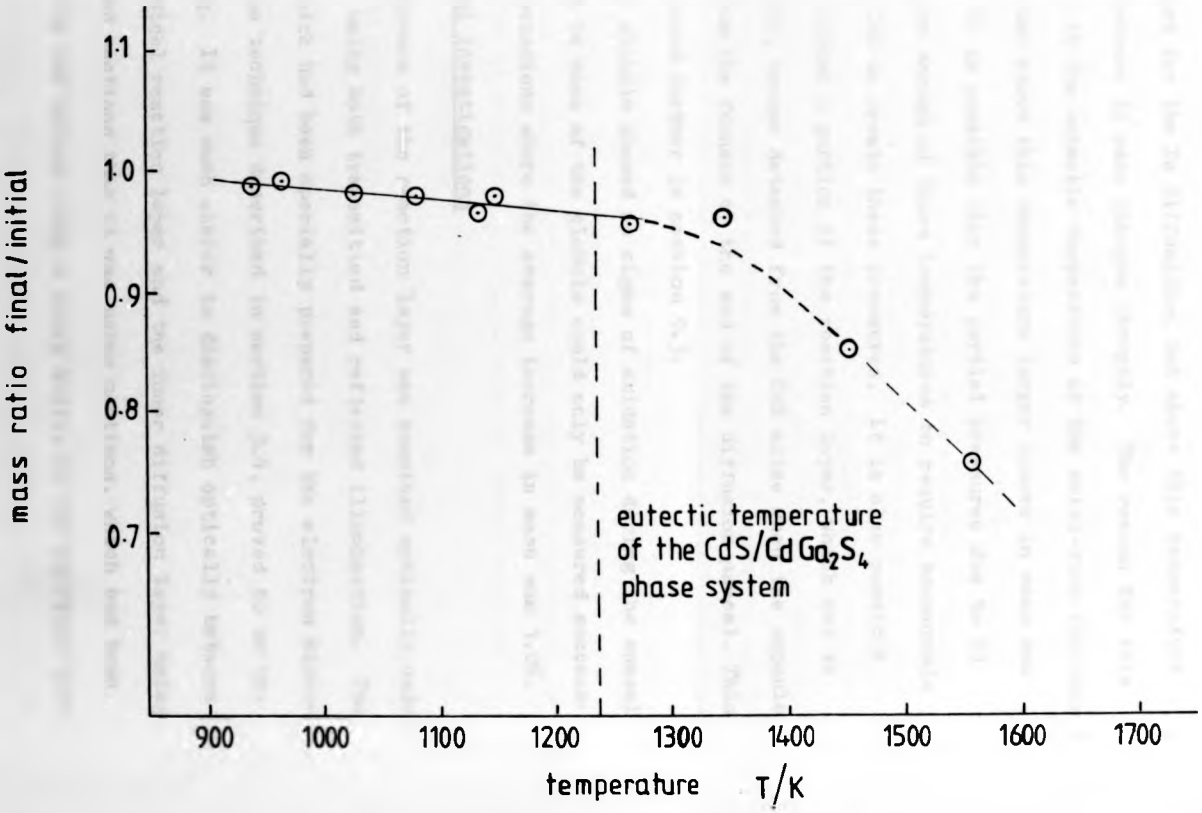

Fig 9·2

these values which are plotted on the graph. At temperatures below 1300 K, the decrease in mass with increasing temperature is similar to that obtained for the In diffusions, but above this temperature the rate of decrease in mass changes abruptly. The reason for this is that 1240 K is the eutectic temperature of the metal-rich $CdS/CdGa_2S_4$ phase diagram and above this temperature larger losses in mass can be expected. It is possible that the partial pressures due to Cd and S_2 are large enough at these temperatures to require measurable loss from the CdS to create these pressures. It is also possible that in these slices a portion of the reaction layer, which was in the liquid phase, became detached from the CdS slice when the ampoule was removed from the furnace at the end of the diffusion anneal. This point is discussed further in section 9.3.

The metal globule showed no signs of oxidation during the anneal, but the change in mass of the globule could only be measured successfully on two occasions where the average increase in mass was 1.0%.

9.1.2. Optical investigations

The appearance of the reaction layer was examined optically under a microscope using both transmitted and reflected illumination. The CdS slices, which had been specially prepared for the electron microprobe using the technique described in section 3.4, proved to be the most revealing. It was much easier to distinguish optically between the outer chemical reaction layer and the inner diffusion layer using highly polished sections than it was using sections, which had been cleaved from the CdS slices using a sharp knife, as the surfaces were too rough.

For diffusion anneals carried out at the lower end of the temperature range, the reaction layer was composed of a single crystal

and appeared to be epitaxial, but the layer became polycrystalline at the centre of the temperature range. As the temperature was increased further beyond the eutectic, which occurred at 1240 K, the layer gave the appearance of having been in the liquid phase during the diffusion anneal. The outside edges of the CdS slices in runs 205, 206 and 207 (table 9.1) took on a curved shape, which was indicative of having been liquid, instead of the straight sides which were obtained at lower temperatures. This point is illustrated in the photograph in figure 9.3. The reaction layer has been observed on specimen 207f but its absence in figure 9.1a was probably due to the reaction layer breaking off in the mounting or cleaving operations. If the temperature of the anneal was increased further, the CdS slices suffered a very high mass loss and the reaction layer could not be seen at all, as in run 210. This was possibly due to the diffusion anneal being carried out at a sufficiently high temperature either for the compound to decompose, or for the liquid to be sufficiently fluid for it to become detached from the slice in some manner.

9.1.3. X-ray investigations

X-ray powder diffraction techniques were used to investigate the properties of the diffusion layer and the reaction layer of the Ga-doped specimens. The details of the investigations are discussed in appendix A3. The main conclusions reached were that the diffusion layer possessed the wurtzite crystal structure and that the lattice parameter, for one particular case, was (2.8 $\pm$ 0.2)% less than that for the pure crystal. There was no detectable change in the c/a ratio. The structure of the reaction layer was identified as due to $CdGa_2S_4$ which has a derivative structure related to zinc blende and wurtzite (3, 4).

TABLE 9.1. DETAILS OF MEASUREMENTS CARRIED OUT USING THE OPTICAL TECHNIQUE FOR THE DIFFUSIONS OF Ga INTO CdS

Run number	T	1000/T	$D_{o_\perp} = 0.3811\left(\frac{X_\perp^2}{t}\right)$	$D_{o_\parallel} = 0.3811\left(\frac{X_\parallel^2}{t}\right)$	Ratio $\left[\frac{\text{Ga atoms}}{\text{cation sites}}\right] \times 100$	$D'_{o_\perp} = 0.3811\left(\frac{X_\perp^2 C_f}{t C_o}\right)$	$D'_{o_\parallel} = 0.3811\left(\frac{X_\parallel^2 C_f}{t C_o}\right)$	$X_\perp/X_\parallel$	Number of experimental points	Duration of the longest anneal
	K	K^{-1}	$m^2 s^{-1}$	$m^2 s^{-1}$		$m^2 s^{-1} (\%)^{-1}$	$m^2 s^{-1} (\%)^{-1}$			s
204	1150	0.870	2.356,-13	1.764,-13	7.6	3.10,-14	2.32,-14	1.335	7	7.099,4
205	1267	0.789	9.379,-13	8.533,-13	14.8	6.34,-14	5.77,-14	1.099	5	1.548,4
206	1350	0.741	1.340,-12	1.334,-12	8.5	1.57,-13	1.57,-13	1.005	6	1.668,4
207	1455	0.687	2.514,-12	2.442,-12	4.65	5.41,-13	5.25,-13	1.029	5	9.061,3
208	1083	0.923	4.085,-14	2.534,-14	4.75	8.60,-15	5.33,-15	1.612	9	3.768,3
209	968	1.033	6.948,-16	3.872,-16	1.78	3.90,-16	2.17,-16	1.794	6	8.197,6
210	1558	0.642	3.070,-12	3.423,-12	2.85	1.08,-12	1.20,-12	0.897	5	3.600,3
211	1136	0.880	1.906,-13	1.270,-13	6.5	2.93,-14	1.95,-14	1.500	5	2.511,5
212	1029	0.972	7.371,-15	4.459,-15	3.05	2.42,-15	1.46,-15	1.653	6	2.322,6
214	941	1.063	3.520,-16	2.038,-16	1.36	2.59,-16	1.50,-16	1.727	6	3.050,7

MENISCUS EFFECT OF THE REACTION LAYER
FOR THE DIFFUSION OF Ga INTO CdS

specimen 206 d magnification x 125

Fig 9.3

9.2. Discussion of the optical measurements

The optical measurements, which are discussed in section 6.1, were analysed in the same way as for the In-doped CdS slices, and the thickness of the reaction layer has been included in the measured values of X.

The full details of the ten runs carried out are summarised in table 9.1 and a typical X^2 versus t plot is shown in figure 9.4. It can be seen that, to within the limits of experimental error, the relationship is linear and passes through the origin. The gradient of the best straight line through the set of measurements, obtained at each temperature, was calculated and the corresponding values of D_o are shown as Arrhenius plots in figure 9.5. The results, which occur in the temperature range 941 K to 1150 K inclusive, can be represented by the following Arrhenius relationships:-

PARALLEL $$D_{o_{\parallel}} = (7^{+9}_{-4})\ (m^2 s^{-1})\ \exp\left[\frac{-(3.10 \pm 0.07)\ eV}{kT}\right] \qquad 9.1$$

PERPENDICULAR $$D_{o_{\perp}} = (4^{+4}_{-2})\ (m^2 s^{-1})\ \exp\left[\frac{-(3.00 \pm 0.06)\ eV}{kT}\right] \qquad 9.2$$

It can be seen in figure 9.5 that above 1150 K the experimental points depart from the above relationships to give a flatter distribution and the possible reasons for this are given in section 6.1 for the diffusion of In into CdS. In the case of the Ga diffusions it is possible that this departure from the linear relationship can also be explained by the large loss in mass of the CdS slice, which occurs during the diffusion anneals at the higher temperatures. The calculations to normalise the diffusion coefficients D_o to a near-surface Ga concentration equal to 1.0% are discussed in section 9.3.

A TYPICAL X^2 VERSUS t PLOT FOR THE DIFFUSION OF Ga INTO CdS

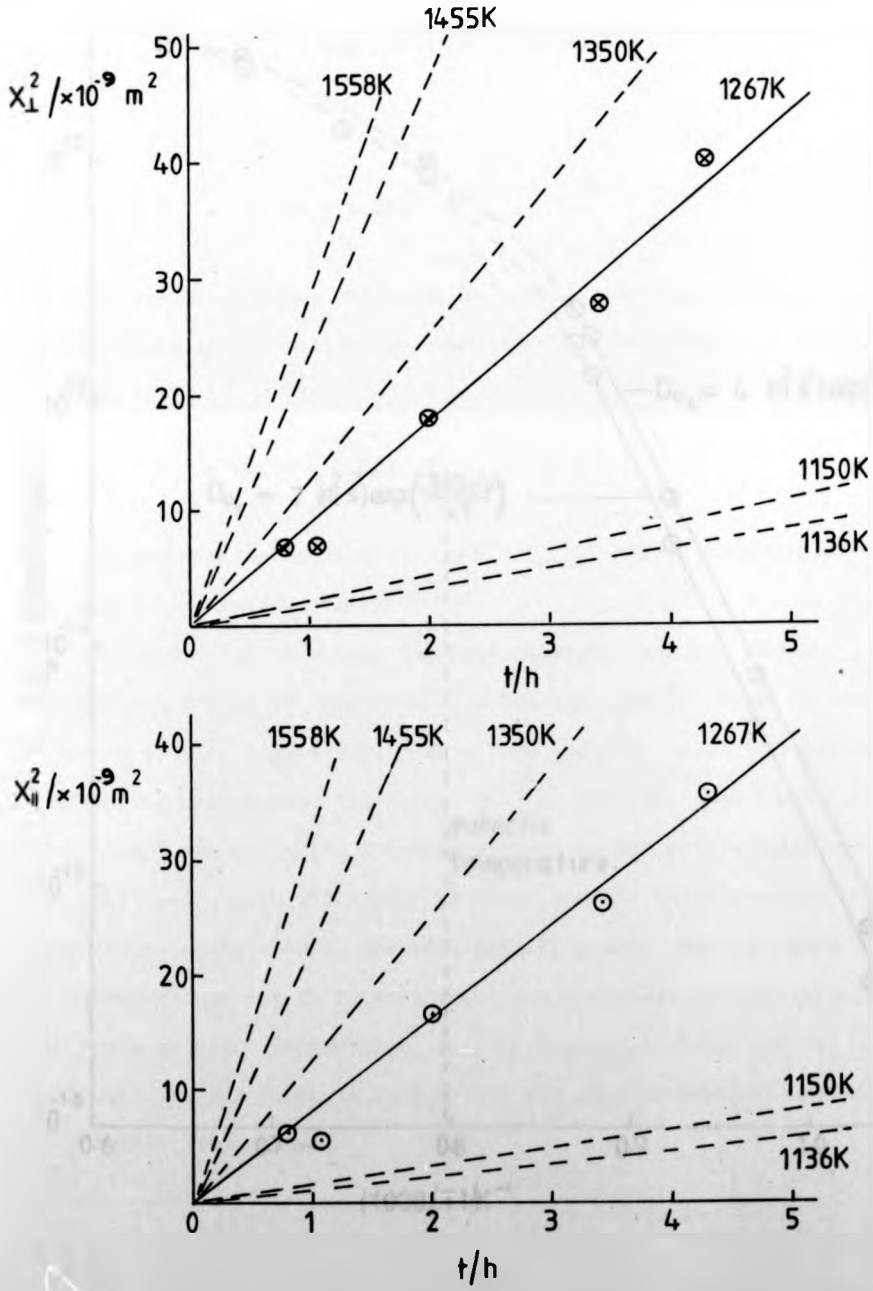

Fig 9.4

AN ARRHENIUS PLOT OF THE DIFFUSION COEFFICIENTS D_o WHICH WERE OBTAINED USING THE OPTICAL METHOD.

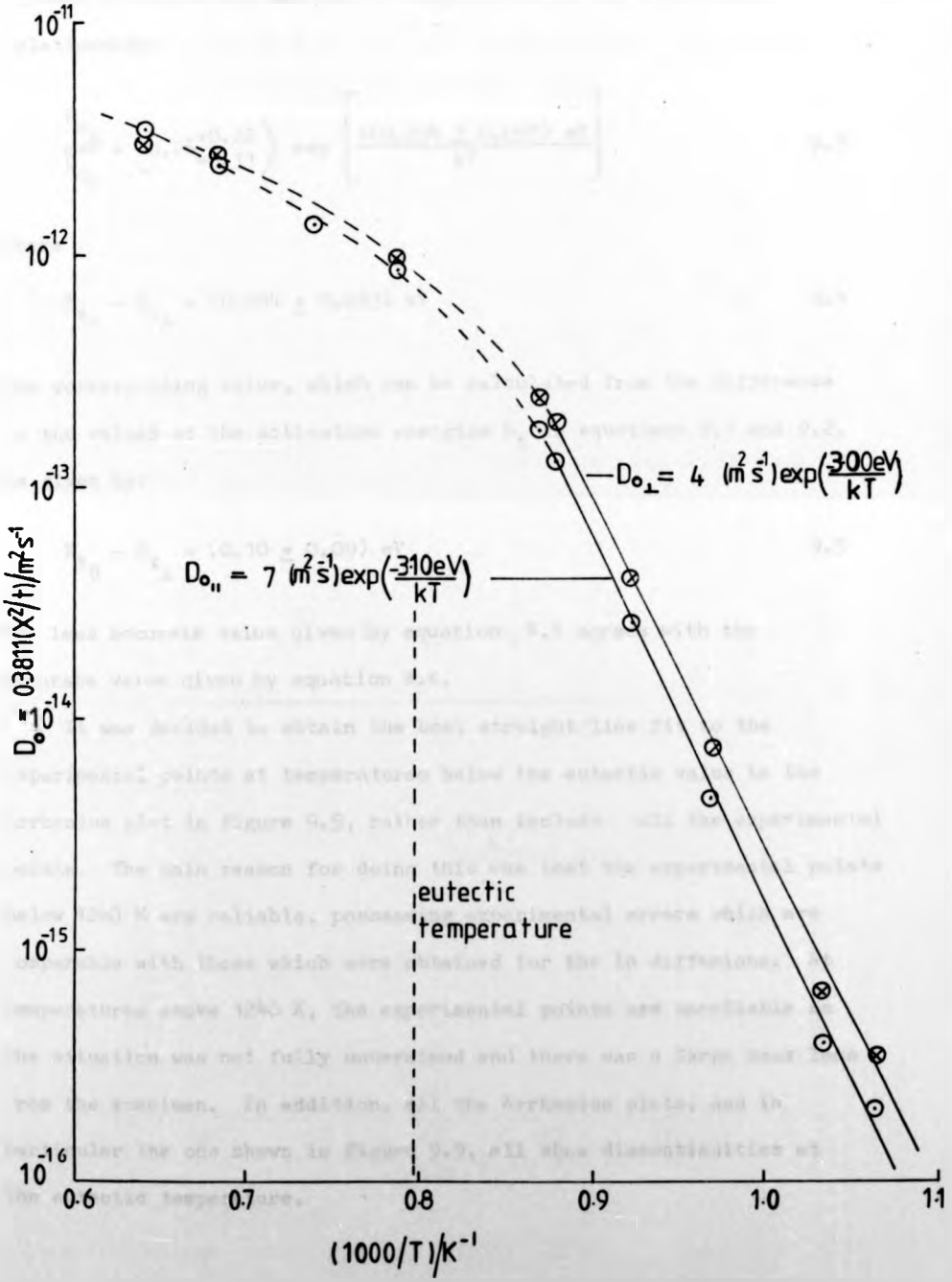

Fig 9·5

The results of the diffusion anisotropy given by $D_{o_\perp}/D_{o_\parallel}$ are plotted in figure 9.6 and can be represented by the following Arrhenius relationship:

$$\frac{D_{o_\perp}}{D_{o_\parallel}} = \left(0.26^{+0.22}_{-0.11}\right) \exp\left[\frac{+(0.204 \pm 0.053)\ eV}{kT}\right] \qquad 9.3$$

where

$$E_{t_\parallel} - E_{t_\perp} = (0.204 \pm 0.053)\ eV \qquad 9.4$$

The corresponding value, which can be calculated from the difference in the values of the activation energies E_t in equations 9.1 and 9.2, is given by:

$$E_{t_\parallel} - E_{t_\perp} = (0.10 \pm 0.09)\ eV \qquad 9.5$$

The less accurate value given by equation 9.5 agrees with the accurate value given by equation 9.4.

It was decided to obtain the best straight line fit to the experimental points at temperatures below the eutectic value in the Arrhenius plot in figure 9.5, rather than include all the experimental points. The main reason for doing this was that the experimental points below 1240 K are reliable, possessing experimental errors which are comparable with those which were obtained for the In diffusions. At temperatures above 1240 K, the experimental points are unreliable as the situation was not fully understood and there was a large mass loss from the specimen. In addition, all the Arrhenius plots, and in particular the one shown in figure 9.9, all show discontinuities at the eutectic temperature.

AN ARRHENIUS PLOT OF THE DIFFUSION ANISOTROPY FOR THE DIFFUSION OF Ga INTO CdS

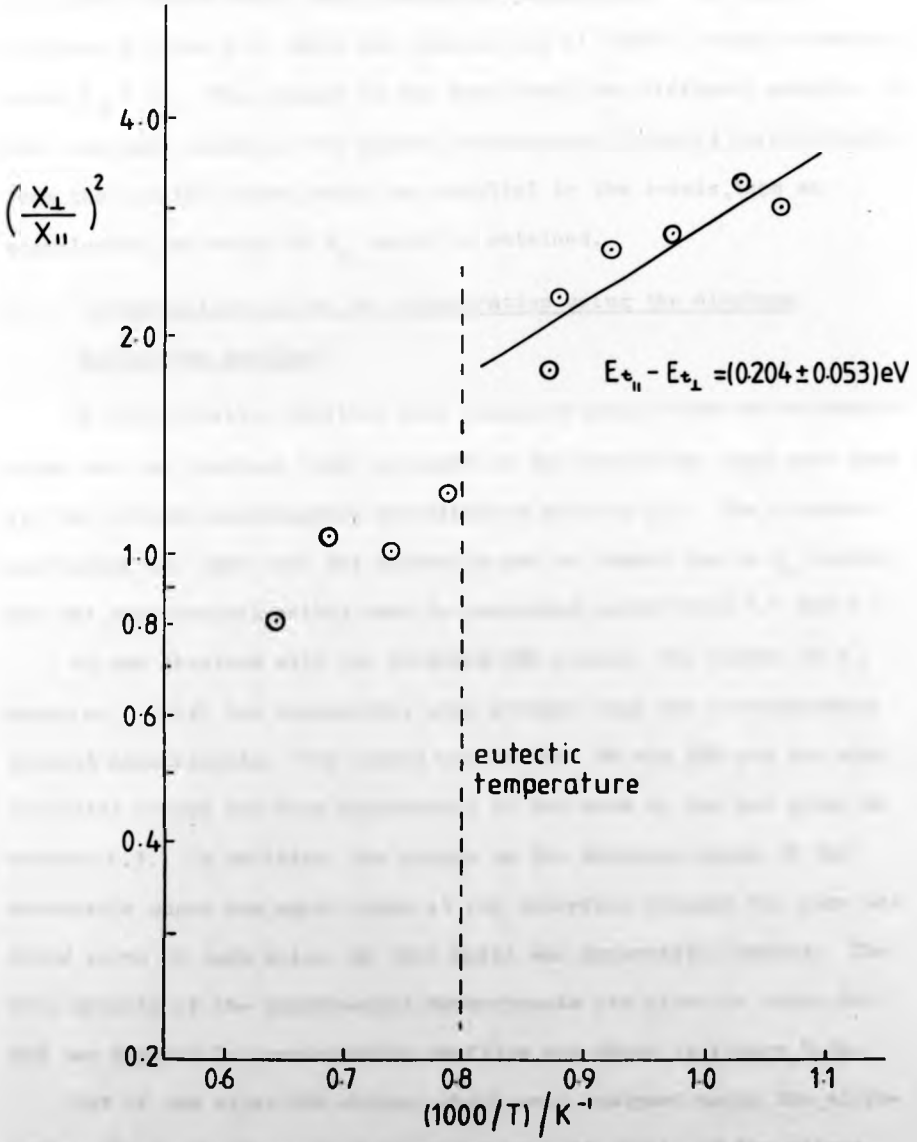

Fig 9.6

It can be seen in figure 9.6 that for the major part of the temperature range over which measurements were taken, the magnitude of the diffusion anisotropy is greater than unity and, as expected, decreases towards unity with increasing temperature. The value obtained for run 210, which was carried out at 1558 K, shows a reversal, where $X_{\parallel} > X_{\perp}$. This result is the mean from five diffusion anneals. If the high mass losses at the higher temperatures occurred preferentially from the crystal planes, which are parallel to the c-axis, then an anomalously low value of $D_{o_{\perp}}$ would be obtained.

9.3. Determination of the Ga concentration using the electron microprobe analyser.

Ga concentration profiles were measured across both the diffusion layer and the reaction layer on eight of the CdS slices that were used for the optical measurements described in section 9.2. The electron microprobe was used with the apparatus set to detect the Ga K_{α} X-rays and the experimental method used is described in sections 3.4 and 6.3.

As was obtained with the In-doped CdS slices the values of $X_{\perp}$ measured with the microprobe, were greater than the corresponding optical measurements. The spread was between 1% and 38% and the most plausible reason for this discrepancy is the same as the one given in section 6.3. In addition, the origin on the distance scale of the microprobe scans was again taken at the interface between the pure and doped parts of each slice, as this point was accurately located. The full details of the experimental measurements are given in table 9.2 and two typical Ga concentration profiles are shown in figure 9.1a.

Out of the eight CdS slices, which were analysed using the microprobe, the chemical reaction layer was present in six of the slices. It was not present on the two slices (207f and 210d) which underwent diffusion anneals at the upper end of the temperature range; this was

TABLE 9.2. DETAILS OF MEASUREMENTS CARRIED OUT USING THE ELECTRON MICROPROBE ANALYSER

Specimen number	Anneal temperature T	1000/T	Anneal duration	Depth of band as measured optically	Ratio $\left(C_o/C_f\right)$
	K	K^{-1}	s	μm	
214f	941	1.063	1.988,7	100.6	0.0157
209e	968	1.033	8.021,6	90.3	0.0165
121f	1029	0.972	2.322,6	160.7	0.030
208d	1083	0.923	5.159,5	177.3	0.0450
211a	1136	0.880	2.321,5	279.2	0.0750
205e	1267	0.789	1.584,4	188.4	0.122
207f	1455	0.687	5.400,3	189.2	0.0600
210d	1588	0.642	3.600,3	183.2	0.0250

above the temperature of the eutectic where large losses in mass occurred. It can be seen from figure 9.1a that the CdS slice used in diffusion 212f (1029 K) shows the presence of the reaction layer. As was mentioned earlier, in run 207f (1455 K) the reaction layer had been observed on the slice before it was mounted in plastic for polishing. In addition to this, the diffusion layer on the second side of the slice, used in diffusion 207f, broke away from the slice in the cleaving operation and consequently it was only possible to measure one concentration profile in this particular case. No reaction layer was observed on specimen 210d (1588 K); this point was mentioned in sub-section 9.1.2.

The highest temperature profiles, as is shown in figure 9.1b, are in reasonable agreement with the Wagner profile and the Ga in these cases is in the highly mobile form $(Ga^{\bullet}_{Cd}\ V''_{Cd})'$. At lower temperatures the agreement is less good, the deviation of these low temperature profiles from the $D \propto C$ relationship at the higher concentrations is almost certainly due to the formation of $(Ga^{\bullet}_{Cd}\ V''_{Cd}\ Ga^{\bullet}_{Cd})^{\times}$ which causes the proportion of the highly mobile defect, expressed as a fraction of the total Ga, to fall off. Similar relationships, which are shown in figure 9.1c, have been observed by Perkins and Rapp (1) and by Minford and Stubican (2). Their curves show a $D \propto C$ relationship at low impurity concentrations with D becoming less sensitive to changes in impurity concentrations at higher values. In their paper on the diffusion of Cr in NiO, Perkins and Rapp discuss the degree of association between double and triple defects of the form $(Cr^{\bullet}_{Ni}\ V''_{Ni})'$ and $(Cr^{\bullet}_{Ni}\ V''_{Ni}\ Cr^{\bullet}_{Ni})^{\times}$ as a function of temperature.

Both types of complexes have been observed (5) by electron spin resonance studies in specimens of Cr-doped NiO at room temperature. A fuller analysis, similar to that performed by Perkins and Rapp, needs to be carried out for the Ga diffusions and, as was mentioned earlier, it is being left to a later time.

For the purpose of this thesis little weighting was placed on the experimental points in the diffusion layer, which were close to the reaction layer, in obtaining the best Wagner fit. In the analysis of the results, the values of C_o and X, which are required to calculate the diffusion parameters, are the ones given by the best Wagner fit through the experimental points assuming a $D \propto C$ relationship. In the case of the phase diagram, which is discussed in section 9.5, the actual concentration at the interface between the reaction layer and the diffusion layer was used.

The Ga count rates obtained from the doped CdS and the metal standard in the microprobe measurements were corrected for the factors which are given in section 3.4. This was done using the computer program which was developed at the University of Birmingham and is described in section 6.3 (6). As with the In diffusions, these correction factors were checked by carrying out a manual calculation using the data due to Theisen (7) where the cation lattice in a CdS slice of stoichiometric composition was assumed to be doped by Ga to an atomic concentration of 2%. The manual calculation indicated that the values of the count rate, which were obtained using the microprobe, should be divided by 0.95 and the corresponding value obtained using the computer program was 0.97. For the diffusion of Ga into CdS, the correction factor which had been determined using the computer program was used as it was probably more reliable.

The experimental error in the values of the concentration was large because the formation of the reaction layer complicated the Wagner model for concentration dependent diffusion. The model is dependent on the surface of the diffusion layer remaining fixed and on the concentration of the diffusing atoms, in contact with the surface of the host lattice, remaining constant. The presence of the reaction layer whose thickness increases at a rate, which is probably $\alpha\ t^{\frac{1}{2}}$, violates both of the above requirements. In the first instance, Ga atoms are entering the diffusion layer from a surface which is moving and not from a stationary one as is assumed in the Wagner analysis. The second violation is that as the thickness of the reaction layer increases, the surface of the diffusion layer is separated from the source of Ga atoms which are in the gaseous phase. It is very likely that the Ga atoms are able to diffuse sufficiently easily through the relatively open cation lattice of the $CdGa_2S_4$ of the reaction layer that its existence did not violate the second requirement. In the case of the diffusion anneals, which were carried out at temperatures above the eutectic temperature, the diffusion of Ga atoms through the reaction layer was certainly sufficiently rapid not to violate the second requirement.

The variation in the depth of the reaction layer as a function of temperature was investigated and the results, which are shown in figure 9.7, for the temperature range 941 K to 1267 K inclusive, can be expressed by the following Arrhenius equation:

$$D_{\parallel} = (0.72^{+4.75}_{-0.63})\ m^2\ s^{-1}\ \exp\left[\frac{-(3.17 \pm 0.18)\ eV}{kT}\right] \qquad 9.6$$

A TEMPERATURE PLOT OF THE DIFFUSIVITY OF THE REACTION LAYER

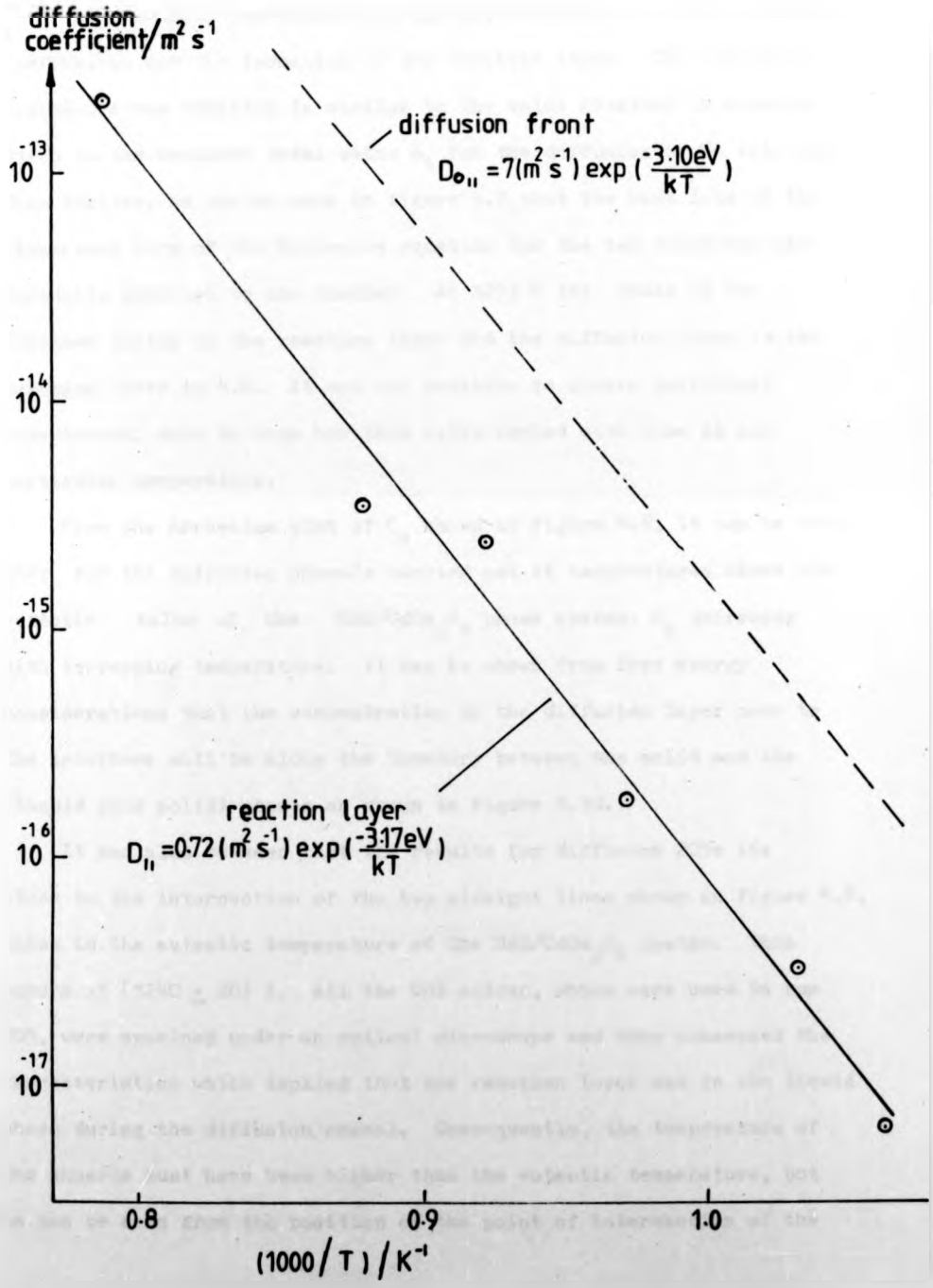

Fig 9.7

The diffusion coefficient in the above equation is the effective coefficient for the formation of the reaction layer. The activation energy for the reaction is similar to the value obtained in equation 9.1 which is the measured total value E_t for the diffusion of Ga into CdS. This implies, as can be seen in figure 9.7, that the best fits of the linearised form of the Arrhenius equation for the two reactions are virtually parallel to one another. At 1273 K the ratio of the combined depths of the reaction layer and the diffusion layer to the reaction layer is 4.8. It was not possible to obtain sufficient experimental data to show how this ratio varied with time at any particular temperature.

From the Arrhenius plot of C_o shown in figure 9.8, it can be seen that for the diffusion anneals carried out at temperatures above the eutectic value of the $CdS/CdGa_2S_4$ phase system, C_o decreases with increasing temperature. It can be shown from free energy considerations that the concentration in the diffusion layer near to the interface will be along the boundary between the solid and the (liquid plus solid) phases as shown in figure 9.10.

It can also be seen that the results for diffusion 205e lie close to the intersection of the two straight lines shown in figure 9.8, which is the eutectic temperature of the $CdS/CdGa_2S_4$ system. This occurs at (1240 $\pm$ 20) K. All the CdS slices, which were used in run 205, were examined under an optical microscope and they possessed the characteristics which implied that the reaction layer was in the liquid phase during the diffusion anneal. Consequently, the temperature of the anneals must have been higher than the eutectic temperature, but as can be seen from the position of the point of intersection of the

AN ARRHENIUS PLOT OF THE NEAR-SURFACE CONCENTRATION OF Ga IN THE DIFFUSION LAYER IN CdS

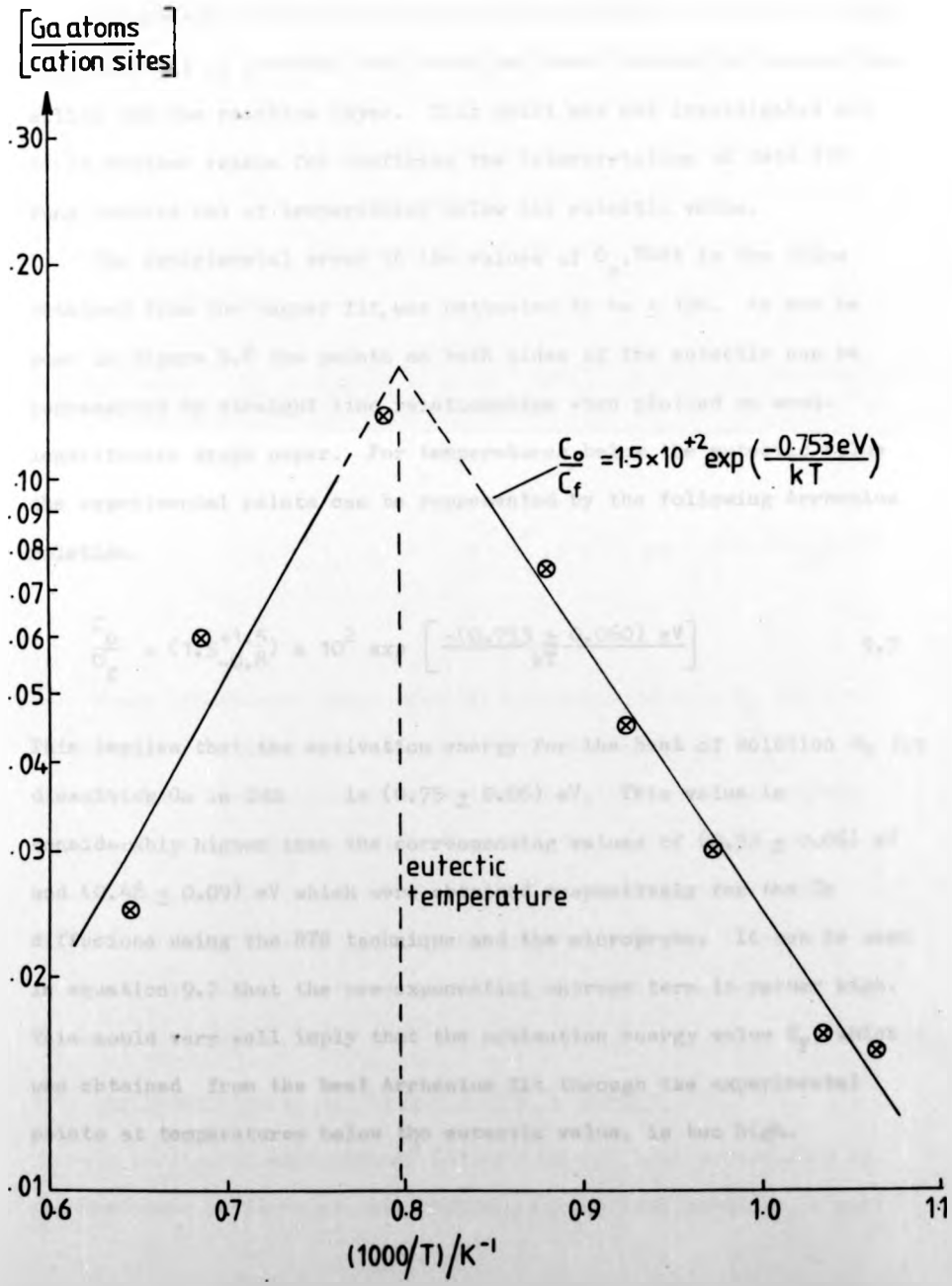

Fig 9·8

two straight lines, the temperature of the anneals must only have been very slightly higher than the eutectic value.

At temperatures above the eutectic value, where the reaction layer was molten, it is possible that there was some interaction between the silica and the reaction layer. This point was not investigated and it is another reason for confining the interpretation of data for runs carried out at temperatures below the eutectic value.

The experimental error in the values of C_o, that is the value obtained from the Wagner fit, was estimated to be $\pm$ 15%. As can be seen in figure 9.8 the points on both sides of the eutectic can be represented by straight line relationships when plotted on semi-logarithimic graph paper. For temperatures below the eutectic value the experimental points can be represented by the following Arrhenius relation:

$$\frac{C_o}{C_f} = (1.5^{+1.5}_{-0.8}) \times 10^2 \exp\left[\frac{-(0.753 \pm 0.060)\ eV}{kT}\right] \qquad 9.7$$

This implies that the activation energy for the heat of solution E_F for dissolving Ga in CdS is (0.75 $\pm$ 0.06) eV. This value is considerably higher than the corresponding values of (0.53 $\pm$ 0.06) eV and (0.48 $\pm$ 0.09) eV which were obtained respectively for the In diffusions using the RTS technique and the microprobe. It can be seen in equation 9.7 that the pre-exponential entropy term is rather high. This could very well imply that the activation energy value E_F, which was obtained from the best Arrhenius fit through the experimental points at temperatures below the eutectic value, is too high.

9.4. Determination of the diffusion parameters at a fixed near-surface Ga concentration

The diffusion coefficients D_o, which were determined optically and are presented in section 9.2, were normalised to give the diffusion coefficient D'_o at the surface of the layer corresponding to a value of (C_o/C_f) of 0.01. The results are presented as Arrhenius plots in figure 9.9 and for the experimental points, which are below the eutectic temperature, the equations of the best fits through the points are given by:

PERPENDICULAR $$D'_{o_\perp} = (2.4^{+3.0}_{-1.3}) \times 10^{-4} \ (m^2 s^{-1} \text{ at } \%^{-1}) \exp\left[\frac{-(2.25 \pm 0.10)eV}{kT}\right] \qquad 9.8$$

PARALLEL $$D'_{o_{||}} = (4.7^{+6.6}_{-2.7}) \times 10^{-4} \ (m^2 s^{-1} \text{ at } \%^{-1}) \exp\left[\frac{-(2.35 \pm 0.12)\ eV}{kT}\right] \qquad 9.9$$

These expressions imply that the activation energy E_M for the migration of the mobile defect, which is probably $(Ga^{\cdot}_{Cd}\ V''_{Cd})'$, through the Cd sub-lattice in directions parallel and perpendicular to the c-axis are (2.35 ± 0.12) eV and (2.25 ± 0.10) eV respectively. In addition, as the values of the diffusion coefficent above the eutectic were calculated ignoring the substantial mass loss, then it is understandable that a discontinuity is likely to occur at the eutectic temperature.

9.5. The phase diagram of the CdS - $CdGa_2S_4$ system

As sufficient experimental information has been accumulated in the preceding sections of this chapter, it has been possible to make

AN ARRHENIUS PLOT OF THE DIFFUSION COEFFICIENTS D'_o FOR THE DIFFUSION OF Ga INTO CdS.

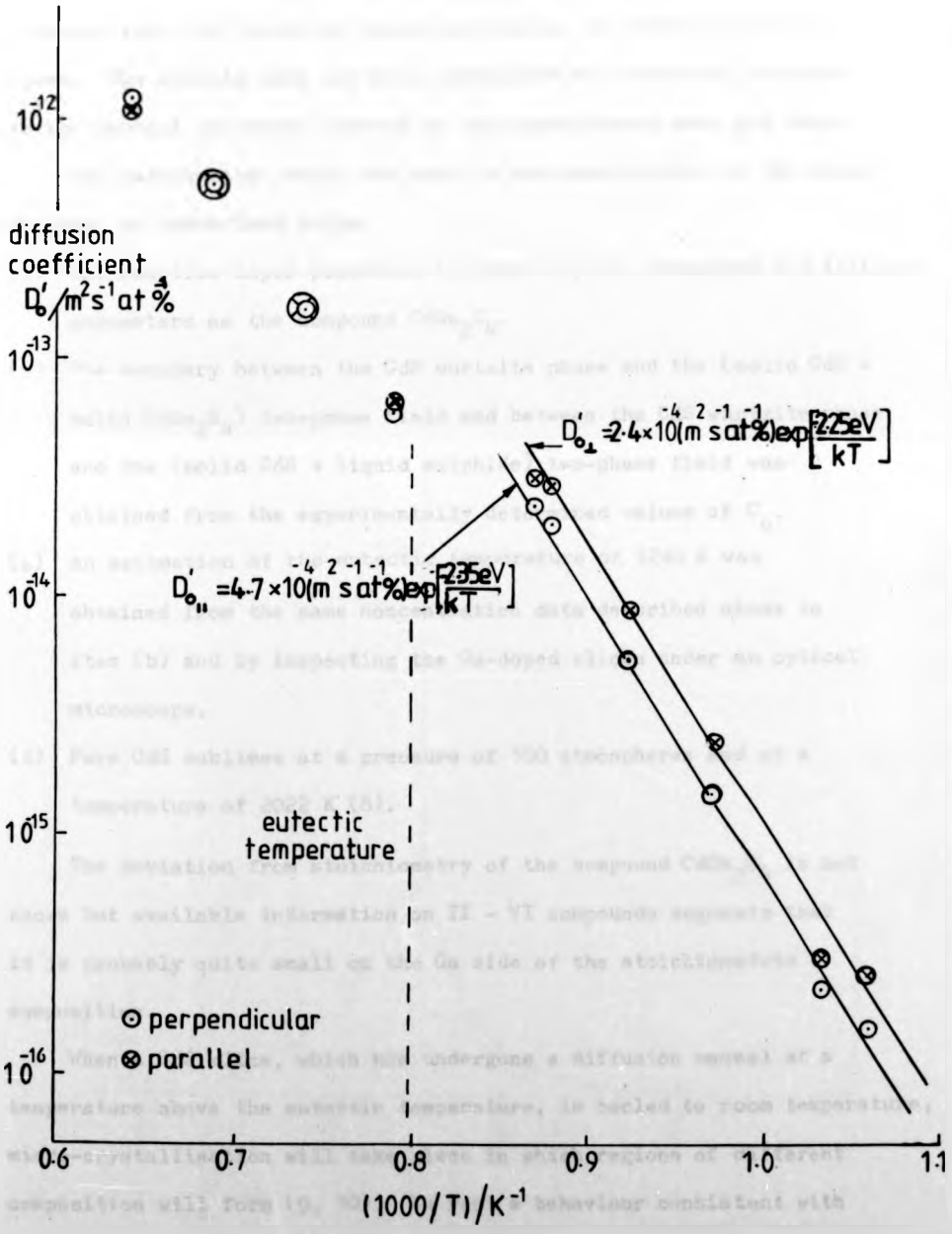

Fig 9.9

an attempt to draw the pseudo-phase diagram for the $CdS/CdGa_2S_4$ system, which is shown in figure 9.10. Accurate information is represented by full lines and the remainder of the phase diagram, which has been obtained from the theory of phase equilibria, is shown as dotted lines. The results have not been normalised to a constant pressure as the partial pressures exerted by the constituents were not known.

The information, which was used in the construction of the phase diagram, is summarised below:

(a) The reaction layer possessed the same crystal structure and lattice parameters as the compound $CdGa_2S_4$.

(b) The boundary between the CdS wurtzite phase and the (solid CdS + solid $CdGa_2S_4$) two-phase field and between the CdS wurtzite phase and the (solid CdS + liquid sulphide) two-phase field was obtained from the experimentally determined values of C_o.

(c) An estimation of the eutectic temperature of 1240 K was obtained from the same concentration data described above in item (b) and by inspecting the Ga-doped slices under an optical microscope.

(d) Pure CdS sublimes at a pressure of 100 atmospheres and at a temperature of 2022 K (8).

The deviation from stoichiometry of the compound $CdGa_2S_4$ is not known but available information on II - VI compounds suggests that it is probably quite small on the Ga side of the stoichiometric composition.

When a CdS slice, which has undergone a diffusion anneal at a temperature above the eutectic temperature, is cooled to room temperature, micro-crystallisation will take place in which regions of different composition will form (9, 10). In fact a behaviour consistent with

THE PROPOSED CdS / $CdGa_2S_4$ PHASE DIAGRAM

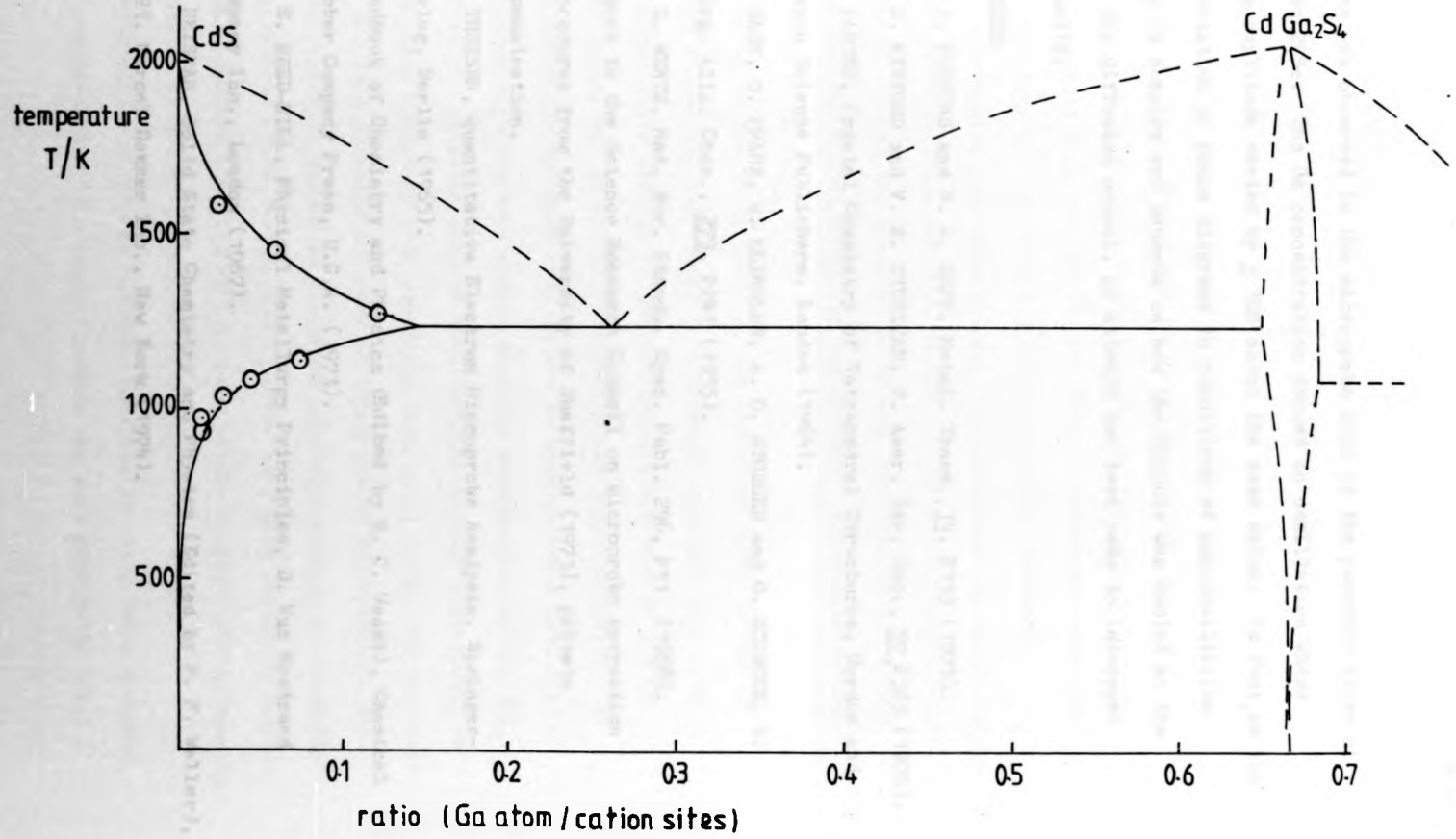

Fig 9·10

this one was observed in the microprobe scan of the reaction layer of specimen 205e. The Ga concentration showed an oscillation whose maximum amplitude varied by ± 30% about the mean value. In fact, as the interpretation of phase diagrams in conditions of non-equilibrium cooling is complex and depends on how the ampoule was cooled at the end of the diffusion anneal, no attempt has been made to interpret the results.

References

1. R. A. PERKINS and R. A. RAPP, Metal. Trans., 14, P193 (1973).
2. W. J. MINFORD and V. S. STUBICAN, J. Amer. Cer. Soc., 57, P363 (1974).
3. E. PARTHE, Crystal Chemistry of Tetrahedral Structures, Gordon and Breach Science Publishers, London (1964).
4. H. HAHN, G. FRANK, W. KLINGLER, A. D. STORGER and G. STORGER, Z. Anorg. Allg. Chem., 279, P241 (1955).
5. J. E. WENTZ, Nat. Bur. Stands. Spec. Publ. 296, P11 (1968).
6. Report to the Science Research Council on microprobe correction procedures from the University of Sheffield (1973), private communication.
7. R. THEISEN, Quantitative Electron Microprobe Analysis, Springer-Verlag, Berlin (1965).
8. Handbook of Chemistry and Physics (Edited by R. C. Weast), Chemical Rubber Company Press, U.S.A. (1973).
9. R. E. REED-HILL, Physical Metallurgy Principles, D. Van Nostrand Company Inc., London (1967).
10. A. REISMAN, Solid State Chemistry and Physics (Edited by P. F. Weller), P721, Marcel Dekker Inc., New York (1974).

10. Diffusion of Al into CdS

The diffusion anneals described in this chapter were carried out with excess Al metal in the ampoule and, as with the In and Ga diffusions, the doped CdS slices possessed sharply defined optically observable diffusion fronts due to the concentration dependent diffusion. The half-lives of the common radioisotopes of Al are not sufficiently long for them to be used as tracers and consequently the OM technique had to be used for measuring the diffusion.

As the results from this series of measurements possessed similar characteristics to those obtained in the In and Ga diffusions, which were carried out in the presence of excess trivalent metal, it was assumed that the defect mechanism was similar. The mobile defect was assumed to be $(Al_{Cd}^{\bullet} \; V_{Cd}^{''})^{'}$.

Similar to the Ga diffusions, the diffusion layer in the Al-doped CdS slices was surrounded by a chemical reaction layer, which appeared optically similar to the low temperature form of the Ga reaction layer, but it was light coloured and polycrystalline. Al is also extremely reactive and, as can be seen in table 3.4, its common oxide Al_2O_3 is more stable than the common oxide of Si, SiO_2, from which the ampoules used in the diffusion anneals were made. As a result many competing side reactions took place during the diffusion anneal and this affected the rate at which the Al diffused into the CdS. It proved difficult to carry out diffusion anneals successfully at temperatures above 1261 K, and also for very long diffusion anneals which were carried out at 1025 K because of the failure of the ampoule. Consequently, as the Al diffusions were complicated by the reactivity of the Al it has not been possible to carry out a complete set of measurements. The available time was more profitably spent

on the In and Ga diffusions.

Successful diffusion anneals were obtained in the temperature range 1025 K to 1336 K inclusive and a summary of the details is given in table 10.1.

Another observation that was made was that the combined thickness of the chemical reaction layer and the diffusion layer on the upper and lower surfaces of the CdS slice were different, and that the ratio of these two depths for each slice remained reasonably constant. As all the CdS slices, which were used in the series of measurements described in this chapter, possessed the same orientation with the c-axis perpendicular to the surface of the slice, the two values of the combined depths were designated using the symbols $X_{\parallel max}$ and $X_{\parallel min}$. In fact it was the greater of the two depths, $X_{\parallel max}$, that was used initially in the determination of the activation energy E_t and the diffusion anisotropy.

10.1. Changes in the physical properties of the CdS

Because of the interaction between the Al and the SiO_2 of the ampoule, only a limited amount of accurate reproducible information could be obtained from the weighings which were carried out on the constituents of the ampoule before sealing, and again after the completion of the diffusion anneals.

For anneals carried out below 1336 K, the competing reactions did not take place at a rate which was sufficiently fast to affect the diffusion, whereas at 1336 K and all temperatures above this value, the side reactions proceeded so quickly that the normal diffusion process was affected. In addition, in some of the very long diffusion anneals, which were carried out at the lowest temperature (1025 K), the walls of the ampoules became porous, air eventually leaked into the ampoules and this caused the CdS to decompose. These points are discussed in

TABLE 10.1. NUMERICAL DATA FOR THE DIFFUSION OF Al INTO CdS

Run number	Temperature T	1000/T	$D_{o_\perp} = 0.3811\left(\frac{X^2_\perp}{t}\right)$	$D_{o_{\parallel max}} = 0.3811\left(\frac{X^2_{\parallel max}}{t}\right)$	$D_{o_{\parallel min}} = 0.3811\left(\frac{X^2_{\parallel min}}{t}\right)$	$\frac{X_\perp}{X_{\parallel max}}$	$\frac{X_\perp}{X_{\parallel min}}$	$\frac{X_{\parallel max}}{X_{\parallel min}}$	Number of anneals in the run
	K	K^{-1}	m^2s^{-1}	m^2s^{-1}	m^2s^{-1}				
301	1261	0.793	1.270,-13	1.221,-13	8.659,-14	1.040	1.467	1.411	8
310	1211	0.826	5.823,-14	4.638,-14	3.229,-14	1.256	1.804	1.436	7
311	1123	0.891	7.115,-15	4.268,-15	3.247,-15	1.667	2.191	1.315	6
312	1169	0.855	2.633,-14	1.826,-14	1.113,-14	1.443	2.366	1.641	8
313	1336	0.749	2.541,-13	2.410,-13	2.072,-13	1.054	1.226	1.163	2
315	1059	0.944	1.453,-15	8.761,-16	7.320,-16	1.658	1.984	1.197	5
316	1025	0.976	2.661,-16	2.083,-16	1.461,-16	1.771	2.525	1.426	5

detail in section 10.3. The changes in the physical properties of the CdS, which took place during the diffusion anneals and are reported in this section, are for the anneals in which consistent results were obtained. The relevant diffusion runs are listed in table 10.1.

After they had been removed from the diffusion furnace, the walls of the ampoules possessed a light orange-yellow deposit at the end where the Al was located. This was the end of the ampoule that entered the hot zone of the furnace first and it was also the end that emerged first from the hot zone when the ampoule was removed from the furnace at the end of the anneal. When the ampoule was opened an odour similar to that of H_2S was detected, which was probably due to Al_2S_3 (1, 2). The odours of these two compounds are similar. The outer surface of the CdS slice possessed a black colouration and the Al globule possessed a hard grey thick coating which was probably an oxide or silicate of Al.

In the diffusion runs summarised in table 10.1, out of the 62 anneals attempted, consistent results were obtained in 41 cases. It was possible to measure the change in mass of the CdS slice in 43 of the anneals, whereas the change in mass of the metal globule and of the total constituents of the ampoule were obtained on only 15 occasions. The average change in mass of the CdS in each run was calculated and the results are plotted in figure 10.1, in which the ratio of the final mass to the initial mass is plotted against temperature.

It can be seen from the graph in figure 10.1 that the ratio tends to decrease gradually as the temperature is increased. The decrease in mass of the slice when averaged over the 43 anneals was 4.5%. The results of the change in mass of the Al globule and the

TEMPERATURE PLOT OF THE MASS CHANGE OF THE CdS SLICES FOR THE DIFFUSION OF Al INTO CdS

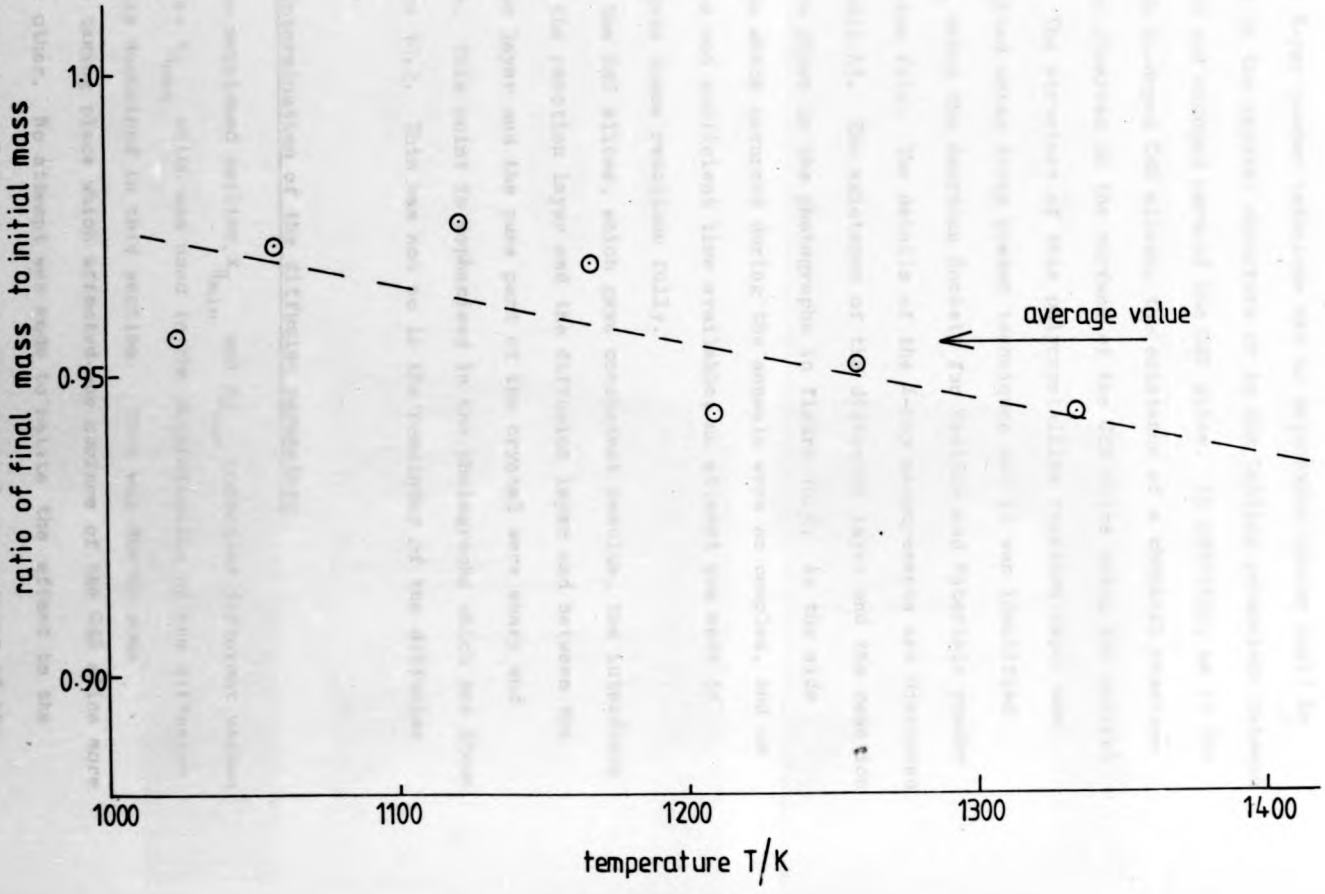

Fig10·1

total contents of the ampoule were omitted from the thesis.

The structure of the doped region of the CdS slice was examined using an X-ray powder technique and no detectable change could be observed in the crystal structure or in the lattice parameters between the doped and undoped parts of the CdS slice. In addition, as in the case with Ga-doped CdS slices, the existence of a chemical reaction layer was observed on the surface of the CdS slice using the optical method. The structure of this polycrystalline reaction layer was investigated using X-ray powder techniques and it was identified as Al_2O_3 using the American Society for Testing and Materials powder diffraction file. The details of the X-ray measurements are discussed in appendix A3. The existence of the diffusion layer and the reaction layer are shown in the photographs in figure 10.2. As the side reactions which occurred during the anneals were so complex, and as there was not sufficient time available, no attempt was made to investigate these reactions fully.

In the CdS slices, which gave consistent results, the interfaces between the reaction layer and the diffusion layer and between the diffusion layer and the pure part of the crystal were sharp and distinct. This point is emphasised in the photographs which are shown in figure 10.2. This was not so in the remainder of the diffusion anneals.

10.2. Determination of the diffusion parameters

As was mentioned earlier, $X_{ll_{min}}$ and $X_{ll_{max}}$ possessed different values and it was $X_{ll_{max}}$ which was used in the determination of the diffusion parameters described in this section. This was due to some reaction taking place which affected one surface of the CdS slice more than the other. No attempt was made to relate the effect to the orientation of the CdS slice or to the physical arrangement of the

PHOTOGRAPHS OF THE CLEAVED SURFACE OF A CdS SLICE WHICH HAS BEEN DIFFUSED IN Al VAPOUR

run 316e
temperature 1025K
duration 2156h

cleaved slice 350μm thick
magnification ×200

(a) transmitted light – reaction and diffusion layers are opaque cleavage steps prominent

(b) incident illumination (not polarised) – polycrystalline reaction layer, dark diffusion layer just visible cleavage steps are prominent and continuous into the diffusion layer

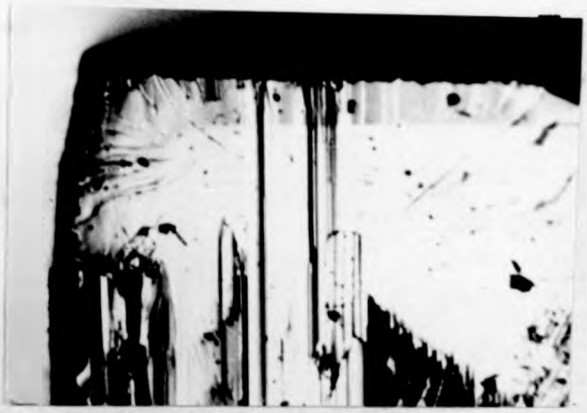

(c) incident illumination polars almost crossed – diffusion layer shows a sharp contrast

Fig 10·2

slice in the ampoule during the anneal. In fact, the physical arrangement, used in the ampoule during the diffusion anneals, was the same for the measurements involving all three metals and no such effect similar to this was observed for the In and Ga diffusions.

The ratio of the thickness of the reaction layer to the total combined thickness of the two layers varied appreciably between slices and the maximum value that was obtained was 0.3. It was the combined thickness of the two layers that was used, in the calculations described in this section, to determine the diffusion coefficients.

A typical straight line plot of X^2 versus t is shown in figure 10.3. Arrhenius plots of the diffusion coefficients D_o for diffusions in two standard directions are shown in figure 10.4. For the experimental points at 1261 K and all temperatures below this value, the equations of the best fits through the points can be represented by the following relationships:

PARALLEL $$D_{o_{\parallel \max}} = \left(0.12^{+0.18}_{-0.07}\right) m^2 s^{-1} \exp\left[\frac{-(2.99 \pm 0.09)\ eV}{kT}\right] \quad 10.1$$

PERPENDICULAR $$D_{o_{\perp}} = \left(0.05^{+0.20}_{-0.04}\right) m^2 s^{-1} \exp\left[\frac{-(2.86 \pm 0.16)\ eV}{kT}\right] \quad 10.2$$

Above 1261 K the experimental points show the same departure from linearity as was obtained with In and Ga, which was to give a flatter distribution.

As there was insufficient time available to measure C_o as a function of T using the electron microprobe, it was not possible to normalise the above values of D_o to a value of C_o/C_r corresponding to 0.01. Despite this, it was possible to obtain just one profile measurement

A TYPICAL PLOT OF X^2 AGAINST t FOR THE DIFFUSION OF Al INTO CdS.

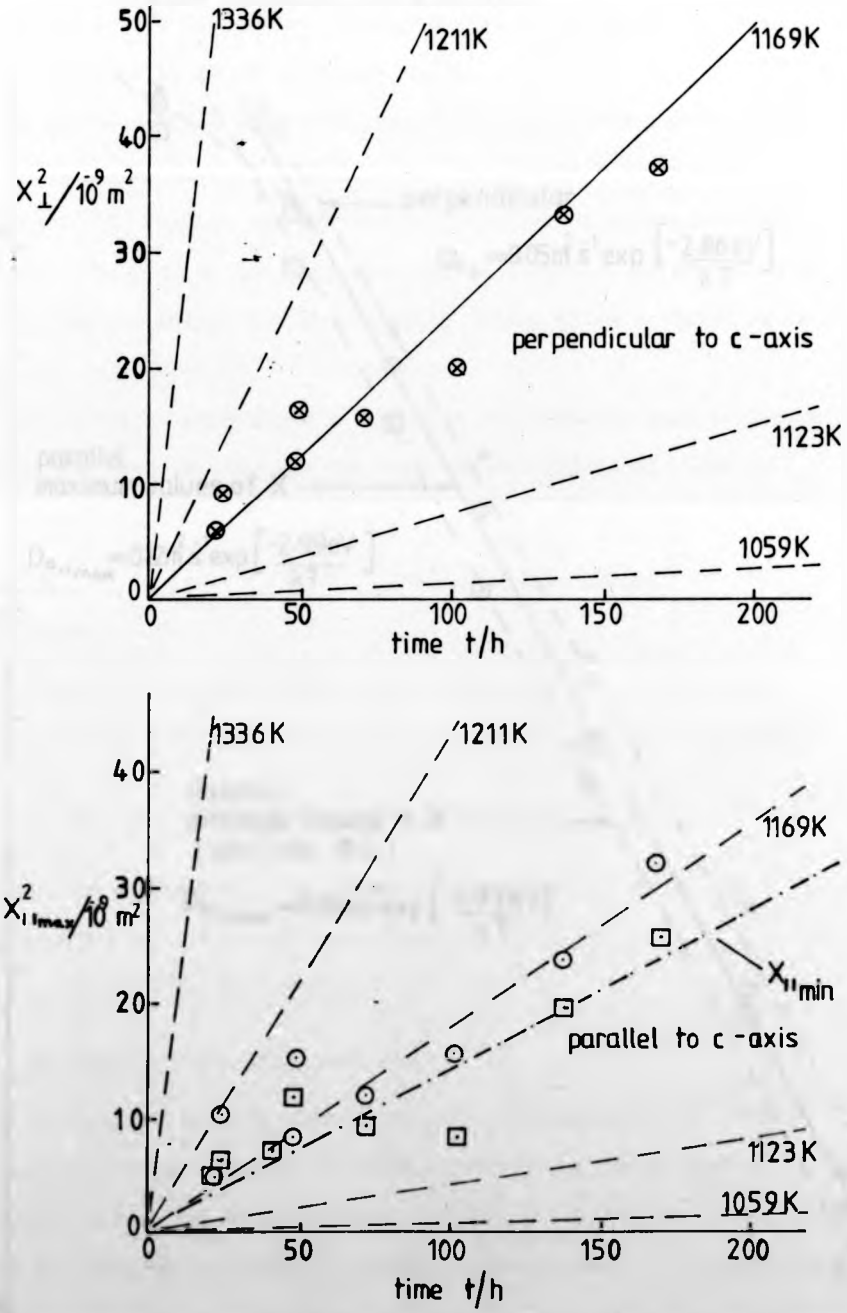

Fig 10.3

AN ARRHENIUS PLOT OF THE DIFFUSION COEFFICIENT D_0 FOR THE DIFFUSION OF Al INTO CdS

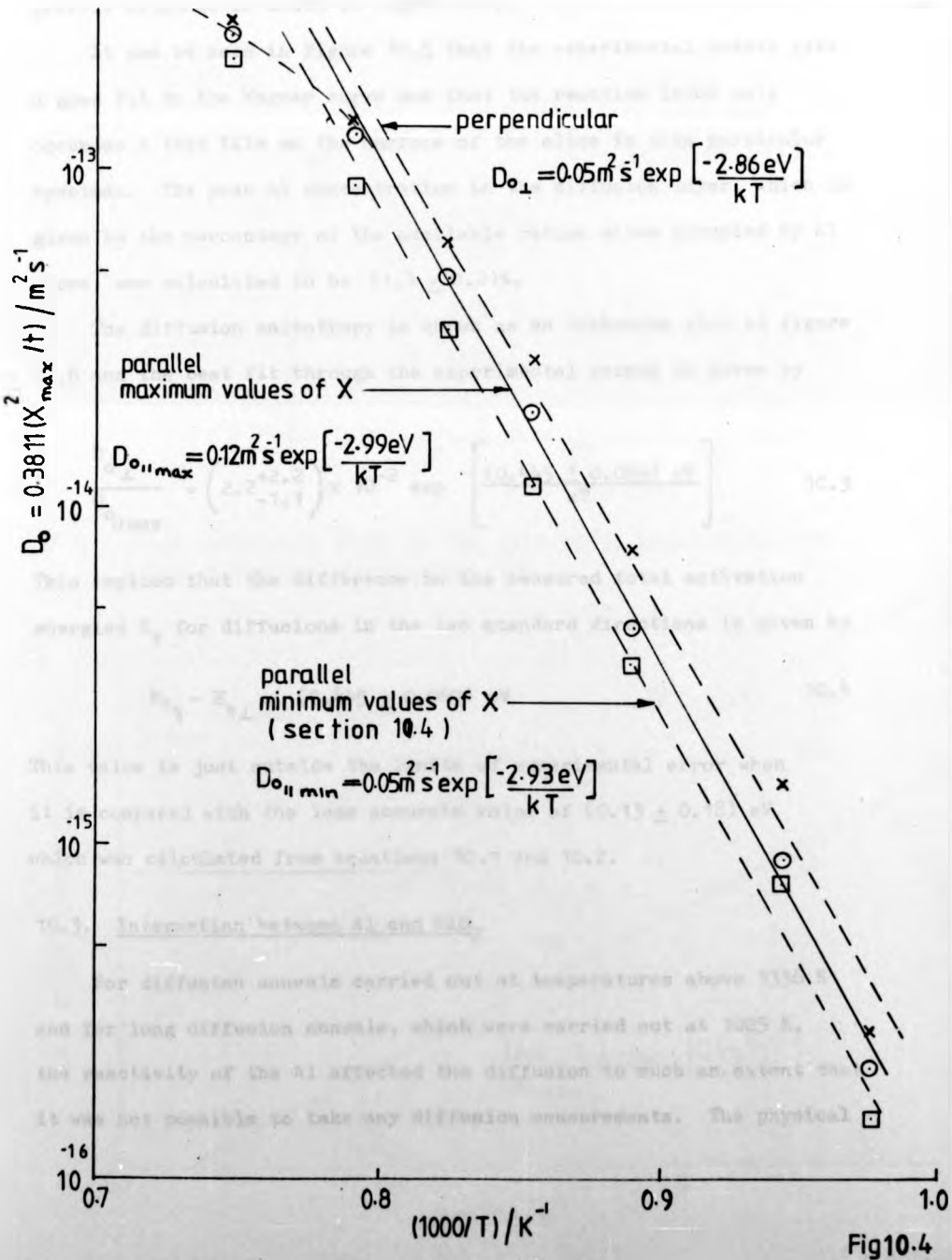

Fig 10.4

for specimen 312e. The same experimental procedure was followed for measuring the profile as was used for the In and Ga measurements except that the apparatus was set up to measure the Al K_α X-rays and the profile obtained is shown in figure 10.5.

It can be seen in figure 10.5 that the experimental points give a good fit to the Wagner curve and that the reaction layer only occupies a thin film on the surface of the slice in this particular specimen. The peak Al concentration in the diffusion layer, which is given by the percentage of the available cation sites occupied by Al atoms, was calculated to be $(1.3 \pm 0.2)\%$.

The diffusion anisotropy is shown as an Arrhenius plot in figure 10.6 and the best fit through the experimental points is given by

$$\frac{D_{o\perp}}{D_{o\parallel max}} = \left(2.2^{+2.2}_{-1.1}\right) \times 10^{-2} \exp\left[\frac{(0.445 \pm 0.069)\ eV}{kT}\right] \qquad 10.3$$

This implies that the difference in the measured total activation energies E_t for diffusions in the two standard directions is given by

$$E_{t_\parallel} - E_{t_\perp} = (0.445 \pm 0.069)\ eV \qquad 10.4$$

This value is just outside the limits of experimental error when it is compared with the less accurate value of (0.13 ± 0.18) eV which was calculated from equations 10.1 and 10.2.

10.3. Interaction between Al and SiO_2

For diffusion anneals carried out at temperatures above 1336 K and for long diffusion anneals, which were carried out at 1025 K, the reactivity of the Al affected the diffusion to such an extent that it was not possible to take any diffusion measurements. The physical

FIG 10.5 AN Al CONCENTRATION PROFILE IN A CdS SLICE

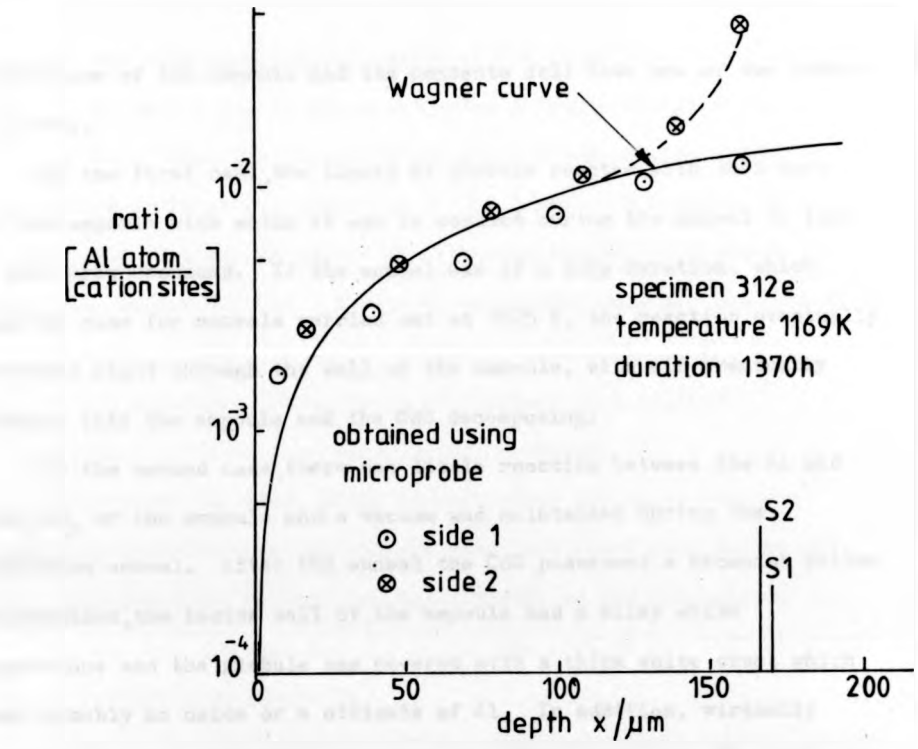

FIG 10.6 AN ARRHENIUS PLOT OF THE DIFFUSION ANISTROPY FOR THE DIFFUSION OF Al INTO CdS

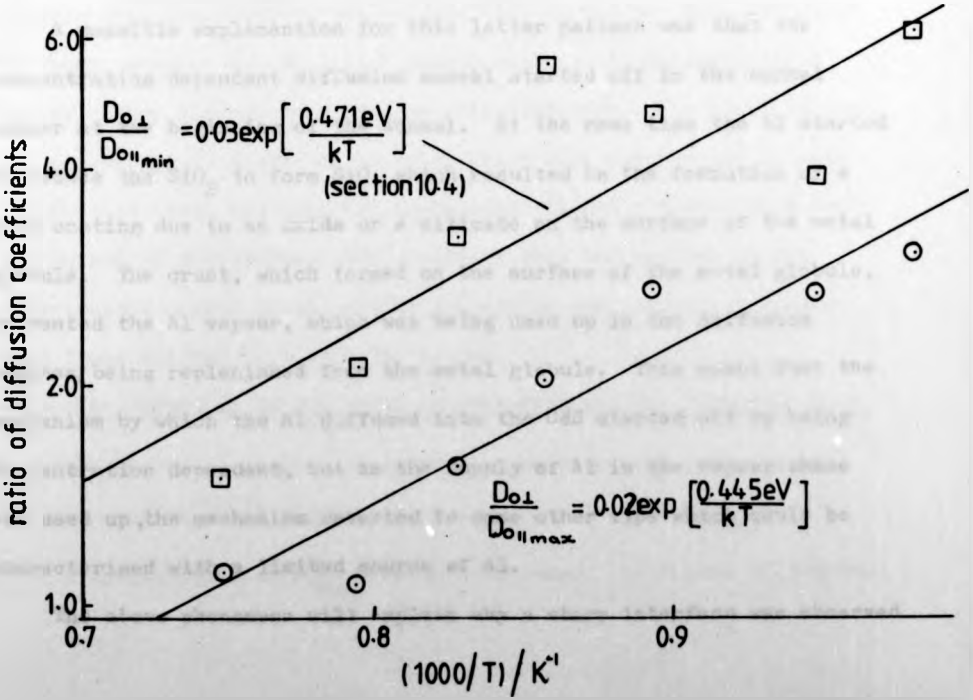

FIGS 10.5, 10.6.

appearance of the ampoule and its contents fell into one of two common patterns.

In the first case, the liquid Al globule reacted with that part of the ampoule with which it was in contact during the anneal to form a hard grey compound. If the anneal was of a long duration, which was the case for anneals carried out at 1025 K, the reaction eventually extended right through the wall of the ampoule, with air eventually leaking into the ampoule and the CdS decomposing.

In the second case, there was little reaction between the Al and the SiO_2 of the ampoule and a vacuum was maintained during the diffusion anneal. After the anneal the CdS possessed a brownish yellow colouration, the inside wall of the ampoule had a milky white appearance and the globule was covered with a thick white crust which was probably an oxide or a silicate of Al. In addition, virtually no concentration dependent diffusion had taken place into the CdS slice and the slice proved very difficult to cleave.

A possible explanantion for this latter pattern was that the concentration dependent diffusion anneal started off in the normal manner at the beginning of the anneal. At the same time the Al started to reduce the SiO_2 to form SiO, which resulted in the formation of a hard coating due to an oxide or a silicate on the surface of the metal globule. The crust, which formed on the surface of the metal globule, prevented the Al vapour, which was being used up in the diffusion process, being replenished from the metal globule. This meant that the mechanism by which the Al diffused into the CdS started off by being concentration dependent, but as the supply of Al in the vapour phase was used up, the mechanism reverted to some other type which could be characterised with a limited source of Al.

The above phenomena will explain why a sharp interface was observed

between the doped and undoped region of CdS slice in certain cases, whereas in others the interface appeared diffuse, or could not be seen at all. When the concentration dependent diffusion mechanism was taking place at the beginning of the anneal the sharp interface was present, but as the amount of Al vapour started to diminish the interface became diffuse. As the Al vapour was used up, the interface became more diffuse because the diffusion eventually took place by a mechanism, which was characterised by a limited source where the interface disappeared completely.

An attempt was made, using several other different physical arrangements, to reduce the effects described above in order to get more successful diffusions. In the majority of the attempts no improvement was obtained and eventually the problem was left as there was no further time available.

Despite the fact that relatively consistent results were obtained from the diffusion anneals listed in table 10.1, there was evidence to show that the interactions between CdS, Al and the SiO_2 did occur in these anneals, but to a much lesser degree. In addition, there are two other factors that confirm this statement. The first is that the percentage of diffusion anneals, which were carried out in this temperature range and were not successful, is still higher than for the In and Ga diffusions. The second is that the scatter in the experimental points on the graphs containing the results is greater than those for the In and Ga diffusions.

224

10.4. Determination of diffusion parameters using the parameter $X_{\parallel_{min}}$

The analysis, which is described in section 10.2, was repeated in this section using the parameter $X_{\parallel_{min}}$ in place of $X_{\parallel_{max}}$.

A typical plot of $X^2_{\parallel_{min}}$ versus t is shown in figure 10.3 along

with the corresponding plot using $X_{\parallel max}$. It can be seen that the points lie along a straight line which passes through the origin. An Arrhenius plot of the diffusion coefficient $D_{o_{\parallel min}}$ is shown in figure 10.4 and the points at 1261 K and all temperatures below this value can be represented by the following relationship:-

$$D_{o_{\parallel min}} = \left(0.05^{+0.11}_{-0.04}\right) m^2 s^{-1} \exp\left[\frac{-(2.93 \pm 0.11)\ eV}{kT}\right] \qquad 10.5$$

Above 1261 K the points show the same tendency, that has been seen in all the other results, which is to give a flatter distribution. The value of $D_{o_{\parallel min}}$ is smaller than the corresponding value of $D_{o_{\parallel max}}$ by 28%. The value of the activation energy is similar, which implies that the diffusion of the mobile defect into the two flat surfaces of the CdS slice takes place using a similar mechanism, but the current of atoms diffusing on the cation lattice is less on one side of the slice than on the other.

The diffusion anisotropy which has been calculated using these results is shown on an Arrhenius plot in figure 10.6 and the best straight line through the points is given by:-

$$\frac{D_{o_\perp}}{D_{o_{\parallel min}}} = \left(3.2^{+8.9}_{-2.4}\right) \times 10^{-2} \exp\left[\frac{(0.471 \pm 0.133)\ eV}{kT}\right] \qquad 10.6$$

To within the limits of experimental error, the slopes of the linearised form of the Arrhenius relationships given in equations 10.3 and 10.6 are similar.

10.5. References

1. F. A. COTTON and G. WILKINSON, Advanced Inorganic Chemistry, Interscience Publishers (1972).

2. Handbook of Chemistry and Physics (Edited by R. C. Weast), Chemical Rubber Company Press, U.S.A. (1973).

11. Conclusions and suggestions for further work

The results which have been obtained on the diffusion of the group III metals In, Ga and Al in CdS will be discussed in this chapter. In the case of the Ga and Al diffusions there was an excess of the trivalent metal in the ampoule throughout each anneal whereas for the In diffusions two sets of conditions were used. In the first one, an excess of In metal was placed in the ampoule and the results were similar to those obtained for the Ga and Al diffusions, whereas in the second an excess of both In and Cd metals were added to the ampoule. The conclusions obtained on the In diffusions are discussed in section 8.3.

When an excess of the trivalent metal was placed in the ampoule, the CdS slices possessed a sharply defined visible interface between the doped and the undoped parts of the slice. The group III metal concentration profiles, which were obtained either with the RTS technique or with the electron microprobe, gave reasonable fits when they were compared with the Wagner (1) curve and with the computed curves of Weisberg and Blanc (2) where it was assumed that $D \propto C$. The diffusion of all three elements displayed diffusion anisotropy with $D_{\perp} > D_{\parallel}$.

In chapter 7 it was proposed that, in the diffusion of In into CdS in the presence of excess In metal, In was incorporated into the CdS by a stoichiometric exchange in which three Cd atoms left the crystal for every two In atoms that entered the crystal and charge neutrality was maintained in this exchange. This lead to an increase in the vacancy concentration on the cation lattice to a value far in excess of the intrinsic vacancy concentration. A proportion of the In ions combined with a vacancy to form a compound defect $(In_{Cd}^{\bullet}\ V_{Cd}^{''})'$ and at high In concentrations some of the In ions also existed as a neutral compound defect $(In_{Cd}^{\bullet}\ V_{Cd}^{''}\ In_{Cd}^{\bullet})^{\times}$. The In diffusion took place via the highly mobile defect $(In_{Cd}^{\bullet}\ V_{Cd}^{''})'$ which had a preferred orientation in the Cd

sub-lattice. This diffusion mechanism can account for all the observations given in the previous paragraph and also account for the high In concentrations that were obtained. A similar defect was assumed by Chern and Kröger (3), in their measurements on the diffusion of In into CdS and CdTe, by Greskovich (4) and by Perkins and Rapp (5) for the diffusion of Cr into NiO.

In the Ga and Al diffusions, which were also carried out in the presence of an excess of the trivalent metal, a similar defect mechanism is involved. In addition, in the case of the Ga diffusions, the Ga concentration was high enough in the low temperature diffusions to show a departure from the $D \propto C$ relationship due to the formation of the neutral immobile defect $(Ga^{\bullet}_{Cd}\ V''_{Cd}\ Ga^{\bullet}_{Cd})^{*}$. Similar observations, as are mentioned in chapter 9, were made by Minford and Stubican (6), for the diffusion of Al in NiO, and by Perkins and Rapp (5) for the diffusion of Cr into NiO.

Both the RTS and the OM techniques proved to be successful for measuring the concentration dependent diffusions, but the latter was much simpler and quicker to use and it possessed one definite advantage over the former. This technique was used to show up the diffusion anisotropy, represented by $D_{o_\perp}/D_{o_\parallel}$, in the wurtzite structure and the results for the three metals are summarised in figure 11.1. The RTS technique, despite its tediousness, was better than the microprobe for measuring the concentration profiles because, as was mentioned in section 3.5, it covered a much wider concentration range.

Arrhenius plots of C_o for In and Ga in the diffused CdS slices, which were obtained using the RTS technique and the electron microprobe, are shown in figure 11.2. The activation energy for the heat of solution for dissolving In and Ga in the CdS was obtained from the slopes.

Fig 11·1 A SUMMARY OF THE ANISTROPY FOR THE DIFFUSION OF THE TRIVALENT METALS In, Ga AND Al INTO CdS

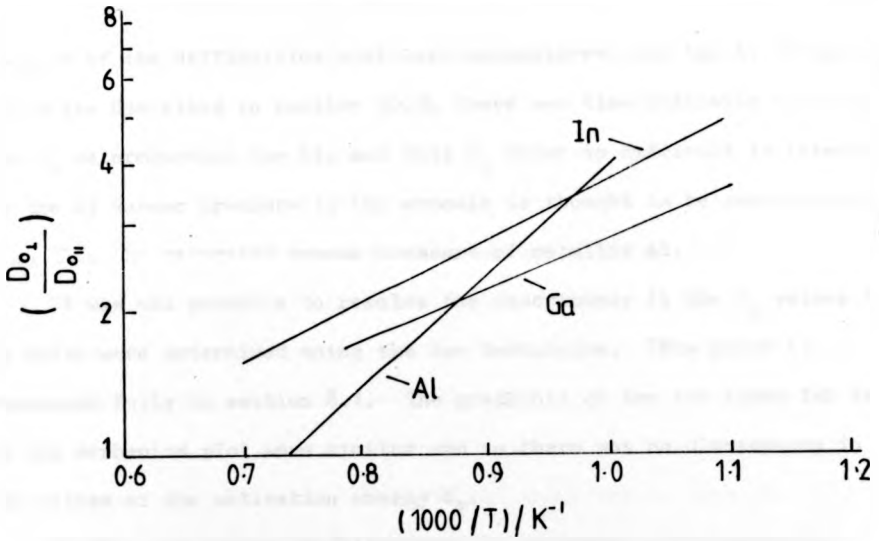

Fig 11·2 A SUMMARY OF THE NEAR-SURFACE CONCENTRATION OF THE TRIVALENT METALS In, Ga AND Al IN CdS

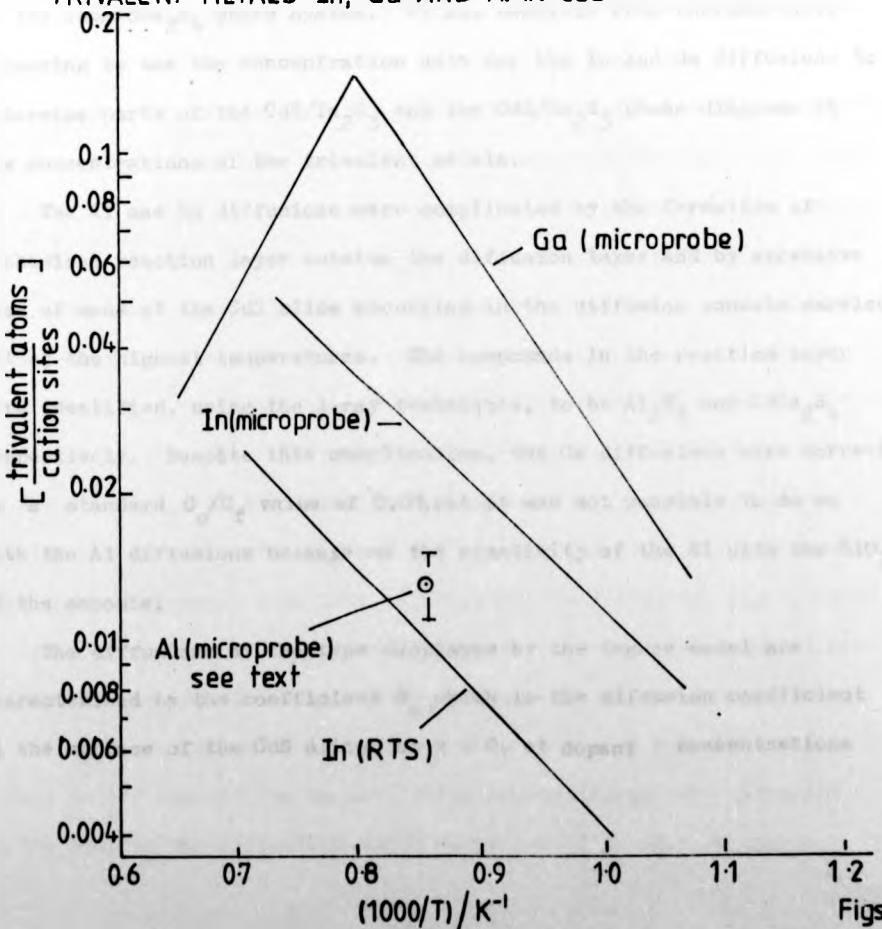

Figs11·1,11·2

Because of the difficulties that were encountered with the Al diffusions, which are described in section 10.3, there was time available for only one C_o determination for Al, and this C_o value is difficult to interpret as the Al vapour pressure in the ampoule is thought to be substantially less than the saturated vapour pressure of metallic Al.

It was not possible to resolve the discrepancy in the C_o values for In which were determined using the two techniques. This point is discussed fully in section 8.1. The gradients of the two lines for In on the Arrhenius plot were similar and so there was no discrepancy in the values of the activation energy E_F.

In the case of the Ga diffusions, C_o decreases with increasing temperature for temperatures above 1240 K which is the eutectic value of the $CdS/CdGa_2S_4$ phase system. It was possible from thermodynamic reasoning to use the concentration data for the In and Ga diffusions to determine parts of the CdS/In_2S_3 and the CdS/Ga_2S_3 phase diagrams at low concentrations of the trivalent metals.

The Al and Ga diffusions were complicated by the formation of a chemical reaction layer outside the diffusion layer and by excessive loss of mass of the CdS slice occurring in the diffusion anneals carried out at the highest temperatures. The compounds in the reaction layer were identified, using the X-ray techniques, to be Al_2O_3 and $CdGa_2S_4$ respectively. Despite this complication, the Ga diffusions were corrected to a standard C_o/C_f value of 0.01, but it was not possible to do so with the Al diffusions because of the reactivity of the Al with the SiO_2 of the ampoule.

The diffusions of the type displayed by the Wagner model are characterised by the coefficient D_o, which is the diffusion coefficient at the surface of the CdS slice, at $x = 0$, at dopant concentrations

equal to C_o. The results for the diffusion of the trivalent metals In, Ga and Al are summarised in the Arrhenius plot in figure 11.3. The range of temperatures over which linear relationships were obtained are indicated by the extent of the straight lines.

In the case of the concentration dependent diffusion all the graphs show the same tendency at the high temperature end of the range which is to depart from the linear relationships to give flatter distributions. The suggested reason for this is that, as the temperature increases, the concentration of the impurity atoms increase to such an extent that other defects and defect complexes become important so that the $(M^{\bullet}_{Cd}\ V^{''}_{Cd})'$ concentration is no longer determined simply by the $(M^{\bullet}_{Cd})$ and $(V^{''}_{Cd})$ interaction. This effect, and the fall-off in D_o for high Ga concentrations at lower temperatures, will require further study and probably an extension of the theory of Perkins and Rapp (5) for a full explanation. The values of D_o for the Al diffusions are much lower than the corresponding results obtained for the In and Ga concentration diffusions; this again is possibly due to the relatively low Al vapour pressure in the ampoule.

The diffusion coefficients D_o, which are given in figure 11.3, were normalised to a C_o value due to the trivalent metal of 1.0 % cation site fraction. The results for the In and Ga diffusions are shown as Arrhenius plots in figure 11.4 and the activation energies E_M for the migration of the mobile defects through the Cd sub-lattice were calculated. As the conditions that existed in the ampoules in the Ga diffusions carried out at temperatures above the eutectic were not fully understood, only the experimental data that was obtained on diffusions carried out at temperatures below the eutectic value were used in the calculations. A complete summary of the activation energies is given in table 11.1.

For the diffusion of In into CdS with excess of both Cd and In metals in the ampoule, the partial pressure conditions were different to the rest of the diffusions where an excess of In only was used.

A SUMMARY OF THE COEFFICIENTS D_o FOR THE DIFFUSION OF THE TRIVALENT METALS In, Ga AND Al INTO CdS

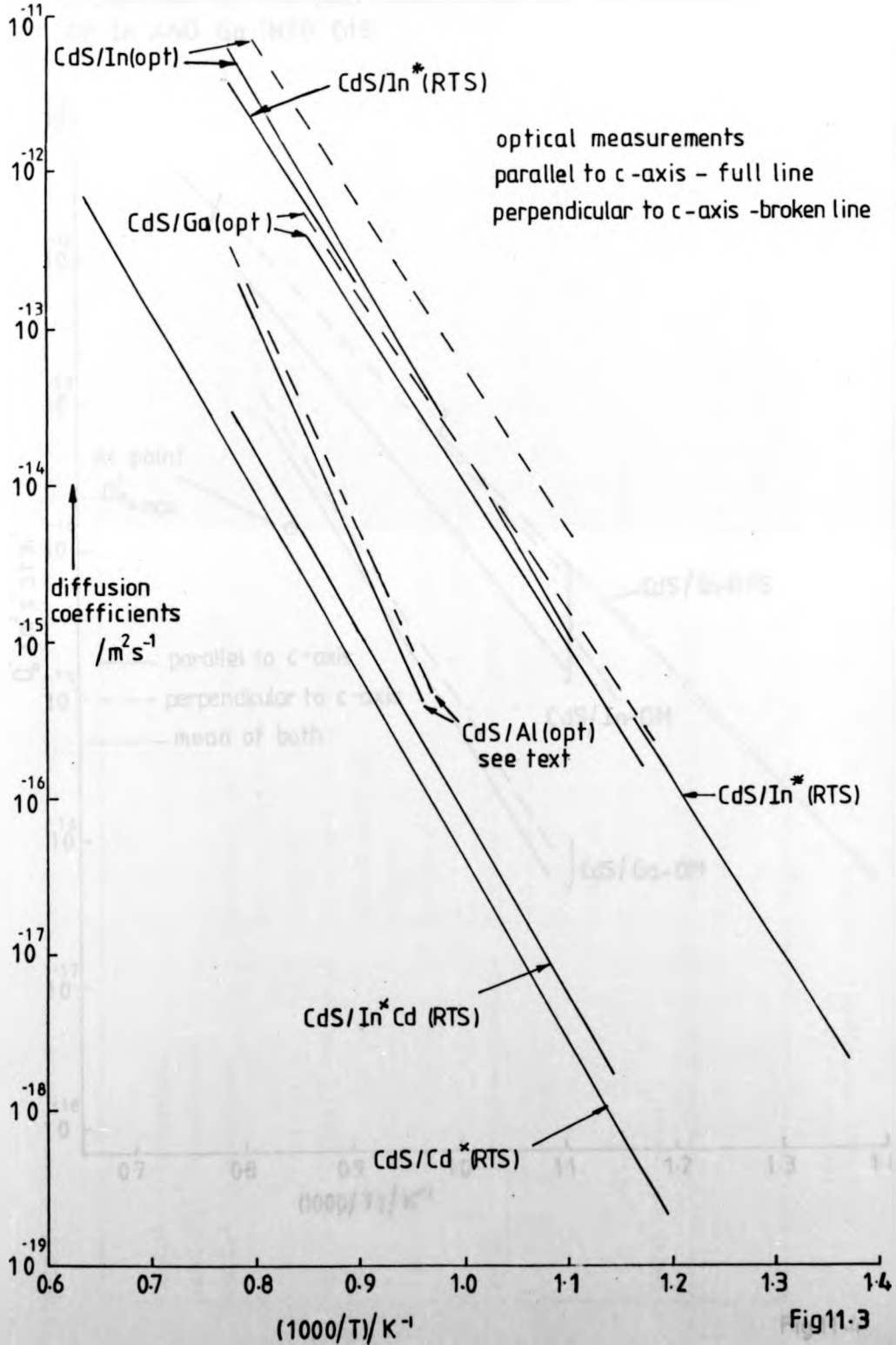

Fig11·3

A SUMMARY OF THE COEFFICIENTS D'_o FOR THE DIFFUSION OF In AND Ga INTO CdS

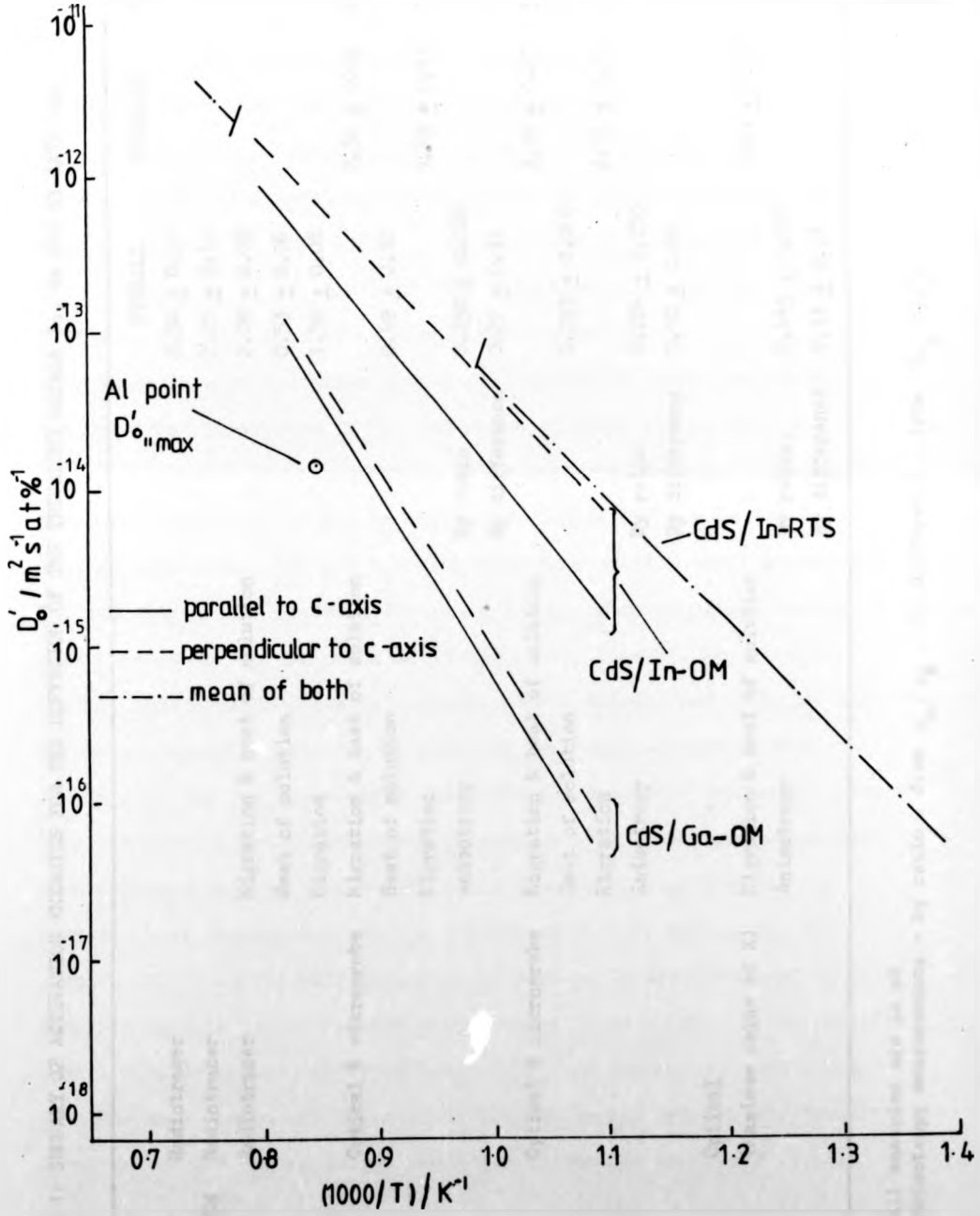

Fig 11.4

TABLE 11.1: SUMMARY OF ACTIVATION ENERGIES FOR THE DIFFUSION OF THE TRIVALENT METALS In, Ga AND Al INTO CdS

				OVERALL	PARALLEL	PERPENDICULAR
CdS/Cd*	Radiotracer			2.30 ± 0.20		
CdS/In*Cd	Radiotracer			2.27 ± 0.12		
CdS/In*	Radiotracer	Migration & heat of solution		2.09 ± 0.08		
		Heat of solution		0.53 ± 0.06		
		Migration		1.54 ± 0.08		
CdS/In	Optical & microprobe	Migration & heat of solution			2.30 ± 0.08	2.03 ± 0.08
		Heat of solution		0.49 ± 0.10		
		Migration			1.80 ± 0.11	1.54 ± 0.11
		Anisotropy	By ratio	0.250 ± 0.008		
			By difference	0.27 ± 0.11		
CdS/Ga	Optical & microprobe	Migration & heat of solution			3.10 ± 0.07	3.00 ± 0.06
		Heat of solution		0.753 ± 0.060		
		Migration			2.35 ± 0.12	2.25 ± 0.10
		Anisotropy	By ratio	0.204 ± 0.053		
			By difference	0.10 ± 0.09		
CdS/Al	Optical					
	(Maximum value of X)	Migration & heat of solution			2.99 ± 0.09	2.86 ± 0.16
		Anisotropy	By ratio	0.445 ± 0.069		
			By difference	0.13 ± 0.18		

All energies are in eV
Anisotropy measurements - by ratio : from $X_{\perp} / X_{\parallel}$, by difference : from $(E_{t_{\parallel}} - E_{t_{\perp}})$

The characteristics of the diffusion were different, being concentration independent and there was no sharply defined diffusion front. The C_o values were low, there was no observable diffusion anisotropy and the diffusion parameters were comparable with those obtained for the self-diffusion of Cd into CdS. The results are included in the graphs and tables given in this chapter. In this case the In is probably incorporated in the Cd sub-lattice as $In^{\bullet}_{Cd}$, but the Cd vacancies are uncharged. Thus the bonding of $In^{\bullet}_{Cd}$ with V^{*}_{Cd} is very weak in contrast to the strong $V^{''}_{Cd}$ to $In^{\bullet}_{Cd}$ interaction, so that pair formation is negligible and diffusion is essentially by a simple vacancy mechanism.

There is only a limited amount of quantitative data available in the published literature on the diffusion of group III metals into II - VI compounds and consequently it is difficult to make comparisons. The defect structure of CdS is extremely complex (7) and it has been studied extensively (8, 9), but some questions still remain unanswered. The majority of the measurements which are reported by other workers were carried out in the presence of the group II metal, where concentration independent diffusion profiles were obtained, and they are not directly comparable with the majority of the results given in this thesis. In the few cases where concentration dependent diffusions have been reported, there is no simple dependency similar to that which has been obtained in this thesis. There is some overlap on the Cd-In-S ternary phase diagram between the conditions used by Kröger and co-workers (8, 9) on the self-diffusion of Cd into In-doped CdS and those reported in this thesis for the diffusion of In into CdS. It is possible that a similar defect, which is $(In^{\bullet}_{Cd}\ V^{''}_{Cd})'$, was present in both cases.

The main reason why there is little similarity between the results obtained for the concentration dependent diffusions described in this

thesis, where $D \propto C$, and the results reported by other workers on the concentration dependent diffusion of group III metals into the chalcogenides of Zn and Cd (3, 10) can possibly be explained by the fact that much higher values of C_o and dC/dx were obtained in the work described in this thesis. In the case of the concentration independent measurements described in section 5.4 very much lower values of C_o and dC/dx were obtained. Concentration independent diffusion profiles have been obtained by other workers (11, 12) who have reported on the diffusion of In into other Cd and Zn chalcogenides. A similar analogy can be made for the diffusion of the group III metals Cr, Sc and Al into NiO and MgO which have been mentioned in several chapters in this thesis. In the case of the results reported by Perkins and Rapp (5), Greskovich (4) and Minford and Stubican (6), in which concentration dependent diffusion profiles were obtained with $D \propto C$, high values of C_o and dC/dx were obtained. This contrasts with the results obtained by Chen et al (13) and Weber et al (14) who obtained concentration independent profiles using low values of C_o and dC/dx.

Further measurements on the diffusion of trivalent metals into II - VI compounds, particularly at low partial pressure due to the group II metal, need to be carried out. In particular there is still a lot of work which could be carried out to establish with certainty the defect mechanism involved in the diffusion of In into CdS over the whole range of M^{3+} concentrations. Measurements of the diffusion coefficient and the electrical conductivity as a function of the Cd and In partial pressures are required. Isoconcentration diffusion studies should also be carried out. Tl should be included with the other trivalent metals which have already been used in this thesis. In fact a small number of diffusion anneals were carried out at the

beginning of the project using CdS and Tl, but it was not possible to observe the diffusion interface optically. In addition, the measurements described in this thesis should be repeated using another chalcogenide of Zn or Cd in place of CdS to investigate if similar diffusion characteristics are obtained.

It is hoped in the near future to carry out a further analysis on the diffusion profiles to evaluate the binding energy of the double and triple defects $(M^{\bullet}_{Cd}\ V^{''}_{Cd})'$ and $(M^{\bullet}_{Cd}\ V^{''}_{Cd}\ M^{\bullet}_{Cd})^{*}$ which form when the trivalent metals In, Ga and Al are diffused into CdS in the presence of excess trivalent metal. A method of analysis, similar to the one described by Perkins and Rapp (5), will be used.

The main conclusions that can be drawn from the work described in this thesis are:

(a) The optical technique, which has been developed, has been shown to give accurate diffusion measurements in conditions where a sharply defined diffusion front occurs, and these are achieved with much less effort than is required by other techniques.

(b) High accuracy for the measurement of the diffusion anisotropy is possible as the diffusion in two or three perpendicular directions can be measured on the same specimen.

(c) The concentration profiles obtained using the RTS technique and the microprobe show that $D \propto C$ when an excess of trivalent metal is placed in the ampoule with the CdS slice.

11.1. References

1. C. WAGNER, J. Chem. Phys., 18, P1227 (1950).

2. L. R. WEISBERG and J. BLANC, Phys. Rev., 131, 4, P1548 (1963).

3. S. S. CHERN and F. A. KRÖGER, Phys. Stat. Sol. (a), 25, P215 (1974).

4. C. GRESKOVICH, J. Amer. Cer. Soc., 53, P498 (1970).

5. R. A. PERKINS and R. A. RAPP, Metal. Trans., 196, 4, P193 (1973).

6. W. J. MINFORD and V. S. STUBICAN, J. Amer. Cer. Soc., 57, 8, P363 (1974).

7. F. A. KRÖGER, Annual Review of Materials Science (Edited by R. A. HUGGINS), Annual Reviews Inc., Palo Alto, California, U.S.A. (1977).

8. V. KUMAR and F. A. KRÖGER, J. Solid State Chem., 3, P387 (1971).

9. C. H. HERSHMAN, V. P. ZLOMANOV and F. A. KRÖGER, J. Solid State Chem., 3, P401 (1971).

10. H. BJERKELAND and I. HOLWECH, Phys. Norv., 6, P139 (1972).

11. H. YOKOZAWA, H. KATO and S. TAKAYANAGI, Denki. Kagaku., 36, 4, P282 (1968).

12. F. KOSHIGA and T. SUGANO, Shinku., 16, 5, P174 (1973).

13. W. K. CHEN, N. L. PETERSON and L. C. ROBINSON, J. Phys. Chem. Solids, 34, P705 (1973).

14. G. W. WEBER, W. R. BITLER and V. S. STUBICAN, J. Amer. Cer. Soc., 60, P61 (1977).

APPENDICES

A1. Self-diffusion of Cd into CdS

In this appendix the results of the measurements on the self-diffusion of Cd into CdS, which are reported in the author's M.Sc. thesis (1) and in a paper, that was published in the Journal of the Physics and Chemistry of Solids (2), are described briefly. A RTS technique was used.

Since the completion of the two publications mentioned above, further experimental work has been carried out on the measurement of the radioactive decay of the two sources, which were made up using some of the Cd from consignments 1 and 2 of radioactive Cd metal that were purchased for the Isotope Production Unit at Harwell. In addition, further work was carried out on the measurement of the purity of the second consignment of radioactive Cd metal using gamma ray analysis. This was an attempt to establish if the diffusion process, which was faster than the bulk diffusion, was due to either another diffusion mechanism involving Cd, or to Ag which was present as an impurity in the samples of radioactive Cd. In the majority of the diffusion anneals carried out on the measurement of the self-diffusion of Cd into CdS, radioactive Cd from the second of the three consignments that were purchased was used. This included CdS slices numbers 5 and 6. The results of this more recent work are described in this appendix.

A1.1 Discussion of the experimental measurements

Diffusion measurements, which covered the temperature range 875 K to 1528 K, were carried out in excess Cd metal and as can be

seen from figure A1.1, the profiles gave reasonable 'erfc' fits. The experimental details are described in the authors M.Sc. thesis.

The variation of the diffusion coefficient with temperature, for the CdS obtained from The General Electric Company Limited, is shown as an Arrhenius plot in figure A1.2, and the best fit through the experimental points is given by

$$D^{*}_{Cd} = \left(1.2^{+3.6}_{-0.4}\right) \times 10^{-4}\left(m^2 s^{-1}\right) \exp\left[\frac{-(2.30 \pm 0.20)\ eV}{kT}\right] \qquad A1.1$$

This can be interpreted in terms of an activation energy of (2.3 ± 0.2) eV. Additional measurements were also carried out using ultra high purity material from Eagle Picher Industries Incorporated and from The Post Office Research Laboratories, and these results are shown in figure A1.3 along with all the other measurements for the self-diffusion of Cd into CdS which were readily available. The key for the experimental data presented in figure A1.3 is given in table A1.1. Accurate results due to Woodbury (3), Pugh (4), Lally (5) and Sysoev et al (6) were available, whereas for Kumar and Krüger (7) and Shaw and Whelan (8) the results given were interpolated from published data. Where diffusion measurements were taken over a range of temperatures, this range is indicated by the extent of the lines on the graphs.

The experimental conditions used by the author are similar to those used by Woodbury. The results reported by the latter for the self-diffusion of Cd, as a function of temperature, are for Cd saturated vapour pressure; the results reported here by the author are for Cd saturated vapour pressure up to 1280 K and, above this temperature, sufficient radioactive Cd was placed in the ampoule to give an excess of Cd. The experimental conditions used by Kumar and Krüger, and Shaw and Whelan were different; the results for the self-diffusion of Cd were reported as a function of Cd

A TYPICAL DIFFUSION PROFILE FOR THE SELF-DIFFUSION OF Cd INTO CdS.

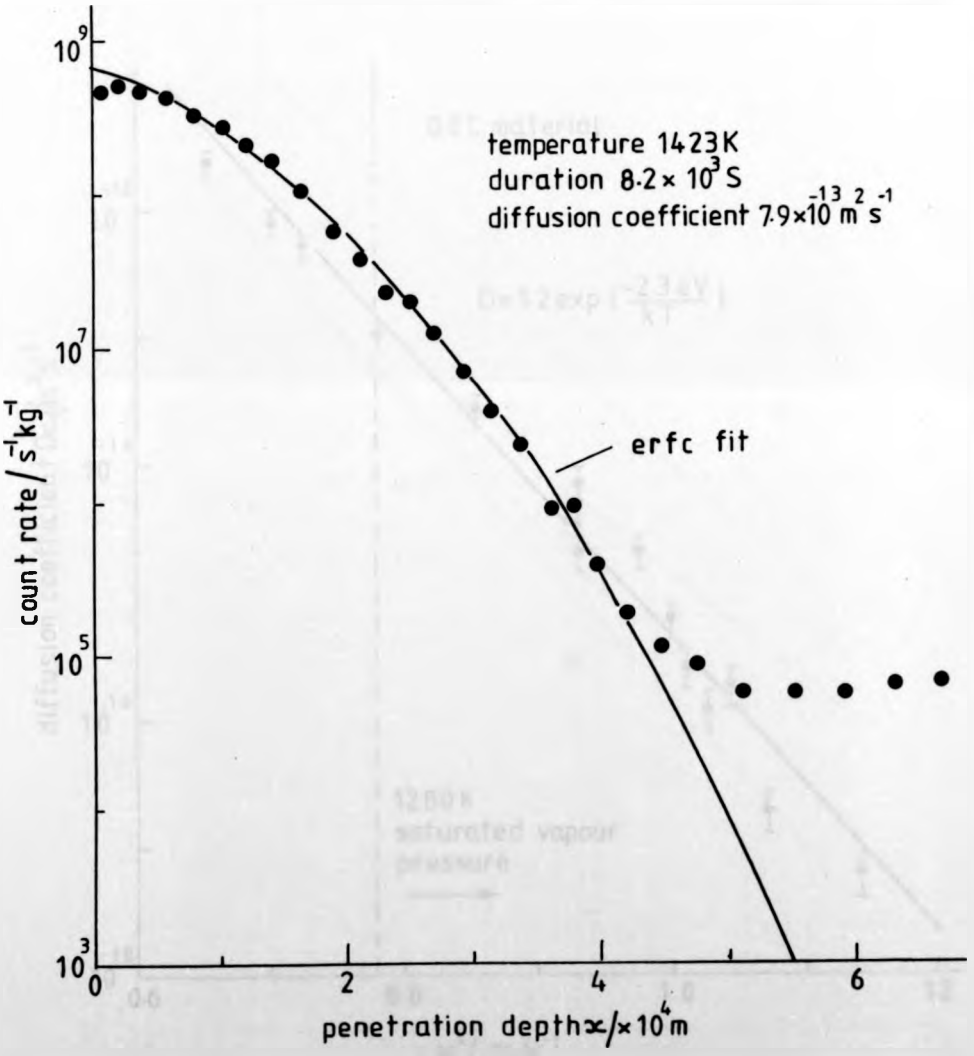

Fig A1.1

AN ARRHENIUS PLOT FOR THE SELF-DIFFUSION OF Cd INTO CdS IN EXCESS Cd VAPOUR.

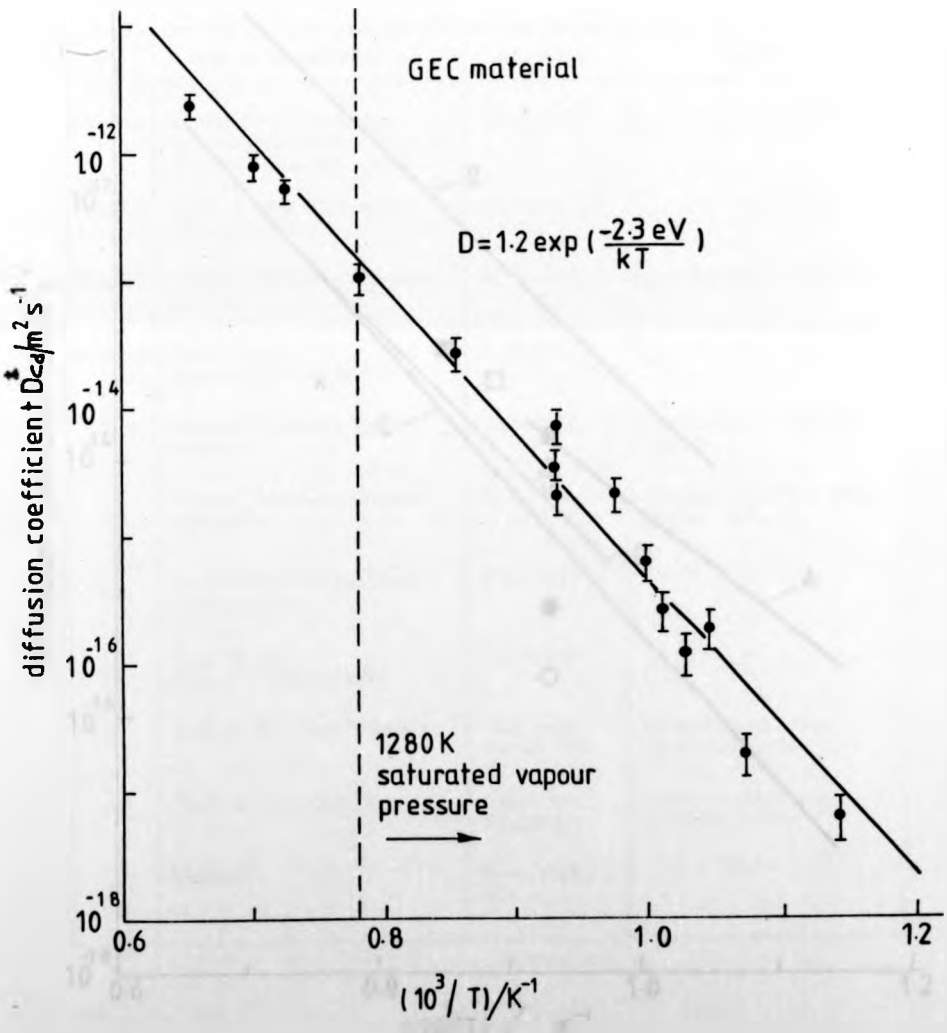

Fig A1·2

COMPILATION OF RESULTS FOR THE SELF-DIFFUSION OF Cd INTO CdS, KEY GIVEN IN TABLE A1.1

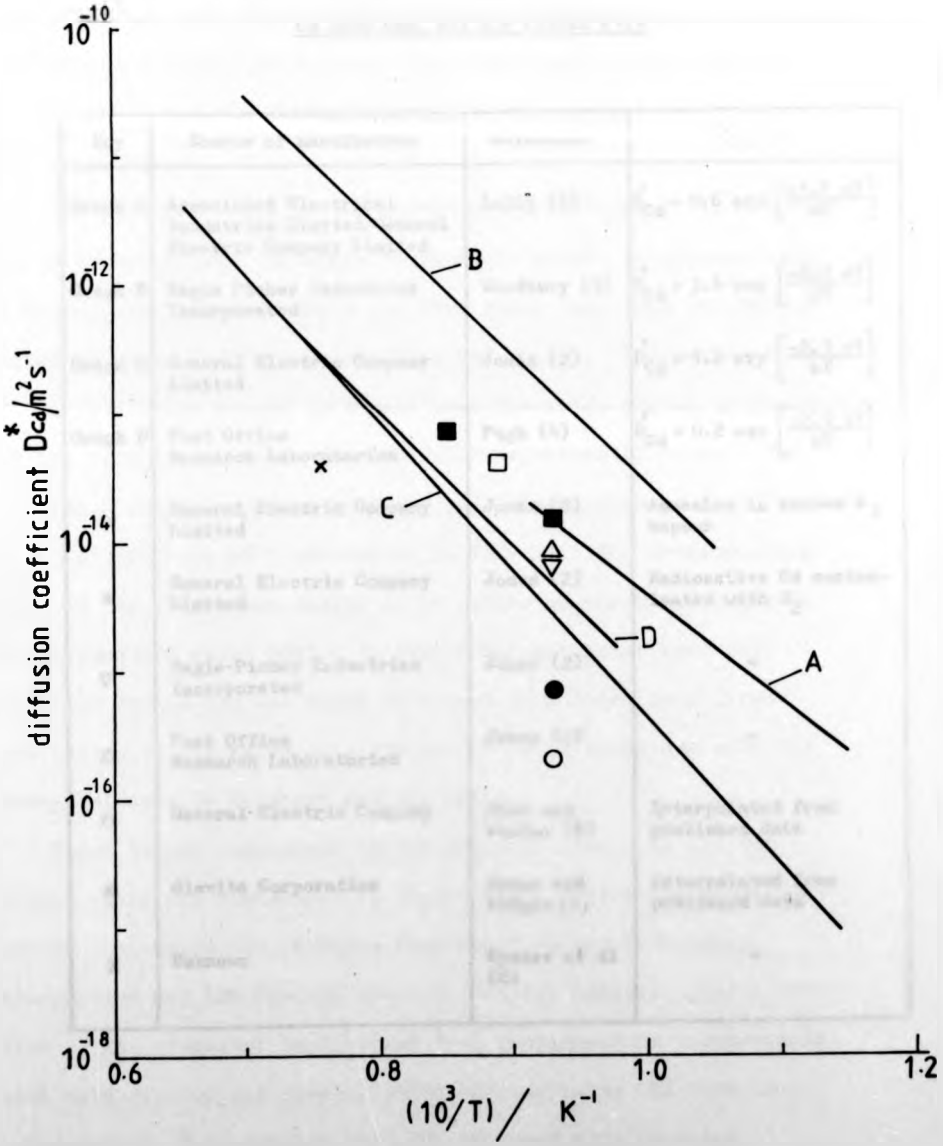

Fig A1.3

TABLE A1.1 COMPILATION OF THE RESULTS FOR THE SELF-DIFFUSION OF Cd INTO CdS. KEY FOR FIGURE A1.3

Key	Source of manufacture	Reference	Comment
Graph A	Associated Electrical Industries Limited/General Electric Company Limited	Lally (5)	$D^{\bullet}_{Cd} = 0.6 \exp\left[\frac{-1.6\ eV}{kT}\right]$
Graph B	Eagle Picher Industries Incorporated	Woodbury (3)	$D^{\bullet}_{Cd} = 3.4 \exp\left[\frac{-2.0\ eV}{kT}\right]$
Graph C	General Electric Company Limited	Jones (2)	$D^{\bullet}_{Cd} = 1.2 \exp\left[\frac{-2.3\ eV}{kT}\right]$
Graph D	Post Office Research Laboratories	Pugh (4)	$D^{\bullet}_{Cd} = 0.2 \exp\left[\frac{-2.0\ eV}{kT}\right]$
○	General Electric Company Limited	Jones (2)	Annealed in excess S_2 vapour
●	General Electric Company Limited	Jones (2)	Radioactive Cd contaminated with O_2
▽	Eagle-Picher Industries Incorporated	Jones (2)	-
△	Post Office Research Laboratories	Jones (2)	-
□	General Electric Company	Shaw and Whelan (8)	Interpolated from published data
■	Clevite Corporation	Kumar and Kröger (7)	Interpolated from published data
×	Unknown	Sysoev et al (6)	-

vapour pressure which was obtained by varying the proportions of elemental S and Cd placed in the ampoule. In addition, the runs were done at constant temperatures of 1073 K for Kumar and Krüger and 1123 K for Shaw and Whelan. The results obtained by Sysoev et al (6) were obtained using CdS crystals, that were melt grown under an inert gas pressure, and the diffusion anneals were carried out at a pressure of 3 atmospheres.

The measured value of the diffusion coefficient at Cd saturated vapour pressure, over the whole temperature range, is approximately 30 times less than Woodbury's and five times less than the values quoted by Kumar and Krüger and Shaw and Whelan. The measured value of the activation energy is higher than the value quoted by Woodbury but the values are within the limits of experimental error. The activation energy reported by Kumar and Krüger, which is at a constant Cd vapour pressure of 1 atmosphere, is 1.26 eV. The corresponding value of the activation energy at Cd saturated vapour pressure in the temperature range 1073 K to 1173 K was estimated from the published curves and was found to be 1.8 eV. There is a large uncertainty in the value of $\pm$ 25% but it is in agreement with the values reported by Woodbury and the author.

There is one consistent factor which is common to all the results which are summarised in figure A1.3. Diffusion measurements carried out, using CdS obtained from Eagle Picher Industries Incorporated and The General Electric Company Limited, give a lower value of the diffusion coefficient than corresponding measurements which were carried out several years earlier using CdS from the same sources. This implies that CdS produced more recently possesses slightly different properties from the CdS produced earlier, which is possibly due to a change in the defect structure

or the purity.

Additional anneals were carried out at 1073 K to determine how certain parameters affected the diffusion coefficient. These results are summarised below:

(a) Anneals were carried out in the presence of excess S_2 vapour where the masses of the elemental S and Cd added to the ampoule were such that the concentration of S_2 molecules exceeded the concentration of Cd atoms by a factor of 2.2. The values of the diffusion coefficient obtained were a decade lower than for the diffusion anneals carried out at the same temperature in the presence of radioactive Cd vapour only, where the pressure in the ampoule equalled the saturated vapour pressure.

(b) Anneals carried out accidentally in the presence of O_2 also gave values of the diffusion coefficient which were a decade lower than anneals carried out in the presence of radioactive Cd vapour only.

(c) Pre-annealing a CdS crystal in an atmosphere of inactive Cd vapour for 41 h did not affect the diffusion coefficient.

(d) The measurement of a diffusion profile in a CdS slice, that possessed a naturally grown facet, gave a value of the diffusion coefficient which was 30% lower than the result obtained from a slice which was prepared for a diffusion anneal by mechanical polishing. This difference was equal to the standard error on the diffusion coefficients. This implied that any stresses or imperfections, that may have been set up in the diffusion surface in the pre-anneal preparation of the CdS slice, diffused out early during the anneal.

(e) CdS possesses a hexagonal structure of the wurtzite arrangement but diffusion measurements into CdS slices, which were cut such

that the diffusion direction was either parallel or perpendicular to the c-axis, showed no significant difference.

A1.2. Gamma-ray spectra of the radioactive Cd

This section deals with the measurements of the gamma-ray spectra emitted by two CdS slices which had been used in the measurement of the self-diffusion profiles. This is a continuation of the measurements, which were obtained using a piece of Cd metal from consignment 2, and is described in the author's M.Sc. thesis. The aim of the more recent measurements was to determine what the fast diffusing constant background, which was obtained in the measurement of the diffusion profiles, was due to. It is due to either the radioactive Cd itself, or possibly the radioactive Ag which was present as an impurity in the radioactive Cd metal. The noble metals Cu, Ag and Au diffuse much faster into CdS than Cd (9, 10).

Radioactive Cd metal contains three long lived radioisotopes, which are:

(a) $^{115m}_{48}Cd(T_{\frac{1}{2}} = 43\ d)$;

(b) $^{109}_{48}Cd(T_{\frac{1}{2}} = 1.3\ yr)$;

(c) $^{113m}_{48}Cd(T_{\frac{1}{2}} = 14\ yr)$;

The initial gamma-ray spectrum measurement, was made on a small piece of Cd metal from the second consignment 377 d after the end of the neutron exposure in order to determine if there were any radioactive impurities present. By this time the sample had started to depart from the 43 d half-life due to the $^{115m}_{48}Cd$, which is the radioisotope in the Cd metal with the predominant activity at the end of the neutron exposure.

The gamma energies that were observed are:

(a) 0.088 MeV due to $^{109}_{48}Cd$ ($T_{\frac{1}{2}}$ = 1.3 yr) which gave the greatest intensity;

(b) twelve gamma energies due to $^{110m}_{47}Ag$ ($T_{\frac{1}{2}}$ = 253 d) which was probably formed due to the presence of Ag as an impurity in the Cd metal;

(c) 0.935 MeV and 1.29 MeV due to $^{115m}_{48}Cd$ ($T_{\frac{1}{2}}$ = 43 d) ;

(d) five gamma peaks of low intensity.

The impurity concentration of the Ag in the Cd metal was calculated to be 50 parts per million by weight and the contribution to the total count rate, due to the $^{110m}_{47}Ag$, at the time when the diffusion profiles were measured was less than 1%.

After the self-diffusion measurements had been completed, two of the CdS slices (numbers 5 and 6), which had been used in the diffusion measurements, were sent to the Analytical Research and Development Unit at Harwell so that the gamma ray spectra emitted by these two slices could be measured. It was mentioned in the introduction that both of these CdS slices underwent diffusion anneals using radioactive Cd from the second consignment. Slice 6 was not given any preparation before it was despatched to Harwell for analysis; it still possessed the bulk diffusion into its reverse side. In the case of slice 5, the centre region only was sent. The outer surfaces were removed completely by lapping the surfaces with emery paper until the only activity that remained on the slice was due to the fast diffusion process.

The gamma-ray spectra were measured with a Quartz-Silica 50×10^{-6} m^3 CV-2556 Ge(Li) semiconductor detector and CL-212

preamplifier which were coupled to an AERE-2151 amplifier and an AERE-2110 analogue-digital converter. The sorted pulses were stored in the memory of a Honeywell DDP-516 computer which was programmed to act as a multichannel analyser in a multi-access mode. The data was then put onto a magnetic tape and transmitted on a fast data-link to a central IBM 370/75 computer, where final printing took place. The samples were measured at a nominal distance of 7.5 mm from the detector. The energy calibration of the analyser was obtained using $^{137}_{55}Cs$ ($T_{\frac{1}{2}}$ = 30.0 yr) and $^{60}_{27}Co$ ($T_{\frac{1}{2}}$ = 5.26 yr) sources and the energy calibration of the multi-channel analyser was 0.91 keV per channel.

These spectrum measurements were carried out approximately 1325 d after the radioactive Cd metal had been removed from the nuclear reactor. This period was sufficiently long for the activity due to $^{115m}_{48}Cd$ ($T_{\frac{1}{2}}$ = 43 d) to have decayed away completely and there was no evidence of any activity due to this isotope having been detected. The activity on both slices was very low and in particular the activity from slice 5 was only just greater than that due to natural background. The observations that were made are summarised in table A1.2 and the conclusion drawn from these measurements is outlined below.

As can be seen from the results of slice 6, some of the Ag, which was present as an impurity in the radioactive Cd metal, had diffused into the outer regions of the slice. The activity from the radioactive Cd, which was detected, was due to the long lived radioisotopes $^{109}_{48}Cd$ ($T_{\frac{1}{2}}$ = 1.3 yr) and $^{113m}_{48}Cd$ ($T_{\frac{1}{2}}$ = 14 yr). It can be seen from the results for slice 5 that the constant background in the diffusion profile is possibly due, in part, to

preamplifier which were coupled to an AERE-2151 amplifier and an AERE-2110 analogue-digital converter. The sorted pulses were stored in the memory of a Honeywell DDP-516 computer which was programmed to act as a multichannel analyser in a multi-access mode. The data was then put onto a magnetic tape and transmitted on a fast data-link to a central IBM 370/75 computer, where final printing took place. The samples were measured at a nominal distance of 7.5 mm from the detector. The energy calibration of the analyser was obtained using $^{137}_{55}Cs$ ($T_{\frac{1}{2}}$ = 30.0 yr) and $^{60}_{27}Co$ ($T_{\frac{1}{2}}$ = 5.26 yr) sources and the energy calibration of the multi-channel analyser was 0.91 keV per channel.

These spectrum measurements were carried out approximately 1325 d after the radioactive Cd metal had been removed from the nuclear reactor. This period was sufficiently long for the activity due to $^{115m}_{48}Cd$ ($T_{\frac{1}{2}}$ = 43 d) to have decayed away completely and there was no evidence of any activity due to this isotope having been detected. The activity on both slices was very low and in particular the activity from slice 5 was only just greater than that due to natural background. The observations that were made are summarised in table A1.2 and the conclusion drawn from these measurements is outlined below.

As can be seen from the results of slice 6, some of the Ag, which was present as an impurity in the radioactive Cd metal, had diffused into the outer regions of the slice. The activity from the radioactive Cd, which was detected, was due to the long lived radioisotopes $^{109}_{48}Cd$ ($T_{\frac{1}{2}}$ = 1.3 yr) and $^{113m}_{48}Cd$ ($T_{\frac{1}{2}}$ = 14 yr). It can be seen from the results for slice 5 that the constant background in the diffusion profile is possibly due, in part, to

TABLE A1.2 A SUMMARY OF THE OBSERVATIONS OBTAINED FROM THE GAMMA RAY SPECTRA OF CdS SLICE NUMBERS 5 AND 6

Slice Number	Experimental observation of gamma energies	Deduction
6	0.0877 MeV present	$^{109}_{48}Cd$ ($T_{\frac{1}{2}}$ = 1.3 yr) present
Same physical state as at end of measurement of profile	0.27 MeV present	$^{113m}_{48}Cd$ ($T_{\frac{1}{2}}$ = 14 yr) present
	0.656 and 0.888 MeV present	$^{110m}_{47}Ag$ ($T_{\frac{1}{2}}$ = 253 d) present, predominant peak in decay scheme
5	0.088 MeV present	$^{109}_{48}Cd$ ($T_{\frac{1}{2}}$ = 1.3 yr) present
All outer surfaces removed	0.27 MeV absent	$^{113m}_{48}Cd$ ($T_{\frac{1}{2}}$ = 14 yr) absent
	0.656 and 0.888 MeV possibly present	$^{110m}_{47}Ag$ ($T_{\frac{1}{2}}$ = 253 d) possibly present

radioactive Ag, but the activity of slice 5 was so low that it was not possible to identify, with any degree of certainty, all the peaks due to $^{110m}_{47}Ag$ ($T_{\frac{1}{2}}$ = 253 d). It is also possible to say, with a fair degree of certainty, that some Cd did diffuse into the centre of the crystal as $^{109}_{48}Cd$ ($T_{\frac{1}{2}}$ = 1.3 yr) was identified.

It was not possible to identify any of the five impurity peaks of low intensity which had been observed in the gamma spectrum of the radioactive Cd metal.

A1.3 Half-life of the radioactive Cd

Two radioactive sources were made up from consignments 1 and 2 of radioactive Cd metal, which were purchased from The Isotope Production Unit, Harwell. Details of the neutron irradiation, the method used for producing the sources and the discussion of the decay curve obtained during the first two years, after the neutron irradiation, are discussed in the author's M.Sc. thesis (1).

The half-lives of these two sources have been checked periodically for over seven years using a low background counter. The stability of the counter was checked throughout using a natural uranium standard which gave approximately 11 x 10^3 counts in 300 s.

Both Cd sources decayed with a half-life of 43 d (due to $^{115m}_{48}Cd$) initially, but the half-lives of both sources 1 and 2 started to depart from this value after periods of 244 d and 143 d respectively after the radioactive Cd metal was removed from the reactor. This is because the contribution to the count rate, due to the long lived Cd isotopes $^{109}_{48}Cd$ ($T_{\frac{1}{2}}$ = 453 d) and $^{113m}_{48}Cd$ ($T_{\frac{1}{2}}$ = 14 yr), started to increase relative to that due to the short lived isotope $^{115m}_{48}Cd$ ($T_{\frac{1}{2}}$ = 43 d). As the time from the end of the

neutron exposure increases the half-lives of the decay curves should approach that due to the longest lived Cd isotope. The last counts, which were made on these sources, were between 20 and 30 times the natural background which was 0.07 counts per second. From the decay curves shown in figure A1.4, it can be seen that the two sources have been decaying with a constant half-life for the five years preceding the last counts, which were taken at the beginning of 1976. The measured half-lives over this period were 10.6 yr and 4.7 yr for Cd sources 1 and 2 respectively. The error on these measurements is $\pm$ 25%.

As can be seen from figure A1.4, the decay curves of the two sources are not identical. Two of the major differences are as follows: The first is that source 1 decayed by a factor of approximately 100 before it started to flatten out whereas source 2 only decayed by a factor of 50. The second is that the long lived activities are decaying with distinctly different half-lives.

It is difficult from the available information to ascribe a reason for the difference in the shapes of the two decay curves, but two possible reasons are:

(a) The effect of Ag which is present as an impurity in source 2.

(b) The relative intensities of the radiation, from the three Cd isotopes, are dependent on the duration of the neutron irradiation and on the energy spectrum of the neutron flux in which the samples were irradiated.

The duration of the neutron exposure for the two samples was similar and so this factor should not produce any variation in the decay curves. It is possible that the two samples were irradiated at different positions in the reactor, where the neutron flux spectrum

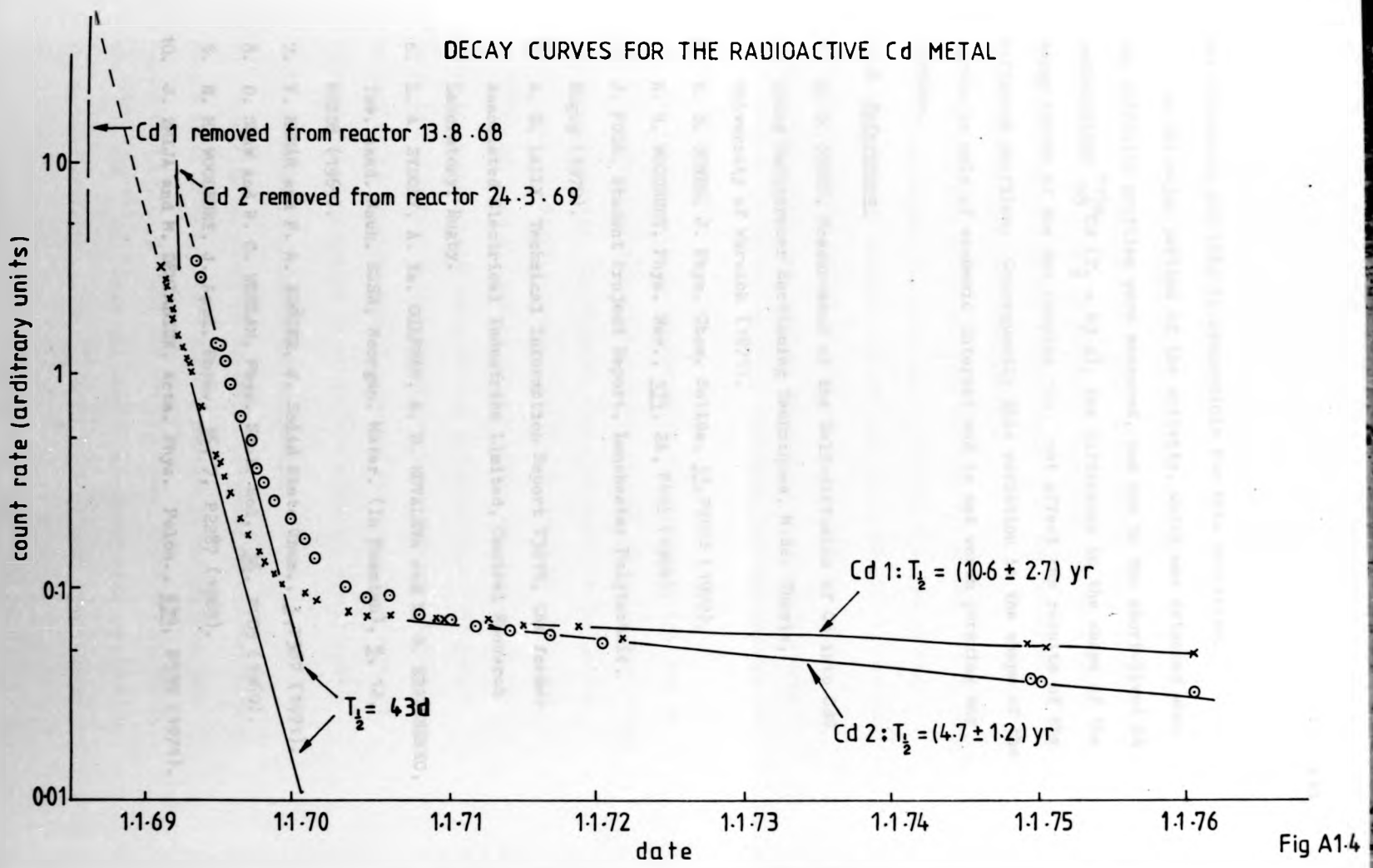
DECAY CURVES FOR THE RADIOACTIVE Cd METAL
Cd 1 removed from reactor 13·8·68
Cd 2 removed from reactor 24·3·69
count rate (arditrary units)
10
1
0·1
0·01
$T_{\frac{1}{2}}$ = 43d
Cd 1: $T_{\frac{1}{2}}$ = (10·6 ± 2·7) yr
Cd 2 : $T_{\frac{1}{2}}$ = (4·7 ± 1·2) yr
1·1·69
1·1·70
1·1·71
1·1·72
1·1·73
1·1·74
1·1·75
1·1·76
date

Fig A1.4

was different, and this is responsible for this variation.

As the major portion of the activity, which was detected when the diffusion profiles were measured, was due to the short-lived Cd radioisotope $^{115m}_{48}Cd$ ($T_{\frac{1}{2}}$ = 43 d), the difference in the shape of the decay curves of the two samples did not affect the results of the diffusion profiles. Consequently this variation in the shape of the curves is only of academic interest and is not worth pursuing any further.

A1.4 References

1. E. D. JONES, Measurement of the Self-diffusion of Cd into CdS using Radiotracer Sectioning Techniques, M.Sc. Thesis, University of Warwick (1971).
2. E. D. JONES, J. Phys. Chem. Solids, 33, P2063 (1972).
3. H. H. WOODBURY, Phys. Rev., 134, 2A, P492 (1964).
4. J. PUGH, Student Project Report, Lanchester Polytechnic, Rugby (1970).
5. A. E. LALLY, Technical Information Report T3215, the former Associated Electrical Industries Limited, Central Research Laboratory, Rugby.
6. L. A. SYSOEV, A. Ya. GILFMAN, A. D. KOVALEVA and N. G. KRAVCHENKO, Izv. Akad. Nauk. SSSR, Neorgan. Mater. (In Russian), 5, 12, P2208 (1969).
7. V. KUMAR and F. A. KRÖGER, J. Solid State Chem., 3, P387 (1971).
8. D. SHAW and R. C. WHELAN, Phys. Stat. Sol., 36, P705 (1969).
9. H. H. WOODBURY, J. Appl. Phys., 36, 7, P2287 (1965).
10. J. ZMIJA and M. DEMIANIUK, Acta. Phys. Polon., A39, P539 (1971).

A2. Measurements on Radioactive In

The aim of the measurements described in this appendix was to establish that the radiation, which was detected and measured in the measurement of the rate of diffusion of In into CdS using the RTS method, was emitted by the radioisotopes of In and not by any impurities that may have been present.

A radioactive source was made up from each of the five consignments of radioactive In, which were purchased from the Isotope Production Unit at Harwell, and the half-lives of all five sources were checked over a period of five years. In addition, four radioactive samples were sent to the Analytical and Development Unit at the Atomic Energy Research Establishment, Harwell for gamma-ray analysis.

The results of these measurements indicated that four out of the five consignments decayed with the correct half-life over three decades of activity. Consignment 2 decayed with a half-life of 47 d, which is slightly shorter than the expected half-life due to $^{114m}_{49}In$ ($T_{\frac{1}{2}}$ = 50 d), but it did not affect the results of the diffusion anneals which were carried out using this consignment. Small traces of long lived radioactive impurities were detected in some of the consignments of In metal, but again they were not of a sufficient intensity to affect the diffusion measurements.

A2.1. Nuclear properties of radioactive In

Naturally occurring In possesses two isotopes and when such a sample of In is placed in a nuclear reactor it can be seen from figure A2.1 (1, 2, 3) that the radioisotopes, which are produced, are $^{116}_{49}In$ and $^{114}_{49}In$. When the sample is removed from the reactor, the induced activity due to $^{116}_{49}In$ ($T_{\frac{1}{2}}$ = 54 m) will decay within

THE NUCLEAR PARAMETERS OF RADIOACTIVE In

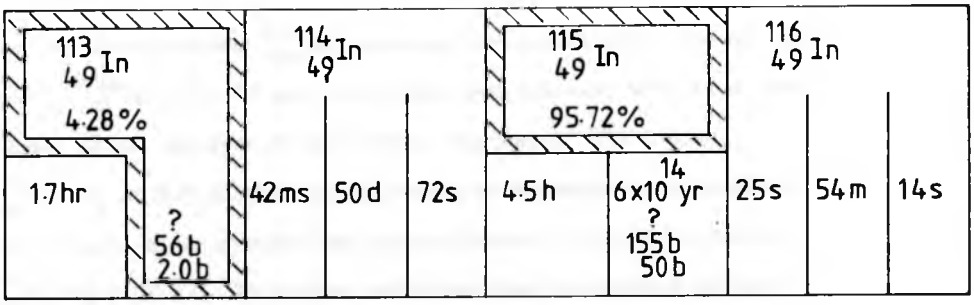

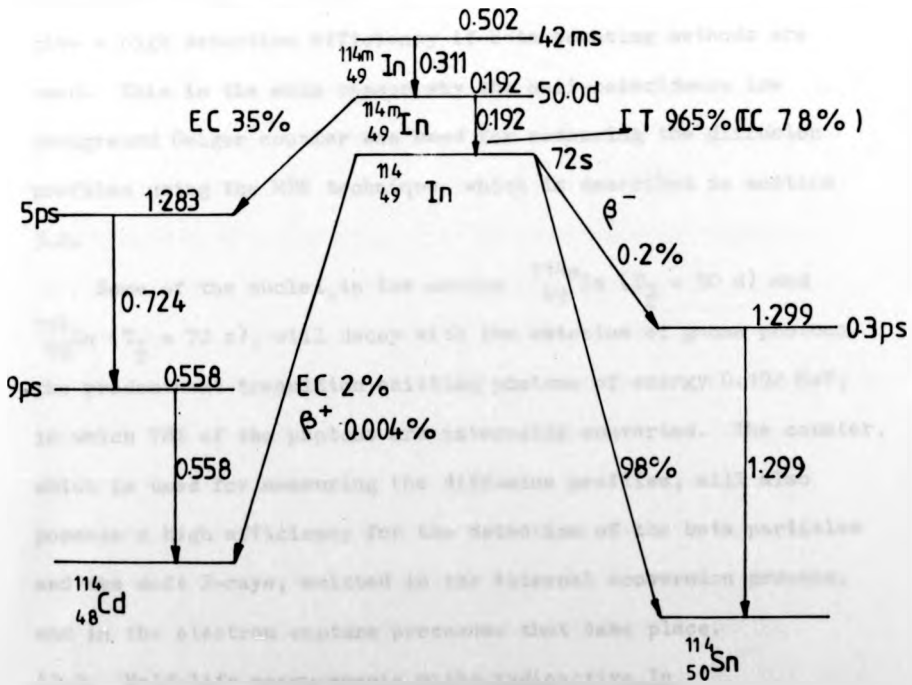

energies are in MeV

Fig A2.1

a few days, leaving that due to $^{114m}_{49}In$ ($T_{\frac{1}{2}}$ = 50.0 d).

The radioisotope $^{114}_{49}In$ possesses three nuclear states but the first, $^{114m}_{49}In$ ($T_{\frac{1}{2}}$ = 42 ms), will have decayed away within a few seconds after the end of the neutron exposure. The second, $^{114m}_{49}In$ ($T_{\frac{1}{2}}$ = 50.0 d), possesses such a relatively long half-life that it will also control the rate of decay of the third state, $^{114}_{49}In$ ($T_{\frac{1}{2}}$ = 72 s). It is the radiation that is emitted in the decay of the second and third radioisotopic states that is measured in the RTS technique.

As 98% of the disintegrations from $^{114}_{49}In$ ($T_{\frac{1}{2}}$ = 72 s) decay straight to the ground state of $^{114}_{50}Sn$ with the emission of beta particles only, the radiation emitted by the radioactive In will give a high detection efficiency if beta counting methods are used. This is the main reason why the anti-coincidence low background Geiger counter was used for measuring the diffusion profiles using the RTS technique which is described in section 3.2.

Some of the nuclei, in the states $^{114m}_{49}In$ ($T_{\frac{1}{2}}$ = 50 d) and $^{114}_{49}In$ ($T_{\frac{1}{2}}$ = 72 s), will decay with the emission of gamma photons, the predominent transition emitting photons of energy 0.192 MeV, in which 78% of the photons are internally converted. The counter, which is used for measuring the diffusion profiles, will also possess a high efficiency for the detection of the beta particles and the soft X-rays, emitted in the internal conversion process, and in the electron capture processes that take place.

A2.2. <u>Half-life measurements on the radioactive In</u>

When the five radioactive sources were made up, one from each consignment of In metal, they gave approximately 100 counts per second when measured on the low background Geiger counter. Their

half-life was checked over a long period of time and a reference source containing sufficient natural uranium salt to give approximately 38 counts per second was used to monitor the variation in the counter efficiency.

The results of the half-life measurements are shown in figure A2.2. The measurement of the activity of the sources was continued until the activity either decayed away to an undetectable level or it flattened out at some level slightly in excess of natural background. In fact, some measurements were still being taken when this thesis was being written.

It can be seen from the decay curves plotted in figure A2.2 that sources 1, 3, 4 and 5, which were made up from consignments bearing the same numbers, decayed with the expected half-life of 50.0 d over an activity range extending over 3 decades. The fifth source, number 2, decayed with a half-life that was somewhat shorter than the expected 50.0 d, due to $^{114m}_{49}In$, which was approximately 47 d extending over the same range of activity. The above observation implied that source 2 contained a radioactive impurity whose half-life was shorter than the expected one of 50.0 d and it would have contributed over 33% of the count rate when the consignment was delivered to Rugby from the Isotope Production Unit at Harwell. Radioactive In from the second consignment was used in all the diffusion anneals in the 109 series of measurements (sections 5.1 and 5.4), except for 109m, and at the time these diffusions were being carried out the impurity contributed 28% to the count rate of source 2. The half-life of this impurity was calculated to be longer than 40 d and it was not possible to identify it on half-life data alone.

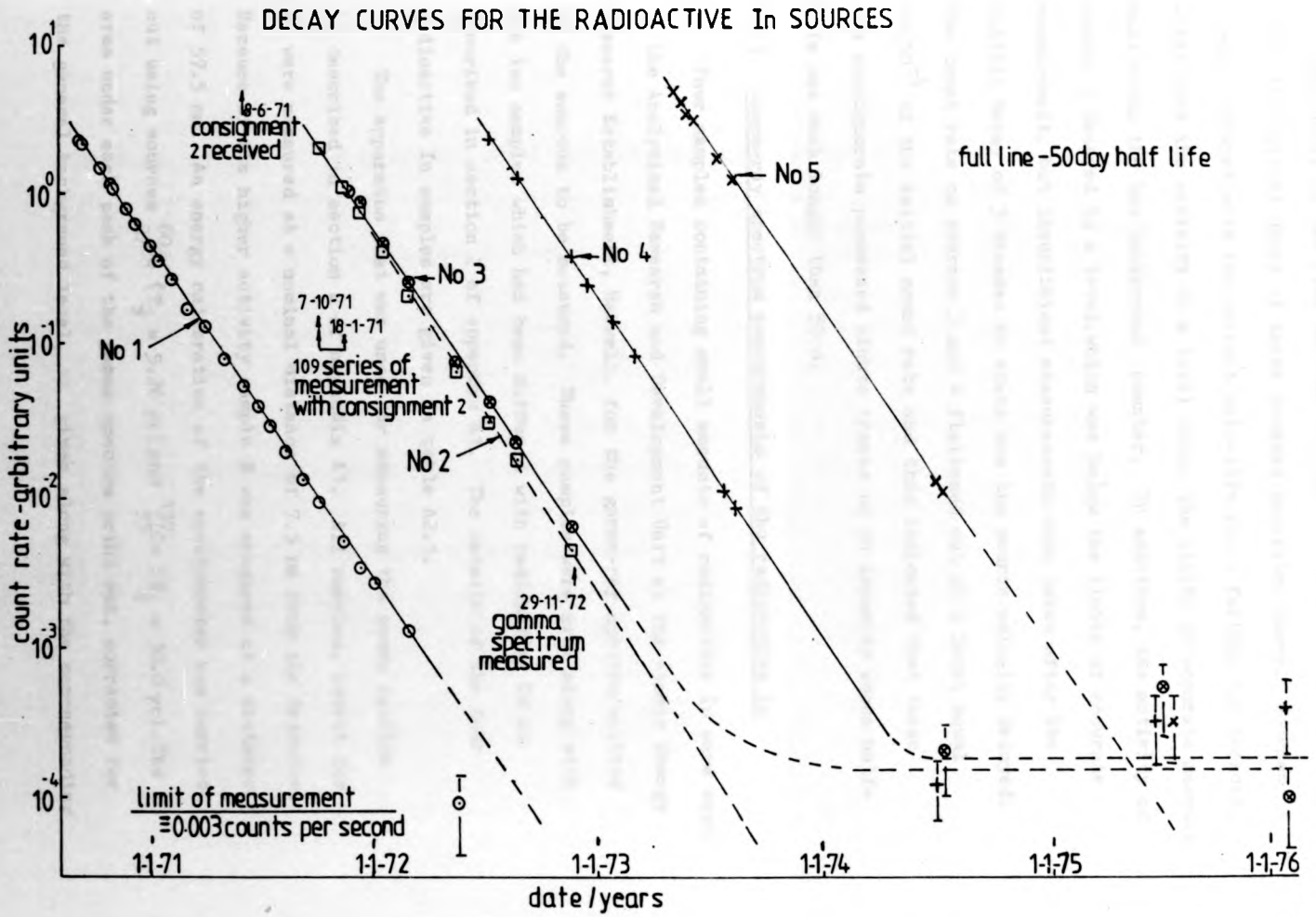
DECAY CURVES FOR THE RADIOACTIVE In SOURCES
full line - 50 day half life
count rate - arbitrary units
date / years
No 1
No 2
No 3
No 4
No 5
18-6-71
consignment
2 received
7-10-71
18-1-71
109 series of
measurement
with consignment 2
29-11-72
gamma
spectrum
measured
limit of measurement
≡ 0·003 counts per second
1-1-71
1-1-72
1-1-73
1-1-74
1-1-75
1-1-76

Fig A 2·2

The decay of the five sources did not follow any common pattern after the initial decay of three decades described above. Sources 1 and 5 decayed with the correct half-life for a further 1.5 decades, which took the activity to a level below the limits of accurate measurement using the low background counter. In addition, the activity of source 2 decayed to a level, which was below the limits of accurate measurement, but insufficient measurements were taken after the initial decay of 3 decades to state how the source actually decayed. The count rate on sources 3 and 4 flattened out at a level equal to 10^{-4} of the initial count rate and this indicated that these two consignments possessed minute traces of an impurity whose half-life was much longer than 50 d.

A2.3. Gamma-ray spectrum measurements of the radioactive In

Four samples containing small amounts of radioactive In were sent to the Analytical Research and Development Unit at the Atomic Energy Research Establishment, Harwell, for the gamma-ray spectra emitted by the sources to be measured. These samples were sent along with the two samples which had been diffused with radioactive Cd as described in section 2 of appendix A1. The details of the four radioactive In samples are given in table A2.1.

TA2.1

The apparatus that was used for measuring the gamma spectra is described in section 2 of appendix A1. All samples, except for B, were measured at a nominal distance of 7.5 mm from the detector. Because of its higher activity sample B was measured at a distance of 57.5 mm. An energy calibration of the spectrometer was carried out using sources $^{60}_{27}Co$ ($T_{\frac{1}{2}}$ = 5.26 yr) and $^{137}_{55}Cs$ ($T_{\frac{1}{2}}$ = 30.0 yr). The area under each peak of the gamma spectra print out, corrected for the general background level, is given along with the corresponding

TABLE A2.1. RADIOACTIVE In SOURCES WHICH WERE USED FOR GAMMA RAY ANALYSIS

Sample	Composition of sample	Approximate activity μCi	Time between removal from reactor and measurement of the gamma spectrum
A	Small piece of In metal from consignment 2	0.5	542 d
B	Small piece of In metal from consignment 4	5	179 d
C	CdS slice whose outer surface was doped with radioactive In. Diffusion details: Excess In metal only Run 121c 1271 K 3.00 h	0.5	179 d
D	CdS slice whose outer surface was doped with radioactive In and whose outer surfaces were removed. Diffusion details: Excess In metal only Run 121c 1271 K 3.00 h	0.001	179 d

channel number of the peaks in table A2.2. All four gamma photons, which are emitted in the decay of $^{114m}_{49}In$ ($T_{\frac{1}{2}}$ = 50.0 d) and $^{114}_{49}In$ ($T_{\frac{1}{2}}$ = 72 s) and are shown in figure A2.1, were identified in the spectra of samples A, B and C. In addition, the In X-rays whose energy is 0.024 MeV was also identified in all three samples. A gamma photon of low intensity was observed in all three samples at 1.283 MeV, but it could not be identified in the available references. It is possible that a small fraction of the nuclei in $^{114m}_{49}In$ ($T_{\frac{1}{2}}$ = 50.0 d), instead of decaying from the 1.283 MeV state in two stages as shown in figure A2.1, decays straight to the ground state with the emission of a single gamma photon of that energy.

The activity of sample D was so low that it was only possible to identify the 0.024 MeV X-rays and the 0.192 MeV gamma photons with any degree of certainty.

Three gamma photons, which were possibly due to the presence of impurities, were observed but their intensity was so low that their presence would not affect the measurement of the diffusion profiles in any way. Two of the gamma photons, which were due to $^{60}_{27}Co$ ($T_{\frac{1}{2}}$ = 5.24 y), were observed in sample A and the third, at 1.400 MeV, in sample B. The presence of $^{60}_{27}Co$ in sample A was not responsible for the departure from the expected half-life of 50 d in the decay of source 2 described in section 2 of this appendix.

The gamma ray intensities of each of the three samples A, B and C were normalised to that of the 0.724 MeV photon and it can be seen from table A2.2 that the normalised values at each energy agree to within the limits of experimental error. It was not possible to do this with sample D as its activity was so low and

TABLE A2.2. TABULATION OF THE GAMMA ENERGIES THAT WERE OBSERVED IN THE RADIOACTIVE In SAMPLES

Gamma energy MeV	Isotope	Sample A In metal consignment 2		Sample B In metal consignment 4		Sample C* CdS slice doped with In		Sample D* In doped slice, outer surfaces removed	
		Channel number	Peak intensity	Channel number	Peak intensity	Channel number	Peak intensity	Channel number	Peak intensity
0.024	In X-rays	20	18328 (5.861)	21	291053 (16.62)	20	35355 (9.832)	17	80
0.192	$^{114m}_{49}In$(50.0 d)	201	67442 (21.57)	200	378734 (21.63)	201	77020 (21.42)	201	123
0.558	$^{114m}_{49}In$(50.0 d)	601	4379 (1.368)	601	23670 (1.352)	602	5155 (1.434)	602	trace
0.724	$^{114m}_{49}In$(50.0 d)	783	3127 (1.000)	782	17512 (1.000)	783	3596 (1.000)	782	trace
1.178	$^{60}_{27}Co$(5.24 yr)	1272	57	-	-	-	-	-	-
1.283	$^{114m}_{49}In$(50.0 d) summation peak	1394	35 (0.0112)	1392	88 (0.0050)	1392	34 (0.0095)	-	-
1.299	$^{114}_{49}In$(72 s)	1412	81 (0.0259)	1410	456 (0.0260)	1412	89 (0.0248)	1412	trace
1.333	$^{60}_{27}Co$(5.24 yr)	1447	58	-	-	-	-	-	-
1.400	Unidentified	-	-	1518	trace	-	-	-	-

* Diffused in excess In metal only.

the X-rays were not included as their intensities could be affected by variations in sample and counter geometry.

The normalised areas under the photo-peaks were also compared with the relative intensities of the photon transitions which occur in the decay schemes of $^{114m}_{49}In$ ($T_{\frac{1}{2}}$ = 50.0 d) and $^{114}_{49}In$ ($T_{\frac{1}{2}}$ = 72 s) and are shown in figure A2.1. There was a correlation between the two sets of figures for each of samples A, B and C, but it was not possible to make an exact comparison as there was no information available on the energy variation of the efficiency of the detector that was used to measure the gamma spectra.

A2.4. Identification of the impurity in the radioactive In of consignment 2

An attempt was made using all the known available data to identify the radioactive impurity, which was present in the radioactive In in consignment 2.

From the half-life measurements on source 2, which are described in section 2 of this appendix, it was deduced that the half-life of the impurity was between 40 d and 50 d. In addition, as the half-life measurement was made using the low background counter the radioactive impurity must emit beta particles whose maximum energy is greater than 0.2 MeV. From the gamma spectra described in section 3 of this appendix, no impurities could be detected in sample A apart from small traces of $^{60}_{29}Co$ ($T_{\frac{1}{2}}$ = 5.24 yr) which were present in trace quantities. The activity of the In in consignment 2 had decayed by more than 3 decades between the time it was delivered to the polytechnic and when the gamma spectrum was measured. So, if the radioactive impurity did emit gamma rays, then it is possible that it had decayed to such a minute proportion by the time the

gamma spectrum was measured, that it was not possible to detect the impurity.

Radioactive In from this consignment was used in all the diffusion anneals of the 109 series, the only exception being 109m. As the results, which were obtained in these particular diffusion anneals, were consistent with all the other results, it must be concluded that this impurity did not diffuse into the CdS in significant amounts during the diffusion anneal.

An attempt was made to identify the radioactive impurity that was present in consignment 2. The radioisotopes (4) that emit beta particles and possess a half-life in the range 40 d to 50 d can be reduced to a possible list of five:

(a) $^{59}_{26}Fe(T_{\frac{1}{2}} = 45\ d)$

(b) $^{103}_{44}Ru(T_{\frac{1}{2}} = 39.6\ d)$

(c) $^{115m}_{49}Cd(T_{\frac{1}{2}} = 43\ d)$

(d) $^{203}_{80}Hg(T_{\frac{1}{2}} = 46.9\ d)$

(e) $^{181}_{72}Hf(T_{\frac{1}{2}} = 42.5\ d)$

The In used in this project was supplied in a spectrographically pure form by Johnson, Matthey and Company Limited. A report on the spectrographic examination carried out by the manufacturers, indicated that Fe was the impurity that was present with the highest concentration, which was three parts per million. It was concluded that Fe would have to be present in the In in much higher concentrations than this if the radiation, emitted by the impurity, was due to the isotope of Fe- $^{59}_{26}Fe(T_{\frac{1}{2}} = 45\ d)$, which would have been formed by the reaction $^{58}_{26}Fe(n, \gamma)$. In addition, the percentage abundance of this isotope

in naturally occurring Fe and the cross section for the reaction are both so low that it rules out this possibility.

It is possible to conclude this appendix by stating that it was not possible to identify the radioactive impurity in consignment 2 with any degree of certainty. The presence of the element has not affected the diffusion anneals which were carried out using In from this consignment.

A2.5. References

1. C. M. LEDERER, J. M. HOLLANDER and I. PERLMAN, Table of Isotopes, John Wiley and Sons Incorporated, New York (1968).
2. Institute of Radiochemistry, Nuclear Research Centre, Karlsruhe, Chart of Nuclides, Esso Petroleum Company Limited, London (1963).
3. The Radiochemical Manual (Edited by B. J. Wilson), The Radiochemical Centre, Amersham (1966).
4. D. N. SLATER, Gamma-Rays of Radionuclides in Order of Increasing Energy, Butterworth and Company (Publishers) Limited, London (1962).

A3. X-ray powder diffraction investigations

The experimental data which is presented in this section has been supplied by the author's project supervisor, who carried out the X-ray powder diffraction investigations at the School of Physics at the University of Warwick.

A3.1. Check on possible lattice parameter changes in the diffusion layer.

Small pieces were cleaved off the edges of the following CdS slices which had been annealed with either excess Ga or excess In in the ampoule. The details of the slices which were used are given below:

In-doped	slice 132a	17.83 h at 1305 K
	slice 132b	57.00 h at 1214 K
Ga-doped	slice 211b	69.75 h at 1136 K

The Ga-doped slice had a comparatively thin diffusion layer. Each specimen was crushed and sorted optically under a microscope to reject the undoped parts. A diffraction specimen was then prepared from each of the diffusion specimens and also from a pure CdS crystal by grinding in a mortar and compacting with 'Durofix'. The powder patterns were taken with a Philips camera of 114.6 mm diameter and Cd K_α radiation, with the tube run at 27 kV to eliminate Cd K fluorescence.

All the specimens showed the 26 sharp lines of wurtzite with the $\alpha_1\alpha_2$ doublet being clearly resolved for the higher Bragg angles. The two In-doped specimens gave lattice parameters that were, to within experimental error, identical with that of pure CdS. For example, line $25\alpha_1$ Bragg angles were 74.75 degrees for the pure

CdS compared with a value of 74.85 degrees for In-doped specimen 132a. The mean lattice spacings of the In-doped specimen for all lines was (0.05 ± 0.05)% less than for pure CdS. Powder pattern photographs for In-doped specimen 132b and for pure CdS are shown in figures A3.1a and A3.1b respectively.

As can be seen in figure A3.1c the Ga-doped specimen gave two sets of sharp wurtzite diffraction lines. This is explained by the presence of some undoped material from the inner part of the doped CdS slice in the fragments used for the X-ray measurements. The lattice parameters were found to be 0.68% and 3.50% less respectively than for the pure CdS sample. The 0.68% increase in $\sin\theta$, and the corresponding 0.68% decrease in lattice spacing is significantly more than the experimental error. However, the results have not been corrected for possible systematic errors, for example, by plotting against $\cos^2\theta$. On the assumption that the lines giving the 0.68% change are due to fragments of undoped CdS, the lattice parameter of the doped parts of specimen 211b are (2.8 ± 0.2)% less than for the pure crystal. There was no change detected in the c/a ratio.

At the end of each diffusion anneal, it was customary to cool the ampoule and its contents down to room temperature as quickly as possible in order to freeze the high temperature equilibrium state that existed in the CdS slice. In the Ga measurements additional diffusion anneals were carried out in which, at the end of the anneal, the ampoule was left in the furnace and the furnace was allowed to cool to room temperature very slowly. On optical examination, these CdS slices were found to contain small isolated regions of a second phase which had segregated out. This was because the rate of cooling was sufficiently slow for the atoms to readjust their positions to

TYPICAL X-RAY POWDER PHOTOGRAPHS OF In-DOPED AND Ga-DOPED CdS

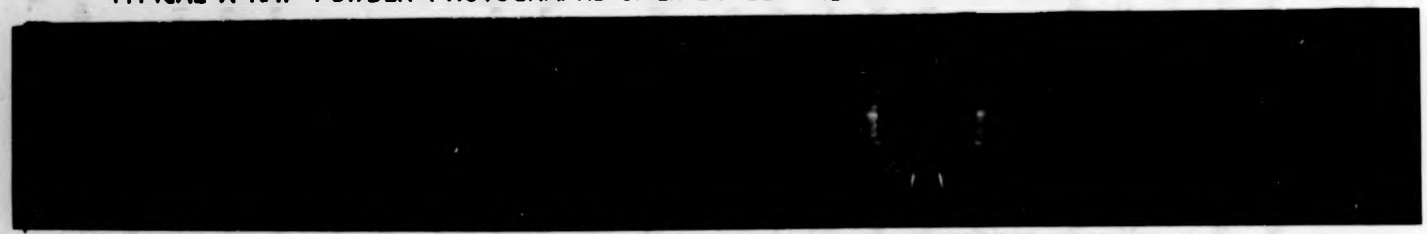

(a) CdS diffused in a saturated vapour of In-specimen 132b – temperature 1214K – duration 57.00h

(b) pure CdS

(c) CdS diffused in a saturated vapour of Ga – specimen 211b – temperature 1136K – duration 69.75h

Fig A3.1

give the equilibrium conditions which exist at room temperature. At the room temperature equilibrium conditions the CdS slice consisted mainly of Ga-doped CdS whose composition corresponded to the boundary between the CdS wurtzite phase and the (CdS + $CdGa_2S_4$) two phase field (figure 9.10). In addition the CdS slice contained small isolated regions of Cd-doped $CdGa_2S_4$ whose composition corresponded with the boundary between the (CdS + $CdGa_2S_4$) two phase field and the Cd-doped $CdGa_2S_4$ phase. This behaviour is shown in the photograph (1) in figure A3.2, where the microscope, which was used to take the photograph, was focussed onto a region of the CdS slice in the vicinity of the diffusion front. The network is visible due to the segregation of second phase particles on dislocations during the reheating of a crystal at 873 K after a diffusion heat treatment at 1173 K.

A3.2. <u>The structure of the reaction layers</u>

Whole diffusion specimen were mounted in the powder camera and rotated so that a small face of the surface was tangential to the X-ray beam. The following slices were used:-

Ga-doped	slice 211d	48.20 h at 1136 K
	slice 212f	645.0 h at 1021 K
Al-doped	slice 313e	4.95 h at 1336 K

In addition to the strong spots due to CdS, a powder pattern was observed. For specimen 212f, all the strongest lines and ten of the twelve recorded lines were identified as due to $CdGa_2S_4$ (2).

The whitish outer layer from specimen 313e gave a clear pattern, which was due to Al_2O_3 (3), along with some weak lines due to pure CdS.

magnification x 1500

PRECIPITATION AROUND A DISLOCATION NETWORK IN AN Ga-DOPED CdS SLICE

Fig A 3·2

A3.3. References

1. D. WILCOX, The Photoconductivity of CdS, Undergraduate Project, Department of Physics, University of Warwick, Coventry, (1975).

2. Powder Diffraction File (Edited by J. V. Smith), Card No. 8-275, American Society for Testing and Materials, Philadelphia.

3. Powder Diffraction File (Edited by J. V. Smith), Card No. 11-661, American Society for Testing and Materials, Philadilphia.

A4. Analysis of the metal globule in the diffusion of In into CdS

Measurements were carried out by the project supervisor to verify that Cd had accumulated in the metal globule. In the diffusions, which had been carried out with excess In metal only sealed in the ampoule with the CdS slice, the metal globule became a dilute Cd/In alloy when the diffusion anneal got under way. Three metal globules were chosen where specimen 122c was expected to give a low final Cd/In ratio, 122q a higher ratio than 122c, and 150a, which was diffused right through, was expected to give a much higher ratio than 122q. This trend is confirmed by the results which are tabulated at the end of this appendix. The measurements were carried out using a 100 keV transmission electron microscope and a Li-drifted Si detector was used for the measurement of the characteristic K_α X-rays.

Diffusion number		150a	122c	122q
Temperature	K	1241	1120	1120
Duration	S	1.555,5	1.44,4	7.92,4
Fraction of CdS doped with In		1.0	0.35	0.69
Cd weight in the In/Cd alloy	%	21 $\pm$ 3	3 $\pm$ 1	8 $\pm$ 2

J. Phys. Chem. Solids. 1978. Vol. 39, pp. 11–18. Pergamon Press. Printed in Great Britain

DIFFUSION OF INDIUM INTO CADMIUM SULPHIDE

E. D. JONES
Department of Applied Sciences, Lanchester Polytechnic, Rugby CV21 3TG, England

and

H. MYKURA
Physics Department, University of Warwick, Coventry CV4 7AL, England

(*Received* 24 *January* 1977; *accepted* 20 *May* 1977)

Abstract—The diffusion of In into CdS was studied using optical, microprobe and radiotracer methods over a temperature range from 729 to 1411 K. When diffusion occurred with a large excess of In metal, the diffusion coefficient was found to be linearly proportional to In concentration in the CdS and a sharp, optically observable diffusion front existed. Varying the Cd/In atomic ratio in the metal produced a transition to normal, concentration independent diffusion for Cd/In ratios greater than unity. The diffusion is markedly anisotropic, with fast diffusion perpendicular to the crystal c-direction. Very high values were measured for the diffusion coefficient in the concentration dependent regime (up to $2\times10^{-11}m^2s^{-1}$) and the mobile specie is thought to be the (InV) complex. The total apparent activation energy was found to be 2.03 and 2.30 eV (perpendicular and parallel to the c-direction respectively) and the anisotropy of the activation energy measured directly was 0.250 eV. On converting the concentration dependent diffusion coefficients to a standard concentration a straight line Arrhenius plot was obtained below 1200 K, which gave an activation energy for defect motion of 1.56 ± 0.12 eV perpendicular to the c-direction and 1.81 ± 0.12 eV parallel to the c-direction.

INTRODUCTION

It is well known that, when an impurity of higher valency is introduced into an ionic crystal, the requirement for charge neutrality in the crystal can be satisfied by introducing compensating vacancies (Kittel[1]). For instance, Ca in solid solution in KCl crystals produces one cation sublattice vacancy for every Ca atom in the lattice. Such vacancies in the positive ion sublattice can greatly increase diffusion on that sublattice when diffusion is by a vacancy mechanism. When the vacancies introduced by impurities are very much greater than the intrinsic vacancy concentration, the diffusion can become linearly proportional to concentration (Wagner[2]). Semiconductors often show complex concentration dependencies for impurity diffusion and a brief report on concentration dependent diffusion in this system (Chern and Kröger,[3]) has appeared. We provide evidence here that CdS, which, though a semiconductor, is also recognised to be a markedly "ionic" II–VI compound, behaves rather like the classical ionic crystal for the diffusion of trivalent In. The solubility of In in CdS (i.e. replacement of $1.5x$ Cd atoms by x In atoms in the positive ion sublattice) occurs readily, so that high vacancy concentrations and correspondingly high In diffusion coefficients are found.

Radio-tracer sectioning methods and electron microprobe measurements across diffusion specimen sections were used to obtain concentration profiles after diffusion. The profiles are in agreement with the theoretical profiles calculated for $D \propto C$ with the very sharp diffusion fronts predicted by the theory (see Figs. 1 and 2). Because of the change in optical properties of CdS on In doping, these fronts are comparatively easily observed by optical microscopy. This makes it possible to study the diffusion behavior very economically using optical microscopy and to determine the anisotropy of diffusion accurately. Absolute measurement of the near-surface concentration of In in the diffusion samples (by microprobe and tracer methods) enables the solubility-temperature relation to be obtained and the gross diffusion coefficient to be converted to a diffusion coefficient at a standard concentration for all temperatures. The activation energy of this normalised diffusion coefficient then gives the activation energy of motion of the mobile defect directly.

INTERPRETATION OF CONCENTRATION DEPENDENT DIFFUSION

The initial experiments showed that the concentration profile for In diffusion did not follow the "integral error function" penetration profile, that is expected for an effectively infinite source, when the diffusion coefficient is independent of concentration. Instead, the concentration profile was convex upward everywhere and showed a sharp diffusion front. The solutions of the diffusion equation for a wide variety of concentration dependencies have been discussed in detail by Crank[4]. The solution for the case of a diffusion coefficient linearly proportional to concentration was first obtained by Wagner[2] and power law ($D \propto C^n$) diffusion profiles have been computed by Weisberg and Blanc[5]. Our measured concentration-distance curves fitted the Wagner solution ($D \propto C$) very well, as is shown in Figs. 1(b) and 2.

The Wagner solution gives the diffusion coefficient D_S for the concentration at the free surface of the crystal in terms of the diffusion time t and the penetration distance x_{max} by $D_S = 0.3811 x_{max}^2/t$. The diffusion coefficient at the annealing temperature for any other In concentration is then given by $D^C = D_S \cdot C/C_S$, where C_S is the near-

J. Phys. Chem. Solids, 1978, Vol. 39, pp. 11–18 Pergamon Press Printed in Great Britain

DIFFUSION OF INDIUM INTO CADMIUM SULPHIDE

E. D. JONES
Department of Applied Sciences, Lanchester Polytechnic, Rugby CV21 3TG, England

and

H. MYKURA
Physics Department, University of Warwick, Coventry CV4 7AL, England

(*Received* 24 *January* 1977; *accepted* 20 *May* 1977)

Abstract—The diffusion of In into CdS was studied using optical, microprobe and radiotracer methods over a temperature range from 729 to 1411 K. When diffusion occurred with a large excess of In metal, the diffusion coefficient was found to be linearly proportional to In concentration in the CdS and a sharp, optically observable diffusion front existed. Varying the Cd/In atomic ratio in the metal produced a transition to normal, concentration independent diffusion for Cd/In ratios greater than unity. The diffusion is markedly anisotropic, with fast diffusion perpendicular to the crystal *c*-direction. Very high values were measured for the diffusion coefficient in the concentration dependent regime (up to $2 \times 10^{-11} m^2 s^{-1}$) and the mobile specie is thought to be the (InV) complex. The total apparent activation energy was found to be 2.03 and 2.30 eV (perpendicular and parallel to the *c*-direction respectively) and the anisotropy of the activation energy measured directly was 0.250 eV. On converting the concentration dependent diffusion coefficients to a standard concentration a straight line Arrhenius plot was obtained below 1200 K, which gave an activation energy for defect motion of 1.56 ± 0.12 eV perpendicular to the *c*-direction and 1.81 ± 0.12 eV parallel to the *c*-direction.

INTRODUCTION

It is well known that, when an impurity of higher valency is introduced into an ionic crystal, the requirement for charge neutrality in the crystal can be satisfied by introducing compensating vacancies (Kittel[1]). For instance, Ca in solid solution in KCl crystals produces one cation sublattice vacancy for every Ca atom in the lattice. Such vacancies in the positive ion sublattice can greatly increase diffusion on that sublattice when diffusion is by a vacancy mechanism. When the vacancies introduced by impurities are very much greater than the intrinsic vacancy concentration, the diffusion can become linearly proportional to concentration (Wagner[2]). Semiconductors often show complex concentration dependencies for impurity diffusion and a brief report on concentration dependent diffusion in this system (Chern and Kröger,[3]) has appeared. We provide evidence here that CdS, which, though a semiconductor, is also recognised to be a markedly "ionic" II–VI compound, behaves rather like the classical ionic crystal for the diffusion of trivalent In. The solubility of In in CdS (i.e. replacement of $1.5x$ Cd atoms by x In atoms in the positive ion sublattice) occurs readily, so that high vacancy concentrations and correspondingly high In diffusion coefficients are found.

Radio-tracer sectioning methods and electron microprobe measurements across diffusion specimen sections were used to obtain concentration profiles after diffusion. The profiles are in agreement with the theoretical profiles calculated for $D \propto C$ with the very sharp diffusion fronts predicted by the theory (see Figs. 1 and 2). Because of the change in optical properties of CdS on In doping, these fronts are comparatively easily observed by optical microscopy. This makes it possible to study the diffusion behavior very economically using optical microscopy and to determine the anisotropy of diffusion accurately. Absolute measurement of the near-surface concentration of In in the diffusion samples (by microprobe and tracer methods) enables the solubility-temperature relation to be obtained and the gross diffusion coefficient to be converted to a diffusion coefficient at a standard concentration for all temperatures. The activation energy of this normalised diffusion coefficient then gives the activation energy of motion of the mobile defect directly.

INTERPRETATION OF CONCENTRATION DEPENDENT DIFFUSION

The initial experiments showed that the concentration profile for In diffusion did not follow the "integral error function" penetration profile, that is expected for an effectively infinite source, when the diffusion coefficient is independent of concentration. Instead, the concentration profile was convex upward everywhere and showed a sharp diffusion front. The solutions of the diffusion equation for a wide variety of concentration dependencies have been discussed in detail by Crank[4]. The solution for the case of a diffusion coefficient linearly proportional to concentration was first obtained by Wagner[2] and power law ($D \propto C^n$) diffusion profiles have been computed by Weisberg and Blanc[5]. Our measured concentration-distance curves fitted the Wagner solution ($D \propto C$) very well, as is shown in Figs. 1(b) and 2.

The Wagner solution gives the diffusion coefficient D_S for the concentration at the free surface of the crystal in terms of the diffusion time t and the penetration distance x_{max} by $D_S = 0.3811 x^2_{max}/t$. The diffusion coefficient at the annealing temperature for any other In concentration is then given by $D^C = D_S C/C_S$, where C_S is the near-

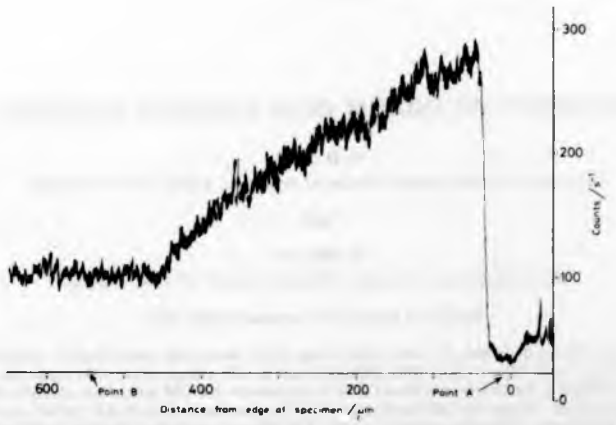

Fig. 1(a). Microprobe intensity scan, half way across a cleaved surface of a diffusion specimen in a direction parallel to the diffusion (i.e. parallel to the c-axis). The detection system was set on the In L_α X-ray line peak. Point A, outer edge of the specimen; point B, centre of specimen. Diffusion details: duration 1.8×10^4 s, temperature 1273 K.

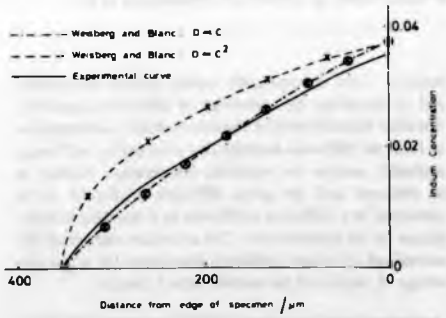

Fig. 1(b). The In concentration profile obtained from (a) after the "white" X-ray contribution is subtracted and the counting rate is normalised and corrected using a pure In sample. The shapes of the expected profiles for $D \propto C$ and $D \propto C^2$ are included for comparison.

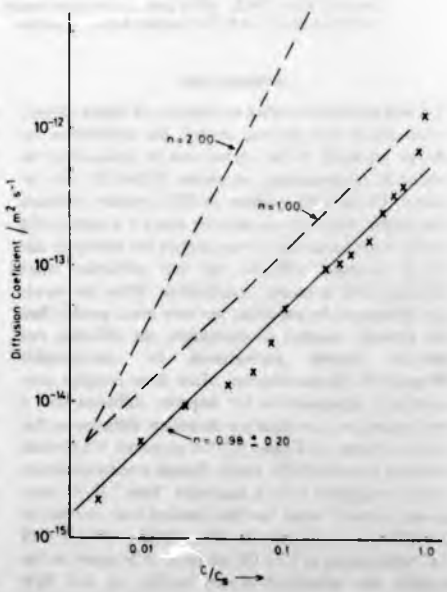

Fig. 2. Concentration dependence of In diffusion in CdS from radio-tracer sectioning analysed by the Boltzmann–Matano technique. Lines have been drawn with slopes of 1.00 and 2.00 corresponding to the cases of $n = 1$ and 2 in $D \propto C^n$ for comparison. Diffusion details: temperature 1126 K and duration 1.8×10^4 s.

surface concentration. The measurement of C_S (by calibrated microprobe or radiotracer measurement) therefore enables the diffusion coefficient at any standard concentration to be calculated. We chose to use 1% In atoms on the cation sublattice as the standard concentration and call the diffusion coefficient at this concentration D_S'. The variation of D_S' with temperature should then give the activation energy of motion of the mobile defect directly, provided we can assume that the nature and proportion of the defects remains constant over the temperature range covered. Thus $D_S' = D_0' \exp(-E_M/kT)$. The solubility of In is found to increase exponentially with temperature, so that $C_S = C_0 \exp(-E_I/kT)$ and the measured diffusion coefficient varies with temperature according to $D_S = D_0 \exp[-(E_I + E_M)/kT]$.

Diffusivity is a second rank tensor property (Nye[6]). As CdS is a hexagonal crystal, the unique principal axis of the tensor will be along the c-axis and diffusion will be isotropic perpendicular to the c-axis. We therefore require two independent diffusion coefficients, which we

call $D_\perp$ and $D_\parallel$, and will obtain two activation energies for defect motion, $E_{M_\perp}$ and $E_{M_\parallel}$, perpendicular and parallel to the c-axis, respectively.

EXPERIMENTAL TECHNIQUES

CdS single crystals from Eagle–Picher Company (Ultra High Purity grade) were used and sliced into discs 1 mm thick using a diamond wheel and mechanically polished. Pure In metal and one piece of crystal were sealed into silica ampoules under high vacuum and annealed in an electric furnace for the required time. For the radiotracer experiments the In used had been previously neutron irradiated at AERE, Harwell and approx. 150 mg of crystal and 15 mg of metal used. The microprobe and optical work was done with crystals of about 60 mg and about 50 mg of metal. During the diffusion anneal, the metal became an In–Cd alloy. To investigate the effect of the Cd/In atomic ratio in the alloy on the diffusion behaviour, a range of ampoules, containing up to 2 g of In at one extreme and 15 mg In plus 50 mg Cd metal at the other extreme were used. Crystal and metal were weighed before and after the anneal to determine mass transfer and check on possible mass loss.

The radio-tracer "sectioning" was done by grinding off successive layers of crystal onto emery paper after the edges of the crystal had been trimmed. The thickness removed was calculated from the mass change and the area and density of the crystal. The piece of emery paper was then counted on a low background β-counting system, appropriate corrections for background counting rate being made. The decay rate of some of the irradiated In and of some diffused specimens was checked to ensure that the measured activity was actually due to ^{114}In (half-life 40.0 d) and all the count rates were corrected for decay. The absolute In concentration in the diffusion specimens was determined by dissolving 3 9 mg of irradiated In in HCl, diluting and taking 10^{-4} of the solution onto a planchet and evaporating to dryness, counting it with the same counter system and comparing counting rates with this standard. More details of this radio-tracer method have already been given (Jones[7]).

The microprobe measurements were performed at the Centre for Materials Science, Birmingham University, using an Associated Electrical Industries' instrument. Diffusion specimens were mounted in a conducting plastic holder, sectioned and polished. Using a 30 keV electron beam focussed to about 1 μm dia., the In L_α X-ray intensity (selected by crystal diffraction and measured by gas proportional counter) was recorded continuously, while the specimen was traversed. This gave two profiles for each traverse, with the central, undoped part of the crystal giving the zero In reading. A piece of pure In was used as a comparison standard to enable absolute In concentrations to be evaluated. For this purpose a computer programme (provided by the Centre) was used to estimate self-absorption and Z-number corrections to the measured counting rates.

The bulk of the optical measurements were made with polarised, incident light. This gave sufficient contrast to enable the diffusion front to be seen. Much better contrast is obtained with transmitted light, but the difficulty of cleaving complete thin (of approximately 100 μm thickness) sections out of the crystals and perpendicular to the principal surfaces of the specimen required that the bulk of the optical measurements were done with incident illumination. The normal optical specimens were oriented so that the depth of the diffused zone in the [0001] and [11$\bar{2}$0] directions could be measured on the same cleavage surface. The distance of the diffusion front from the crystal surface was measured with an eyepiece micrometer, which was occasionally calibrated with a stage micrometer.

The reverse diffusion of Cd out of the CdS crystal was checked for a few specimens by measuring the Cd concentration in the In globule after the end of the diffusion anneal. Using an energy-dispersive analyser and a 100 keV electron beam, the K lines of In and Cd were easily separated and Cd concentrations down to 1% could be detected.

MICROPROBE AND OPTICAL RESULTS

The optical measurements for the penetration depth were very much simpler to do and were more accurate than those obtained using the radiotracer sectioning technique. Therefore the microprobe measurements were limited to showing that the "Wagner" concentration dependent profiles occurred and for determining the surface concentration of In, which is also the solubility, over the temperature range investigated. A typical microprobe trace is shown in Fig. 1(a) and the In concentration depth profile derived from it in Fig. 1(b). The surface concentration of In as a function of annealing temperature, derived from the microprobe traces, is shown in Fig. 3, and the best straight line through the points can be represented by $C_s/C_0 = (3.0^{+4}_{-2}) \exp[-(0.48 \pm 0.09)/kT]$, where the activation energy is in eV.

At each diffusion temperature a number of specimens were annealed together in the furnace and removed sequentially for measurement. This enabled a penetration depth-time graph to be drawn; a typical example is shown in Fig. 4. For each specimen several individual readings of the penetration depth parallel and perpendicular to the c-axis were taken, and the two mean values

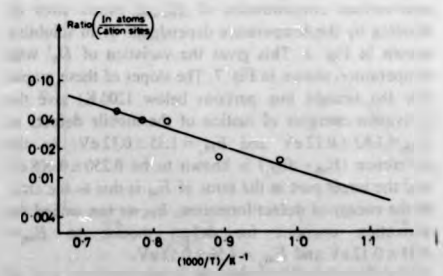

Fig. 3. An Arrhenius plot of the surface concentration of In in CdS, expressed as the concentration of In atoms per cation site, as derived from the microprobe traces. The best straight line through the experimental points can be represented by $C_s/C_0 = (3.0 \pm \frac{4}{2}) \exp[-(0.48 \pm 0.09)\text{eV}/kT]$.

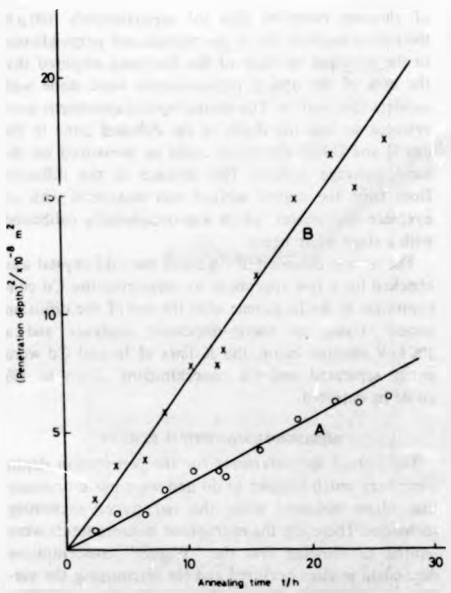

Fig. 4. Typical (penetration depth)² time graph for the In diffusion front which was obtained with the optical measurements. Line A, parallel to the c-axis; line B, perpendicular to the c-axis. Diffusion details: temperature 1120 K and maximum duration 9.54×10^5 s.

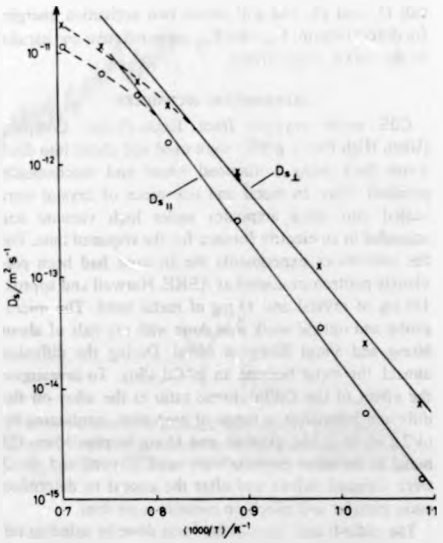

Fig. 5. Crude diffusion coefficients D_S for In diffusion in the two principal directions as a function of temperature. The deviation from the straight line relation at temperatures above 1200 K is marked. Equations for the straight line portions of the curves at lower temperatures are given by

$$D_{S_\parallel} = (6^{+6}_{-4}) \times 10^{-3} (\mathrm{m^2 s^{-1}}) \exp\left[\frac{-2.30 \pm 0.08\ \mathrm{eV}}{kT}\right]$$

and

$$D_{S_\perp} = (1^{+2}_{-1}) \times 10^{-3} (\mathrm{m^2 s^{-1}}) \exp\left[\frac{-2.03 \pm 0.08\ \mathrm{eV}}{kT}\right].$$

for each annealing time were plotted. The value of x^2/t was calculated from the slope of the graph. The values of D_0 obtained are shown as a function of reciprocal temperature in Fig. 5. The ratios $(x_\perp/x_\parallel)^2$ for individual specimens were also evaluated. These give the diffusion anisotropy directly and much more accurately, because the errors of timing and temperature cancel out. They are plotted against reciprocal temperature in Fig. 6; from this curve the difference in activation energy of diffusion in the two principal directions is (0.250 ± 0.008) eV.

The diffusion coefficients shown in Fig. 5 can be converted to diffusion coefficients at our standard In near-surface concentration of 1% of cation sites by dividing by the temperature dependence of In solubility shown in Fig. 3. This gives the variation of $D_S^{\ I}$ with temperature, shown in Fig. 7. The slopes of these graphs (for the straight line portions below 1200 K) give the activation energies of motion of the mobile defects as $E_{M_\parallel} = 1.82 \pm 0.12$ eV and $E_{M_\perp} = 1.55 \pm 0.12$ eV. As the difference $(E_{M_\parallel} - E_{M_\perp})$ is known to be 0.250 ± 0.008 eV and the larger part in the error of E_M is due to the error in the energy of defect formation, E_F, we can amend the activation energies for defect motion to $E_{M_\parallel} = 1.81 \pm 0.12$ eV and $E_{M_\perp} = 1.56 \pm 0.12$ eV.

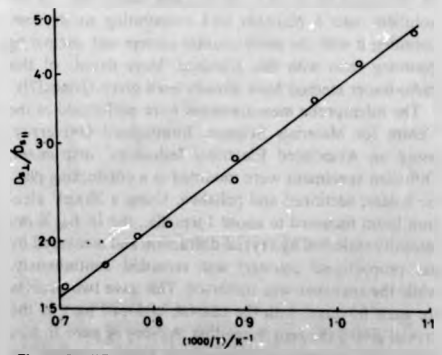

Fig. 6. In diffusion anistropy in CdS plotted as log (penetration depth ratio)² against reciprocal temperature. The difference in activation energy of diffusion in the two principal directions is (0.250 ± 0.008) eV.

RADIOTRACER RESULTS

The tracer experiments were done with larger crystals (to have a large enough area for convenient sectioning) and a smaller amount of In metal, to save on costs of radioactive material. This meant that the annealing conditions were not exactly comparable with the optical and microprobe measurements and this is discussed further in the next section.

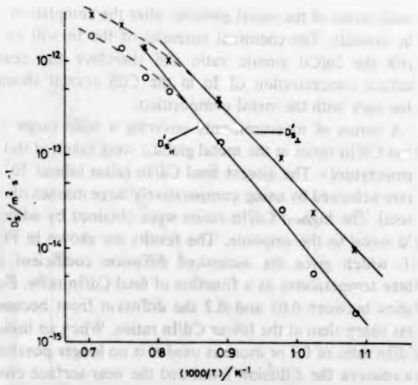

Fig. 7. Arrhenius plots of the standardised In diffusion coefficient D_S' for 1 atomic per cent In in CdS for the two principal crystal directions. The curves show the same deviation from the straight line relationship as is shown in Fig. 5. The relationships for the straight line portion (that is below 1200 K) are given by

$$D_{S\parallel}' = \left(2^{+3}_{-1}\right) \times 10^{-1}\,(m^2s^{-1}) \exp\left[\frac{-(1.82 \pm 0.12)\,eV}{kT}\right]$$

and

$$D_{S\perp}' = \left(3^{+5}_{-2}\right) \times 10^{-4}\,(m^2s^{-1}) \exp\left[\frac{-(1.55 \pm 0.12)\,eV}{kT}\right].$$

The tracer technique was more sensitive than the microprobe technique and enabled a more accurate comparison of the measured concentration profile with the Wagner theory to be made. Such a profile is shown in Fig. 8. It was usually possible to follow the In concentration down to less than 10^{-3} of the surface concentration, whereas the microprobe method could not go below 3% of the surface concentration. However, there was more scatter in the penetration depth measurements for the tracer experiments and as far fewer measurements were made, the overall results were not so accurate. The results for D_S by the tracer technique are shown in Fig. 9 as a function of $1/T$. It was not possible to show the diffusion anistropy unambiguously so the average of all measurements is given. This produces an activation energy of 2.09 ± 0.08 eV compared to the mean of the two optical values of 2.16 eV.

The near-surface concentration of In after annealing over a range of temperatures was determined using a calibrated In source as a comparison. The plot of log (concentration) against $1/T$ gave an energy of solution of (0.53 ± 0.006) eV, compared to (0.48 ± 0.09) eV obtained from the microprobe results. While the activation energies are in tolerable agreement the absolute value of In solubility for the tracer results are almost a factor of two lower. The results are shown in Fig. 10 and the discrepancy is discussed in the next section.

THE EFFECT OF THE Cd/In RATIO IN THE METAL

During the diffusion of In into the CdS, Cd atoms diffuse outwards and are liberated from the crystal. The Cd atoms will dissolve in the liquid In globule and the

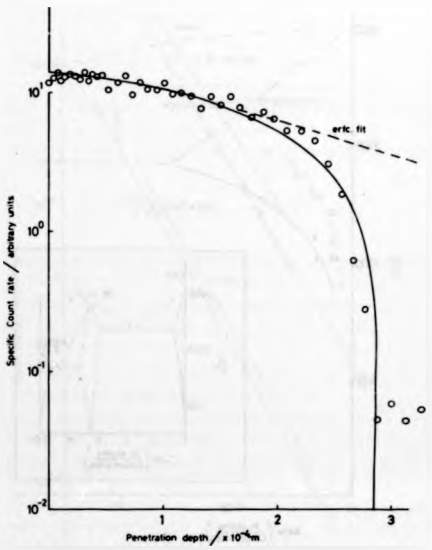

Fig. 8. Typical radiotracer In^{α} counting rate versus penetration depth profile obtained by sectioning. The solid line shows the best Wagner curve fit whereas the dotted line shows the corresponding error function complement curve. Diffusion details: temperature 1027 K, duration 7.74×10^5 s.

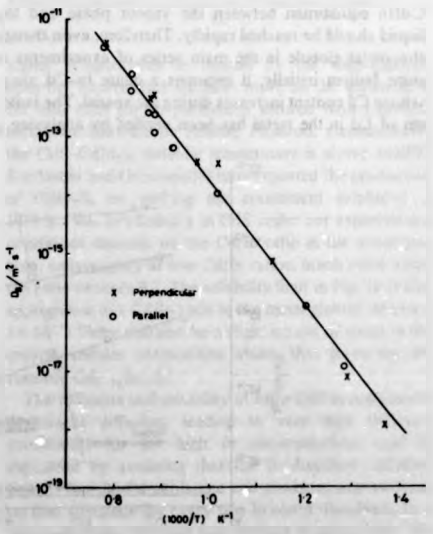

Fig. 9. An Arrhenius plot of the crude In diffusion coefficient in CdS obtained from the tracer measurements. The best straight line through the experimental points is given by $D_S = (6^{-4}_{-3}) \times 10^{-4}\,(m^2s^{-1}) \exp[-(2.09 \pm 0.08)\,eV/kT]$. It was not possible to show the diffusion anisotropy unambiguously so the average of all the measurements is given.

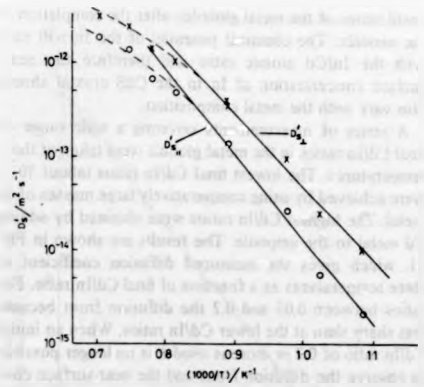

Fig. 7. Arrhenius plots of the standardised In diffusion coefficient D_S' for 1 atomic per cent In in CdS for the two principal crystal directions. The curves show the same deviation from the straight line relationship as is shown in Fig. 5. The relationships for the straight line portion (that is below 1200 K) are given by

$$D'_{S_\perp} = \left(2^{+3}_{-1}\right) \times 10^{-4}\,(\mathrm{m^2 s^{-1}}) \exp\left[\frac{-(1.82 \pm 0.12)\,\mathrm{eV}}{kT}\right]$$

and

$$D'_{S_\parallel} = \left(3^{+5}_{-2}\right) \times 10^{-4}\,(\mathrm{m^2 s^{-1}}) \exp\left[\frac{-(1.55 \pm 0.12)\,\mathrm{eV}}{kT}\right].$$

The tracer technique was more sensitive than the microprobe technique and enabled a more accurate comparison of the measured concentration profile with the Wagner theory to be made. Such a profile is shown in Fig. 8. It was usually possible to follow the In concentration down to less than 10^{-3} of the surface concentration, whereas the microprobe method could not go below 3% of the surface concentration. However, there was more scatter in the penetration depth measurements for the tracer experiments and as far fewer measurements were made, the overall results were not so accurate. The results for D_S by the tracer technique are shown in Fig. 9 as a function of $1/T$. It was not possible to show the diffusion anistropy unambiguously so the average of all measurements is given. This produces an activation energy of 2.09 ± 0.08 eV compared to the mean of the two optical values of 2.16 eV.

The near-surface concentration of In after annealing over a range of temperatures was determined using a calibrated In source as a comparison. The plot of log (concentration) against $1/T$ gave an energy of solution of (0.53 ± 0.006) eV, compared to (0.48 ± 0.09) eV obtained from the microprobe results. While the activation energies are in tolerable agreement the absolute value of In solubility for the tracer results are almost a factor of two lower. The results are shown in Fig. 10 and the discrepancy is discussed in the next section.

THE EFFECT OF THE Cd/In RATIO IN THE METAL

During the diffusion of In into the CdS, Cd atoms diffuse outwards and are liberated from the crystal. The Cd atoms will dissolve in the liquid In globule and the

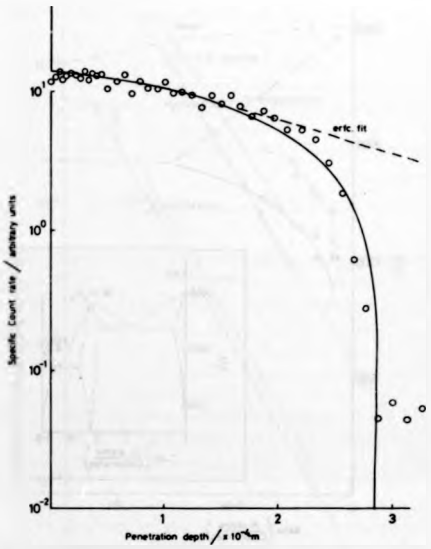

Fig. 8. Typical radiotracer In* counting rate versus penetration depth profile obtained by sectioning. The solid line shows the best Wagner curve fit whereas the dotted line shows the corresponding error function complement curve. Diffusion details: temperature 1027 K, duration 7.74×10^5 s.

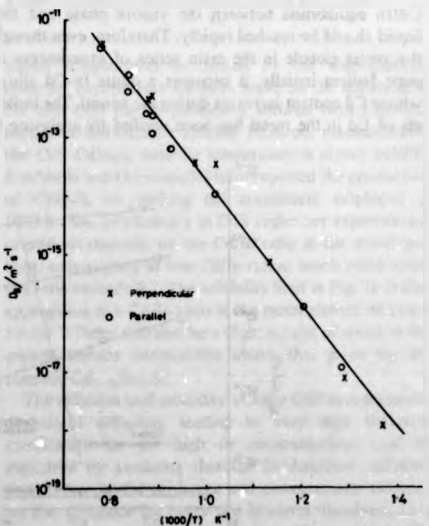

Fig. 9. An Arrhenius plot of the crude In diffusion coefficient in CdS obtained from the tracer measurements. The best straight line through the experimental points is given by $D_S = (6^{+3}_{-2}) \times 10^{-4}\,(\mathrm{m^2 s^{-1}}) \exp[-(2.09 \pm 0.08)\,\mathrm{eV}/kT]$. It was not possible to show the diffusion anisotropy unambiguously so the average of all the measurements is given.

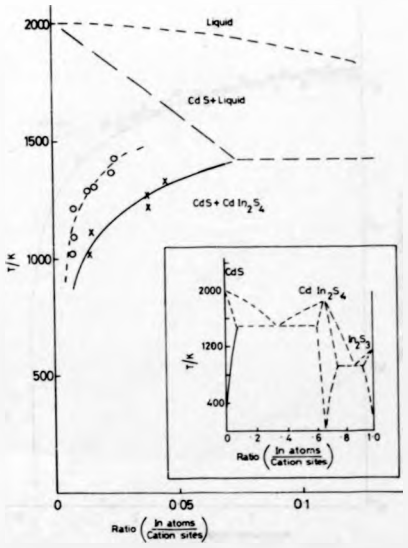

Fig. 10. The In solubility in CdS expressed in the form of a phase diagram. The final Cd/In ratio in the liquid metal = 2×10^{-4}. Experimental points: crosses, microprobe results; circles, radiotracer results. The reason for the discrepancy in the two sets of results is explained in the text. The possible form of the whole phase diagram indicating the existence of $CdIn_2S_4$ is shown in the inset diagram.

Cd/In equilibrium between the vapour phase and the liquid should be reached rapidly. Therefore, even though the metal globule in the main series of experiments is pure Indium initially, it becomes a dilute In–Cd alloy, whose Cd content increases during the anneal. The build-up of Cd in the metal has been verified by analysing a small series of the metal globules after the completion of the anneals. The chemical potential of the In will vary with the In/Cd atomic ratio and therefore the near-surface concentration of In in the CdS crystal should also vary with the metal composition.

A series of measurements covering a wide range of final Cd/In ratios in the metal globule were taken at three temperatures. The lowest final Cd/In ratios (about 10^{-5}) were achieved by using comparatively large masses of In metal. The highest Cd/In ratios were obtained by adding Cd metal to the ampoule. The results are shown in Fig. 11, which gives the measured diffusion coefficient at three temperatures as a function of final Cd/In ratio. For ratios between 0.03 and 0.2 the diffusion front became less sharp than at the lower Cd/In ratios. When an initial Cd/In ratio of 0.2 or more is used it is no longer possible to observe the diffusion front and the near-surface concentration of In has decreased substantially. For Cd/In ratios higher than unity the diffusion becomes essentially independent of concentration and both the radiotracer and mocroprobe results give "integral error function" penetration profiles (of which Fig. 12 is a typical example) and which can be interpreted in the normal way. The change in the Cd/In ratio in the metal globule during the diffusion anneal should cause a slight drop in the surface In concentration C_{Si} in the crystal during the later stages of each anneal. This should produce a slight deviation from the Wagner profile in the measured profile. The effect is expected to be near our experimental measurement accuracy limit, but it may account for the low C_S values in Fig. 1(b) and Fig. 8, and (as it causes high values of dx/dC) for the high values near $C/C_S = 1$ in Fig. 2.

The difference in the result obtained by the microprobe-optical method and by the radiotracer method for the In solubility in CdS differ in part due to the difference in Cd/In ratio. However, when the radiotracer results in Fig. 10 have been corrected for this (using the data in

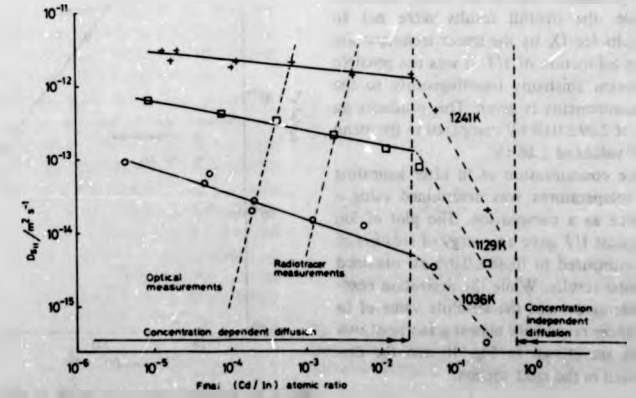

Fig. 11. Effect of the final Cd/In ratio in the metal globule during the anneal on the diffusivity (& solubility) of In in CdS. The three temperatures used were 1036, 1129 and 1241 K. For ratios between 0.03 and 0.2 the diffusion front becomes less sharp than at the lower Cd/In ratios. When an initial Cd/In ratio of 0.2 or more is used it is no longer possible to observe the diffusion front and the near-surface In concentration has decreased substantially. For Cd/In ratios higher than unity the diffusion becomes essentially independent of concentration.

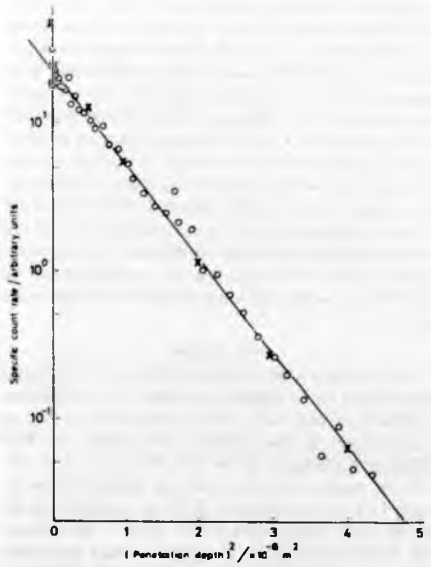

Fig. 12. A radiotracer In* diffusion profile in the presence of excess Cd (Final Cd/In ratio in the metal ≈ 3.4) showing a diffusion coefficient independent of In concentration. Diffusion details: temperature, 1275 K, duration 5.06×10^4 s. Notation: Circles, experimental points; full line, best Gaussian fit through experimental points giving $D = 3.34 \times 10^{-14} m^2 s^{-1}$; crosses, best erfc fit through experimental points giving $D = 3.81 \times 10^{-14} m^2 s^{-1}$.

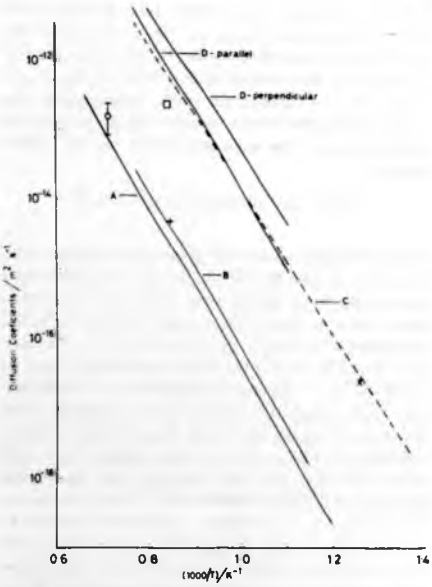

Fig. 13. Comparison of diffusion data in CdS. Lines: A, Cd* tracer self-diffusion see Jones[7]; B, In* tracer, excess Cd metal in ampoule Cd/In ratio ≈ 3.4; C, In* tracer, Cd/In ratio ≈ 10^{-3}; D, In optical, Cd/In ratio ≈ 2×10^{-4}. Points: O, By microprobe, excess Cd metal in ampoule; +, from Woodbury[11], excess In and S; ×, from O'Tuama and Richter[12], excess In; □, from Chern and Kröger [3], concentration dependent. Present work; lines B, C and D.

Fig. 11 to estimate what the tracer results would have been, had they been carried out at the lower final Cd/In ratio) there remains a substantial discrepancy. The tracer result is still about 40% lower than the microprobe result. The optical and microprobe results were much more extensive and consistent, and each microprobe measurement was individually calibrated. The absolute value of the tracer solubility measurements presented in Fig. 10 however depended on a single calibration, involving acid solution of a very small mass of radioactive In and dilution of the solution prior to counting. The calibration was later checked by carrying out three further independent calibrations and the results confirmed the results which are presented in Fig. 10. At present we feel that we are unable to explain the discrepancy between the results obtained by the two methods.

A total of 27 tracer diffusion and 80 optical diffusion specimens were used; the majority of the optical specimens gave four separate (two parallel and two perpendicular) diffusion penetration results.

INTERPRETATION OF THE RESULTS

We can conveniently represent the solubility data of In in CdS as a pseudo-CdS–In_2S_3 phase diagram, though we are dealing with the Cd–In–S ternary system. There is a $CdIn_2S_4$ intermediate phase in this system, though the presence of this compound was not demonstrated in these experiments. We believe the In solubility in CdS at higher temperatures is limited by the CdS–$CdIn_2S_4$ eutectic; experiments we have made on the diffusion of Ga into CdS (to be published) showed both $CdGa_2S_4$ formation and eutectic melting. From our measurements the CdS–$CdIn_2S_4$ eutectic temperature is above 1420 K; Koelmans and Grimmeis[8] have reported the production of $CdIn_2S_4$ by melting the constituent sulphides at 1423 K. The In solubility in CdS under our experimental conditions depends on the Cd/In ratio in the metal globule: only slightly at low Cd/In ratios, much more when the ratio exceeds 0.2. The solubility limit in Fig. 10 is that appropriate to a Cd/In ratio in the metal globule of about 3×10^{-4}. There will also be a slight excess of metal in the crystal surface composition above that given by the formula $Cd_{1-3x}In_{2x}S$.

The diffusion and solubility of In in CdS concentration dependent diffusion, leading to very high diffusion coefficients for the high In concentrations, can be explained by assuming that the In dissolves substitutionally on the Cd sublattice and produces one vacancy on that sublattice for every two In atoms dissolved, as is expected when trivalent ions replace divalent ions. We also believe that there is substantial association of the vacancies with In atoms to form (InV) pairs and that such pairs, diffusing by the vacancy mechanism, are very much more mobile than the other In atoms. Following Wagner[2], we can assume in our case that the concen-

tration of vacancies ($[V_{Cd}]$ in the usual notation) is half the In concentration $[In_{Cd}]$, i.e. $[In_{Cd}] = 2[V_{Cd}]$. If both are randomly distributed on the Cd sublattice, the concentration of the associated defect would be $[In_{Cd}V_{Cd}] = [In_{Cd}] \times [V_{Cd}] = 1/2[In_{Cd}]^2$ for small concentrations. Due to the bonding between a vacancy and an In atom, the concentration of the associated defect will be k times greater,

$$[In_{Cd}V_{Cd}] = k[In_{Cd}] \times [V_{Cd}] \simeq \frac{k}{2}[In_{Cd}]^2$$

where k depends on the binding energy and temperature. If we now assume that the $(In_{Cd}V_{Cd})$ is very much more mobile than In as substitutional atoms or in other complexes such as $(In_{Cd}V_{Cd}In_{Cd})$, then we find the In flux proportional to $[In_{Cd}]^2$, the amount of In to be transported is [In], so that the diffusivity should depend on $[In]^2/[In]$, i.e. be linearly proportional to In concentration. Such simple considerations are adequate when $[In_{Cd}]$ and $[V_{Cd}]$ are both small, $[In_{Cd}]^2 < 1/k$ and larger complexes can be neglected. Some $(In_{Cd}V_{Cd}In_{Cd})$ complexes will exist and their formation and dissociation keeps the total In distribution in approximate equilibrium with the $(In_{Cd}V_{Cd})$ distribution. A fuller theory must take account of the fact that $[In_{Cd}]$ is not the total (measured) In concentration, but that this needs to be corrected for the In in $(In_{Cd}V_{Cd})$ and $(In_{Cd}V_{Cd}In_{Cd})$ complexes. Such a fuller theory is needed to explain the fall-off in the measured diffusion coefficient above 1200 K (Figs. 5 and 7), but we restrict ourselves in this paper to the linearly concentration dependent diffusion.

Dr. D. Shaw (University of Hull) has determined for us the room temperature electrical properties by the Van der Pauw method of a CdS crystal which was uniformly doped to 2% In at 1241 K. This gave a carrier concentration of $5.6 \times 10^{25} m^{-3}$, showing that at room temperature only about 13% of the In was electrically active. This is not necessarily inconsistent with our model, which assumes that at high temperatures the In is mainly in the form of simple substitutional atoms (which are expected to produce n-doping) and $(In_{Cd}V_{Cd})$ complexes, as the proportion of $(In_{Cd}V_{Cd}In_{Cd})$ complexes, which should be electrically inactive, will be much larger at low temperatures and higher In concentrations.

The anisotropy of In diffusion is unexpectedly large for a crystal whose c/a ratio (1.623, Wyckoff[9]) is so near to the close-packed value of 1.633. In fact, simple theory predicts faster diffusion in the c-direction when the c/a ratio is less than 1.633. We consider that the large observed anisotropy, with $D_\perp > D_\parallel$, can be explained by assuming that the (InV) complex has a preferred orientation in the basal plane, possibly due to the effect of the crystal field on the defect complex. The measured difference in activation energy diffusion is thus related to orientation dependence of the defect energy.

The effect of the Cd/In ratio in the metal globule during the anneal is to decrease the In solubility slightly, without affecting the concentration dependent diffusion behaviour, when the ratio is less than about 0.03. For higher values of the ratio there is a gradual transition from concentration dependent diffusion to concentration independent behaviour with a much lower value of the diffusion coefficient. This is consistent with the known self-diffusion of Cd in CdS. From the pressure dependence of Cd self-diffusion of CdS crystals heated in Cd vapour it is known that (at least for high Cd partial pressures) the Cd diffusion is predominantly interstitial (Kumar and Kröger[10]). Therefore an increase in the Cd partial pressure would be expected to suppress vacancy formation on the Cd sublattice and reduce In solubility, as is found experimentally. The whole diffusion data for In and Cd diffusion in CdS is summarised in Fig. 12 and shows the striking increase in In diffusion in the presence of low Cd/In metal ratios, over the In diffusion and Cd self-diffusion when high Cd vapour partial pressures are used.

CONCLUSIONS

We have shown that, when In diffuses into CdS during annealing in an In vapour atmosphere, the In diffusion coefficient is very large and is proportional to the In concentration in the crystal. We ascribe the high diffusion coefficients to the introduction of vacancies into the cation sublattice during the solution of the In, caused by the requirement of charge neutrality in the lattice on the replacement of Cd^{2+} by In^{3+}. We consider the mobile defect to be a charged vacancy associated with an In^{3+} ion. The large crystallographic anisotropy found in this system is attributed to a preferred orientation of the (InV) associated defect in the CdS basal plane.

A transition from concentration dependent diffusion to normal concentration independent diffusion occurs when the In vapour annealing atmosphere is diluted with Cd vapour. This is associated with a decrease in the In diffusion coefficient to "normal" values.

Acknowledgments—We wish to thank (a) Dr. D. Shaw (Physics Department, University of Hull) for the electrical measurements on the doped CdS crystals and for comments on the work; (b) Dr. M. Hall of the Centre for Materials Science of the University of Birmingham for producing the microprobe analyser profiles and computing the corrections; and (c) Mr. C. Gilson and Mrs. P. Gillison of the Lanchester Polytechnic, Rugby, for technical assistance with the sealing of silica ampoules and the diffusion runs.

REFERENCES

1. Kittel C., *Introduction to Solid State Physics*, 3rd Edn, Chap. 18. Wiley, New York (1966).
2. Wagner C., *J. Chem. Phys.* 18, 1227 (1950).
3. Chern S. S. and Kröger F. A., *Phys. Status Solidi* A25, 215 (1974).
4. Crank J., *Mathematics of Diffusion*, 2nd Edn, Chap. 7. Clarendon Press, Oxford (1975).
5. Weisberg L. R. and Blanc J., *Phys. Rev.* 131, 1548 (1963).
6. Nye J. F., *Physical Properties of Crystals*. Clarendon Press, Oxford (1967).
7. Jones E. D., *J. Phys. Chem. Solids* 33, 2063 (1972).
8. Koelmans H. and Grimmeis H. G., *Physica* 25, 1287 (1959).
9. Wyckoff R. W. G., *Crystal Structures*, Vol. 1. Interscience, New York (1963).
10. Kumar V. and Kröger F. A., *J. Solid State Chem.* 3, 381 (1971).
11. Woodbury H. H., *Physics and Chemistry of II-VI Compounds* (Edited by M. Aven and J. S. Prener). North Holland, Amsterdam (1967).
12. O'Tuama S. S. and Richter J., *J. Appl. Phys.* 41, 1861 (1970).